Deregulated Notch and CD40 signaling

in murine B lymphocytes

Dissertation der Fakultät für Biologie der

Ludwig-Maximilians-Universität München

Anne Draeseke

München 2013

Erklärung

Diese Dissertation wurde von Januar 2009 bis Dezember 2012 am Institut für Klinische Molekularbiologie und Tumorgenetik des Helmholtz Zentrums München (später Abteilung für Genvektoren) in der Arbeitsgruppe von PD Dr. Ursula Zimber-Strobl erstellt und von Prof. Dr. Dirk Eick betreut.

Eidesstattliche Erklärung

Hiermit erkläre ich, Anne Draeseke, geboren am 07. Januar 1983 in Bonn, an Eides statt, dass ich die vorliegende Arbeit selbständig und nur unter Verwendung der angegebenen Hilfsmittel und Quellen angefertigt habe.

Diese Dissertation hat weder in gleicher oder ähnlicher Form einem anderen Prüfungsverfahren vorgelegen. Ich habe weder bereits früher Doktorgrade erworben noch versucht zu erwerben.

München, den 10.06.2013   Anne Draeseke

Erstgutachter: Prof. Dr. Dirk Eick

Zweitgutachterin: Prof. Dr. Elisabeth Weiß

Tag der Abgabe: 11.06.2013

Tag der mündlichen Prüfung: 09.12.2013

TABLE OF CONTENTS

LIST OF TABLES

LIST OF FIGURES

LIST OF ABBREVIATIONS

APC	antigen-presenting cell
B-CLL	B-cell chronic lymphocytic leukemia
BCR	B-cell receptor
BM	bone marrow
bp	base pairs
BrdU	Bromodesoxyuridin
BSA	bovine serum albumin
CD	cluster of differentiation
cDNA	complemetary DNA
CFSE	Carboxyfluorescein succinimidyl ester
Cre	protein recombinase of the phage P1 ("Causes Recombination")
CXCR	cysteine-X-cysteine chemokine receptor
DLBCL	Diffuse Large B-cell lymphoma
DC	dendritic cell
Dll	Delta-like
DNA	deoxyribonucleic acid
EBNA	EBV nuclear antigen
EBV	Epstein-Barr Virus
FCS	fetal calf serum
FACS	fluorescence-activated cell scanning/sorting
FL	Follicular lymphoma
Fo	follicular
Foxp3	Forkhead box P3, transcription factor
FSC	forward scatter
g	gram
GC	germinal center
(c)HL	(classical) Hodgkin Lymphoma
hi	high
HIV	human immunodeficiency virus
HRS cells	Hodgkin-Reed-Sternberg cells
hrs	hours
IHC	immunohistochemistry
IFN	interferon
Ig	immunoglobulin
IL	interleukin
int	intermediate
kb	kilobase
LMP	latent membrane protein
LN	lymph node
LPS	lipopolysaccharide
LT	lymphotoxin
MACS	magnetic cell separation
MALT	mucosal-associated lymphoid tissue
MDSC	myeloid-derived suppressor cell
mRNA	messenger RNA

MZ	marginal zone
neg	negative
NF-κB	nuclear factor κ B
NotchIC	intracellular part of the Notch receptor
o/n	overnight
PCR	polymerase chain reaction
pos	positive
qPCR	quantitative real-time polymerase chain reaction
RBP-Jκ	recombination signal binding protein for immunoglobulin κ J region
RNA	ribonucleic acid
SCID	Severe Combined Immunodeficiency
SMZL	splenic marginal zone lymphoma
SP	spleen
S1PR3	sphingosine 1-phosphate receptor 3
SSC	side scatter
TD	T-cell dependent
TCR	T-cell receptor
TGFβ	transforming growth factor-β
TI	T-cell independent
TNFR	tumor necrosis factor receptor
TRAF	TNF receptor associated factor
T_{regs}	T regulatory cells

1. INTRODUCTION

1.1 CD40 and Notch

CD40 and Notch represent two signaling transmembrane receptors that are expressed in a multitude of different cells and influence various signaling contexts initiated through cell-cell contact during cellular proliferation and differentiation processes. Both have numerous intersection points with other signaling pathways and consequently their activation or inactivation can have significant impact on health or disease states of the individual.

Since the work at hand is at the crossroads of immunology and oncology the molecules as such will be introduced, B- and T-cell development will be laid out and the impact the respective molecule has on the lymphocyte compartment as well as their roles in malignancies will be pointed out.

1.2 Notch signaling

The family of Notch receptors is found on a large number of different cell types and is involved in a multitude of different cellular processes. Notch signaling was originally discovered in *Drosophila melanogaster*, but has been shown to be conserved throughout evolution (Artavanis-Tsakonas et al., 1999).

This family of receptors consists of four members in mammals (Notch1-4) sharing structural and sequence homologies (Radtke et al., 2010). The Notch protein belongs to the family of LNG proteins (LIN12 and GLP1 in *Caenorhabditis elegans*; Notch in *Drosophila melanogaster*). In the extracellular part Notch presents three LNG and 10–36 copies of EGF (epidermal growth factor)-like repeats, where ligand-binding is mediated by the latter (Rebay et al., 1991). The intracellular region of Notch contains a PEST sequence (proline-, glutamate-, serine-, threonine- rich) important for the degradation of the protein, a RAM domain (RBPJк-associated molecule) and six to seven ankyrin repeats, both sequence of which are crucial for nuclear interaction with other proteins. Notch1 and Notch2 additionally feature a TAD domain (transcriptional activator domain).

Notch receptors have five different membrane-bound ligands in mammals that can be subdivided into two groups, according to the homology with the Drosophila genes *serrate* or *delta*; the first mentioned comprises Jagged 1 and 2, the latter Delta-like-1, -3 and -4 (Dll-1, -3 and -4). Delta and Serrate form part of the family of DSL (Delta/Serrate/Lag2) proteins. They consist of a small

intracellular part, and in the extracellular space they have varying number of EGF-like repeats and a DSL domain in the N-terminus. This DSL domain was also identified to be responsible for the interaction with Notch (Fitzgerald et al., 1995).

Notch receptors -like their ligands- are type I single pass transmembrane proteins. From their maturation until activation the Notch receptor undergoes three distinct proteolytic cleavage events (Fig. 1.1). The first cleavage (S1 cleavage) is mediated by a furin-like protease in the trans-Golgi network during synthesis (Logeat et al., 1998). Loss of S1 cleavage leads to loss of function of the Notch receptor (Lake et al., 2009). S1 cleavage results in a bipartite protein, composed of a small transmembrane and intracellular part linked to the larger extracellular part. After localization in the membrane the receptor can interact with its respective ligand. Crosslinking of the extracellular part then leads to a cascade of proteolytic cleavage events: first a metalloproteinase such as ADAM 10 or ADAM 17/TACE (a disintegrin And metalloproteinase/tumor necrosis factor-α-converting enzyme) (Gibb et al., 2010; Murthy et al., 2012) leads to membrane shedding of the extracellular portion of the protein (NotchEC; S2 cleavage). Subsequently, a presenilin-dependent γ-secretase (De Strooper et al., 1999) cuts within the membrane spanning domain of the receptor (S3 cleavage) so that the intracellular part (NotchIC) is released and can translocate to the nucleus.

In the absence of NotchIC in the nucleus its nuclear binding partner CSL (C promoter binding factor1/Suppressor of Hairless/Lag1) in humans and RBP-J in mice (recombination-signal-binding protein-J) (Matsunami et al., 1989) is bound to DNA with co-repressors including SMRT (silencing mediator of retinoid and thyroid receptors), HDAC1 and HDAC2 (histone deacetylase) which leads to suppression of Notch-target genes. Once NotchIC enters the nucleus, it binds to RBPJ via its ankyrin repeats and RAM domain (Kurooka et al., 1998). Subsequently, co-repressors are released from the complex and co-activators such as PCAF (P300/CBP-associated factor), p300 itself, and MAML1-3 (mastermind-like 1-3) are recruited which turn the complex into an activator complex. This eventually results in the expression of Notch-responsive genes such as *hes1* (hairy and enhancer of split 1) and *deltex1*. Via direct and indirect effectors expression of Notch-responsive genes influences diverse processes such as cell-fate decisions, cell migration (CCR4, CCR6, CCR7; CC chemokine receptors), angiogenesis (VEGF; vascular endothelial growth factor) and cell proliferation (c-myc, p21, p27, Cyclin D1). Ubiquitination of the PEST domain of NotchIC by E3 ligases terminates signaling and Notch is subsequently degraded in the proteasome (Hubbard et al., 1997; Fostier et al., 1998; Cornell et al., 1999; Oberg et al., 2001; Wu et al., 2001).

The largest body of research with regard to Notch signaling has probably been compiled in developmental studies (e.g. in embryonic pattern formation such as during somitogenesis) and

outside the lymphocyte compartment. Nonetheless, Notch signaling is also of key importance in the development of T cells as well as in the development of marginal zone (MZ) B cells (Tanigaki et al., 2002).
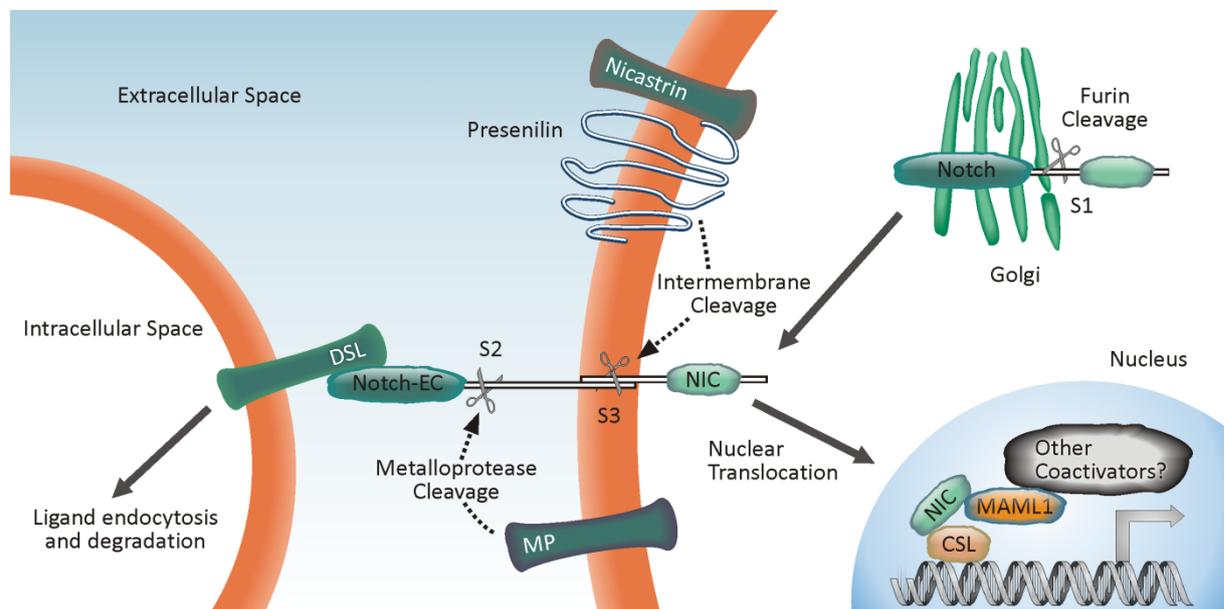
Fig. 1.1 Notch maturation and signaling cascade.
In its lifetime Notch undergoes three cleavage events: cleavage at S1 during transit to the cell surface in the Golgi apparatus by a furin-like protease after which it functions as a transmembrane receptor. Upon engagement with its membrane-bound ligands of the family of DSL proteins Notch undergoes cleavage at S2 extracellularly by a metalloprotease and S3 within the membrane by a presenilin-dependent γ secretase. NotchIC then translocates to the nucleus transforming the transcriptional repressor CSL into a transcriptional activator by recruiting MAML1 and possibly other co-activators leading to expression of Notch-responsive genes. CSL, human C protein binding factor1/Suppressor of Hairless/Lag1; DSL, Delta/Serrate/Lag2 proteins; MAML1, mastermind-like 1; MP, metalloprotease; NotchEC, Notch extracellular portion; NotchIC, Notch intracellular portion; S, site. (adapted from (Nam et al., 2002; von Boehmer, 2005)

1.3   T-cell development

Like all cells of the adaptive immune system T cells are derived from the common lymphoid progenitor (CLP) in the bone marrow, but they undergo their final developmental stages in the thymus. Each compartment gives important developmental cues: for example both B and T cells in the bone marrow depend on interleukin7 receptor (IL7R) signaling. Mice deficient for this non-redundant cytokine or its receptor display lymphopenia of both the B- and T- cell lineage (Peschon et al., 1994; von Freeden-Jeffry et al., 1995; Rich, 1997). Afterwards, the lobules of the thymus with their different compartments (i.e. the cortex and the medulla) provide the appropriate environment for the T-cell progenitors to develop into mature T cells.

T-cell progenitors still do not bear any of the distinct lineage markers of T cells, namely the T-cell receptor (TCR) complex, with the co-receptors CD4 and CD8. With reference to the CD4/CD8

status the progenitors are termed double negative (DN). They develop through distinct DN phases (DN 1-4), characterized by consecutive rearrangement of the Variable (V), Diverse (D), and Joining (J) gene segments of the TCR and change in surface marker expression of CD25 and CD44 (D'Acquisto et al., 2011) to finally becoming double-positive (DP) for CD4 as well as CD8. At this stage T-cell precursors stop proliferating and finally an α:β TCR-CD3 complex is presented at the cell surface and the cells are able to undergo positive selection (in the medullary areas of the thymus) and subsequently negative selection (in the cortical areas of the thymus). Only 2-4 % of T cells will successfully accomplish the process of selection and then migrate into the periphery as naïve single-positive T cells (CD4^{pos} or CD8^{pos}), i.e. functional T helper or cytotoxic T cells, respectively, that can further develop into effector T cells upon antigen encounter. CD4^{pos} T cells can further differentiate into Th(helper)1 and Th2 cells. These distinct cell types are characterized e.g. the type of cytokines the respective cell produces and whether it rather promotes humoral or cellular immune responses.

There are two other distinct groups of DN cells that already acquire their effector potential in the thymus before their emigration to the periphery: natural killer (NK) T cells and T cells that belong to the γ:δ lineage (as opposed to the α:β lineage).

NK T cells are a small group of T cells (0.01 %–1 % of CD3^{pos} lymphocytes in humans) expressing the surface marker NK1.1 and in contrast to conventional T cells they respond to CD1d-restricted lipid ligands (Juno et al., 2012). The various functions of NK T cells are mediated mainly by a rapid release of large amounts of cytokines, including IL4 and IFNγ (Oki et al., 2004).

γ:δ T cells, like NK T cells, are a quite small group of T cells. They diverge from α:β T cells at the DN2/DN3 stage (D'Acquisto et al., 2011). In humans and mice, the vast majority of T cells (>90 %) in peripheral blood and conventional lymphoid organs express the α:β-TCR and only a minority (<10 %) express the γ:δ- TCR (Haas et al., 1993).

Interestingly, another T-cell population called T regulatory cells (T$_{regs}$) is able to prohibit the developmental step from naïve CD8^{pos} T cells into effector T cells in the periphery (McNally et al., 2011). T$_{regs}$ themselves develop from the late DP stage (i.e. from α:β TCR-positive cells) (Fontenot et al., 2005) in the thymus and are characterized by the expression of transcription factor Foxp3 (Forkhead box P3), and the surface markers CD4 and CD25. The expression and activity of Foxp3 is essential to the development of this cell population which in some instances can also be induced in the periphery upon antigenic stimulation in the presence of transforming growth factor-β (TGFβ) (Chen et al., 2003; Apostolou et al., 2004; Coombes et al., 2007), IL2 (Laurence et al., 2007) and retinoic acid (Benson et al., 2007; Mucida et al., 2007; Sun et al., 2007). However, it is still a topic of debate whether these so-called induced T$_{regs}$ (iT$_{regs}$) are functionally stable in vivo (Floess et al., 2007).

Natural T$_{reg}$ from the thymus play a role critical for the maintenance of peripheral immunological tolerance (Dejaco et al., 2006), thereby suppressing autoimmunity, inflammatory bowel disease and allergies. T$_{reg}$ are of quintessential importance to keep self-reactive cells under control. However, this property seems to be mostly detrimental with regard to the role of T$_{reg}$ in cancer, where they are suspected to dampen adaptive and innate immune responses leading to anti-tumor cytotoxicity (Wang et al., 2011). Nonetheless, it is not yet clarified whether their presence in tumors is really causal or rather correlative and it is now thought that the role of T$_{reg}$ might be much more versatile and strongly context-dependent (deLeeuw et al., 2012; Savage et al., 2012).

1.3.1   Notch in T-cell development

With regard to hematopoiesis Notch signaling is best studied in T-cell lymphopoiesis. It is instructive for T-cell development as such and it remains important throughout T-cell development and differentiation. Notch1 expression in early lymphopoiesis influences B- versus T-cell lineage determination and constitutive Notch signaling in the very early pro-B-cell stage leads to formation of an aberrant T-cell population in the bone marrow while blocking B2 B-cell development (Pui et al., 1999; Hampel et al., 2011). In the thymus, T cells express the Notch1 receptor and cells of the thymic stroma express the Notch-ligand Dll4. Genetic inactivation of *notch1* (Radtke et al., 1999; Wilson et al., 2001) or of *dll4* on thymic stroma cells (Koch et al., 2008) leads to a complete block in T-cell development. Moreover, interference with Notch signaling such as through a dominant negative form of MAML1 results in a similar phenotype (Maillard et al., 2004).

In later developmental stages Notch signaling is thought to play a role in the α:β versus γ:δ T-cell lineage choice (Wolfer et al., 2002) and seems to be important for the development of IL17-producing γ:δ T cells (Shibata et al., 2011). Expression of active Notch3 in T cells and transgenic expression of Jagged1 by B lymphocytes significantly increases the pool of T$_{reg}$ (Vigouroux et al., 2003; Anastasi et al., 2003). Notch has also repeatedly been discussed to be involved in differentiation of Th1 cells, Th2 cells, or both. However, to date the issue remains unresolved. (Minter et al., 2005; Tu et al., 2005; Sun et al., 2008; Ong et al., 2008; Amsen et al., 2009).

1.4   B-cell development

Under many aspects B-cell development parallels T-cell development. B cells also rely on the surrounding stroma in the bone marrow for developmental cues, both through cell-cell contact as well as through secreted growth factors (Nagasawa, 2006). The developmental process of B

cells resembles that of T cells with regard to successively rearranging V(D)J-gene segments in a gradual and coordinated fashion, testing whether the rearrangement was successful, which finally results in the formation of a heterodimeric, disulfide bridge-linked antigen-receptor. Also, like in T cells, these stages are marked by characteristic expression of certain surface molecules and intracellular proteins. Striking differences in development are however that B cells are continually produced over the lifetime of the individual in the bone marrow (Nunez et al., 1996), whereas development of T cells occurs in the thymus and slows down with the thymus eventually undergoing involution during puberty.

One of the very first decisive factors for the commitment of an uncommitted progenitor cell towards the B-cell as opposed to T-cell lineage and further maturation of the B cell is the transcription factor Pax5 (paired box 5). Pax5 encodes the B-cell lineage specific activator protein (BSAP) (Rolink et al., 1999; Nutt et al., 1999). From the early pro-B-cell phase the germline conformation of the heavy chain IgH-locus with its V(D)J segments is rearranged, through action of RAG-1 and RAG-2 (Recombination Activating proteins) (Oettinger, 1996) resulting in a pre-B-cell-receptor at the large pre-B-cell stage. Only if the rearrangement of the heavy chain was successful subsequent rearrangement first of the light κ- and then λ-chain gene locus in the now committed B cell is initiated. Upon successful completion of this process IgM is expressed on the surface of the immature B cell. Only B cells expressing a non-self-reacting B-cell receptor (BCR) can further differentiate. B cells expressing a self-reactive BCR have been observed to re-induce RAG expression and to subsequently undergo additional Ig-gene rearrangements. These usually occur at the light chain locus in response to encountering self-antigens in the bone marrow (Gay et al., 1993; Tiegs et al., 1993). This mechanism has been termed receptor editing and if cells fail to undergo it successfully development of the respective cell is arrested and the cell dies by apoptosis, which has been termed clonal deletion (Nemazee et al., 1989; Hartley et al., 1993). Therefore, at the end of the development in the murine bone marrow only 10-20 % of the $\sim2\times10^7$ IgM^{pos} immature B cells that are produced daily leave the bone marrow as transitional B cells (Osmond, 1991), enter the blood stream and initially home to the spleen (Osmond, 1986; Allman et al., 1993; Rolink et al., 1998).

Via different transitional stages (termed T1-3) these B cells mature into naïve follicular B cells (Fo B cells) and into MZ B cells in the spleen (Loder et al., 1999; Su et al., 2002; Chung et al., 2003; Pillai et al., 2009). With 75 % of all mature B cells Fo B cells represent the largest group. They express high levels of surface IgD and CD23. As their name suggests, they are rather found in the follicular areas in the white pulp of the spleen and lymph nodes, but they have the ability to recirculate, entering and exiting follicular niches in secondary lymphoid organs until they encounter antigen (Hardy et al., 1983; Waldschmidt et al., 1988). With only 5 % of total splenic B

cells MZ B cells represent the smaller group of mature B cells. In mice they are exclusively found and defined by their anatomical niche in the marginal zone at the rim of splenic follicles, separating the red from the white pulp in the spleen. Unlike Fo B cells they are sessile in this location adjacent to MZ macrophages, reticular fibroblasts and metallophilic macrophages that reside at the inner border of the marginal sinus through which the blood enters the organ. This architectural setup accounts for the fact that the spleen is the largest filter of blood in the body. The MZ therefore presents a highly effective line of defense against blood-borne bacteria (Tanigaki et al., 2002): the macrophages are extremely potent phagocytic and apt for the uptake and clearance of even large foreign particles, such as bacteria and also effete red blood cells. Thereby produced antigenic fragments are taken up by dendritic cells which relay them to the T cells in the PALS (periarteriolar lymphoid sheath). The MZ B cells ($CD1d^{pos}CD9^{pos}CD21^{hi}CD23^{low}$/$IgD^{low}IgM^{hi}B220^{low}S1P1^{hi}S1PR3^{hi}$; sphingosine 1-phosphate receptor 3) are in a pre-activated state (indicated also by higher levels of CD80 and CD86) which allows them to rapidly respond to antigen contact. Not only do they become potent antigen-presenting cells (APCs) after brief antigenic stimulation but they have been shown to be superior activators of naïve $CD4^{pos}$ T cells over Fo B cells both in vivo and in vitro (Oliver et al., 1999; Attanavanich et al., 2004). Moreover, they differentiate quicker into plasma cells upon T-cell-independent (TI) stimuli such as bacterial lipolysaccharide (LPS) (Oliver et al., 1999). Furthermore, our group could demonstrate that they display enhanced proliferation after stimulation, and have an inherent increased basal signaling activity of Akt, extracellular signal-regulated kinase (ERK) and c-Jun N-terminal kinase (JNK) (Hampel et al., 2011).

Localization of the MZ B cells is thought to be managed majorly by expression of S1PR1, but not S1PR3 (Cinamon et al., 2004). However, S1PR3 expression by the endothelial cells lining the MZ is vital for proper establishment of the zone (Girkontaite et al., 2004). For Fo B cells expression of the chemokine receptor CXCR5 is key to access the lymphoid follicles (Forster et al., 1996), as the chemokine ligand CXCL13 is expressed along the dense follicular dendritic cell (Fo DC) network.

In mice there is another subset of mature B cells beside the B2 cell populations (Fo and MZ B cells). These are so called B1 B cells. This self-renewing B cell subset is found mainly in peritoneal and pleural cavities and unlike B2 cells they are not derived postnatally from the bone marrow, but the fetal liver. They share certain characteristics with MZ B cells with regard to their longevity and pre-activated status and high expression of CD9, which is not found on unstimulated Fo B cells (Miller et al., 1975; Won et al., 2002). Furthermore, they respond similarly to common bacterial antigens through their intrinsic ability to differentiate into antibody secreting cells if their Toll-like receptors (TLR) are stimulated by appropriate ligands (Genestier et al., 2007). Therefore, both MZ B cells and B1 B cells have been referred to as "innate B cells".

1.4.1 Notch in B-cell development

Lineage decision between a Fo and MZ B-cell fate is affected by several factors: e.g. BCR-signaling strength (Martin et al., 2000; Girkontaite et al., 2001; Cariappa et al., 2001) and also Notch signaling (Tanigaki et al., 2002; Kuroda et al., 2003). While there is strong evidence that strong BCR signaling rather drives the B cells into adopting a Fo B-cell fate, strong Notch signaling is instructive for B cells to adopt a MZ B-cell fate.

While Dll4, but not Dll1 is quintessential for T-cell development (Koch et al., 2008), Dll1-Notch2 interaction in fact is crucial for proper MZ B-cell development as was evidenced by studies in mice deficient for either one of the interaction partners (Saito et al., 2003; Hozumi et al., 2004). These findings are further supported by studies showing that MZ B-cell generation is similarly affected if a player of the Notch-signaling pathway is affected; such as MAML1 (Oyama et al., 2007; Wu et al., 2007). Dosage of Notch pathway players such as MAML1 in fact correlates with MZ B-cell number (Wu et al., 2007). Furthermore, deletion of negative regulators of Notch and constitutive action of Notch2 led to an increase in the MZ B-cell compartment in the analyzed mice (Kuroda et al., 2003; Hampel et al., 2011).

1.5 The CD40 receptor

The CD40 receptor is involved in T-cell-dependent (TD) activation of B cells. It is like Notch and its ligands a type I single pass transmembrane glycoprotein and belongs to the superfamily of tumor necrosis factor receptors (TNFRs). CD40 is mainly expressed on B cells, DCs and macrophages. Additionally, various levels of CD40 were described on a multitude of different cells such as epithelial cells, monocytes, basophils, eosinophils, T cells and neurons (Banchereau et al., 1994).

The natural ligand of CD40 is CD154 (CD40L), a type II transmembrane molecule that also belongs to the TNF family. Expression has like its receptor CD40 been noted on a variety of different cell types, but is majorly found on activated T cells. Ligand-receptor interaction leads to the clustering of CD40 from monomers into trimeric complexes and subsequent relocation into lipid rafts initiating CD40 signal transduction. Since the CD40 molecule itself lacks enzymatic activity it relies on signaling via its intracellular carboxy-terminal domain via the assembly of adaptor proteins, i.e. TNFR-associated factors (TRAFs) along the cytoplasmatic tail of the receptor. These TRAFs, namely TRAF1, -2, -3, -5 and -6 mediate all downstream effects of active CD40 (Fig. 1.2), resulting in the activation of a variety of kinases including p38, ERK and JNK, PI3K and PLCγ2 (phosphoinositol-3-kinase; phospholipase C-γ2) and the Src family kinases Syk, Lyn and Fyn. CD40-signaling leads to the activation of numerous transcription factors such as members of the

canonical as well as non-canonical NF-κB (nuclear factor κB) family and STAT3 (signal transducer and activator of transcription) (Hanissian et al., 1997). Engagement of the CD40 receptor in in vitro experiments showed that B cells display better survival and proliferation and that they up-regulate numerous activation markers, including CD23, CD80, CD86, CD95 (Fas) and ICAM1 (intercellular adhesion molecule 1). Notably, CD40 activation also triggers production and release of various cyto- and chemokines, including IL1, IL2, IL7, IL10, IL12, IL15, IL17, LTα, which play a role in regulating CD40 function in immunity since these are involved in regulating processes such as Ig-isotype switching and antigen presentation. Its role in immunity has also been highlighted in male individuals carrying CD154-mutations leading to the immunodeficiency X-linked Hyper IgM (HIGM) syndrome, which is characterized by normal to elevated IgM levels, a deficiency in IgG, IgE and IgA antibodies and a reduction of memory B cells, while overall B-cell numbers remain normal. This is recapitulated in CD40- (Kawabe et al., 1994) and CD154-KO mice (Renshaw et al., 1994). As observed for HIGM patients no IgG, IgA, and IgE responses to TD antigens could be mounted by the B cells in these mice and germinal center (GC) formation is severely affected, while the TI response was largely unaffected.

Hence, proper CD40 signaling is of utmost importance in many different processes most notably in B-cell signaling notably in TD-immune responses leading to formation of B-cell memory through the GC-reaction.
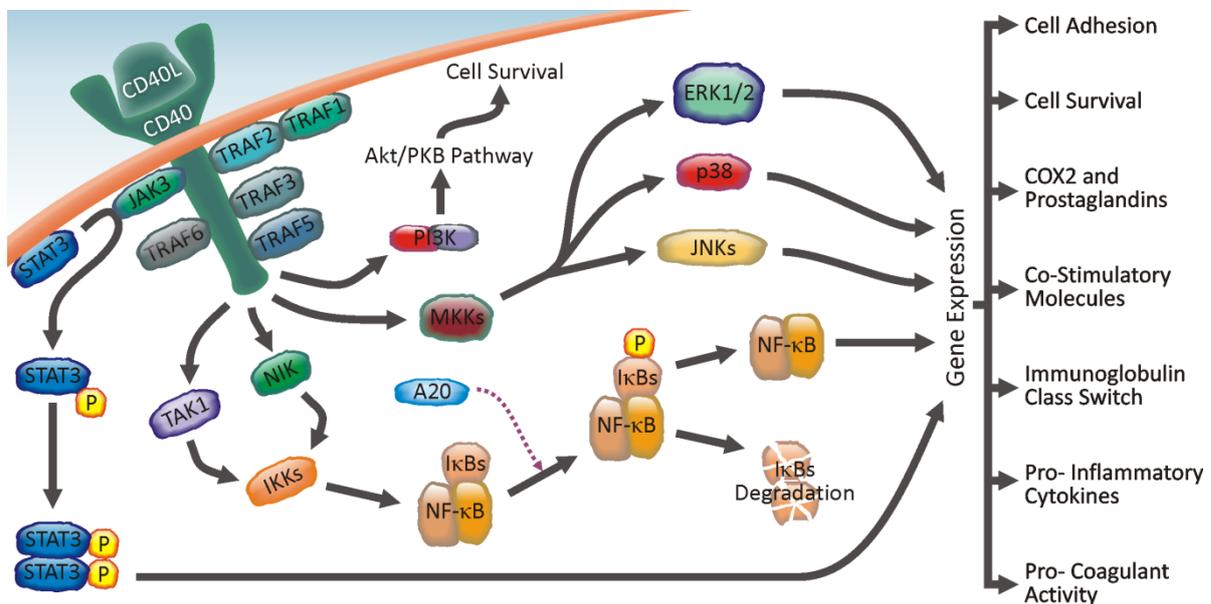
Fig. 1.2 Overview of CD40 activation and impact on signaling pathways.
Upon engagement of CD40 with CD40L and trimerization of the receptor (not shown) signaling is mediated via CD40's intracellular carboxy-terminal domain and the assembly of TRAF adaptor proteins along the cytoplasmatic tail of the receptor. TRAF1, 2, 3, 5 and 6 mediate all downstream effects of active CD40. CD40L: CD154; ERK, extracellular signal-regulated kinase; IKK, IκB kinase; JNK, c-Jun N-terminal kinase; MKK, Mitogen-activated protein kinase kinase; NF-κB, nuclear factor κB family; NIK, NF-κB-inducing kinase;STAT, signal transducer and activator of transcription; TAK1, transforming growth factor-b (TGF-b)-activated kinase 1; TRAF, Tumor necrosis factor receptor (TNFR)-associated factor

1.6   T-cell dependent and T-cell independent immune response

While T cells recognize their cognate antigen mainly in processed form presented on MHCs, B cells are able to directly bind soluble antigen in blood and lymph. Depending on the type of antigen presented the naïve B cell elicits a TD- or TI immune response.

TI antigens can activate B cells without help from a T helper cell (TI response). The TI immune response is fast and yields B-cell antibodies that have low affinity and are often polyreactive. The TI immune response does not lead to generating immunological memory.

TD antigens however, can elicit a much more refined immune response in B cells. When crosslinking the BCR, the TD-antigen is internalized by receptor-mediated endocytosis, intracellularly processed and loaded onto MHCII molecules which are brought to the cell surface. The production of MHCII is up-regulated simultaneously along with other activation molecules, i.e. ICAM and co-stimulatory molecules B7.1 and B7.2 (CD80 and CD86, respectively). In contrast to macrophages and DCs, this process is initiated already at very low antigen concentrations in B cells. These TD antigens are thereby presented to T helper (i.e. CD4^{pos}) cells. In case the T helper cell is specific for the same antigen it is activated by engagement of its TCR binding to the MHCII/peptide-complex and CD28 to the B cell's B7 surface molecules and thereby activate the peptide-presenting B cell.

This T-cell mediated B-cell activation is further based on two components: secreted cytokines and cell-cell contact mediated signals, such as IL4-stimulation and CD40L-CD40-ligation, respectively. Receiving the aforementioned signals the B cell then enters mitosis and can initiate isotype switching to IgG, IgA and IgE. Proliferating B cells are able to form either extra-follicular foci or to migrate to primary lymphoid follicles ultimately forming a GC. In extra-follicular foci, mainly short-lived plasma cells producing low-affinity antibodies are found and the foci quickly involute after some days (Ho et al., 1986; Smith et al., 1996). On the other hand GCs represent sites in secondary lymphoid organs where activated B cells commence to highly proliferate at first. Afterwards they undergo a number of further, crucial genetic modifications in the Ig genes leading to diversification and the refinement of the BCR, while migrating through distinct compartments (dark and light zones) of the GC. These modifications include somatic hypermutation, which alters the V regions of BCR, affinity maturation, which selects for survival of B cells with high affinity for the antigen, and isotype switching. Eventually the positively selected B cells differentiate either into long-lived plasma or memory B cells (McHeyzer-Williams et al., 1999). The latter can be rapidly reactivated upon contact with the same antigen, conferring quick and highly effective protection against previously encountered pathogens.

1.7   CD40 and Notch signal deregulation in human malignancies

Both CD40 and Notch signaling molecules have been implicated in the development of many human malignancies, both within and apart from the lymphocyte context. Given that CD40 as well as Notch can induce a variety of signaling cascades in the cell it is not surprising that the results of deregulated signaling can be quite disparate.

1.7.1   Notch signaling in cancer

At multiple stages during development Notch signaling is involved in maintaining the balance between cell proliferation, differentiation and apoptosis. Therefore it is plausible that disrupting this balance by Notch deregulation can have both tumorigenic as well as anti-proliferative effects and the ultimate outcome is context-dependent. Anti-tumorigenic effects of Notch signaling have been observed in human hepatocellular and small lung carcinoma for example. In in vitro cultures of human esophageal cells a Notch3-mediated program has been shown to induce squamous differentiation and to counter-regulate invasive growth (Ohashi et al., 2011). Suppressing Notch1 signaling in murine keratinocytes undercuts the Notch-induced expression of *p21* that usually leads to cell cycle withdrawal and terminal differentiation (Rangarajan et al., 2001). Moreover, it abrogates Notch activation of caspase3 which as well leads to the terminal differentiation of the cells (Okuyama et al., 2004). Epidermal deletion of the *notch1* gene leads to extensive epidermal hyperplasia and the *notch1* conditional knock-out mice spontaneously develop cutaneous basal cell carcinoma (Nicolas et al., 2003). These experiments showed a role for Notch1 in the murine skin as a tumor suppressor.

Nonetheless, most studies were able to show the tumor promoting effects of aberrant Notch signaling due to up-regulation of the receptor and/or its ligands, such as in colon, head and neck carcinoma and renal carcinoma and pancreatic cancer. High expression levels of Notch1 and Jagged1 in patients with breast, bladder and prostate cancer are correlated with a poor prognosis (Santagata et al., 2004; Reedijk et al., 2005; Reedijk et al., 2008; Shi et al., 2008). This underscores the effect Notch has by activating expression of its responder genes as well as its cross-talk with other pathways, such as sonic hedgehog (SHH) and Wnt signaling, EGF- and platelet-derived growth factor- (PDGF) signaling. Cross-talk with other pathways such as TGFβ and SMAD signaling is important during epithelial mesenchymal transition (EMT) - a central process in carcinoma progression in which Notch was found to be an inducing key player (Zavadil et al., 2004; Wang et al., 2010; Matsuno et al., 2012).

The first connection between Notch dysregulation and cancer was made in 1991 by Ellisen and colleagues showing that the human homologue TAN1 of the Drosophila's Notch gene was

disrupted in patients suffering from T-cell lymphoblastic leukemia (Ellisen et al., 1991). Since then the extensive involvement of Notch especially with regard to the development of T-cell malignancies has been progressively elucidated. However, considering direct effects on B-cell tumorigenesis the role of Notch is somewhat unclear. Like for other cell types the up-regulation of the receptor and/or its ligands was also found in the B-lymphocyte compartment, such as in Hodgkin Lymphoma (HL). It is under discussion whether HL could be distinguished from Non-HL on the basis of a Notch-associated gene expression profile (Kochert et al., 2011). In B-cell chronic lymphocytic leukemia (B-CLL) the oncogenic effects of Notch were found to be due to its capacity to up-regulate CD23 expression (Hubmann et al., 2002), while Lee and colleagues could identify gain of function mutations in the PEST domain – usually ubiquitinated before Notch degradation in the proteasome- in Diffuse Large B-cell lymphoma (DLBCL) samples (Lee et al., 2009). Consistent with the role of Notch in developmental decision of the B-cell lineage in the periphery (i.e. its capacity to push B cells towards a MZ B-cell fate) Notch2 and other molecules involved in the Notch signaling pathway were recently found to be the most frequent lesions in splenic marginal zone lymphoma (SMZL) as determined by whole-exome and –genome sequencing and copy-number analysis (Rossi et al., 2012; Kiel et al., 2012). The concomitant presence of viruses within the B cells such as Kaposi's sarcoma herpes virus (KSHV) and Epstein-Barr Virus (EBV) (Hsieh et al., 1997) also seems to support the oncogenic capacities of Notch in the B cell (He et al., 2009) as shown in primary effusion lymphoma (PEL) (Lan et al., 2009; Lan et al., 2007) and Burkitt lymphoma (BL) (He et al., 2009).

Nonetheless, the role of Notch in B cells remains controversial: while on the one hand synergistic effects of Notch with BCR and CD40 signaling have been shown in the promotion of proliferation (Thomas et al., 2007; He et al., 2009), Notch has also demonstrated to induce apoptosis and cell cycle arrest at both immature and mature developmental stages (Morimura et al., 2000; Romer et al., 2003; Kohlhof et al., 2009) as well as in B-cell malignancies (Zweidler-McKay et al., 2005).

1.7.2   CD40 signaling in cancer

CD40 signaling has been shown to play a role in multiple myeloma, both B-CLL and B-ALL (B-cell acute lymphocytic leukemia), MALT (low-grade mucosal-associated lymphoid tissue) lymphoma, BL and HL. The background for this effect becomes evident when looking at the effects that active CD40 signaling has on the cell. CD40 can promote cell growth and inhibit the induction of apoptosis, since it increases the level of anti-apoptotic proteins of the Bcl-family of proteins, protecting the cell from TRAIL- (TNF-related apoptosis-inducing ligand) and Fas-induced apoptosis (Benson et al., 2006; Travert et al., 2008). The ability of CD40 to induce IL6 production

for example has a stimulatory effect on tumor cell types such as multiple myeloma, in which IL6 is a key feature (Urashima et al., 1995). In melanoma, CD40 leads to self-stimulation through the up-regulation of its ligand CD154 (van den Oord et al., 1996). On the other hand down-regulation of CD154 on T cells results in decreased activation of the T lymphocytes in colon and pancreatic carcinoma cell lines and growth of the tumor cells (Batrla et al., 2002). Indirectly, CD40 can have a positive effect on tumor growth by inducing and supporting neo-vascularization of the tumor by relaying strong angiogenic signals (Melter et al., 2000; Chiodoni et al., 2006).

On the other hand CD40 also supplies anti-tumorigenic signals, this has been shown primarily in solid tumors but it also holds true for some lymphomas. For example, anti-CD40 treatment in B-cell lymphomas can have growth inhibiting effects in vitro and in vivo after transfer into SCID (Severe Combined Immunodeficiency) mice (Funakoshi et al., 1994). Moreover, CD40 on B cells promotes the stimulation of other APCs, in fact turns the tumor cells themselves into potent APCs leading to the attraction of cytotoxic T cells in turn leading to eradication of the tumor cell. Therefore, whether engagement of CD40 has tumorigenic or anti-tumorigenic effects depends largely on cell type, experimental conditions (in vitro, in or ex vivo) and type of stimulus used (soluble versus membrane-bound CD154).

1.8 B-cell lymphoma

As described in the previous sections both CD40 and Notch play a role in diseases of the lymphatic system and therefore also in the B-cell compartment. B-cell lymphomas comprise both HL and non-HL, the latter of which represent the majority of cases. HL can then be differentiated into two larger groups: classical HL (cHL; 95 % of cases) and nodular lymphocyte predominant HL (NLPHL; 5 % of cases). Of the non-HL, DLBCL, MALT and Follicular lymphoma (FL) are the most common types, while primary effusion lymphoma (PEL) and Burkitt lymphoma (BL) are more rare (however with endemic differences).

Most B-cell lymphoma develop upon recombination processes in B cells. This can happen during the maturation of a B cell and its BCR at two distinct time points: A) during development in the bone marrow and B) during the GC reaction, i.e. somatic hypermutation and class switch recombination. HL, like FL, marginal zone B-cell lymphoma (MZBL) and DLBL display a clear post-GC phenotype, as indicated by the Ig-configuration of the B cell that has undergone somatic hypermutation (Kanzler et al., 1996; Lossos et al., 2003). These mutations are usually unfavorable and would force the B cells to undergo apoptosis, but due to simultaneously occurring genetic lesions in genes such as p53, c-myc etc. these cells rather receive growth promoting cues (Lossos et al., 2003).

As with most GC lymphomas the neoplastic follicles do not only comprise the malignant cells themselves but also increased numbers of non-neoplastic, but highly reactive cells such as myeloid cells, DCs, macrophages and T cells. This is probably most pronounced in cHL. This type of lymphoma can be particularly characterized by the fact that the actual tumor cells, the so-called Hodgkin-Reed-Sternberg (HRS) cells, only constitute roughly 0.1 - 10 % of the tumor mass (Kuppers, 2009). The rest of the cells in the mass consists of infiltrates of reactive cells with varying composition according to which the type of HL can be further classified. Members of the innate immune system are key constituents of the HL tumor microenvironment. Their abundant cytokine production adds significantly to maintaining the inflammatory background in cHL (Aldinucci et al., 2010). However, of course, these cellular infiltrates cannot only be found in HL but in various tumors not only of the lymphatic system. Therefore, a short excursus will be made at this point to illustrate the physiological role of these innate immune cells.

1.8.1   Innate immune cells

The innate immune system is in its cellular part represented by granulocytes, monocytes and macrophages. These are myeloid cells derived from common myeloid progenitor cells (CMPs) in the bone marrow.

The first cell type a pathogen is likely to encounter in solid tissues is macrophages. While for long having been regarded to be inflammation mediators and phagocytes only, their role seems to be more refined with regard to the effect they have on T cells and the extracellular matrix (Mosser, 2003). Therefore, macrophages are now usually divided into type 1- and type 2-activated macrophages, which refers to the way in which the macrophage ultimately serves as an effector cell in type 1 or type 2 T helper cell immune responses elicited by IFN-γ or IL4 (Ding et al., 1988; Stein et al., 1992; Mantovani et al., 2004). Activated macrophages secrete a range of cytokines having both local and systemic effects; such as IL8 for example which leads to the recruitment of neutrophil granulocytes to the site of infection (Mosser et al., 2008; Cailhier et al., 2006). Neutrophils are then the first cells to arrive in large numbers at the site of inflammation. They limit the expansion and spread of pathogens directly at the site by phagocytosis, release of anti-microbial peptides and pro-inflammatory cytokines (Cassatella, 1999; Denkers et al., 2003). Neutrophils further attract and activate other effector cells such as monocytes and DCs by the secretion of chemokines, which ultimately aids in mounting an adaptive immune response. DCs are further cellular representatives of the innate immune system. They are the most potent and therefore major APCs. The DCs key role is T-cell activation, providing a highly critical link to the adaptive immune system (Clark et al., 2000).

Furthermore, there are cells derived from the CLP, which unlike B- and T-lymphocytes, lack antigen specificity and form part of the innate immunity such as NK cells. NK cells develop in the bone marrow and are activated in response to cytokines and interferons secreted by macrophages and like cytotoxic T cells they release granules onto the surface of the respective target cell leading to its demise (Gapin et al., 2001).

Looking only at these few cell types one can already fathom that cytokines and chemokines play a key role both in the initiation and amplification of the inflammatory response, as well as in the orchestration of the different cell types involved and finally in the initiation of the adaptive immune response. And this gives an impression that deregulation of these mechanisms can have quite detrimental effects for the individual such as seen not only in allergies but of course also in cancer.

1.9   Rationale for studying deregulated CD40- and deregulated Notch2IC signaling

In a number of lymphomas (i.e. HRS cells in cHL) the tumorigenic cells display an up-regulation of both CD40 and Notch. In fact Notch1 is thought to be one of the key players during malignant re-programming of the cells (Jundt et al., 2008). CD40 has been shown to be strongly expressed in the cytoplasmatic and membrane sections in samples of HL patients and is now accepted as a hallmark of the disease (Aldinucci et al., 2010). Moreover, T cells in the neoplastic follicles express high amounts of CD40L (Carbone et al., 1995).

Furthermore, HRS-cells in 40 % of all cHL cases are positive for EBV-infection. Interestingly, in EBV-infection the virus hijacks the cellular machinery to express viral genes that are functional mimics of cellular proteins. Latent membrane protein 1 (LMP1), is a functional homologue of CD40, whereas EBV nuclear antigen 2 (EBNA2) mimics a Notch receptor and LMP2A a BCR signal. All of these viral proteins target the same pathways as their cellular counterparts yet with the key difference that they are constitutively active forms. LMP1 is critical for B-cell transformation, a quality that has first been discovered in rodent fibroblasts. With regard to EBNA2 and Notch Hella Kohlhof from our group was able to show that although EBNA2 and Notch interact with RBP-J resulting in the activation of target genes their respective function has still differential outcomes (Kohlhof et al., 2009). While Notch-IC like EBNA2 is able to bring quiescent B cells to actively cycle again, an mRNA-screen revealed that it also up-regulates genes related to apoptosis. EBNA2 mimics this physiological function, yet simultaneously leads to the up-regulation of anti-apoptotic genes. In case Notch signaling is active, LMP1- or constitutively active CD40-signaling could provide anti-apoptotic signals leading to onset of tumorigenesis. And indeed, Thomas and

colleagues were able to show that Notch and CD40 together with BCR-signaling in vivo lead to an enhancement of B-cell activation, also leading to an increase in proliferation of the B cells (Thomas et al., 2007), which is a necessary prerequisite for lymphoma. To study the immediate effects of deregulated CD40- and Notch2IC- signaling in an in vivo situation also with regard to lymphomagenesis was the aim of this project at hand.

1.10 The LMP1/CD40 and Notch2IC transgenic mouse strains

In order to examine deregulated signaling of the Notch receptor as well as the CD40-receptor two conditional mouse strains were generated in our lab that allow for tissue- and developmental stage-specific deregulation of the two molecules; the Notch2ICflSTOP and the LMP1/CD40flSTOPP mouse (Homig-Holzel et al., 2008; Hampel et al., 2011).

1.10.1 The LMP1/CD40^{flSTOP} mouse strain (Homig-Holzel et al., 2008)

The LMP1/CD40 molecule represents a fusion protein, consisting of the membrane spanning domain of the viral protein LMP1 and the intracellular part of the cellular CD40 molecule. Thereby, we are able to exploit the ability of the six membrane spanning domain of LMP1 to signal ligand-independently via self-oligomerization. This N-terminal domain that tethers the fusion protein to the cell membrane and leads to its self-aggregation was fused to the C-terminal signaling domains of CD40. Thus, this construct conveys constitutively active CD40 signals to the respective cell in which it is expressed.

The targeting construct was inserted into the Rosa26 locus and is under the control of the endogenous Rosa26 promoter. This locus is ubiquitously expressed and even a complete knock-out of the locus has no deleterious effects on the cell (Zambrowicz et al., 1997; Casola, 2010).

The construct is preceded by a loxP site flanked STOP cassette, which is removed upon Cre-expression leading to the expression of the fusion protein. Hence, crossing the LMP1/CD40flSTOP mice to mice expressing Cre recombinase in a developmental stage- and tissue-specific manner allows for cell type and differentiation stage-specific expression of the transgene.

Overall, in the LMP1/CD40 mouse strain the CD40 signaling is deregulated in the sense of it being constitutively active, yet the signaling pathways that are involved are still physiological CD40 targets. This is important because even though LMP1 is the viral homologue for CD40, there are subtle differences in the regulation of those targets and the effect the expression of LMP1, respectively CD40, has on the cell (Lam et al., 2003; Rastelli et al., 2008).

Crossing these mice to CD19-cre mice leads to expression of the transgene in the CD19-expressing B cells of those mice. Already at 8 weeks these mice display splenomegalies due to increased B- and also T-cell numbers in the spleen (eight and three times, respectively). Moreover the numbers of lymphocytes are as well as thrice as high in the inguinal lymph nodes compared to controls. In line with the effects of CD40 signaling LMP1/CD40-expressing B cells display an activated phenotype with regard to both surface expressed activation markers as well as the activation of intracellular signaling pathways, such as MAP kinase signaling (ERK, JNK). TD-immunization of the LMP1/CD40^{flSTOP}//CD19-cre mice does neither lead to the formation of GCs in those mice, nor to the subsequent production of high-affinity antibodies by plasma cells. B cells of the LMP1/CD40^{flSTOP}//CD19-cre mice do not only show increased survival and diminished apoptosis in vitro but develop lymphomas with a very high incidence from the age of 12 months onward compared to controls. These lymphomas are very diverse with regard to the activation of their signaling pathways. Interestingly, we further found that these aged mice also develop tumors in the lower neck region.

1.10.2 The Notch2IC^{flSTOP} mouse strain (Hampel et al., 2011)

The Notch2IC mouse was also generated in our lab in a similar manner as was the LMP1/CD40 mouse. The murine cDNA coding for the intracellular portion of the Notch receptor was inserted into the Rosa26 locus and also contains a loxP flanked STOP cassette like the LMP1/CD40 mouse strain. Unlike the LMP1/CD40 transgene however, the Notch2IC sequence was moreover preceded by an endogenous ATG-Kozak site (serving as a translational start site) as well as a sequence coding for the CAGGS promoter (Cytomegalovirus early enhancer/chicken β-actin/rabbit globin promoter). This promoter was chosen in order to ensure strong and consistent expression, as has been shown in various cellular systems (Niwa et al., 1991; Daly et al., 1999a; Daly et al., 1999b). Another crucial point of distinction between the Notch2IC and LMP1/CD40 mouse strain is that in the Notch2IC mouse an IRES-hCD2 (internal ribosomal entry site-human CD2) cassette is inserted downstream of the sequence coding for Notch2IC. Thereby, Notch2IC expression in any given cell can be monitored via concomitant surface expression of a truncated form of human CD2.

Crossing the Notch2IC mice to CD19Cre mice led to a shift towards MZ B cells at the expense of Fo B cells in the spleen of the Notch2IC mice compared to controls. These Notch2IC-expressing B cells exhibit MZ B-cell characteristics with regards to their localization, their pre-activated phenotype: i.e. expression of surface markers, activation of Akt, ERK and JNK signaling and

enhanced response to stimulation by LPS and CD40 in vitro. This was found to be true even in the absence of a functional CD19 receptor in those Notch2IC-expressing B cells.

1.10.3 The CD19-cre mouse strain (Rickert et al., 1997)

The CD19-cre mouse strain has been described in 1997 by Rickert and colleagues (Rickert et al., 1997) and it is by now widely used throughout the B-cell research community. CD19 functions as a co-receptor of the B-cell receptor and is expressed from the pro B-cell stage in the bone marrow onward with expression increasing as the B cell matures and migrates to the spleen. Hence, crossbreeding this mouse into the Notch2IC^{flSTOP} and LMP1/CD40^{flSTOP} mouse strains allows for a deletion of the STOP cassette preceding the Notch2IC as well as the LMP1/CD40-transgene from B-cell precursor stages in the bone marrow onwards and allows an easy approach to test the effect of the two transgenes in the B-cell context.

2. AIM

The Notch receptor as well as the CD40 receptor have well established roles in the biology of B lymphocytes. While CD40 is known to be essential to promote class switch in activated B cells, Notch2 plays a crucial role in the development of marginal zone (MZ) B cells. Contribution of constitutive Notch1 signaling in the development of T-cell lymphomas is well established, however the potential role of constitutive Notch signaling in B-cell lymphoma is less elucidated.

Mice expressing either the CD40 or the Notch2 receptor in a constitutively active form and B-cell-specific fashion have previously been established and characterized in our lab (LMP1/CD40//CD19-cre and Notch2IC//CD19-cre; Homig-Holzel et al., 2008; Hampel et al., 2011). Notch2IC//CD19-cre mice show an expansion of MZ B cells at the expense of the follicular (Fo) B cells, while B- and T-cell numbers resemble those of CD19-cre control mice. With age these mice do not develop B-cell lymphomas. The reason for this observation might be that constitutively active Notch2 signaling in B cells although able to induce proliferation, also leads to higher apoptosis rates. This hypothesis was supported by array data from Kohlhof of our group showing that Notch signaling leads to an up-regulation of both cell cycle genes as well as an increase in pro-apoptotic signals in the B cell (Kohlhof et al., 2009).

In LMP1/CD40//CD19-cre mice on the other hand constitutively active CD40 leads to an expansion not only of B-, but also of T cells and LMP1/CD40-expressing B cells display a better survival rate conveyed by the constitutive CD40 signal that delivers anti-apoptotic signals to the B cell. These mice develop B-cell lymphoma with a high incidence from 12 months onward.

From these findings it was hypothesized that Notch signaling in B cells might eventually lead to B-cell lymphoma in combination with anti-apoptotic signals. These signals could be relayed to the B cell by a constitutive CD40 signal.

With the aim to examine this question in vivo and in vitro, LMP1/CD40//CD19-cre and Notch2IC//CD19-cre mice were cross-bred to analyze their offspring for their B-cell phenotype, the developmental fate of the B cells (Fo versus MZ B cell), the proliferation and survival patterns and the potential effects the transgenic B cells have on the T cells and other cell populations. A small test group of Notch2IC//LMP1/CD40//CD19-cre animals will be kept to evaluate whether lymphomagenesis is potentially favored in this genetic background.

Furthermore, in previous experiments ulcerations in the lower neck region of old LMP1/CD40//CD19-cre mice were observed. The potential reason behind this growth shall be examined and aged Notch2IC//LMP1/CD40//CD19-cre should be monitored for the recurrence of these ulcerations.

3. RESULTS

3.1 Concomitant expression of constitutive Notch2IC and LMP1/CD40 in B cells has synergistic effects on increase in spleen size and weight

LMP1/CD40flSTOPP mice and Notch2ICflSTOPP were crossed to CD19-cre mice, which resulted in the deletion of the floxed STOP cassette in the LMP1/CD40^{flSTOP}//CD19-cre and Notch2IC^{flSTOP}//CD19-cre mice. These mouse strains were cross-bred with each other to express both receptors in a B-cell specific fashion yielding offspring with a Notch2IC^{flSTOP}//LMP1CD40^{flSTOP}//CD19-cre genotype. Mice names were hence forth abbreviated to Notch2IC//CD19-cre, LMP1/CD40//CD19-cre and Notch2IC//LMP1/CD40//CD19-cre mice. All three genotypes were analyzed in parallel with a CD19-cre control mouse.

In these mice deletion of the stop cassette by activation of the CD19 promoter and expression of Cre recombinase starts in the phase of early B-cell development in the bone marrow, but progressively continues as mature B cells migrate to and distribute in the spleen. As the spleen represents the largest secondary lymphoid organ, overt effects of transgene-expression in B cells can easily be monitored by changes in size and weight of the organ.

It has been shown before that the spleens of Notch2IC//CD19-cre mice are slightly and spleens of LMP1/CD40//CD19-cre mice are markedly enlarged and the organs are correspondingly heavier than those of aged-matched CD19-cre control mice (Homig-Holzel et al., 2008; Hampel et al., 2011). This is even potentiated when constitutively active CD40 and constitutively active Notch2 are simultaneously expressed in the B cells of Notch2IC//LMP1/CD40//CD19-cre mice. The spleens of these eight to 20 week-old mice are markedly larger than of aged-matched control CD19-cre and Notch2IC//CD19-cre mice (Fig. 3.1A). And they usually present with an even more pronounced splenomegaly than spleens of LMP1/CD40//CD19-cre and are on the average 1.6-fold as heavy as those of LMP1/CD40//CD19-cre mice (Fig. 3.1B).
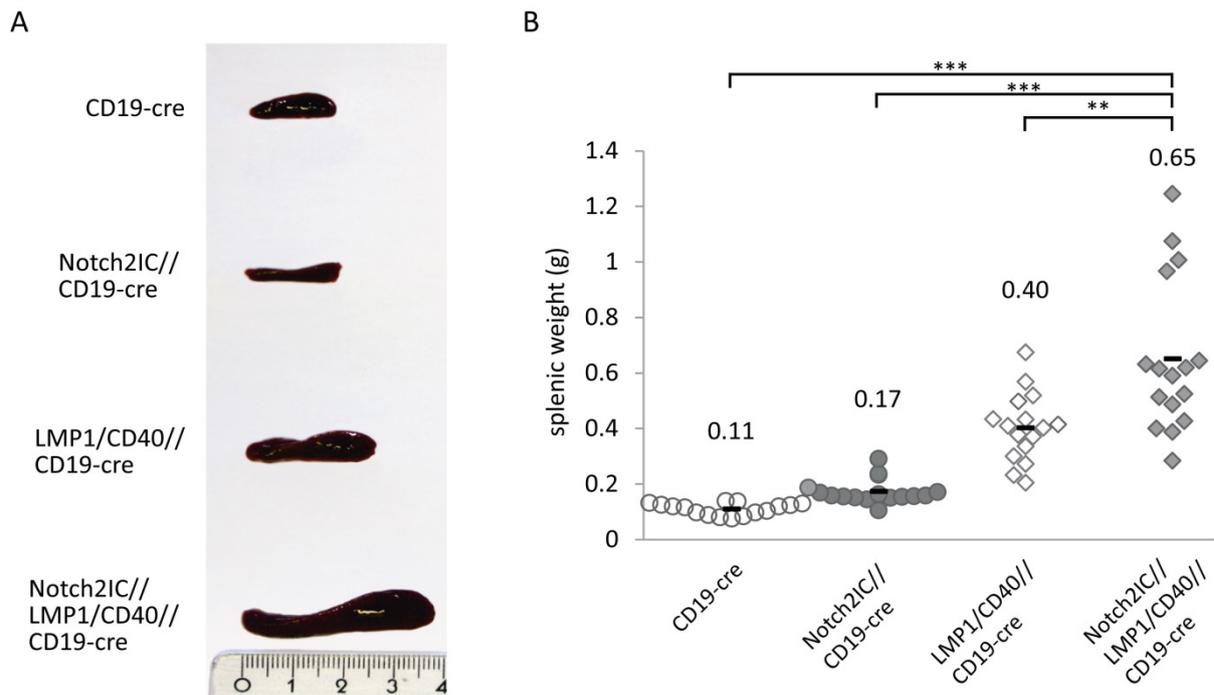
Fig. 3.1 Notch2IC//LMP1/CD40//CD19-cre mice display a splenomegaly and heavier spleens than all control mice.
(A) Spleen size of 10 week-old mice. The ruler indicates the size of the organ in cm. (B) Splenic weight in g. CD19-cre (blank circle), Notch2IC//CD19-cre (filled circle), LMP1/CD40//CD19-cre (blank rhombus), Notch2IC//LMP1/CD40//CD19-cre (filled rhombus). Points represent data from individual mice and horizontal bars mark the mean value indicated in numbers. *p < 0.05, ** p < 0.01, *** p < 0.005.

3.2 Expression of the transgenes Notch2IC and LMP1/CD40 is a B-cell specific event

In order to ensure that there was no leakage of the expression of the two transgenes in any other cell type than in B cells, other cell types including T lymphocytes were analyzed for the presence of the reporter protein hCD2. hCD2 is concomitantly expressed upon the expression of the Notch2IC transgene after deletion of the upstream stop cassette. Flow cytometric analysis (Fluorescence-activated cell sorting, in short FACS) showed that expression of hCD2 could only be detected in splenic B220^{pos} B cells of Notch2IC//CD19-cre and Notch2IC//LMP1/CD40//CD19-cre mice (Fig. 3.2A), but not in B cells of CD19-cre and LMP1/CD40//CD19-cre mice. Furthermore, hCD2 expression was undetectable in CD3^{pos} T cells (Fig. 3.2B) in mice of all genotypes, as well as in any other living cell type present in the spleen (Fig. 3.2C).

The deletion efficiency of the stop cassette upstream of the LMP1/CD40-transgene can be checked indirectly via the highly specific up-regulation of CD95 in B cells of those animals. Therefore, staining cells simultaneously with α-hCD2 and α-CD95 antibodies and performing FACS analysis allows to determine the amount of successful deletion in the B cells of the respective animals with regard to both Notch2IC- as well as LMP1/CD40-expression (Fig. 3.2D).

The results displayed in Fig. 3.2D show that in all three transgene-carrying genotypes (Notch2IC//CD19-cre, LMP1/CD40//CD19-cre and Notch2IC//LMP1/CD40//CD19-cre) the deletion efficiency reached on the average at least 80 % or more according to up-regulation of the respective reporter marker (hCD2 or CD95 or both). In summary, these results show that the stop cassette deletion upstream of the respective transgenes is an unambiguously B-cell-specific event.
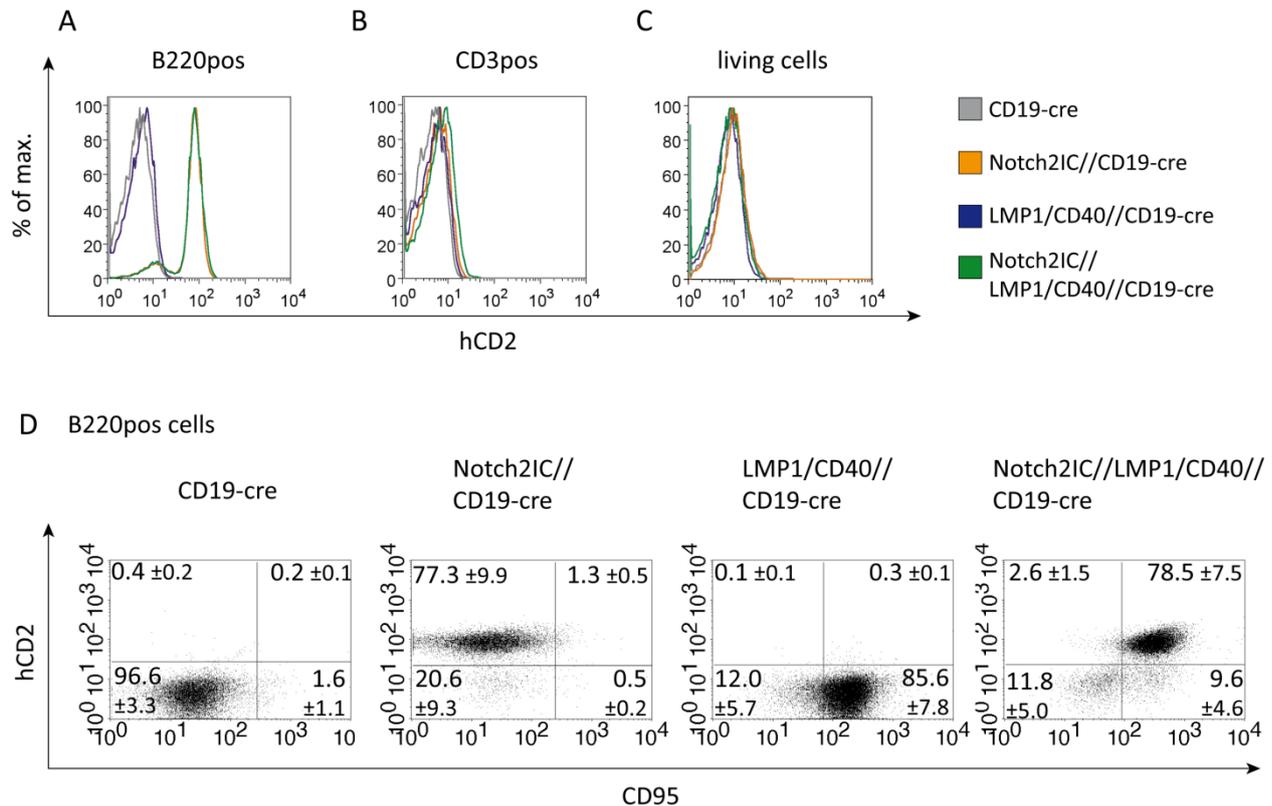
Fig. 3.2 Transgene expression is a B-cell-specific event.
Histograms show overlays of hCD2-expression of (A) lymphocyte-gated, living, B220^{pos} B cells, (B) lymphocyte-gated, living, CD3^{pos} T cells and (C) living, B220^{neg} cells in the spleen of CD19-cre (grey line), Notch2IC//CD19-cre mice (orange line), LMP1/CD40//CD19-cre mice (purple line) and Notch2IC//LMP1/CD40//CD19-cre mice (green line). Data is representative for nine independent experiments. (D) Living, B220^{pos} splenocytes were simultaneously stained for surface expression of hCD2 and CD95. The FACS plots show average percentages and SDs, as determined by antibody staining of whole splenocytes and subsequent flow cytometric analysis. Topro-3^{pos} (dead) cells were excluded from analysis. SD, standard deviation.

3.3 In Notch2IC//LMP1/CD40//CD19-cre mice total splenic cell numbers and B-cell numbers are significantly higher than in control and Notch2IC//CD19-cre mice but B-cell numbers are significantly lower than in LMP1/CD40//CD19-cre mice

In order to determine to what extent the expression of the respective transgenes adds to increase in size and weight the spleens were analyzed with regard to their total splenic cell as well as their splenic B-cell numbers. CD19-cre and Notch2IC//CD19-cre mice display about the same amount of total cells in their spleens, as well as similar B-cell numbers (Fig. 3.3A and B). Notch2IC//LMP1/CD40//CD19-cre mice resemble LMP1/CD40//CD19-cre mice with regard to their total splenic cell numbers of 5.3×10^{8} cells (versus 5.6×10^{8} total splenic cells in LMP1/CD40//CD19-cre mice) and they harbor more than 6-fold more cells than control CD19-cre and Notch2IC//CD19-cre mice (Fig. 3.3A). Also, B- cell numbers of Notch2IC//LMP1/CD40//CD19-cre mice (like LMP1/CD40//CD19-cre mice) display significantly increased splenic B-cell numbers compared to CD19-cre and Notch2IC//CD19-cre mice.
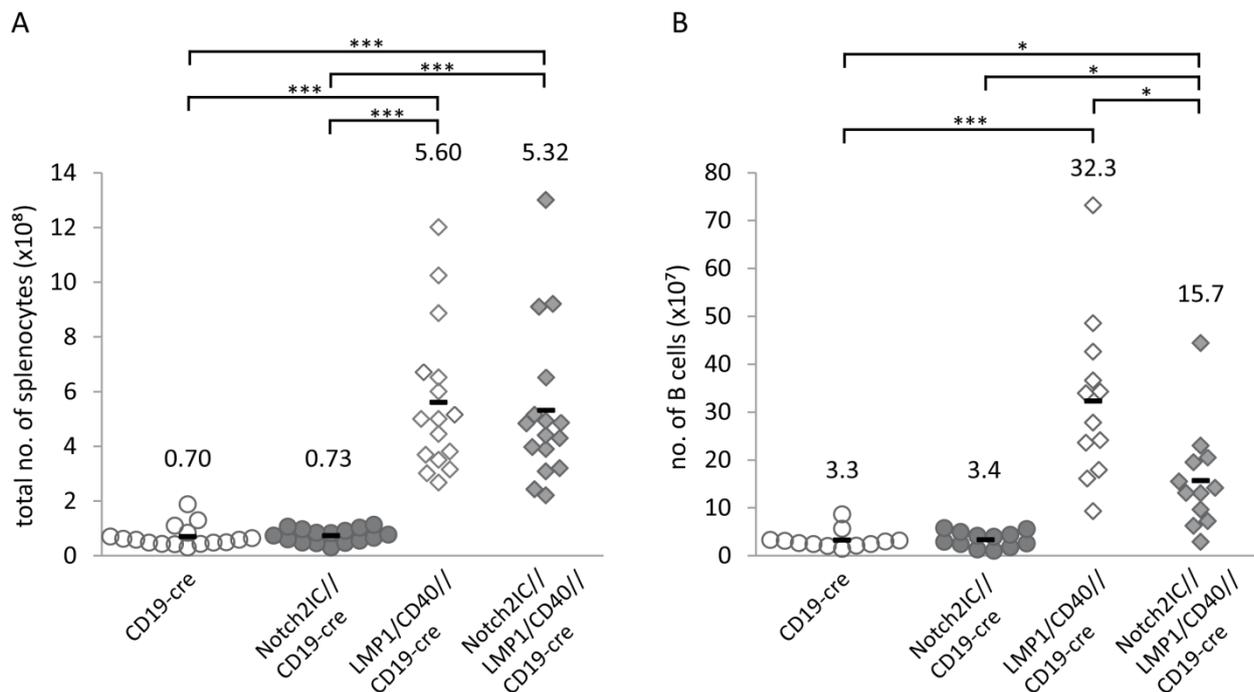
Fig. 3.3 Notch2IC//LMP1/CD40//CD19-cre mice display higher splenic cell numbers and increased B-cell numbers compared to control CD19-cre and Notch2IC//CD19-cre mice, but lower B-cell numbers than LMP1/CD40//CD19-cre mice.
(A) Absolute numbers of counted, living cells and (B) living, lymphocyte-gated, B220^{pos} B cells in the spleen of CD19-cre, Notch2IC//CD19-cre, LMP1/CD40//CD19-cre and Notch2IC//LMP1/CD40//CD19-cre mice as determined by antibody staining of whole splenocyte peparations and subsequent flow cytometric analysis. Topro-3^{pos} (dead) cells were excluded from analysis. Points represent data from individual mouse and horizontal bars mark the mean value indicated in numbers above each data set for the respective genotype. *p < 0.05, ** p < 0.01, *** p < 0.005.

However, when comparing splenic B-cell numbers of Notch2IC//LMP1/CD40//CD19-cre with LMP1/CD40//CD19-cre mice, the LMP1/CD40//CD19-cre mice display still significantly increased B-cell numbers versus Notch2IC//LMP1/CD40//CD19-cre mice (1.6×10^8 cells versus 3.2×10^8 splenic B cells in LMP1/CD40//CD19-cre mice).

Therefore surprisingly, Notch2IC//LMP1/CD40//CD19-cre mice display higher total splenic cell numbers and increased splenic B-cell numbers compared to control CD19-cre and Notch2IC//CD19-cre mice, but lower splenic B-cell numbers than LMP1/CD40//CD19-cre mice. Hence, the enlargement of the spleen had to be due to other cell populations.

3.4 Notch2IC//LMP1/CD40//CD19-cre mice display an increased number of splenic accessory cells

As aforementioned the elevated numbers of splenic B cells alone cannot account for the overall elevated total splenic cell numbers. This invited a broader look at cell populations that might be expanded in Notch2IC//LMP1/CD40//CD19-cre mice. In the forward scatter (FSC) versus side scatter (SSC) during flow cytometric analysis a population characterizing myeloid cells (Givan, 2013) showed up unexpectedly in the splenic cell preparations of Notch2IC//LMP1/CD40//CD19-cre mice repeatedly, however to varying extent (Fig. 3.4). Myeloid cells comprise all blood cells that do not belong to the group of lymphocytes and include mast cells, but also myeloblasts which can differentiate into neutrophils and monocytes the latter of which can further develop into macrophages and dendritic cells upon activation. In Notch2IC//CD19-cre and LMP1/CD40//CD19-cre mice percentages of these myeloid cells are with ≈3.6 % more or less on level of the spleens of control CD19-cre mice (with 2.8 %). However, since there is an overall increase in the splenic cell number of LMP1/CD40//CD19-cre mice this also translates into an increase in total myeloid cell numbers in these mice although the percentages vary strongly (±1.7-3.7 %). In Notch2IC//LMP1/CD40//CD19-cre mice there is a defined increase in the myeloid cell population which harbor on average 7.2 % myeloids in the splenocytes population. However, this varies strongly (±5.55 %), which indicates that spleens of Notch2IC//LMP1/CD40//CD19-cre mice have a tendency to harbor or attract more myeloid cells to the organ, but this cannot be observed to the same extent in all animals analyzed.
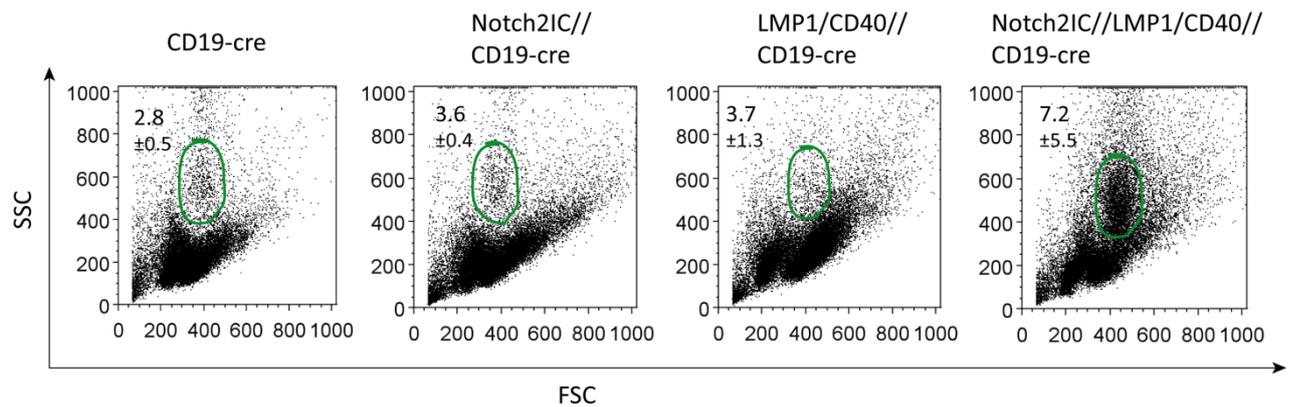
Fig. 3.4 Spleens of Notch2IC//LMP1/CD40//CD19-cre display an increase in the myeloid cell population.
Myeloid cell population (green circle, Givan, 2013) as detected by FSC/SSC-analysis during FACS. Averages
and SDs are given. FSC, forward scatter; SSC, sideward scatter; SD, standard deviation.

3.4.1   Notch2IC//LMP1/CD40//CD19-cre mice display an increased number of granulocytes and macrophages

Monocytes are an important subpopulation of myeloid cells. They are recruited to sites of tissue
injury and inflammation where they help to resolve the infection and are important for tissue
repair. Arriving at the site of infection or injury they quickly differentiate into DCs and
macrophages. Therefore, the spleens of all mice were analyzed for the presence of macrophages
and DCs and granulocytes which contribute to the myeloid cell population.

A Gr1/Mac1 surface marker staining allows differentiating Gr1^{hi} Mac1^{pos} granulocytes from the
Gr1^{pos} Mac1^{pos} macrophages (Zohren et al., 2012) (Fig. 3.5A) and permits to determine the
number of macrophages and granulocytes in the respective sample as given in the methods
section ("isolation of primary lymphocytes" and "Cell number calculations"). The results revealed
an increase in macrophage cell numbers in LMP1/CD40//CD19-cre by roughly 3-fold in
comparison to both Notch2IC//CD19-cre and CD19-cre mice (Fig. 3.5B). In
Notch2IC//LMP1/CD40//CD19-cre mice however, the numbers were markedly increased by 10-
fold with respect to spleens of control CD19-cre mice. Fig. 3.5C displays the actual granulocyte
cell numbers for the respective genotype. Again, the numbers found in Notch2IC//CD19-cre and
CD19-cre mice are roughly the same, while in comparison those in LMP1/CD40//CD19-cre are
increased by 4-fold and those in Notch2IC//LMP1/CD40//CD19-cre mice are increased by 10-fold
in comparison.

Performing immunofluorescent staining using the macrophage/granulocyte marker Mac1 on
histological sections one can analyze the location of these macrophages and granulocytes within
the spleen (Fig. 3.5D). In all four genotypes these cell populations are retained within the red
pulp of the spleen, while the follicles are discernible as dark areas. One can see that the cells sit
rather loosely in the red pulp in the spleens of CD19-cre and seem to be a little more clustered in

Notch2IC//CD19-cre mice. As expected due to the enlarged spleens the follicles in LMP1/CD40//CD19-cre and Notch2IC//LMP1/CD40//CD19-cre are rather large in comparison to Notch2IC//CD19-cre and CD19-cre (and will be analyzed in detail in section 3.11). In LMP1/CD40//CD19-cre and Notch2IC//LMP1/CD40//CD19-cre mice the macrophages and granulocytes also populate the red pulp areas where they seem to sit rather densely, while the follicles are devoid of Mac1^{pos} cells.
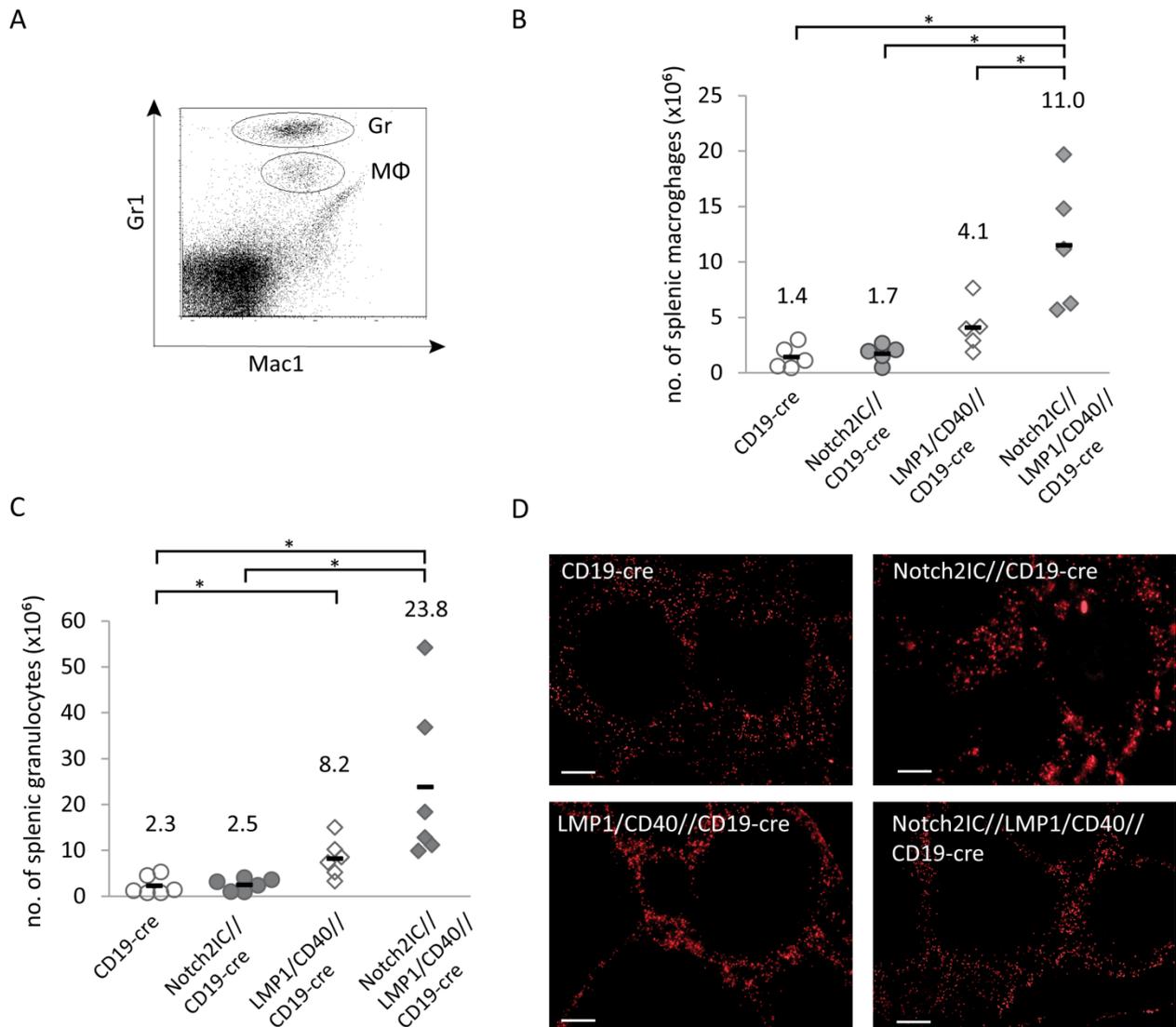
Fig. 3.5 Notch2IC//LMP1/CD40//CD19-cre mice display an increased number of granulocytes and macrophages.
(A) Exemplary gating to differentiate Gr1^{hi} Mac1^{pos} granulocytes (Gr) from the Gr1^{pos} Mac1^{pos} macrophages (MΦ)(as described in e.g. Zohren et al., 2012). Cell numbers for the splenic macrophages (B) population and for the splenic granulocyte population (C) as determined by Mac1/Gr1-antibody staining and FACS analysis. Points represent data from individual mouse and horizontal bars mark the mean value indicated in numbers above each data set for the respective genotype. (D) Mac1-antibody was used in immunofluorescent stainings to determine the localization of macrophages/granulocytes in the spleen of different genotypes on splenic cryosections. Bar: 100 μm; *p < 0.05.

3.4.2 Notch2IC//LMP1/CD40//CD19-cre mice display an increased number of activated dendritic cells

Next, since DCs are the other cell population into which monocytes can differentiate the spleens of all genotypes were analyzed for the presence of DC population. Although CD11c is being considered a marker for DCs as such (Metlay et al., 1990; Brocker et al., 1997) CD11c is also found on monocytes, tissue macrophages and NK cells (Hogg et al., 1986; Blasius et al., 2007; Drutman et al., 2012). Conventional DCs in the murine spleen however can be identified through examining the expression of both surface markers CD11c and CD8. FACS analysis was performed in order to determine whether this cell population was increased in Notch2IC//LMP1/CD40//CD19-cre mice. An increase in lymphocyte-gated, CD11c^{pos} cells is detectable both in LMP1/CD40//CD19-cre and in the Notch2IC//LMP1/CD40//CD19-cre mice in which also the population of both CD11c and CD8^{pos} conventional DC population is clearly discernible (Fig. 3.6A).
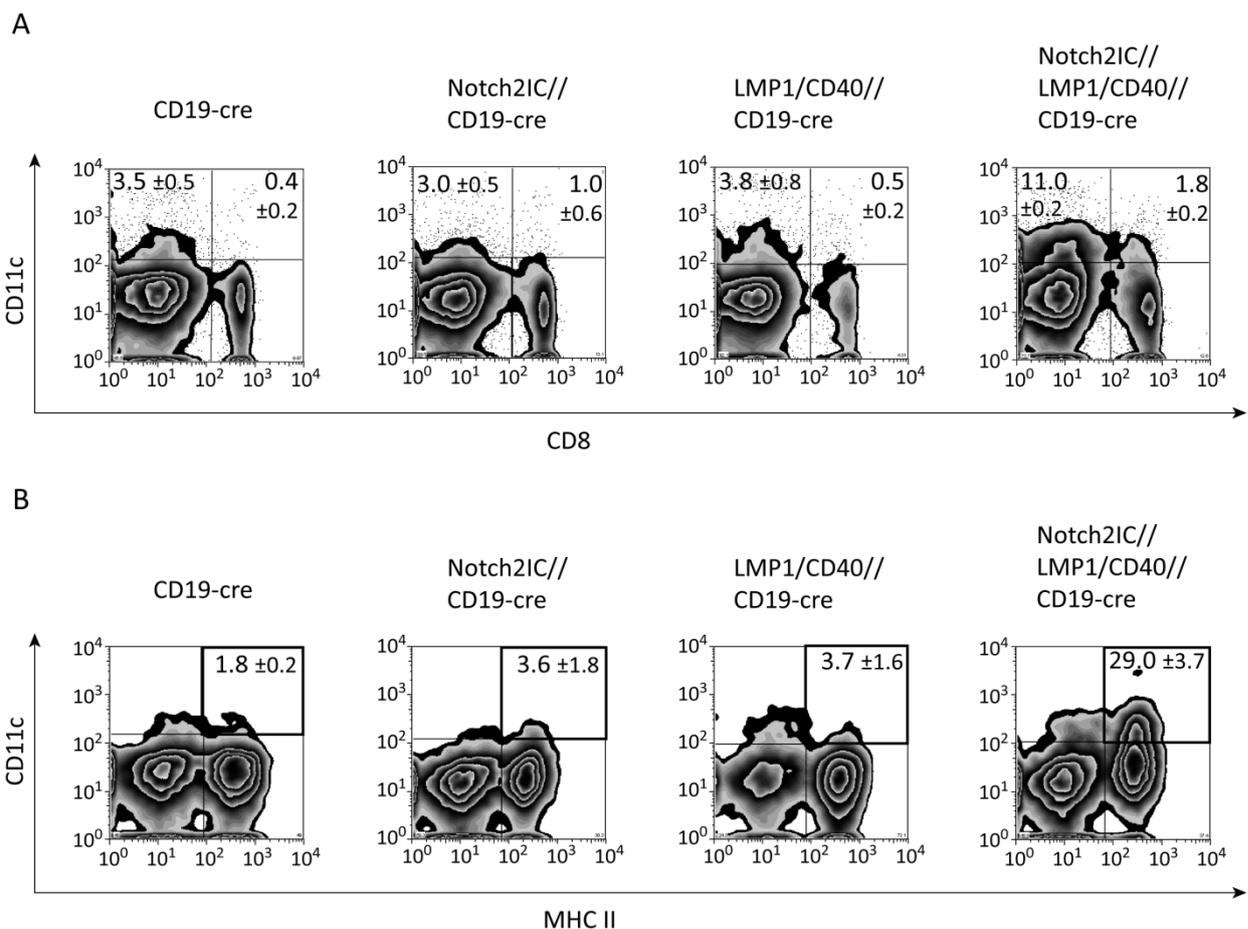
Fig. 3.6 Notch2IC//LMP1/CD40//CD19-cre mice display an increased number of activated dendritic cells. (A) FACS analysis results of the different genotypes after staining splenocytes for CD11c and CD8 surface markers indicative of conventional murine splenic DCs (lymphocyte-gated, CD8^{pos} and CD11c^{pos} population). (B) Dot plot of lymphocyte-gated, MHCII versus CD11c^{pos} cells as determined by flow cytometry in splenocytes preparations of all four genotypes with average and SDs. Data are representative for three independent experiments. DC, dendritic cell. SD, standard deviation.

Activated DCs -as other professional APCs- are characterized by up-regulation of MHCII. Interestingly, analyzing the CD11c^{pos} cell population revealed not only that CD11c^{pos} population is increased as such but these also up-regulate MHCII (Fig. 3.6B).

Altogether, numbers of accessory cells as myeloid cells, macrophages and DCs were found to be elevated in Notch2IC//LMP1/CD40//CD19-cre mice. All these cell types are involved in inflammatory responses, which suggested also looking further into the activation states of the T lymphocytes.

3.5 Notch2IC//LMP1/CD40//CD19-cre mice display significantly increased numbers of splenic T cells

Next, the splenic T cells -representing the other large lymphocyte population besides B cells- were examined by flow cytometric analysis.
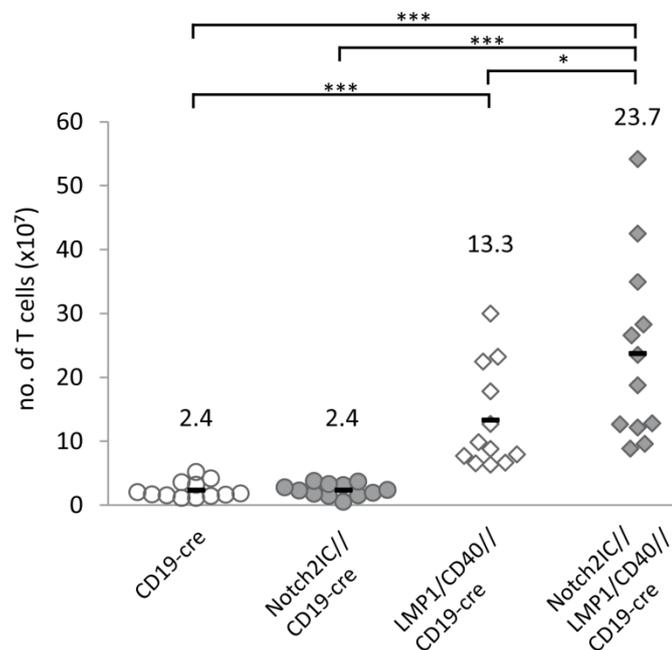
Fig. 3.7 Notch2IC//LMP1/CD40//CD19-cre mice display higher splenic T-cell numbers compared to control CD19-cre, Notch2IC//CD19-cre and LMP1/CD40//CD19-cre mice.
Number of living, lymphocyte-gated, CD3^{pos} T cells in the spleen of CD19-cre, Notch2IC//CD19-cre, LMP1/CD40//CD19-cre and Notch2IC//LMP1/CD40//CD19-cre mice as determined by antibody staining of whole splenocytes and subsequent flow cytometric analysis. Topro-3^{pos} (dead) cells were excluded from analysis. Points represent data from individual mouse and horizontal bars mark the mean value indicated in numbers above each data set for the respective genotype. *p < 0.05, ** p < 0.01, *** p < 0.005

Splenic T-cell numbers in Notch2IC//CD19-cre mice are on the level of CD19-cre control mice, while they are roughly increased by 6-fold in LMP1/CD40//CD19-cre mice, as has been previously documented. Surprisingly, the splenic T-cell population (with an overall average number of roughly 2.4×10^8 cells) is even further increased in Notch2IC//LMP1/CD40//CD19-cre mice: this amounts to a 10-fold increase compared to CD19-cre control mice (Fig. 3.7). It is striking to see that although T cells do not express the transgenes (i.e. display an expression of hCD2; Fig. 3.2B) this lymphocyte population is vastly expanded in Notch2IC//LMP1/CD40//CD19-cre in the spleens of these animals.

3.5.1   Notch2IC//LMP1/CD40//CD19-cre mice display a shift from CD4^{pos} towards CD8^{pos} splenic T cells

Beyond their developmental stages in the thymus T cells can be grouped into CD4^{pos} and CD8^{pos} cells in the periphery.

As displayed in Fig. 3.8A CD19-cre mice majorly have CD4^{pos} T cells, while exhibiting lower percentages for CD8^{pos} T cells. The same distribution pattern can be observed in Notch2IC//CD19-cre mice. This is also reflected in similar cell numbers for the different T-cell populations in those two genotypes (Fig. 3.8B). In LMP1/CD40//CD19-cre mice however, the percentages for CD4^{pos} cells are even increased, while the percentages for CD8^{pos} cells are slightly reduced in comparison to CD19-cre and Notch2IC//CD19-cre mice. This is also reflected in the actual cell numbers of CD4^{pos} cells in LMP1/CD40//CD19-cre mice which are significantly increased compared to CD19-cre control mice. However, since these mice harbor more T cells in their spleens as such also the actual numbers for CD8^{pos} cells are significantly increased in these mice versus the control mice. Interestingly, in comparison to CD19-cre mice the percentages for splenic CD4^{pos} T cells are slightly decreased and the percentages of CD8^{pos} are increased in Notch2IC//LMP1/CD40//CD19-cre mice, however due to the high number of T cells in these mice the actual cell numbers as such are in both cases still significantly higher than in control CD19-cre and Notch2IC//CD19-cre mice. With regard to the CD8^{pos} cells Notch2IC//LMP1/CD40//CD19-cre mice harbor significantly higher numbers than LMP1/CD40//CD19-cre mice.

A

CD3pos

B
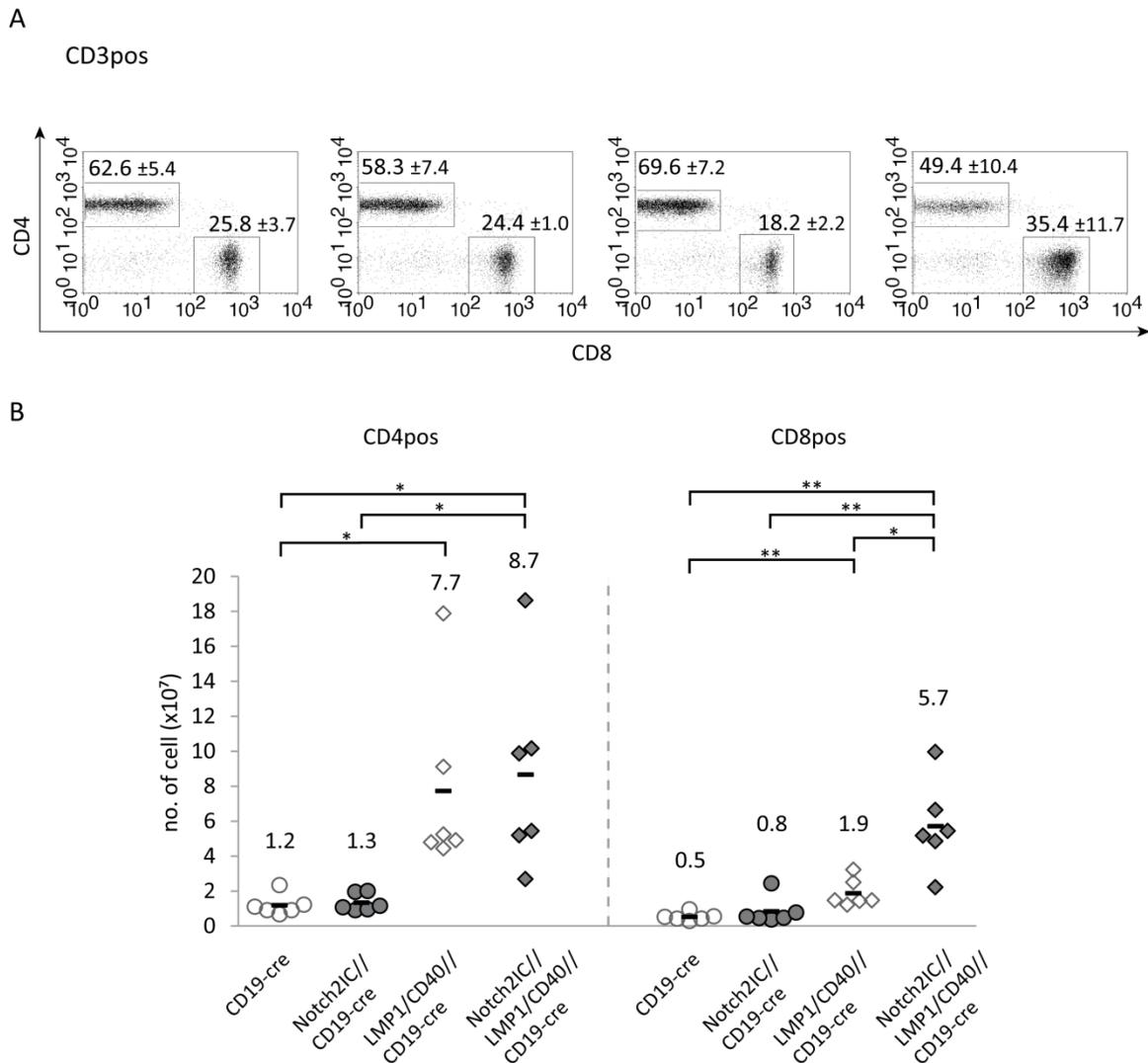
Fig. 3.8 Notch2IC//LMP1/CD40//CD19-cre mice display higher CD4^pos and CD8^pos splenic T-cell numbers compared to CD19-cre, Notch2IC//CD19-cre and LMP1/CD40//CD19-cre mice.
(A) Average percentages and SDs of CD3^pos/CD4^pos or CD3^pos/CD8^pos splenic T cells of CD19-cre, Notch2IC//CD19-cre, LMP1/CD40//CD19-cre and Notch2IC//LMP1/CD40//CD19-cre mice as determined by FACS analysis. Data is representative of six independent experiments. Plots are gated on living lymphocytes. (B) Number of living, CD3^pos and CD4^pos (left panel) and CD3 and CD8^pos (right panel) T cells in the spleen of CD19-cre, Notch2IC//CD19-cre, LMP1/CD40//CD19-cre and Notch2IC//LMP1/CD40//CD19-cre mice as determined by antibody staining of whole splenocytes and subsequent flow cytometric analysis. Topro-3^pos (dead) cells were excluded from analysis. Points represent data from individual mouse and horizontal bars mark the mean value indicated in numbers above each data set for the respective genotype. *p < 0.05, ** p < 0.01, *** p < 0.005; SD, standard deviation.

3.5.2   Notch2IC//LMP1/CD40//CD19-cre mice display activation of splenic T cells

In order to characterize the abnormally expanded splenic T-cell population in these mice and to determine which T-cell populations are majorly responsible for the observed expansion and activation levels of T cells, the distribution of naïve, memory and effector T cells and the populations (Th1, Th2, T_reg) as such were examined more closely in murine spleens. This was

achieved mainly via flow cytometric analysis using antibodies binding to several different surface (α-CD62L, α-CD25, α-CD28, α-CD69) as well as intracellular markers (IFNγ, IL4 and Foxp3).

3.5.2.1   Splenic T cells of Notch2IC//LMP1/CD40//CD19-cre mice show an enhanced expression of T-cell activation markers CD25 and CD69, but not of CD28

The splenic T cells were examined for a number of surface antigens that are up-regulated if the T cells are activated. CD28 is one of these markers that can engage with the B7 proteins (CD80 and CD86) on APCs (such as DCs and B cells) and provides co-stimulatory signals. Unexpectedly, none of the four genotypes tested show an upregulation of CD28 (data not shown).

Another molecule providing co-stimulatory signals to the T cell after the TCR has been engaged is CD69. Together with CD25, CD69 is one of the earliest and most prominent markers expressed by T cells upon activation and therefore has been dubbed very early antigen (VEA) (Yokoyama et al., 1989; Hamann et al., 1993). When testing Thy1.2^{pos} T cells for the expression level of CD69, Notch2IC//LMP1/CD40//CD19-cre and LMP1/CD40//CD19-cre mice display an increased number of splenic T cells with higher CD69 levels than CD19-cre and Notch2IC//CD19-cre mice (Fig. 3.9B). CD25 however is specifically up-regulated in the splenic T cells of Notch2IC//LMP1/CD40//CD19-cre mice compared to all other genotypes tested (Fig. 3.9A).
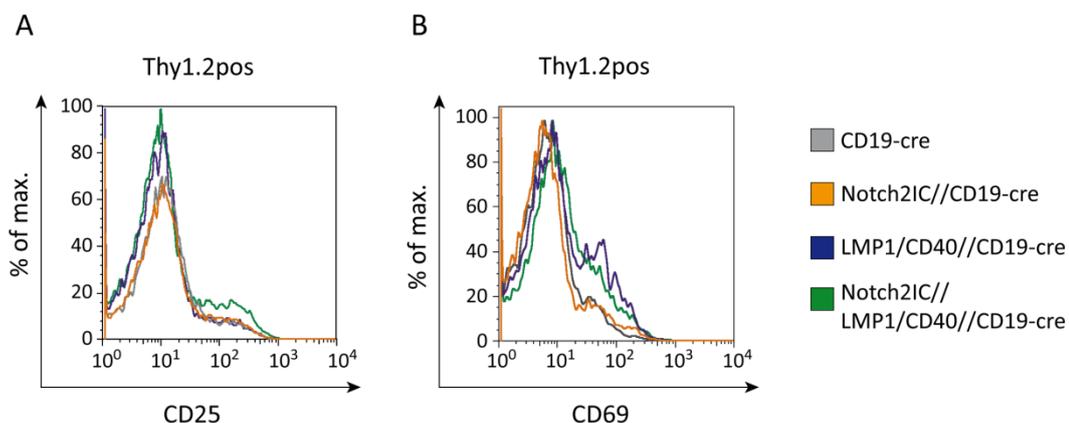
Fig. 3.9 Splenic T cells of Notch2IC//LMP1/CD40//CD19-cre show an enhanced expression of the T-cell activation markers CD25 and CD69.
Splenocytes from two to five-month-old mice with genotypes as indicated were stained with antibodies specific for Thy1.2, CD25 (A) or CD69 (B) and subjected to FACS analysis. Histograms show overlays of representative FACS plots (pre-gated on lymphocytes and Thy1.2^{pos} cells) of surface expression of the indicated molecules from CD19-cre (grey line), Notch2IC//CD19-cre mice (orange line), LMP1/CD40//CD19-cre mice (purple line) and Notch2IC//LMP1/CD40//CD19-cre mice (green line). Representative data from three independent experiments are shown.

3.5.2.2 Splenic T cells of Notch2IC//LMP1/CD40//CD19-cre mice show an increase in the percentage of both central memory as well as effector memory T cells

Analyzing splenic T lymphocytes by staining of the surface markers CD4, CD8, CD62L and CD44, allows determining the percentages of naïve (CD62L^{hi} CD44^{neg}), central memory (CD62L^{hi} CD44^{hi}) and effector cells (CD62L^{neg} CD44^{hi}) in the respective CD4^{pos} or CD8^{pos} T-cell population.

The FACS analysis results revealed that Notch2IC//CD19-cre, LMP1/CD40//CD19-cre mice and Notch2IC//LMP1/CD40//CD19-cre compared to CD19-cre mice have a reduction in the naïve T cell compartment (CD62L^{hi} CD44^{low}) in their spleens (Fig. 3.10A (CD4^{pos}) and Fig. 3.10B (CD8^{pos})). This is observable for all three genotypes both in the CD4^{pos}, as well as in the CD8^{pos} T-cell population (upper and lower panel). In Notch2IC//CD19-cre mice the compartment of splenic central memory T cells (CD62L^{hi} CD44^{hi}) for both the CD4^{pos} and CD8^{pos} cells resembles that of CD19-cre mice, since there are roughly 8 % CD4^{pos} memory T cells and roughly 18 % CD8^{pos} memory T cells. With regard to the splenic effector T cells (CD62L^{low} CD44^{hi}) in Notch2IC//CD19-cre mice however, there is a distinct increase both in the CD4^{pos} (≈ 41 %) as well as the CD8^{pos} population (≈ 26 %) compared to that of CD19-cre mice (26% in the CD4 and 17 % in the CD8^{pos} cell populations).

With regard to CD4^{pos} splenic T cells Notch2IC//CD19-cre and Notch2IC//LMP1/CD40//CD19-cre mice display very similar patterns of expansion of splenic T-cell subgroups, although the subgroup of CD4^{pos} central memory T cells is slightly decreased in Notch2IC//LMP1/CD40//CD19-cre mice and the splenic effector T cells are even more expanded in these mice (on the average 42 % in Notch2IC//CD19-cre versus 55 % in Notch2IC//LMP1/CD40//CD19-cre and only 26 % in CD19-cre mice). LMP1/CD40//CD19-cre mice have slightly increased CD4^{pos} memory T cells and a stronger increase in the CD4^{pos} effector cell compartment in comparison to CD19-cre mice. With respect to CD8^{pos} splenic T cells the subgroup of central memory T cells is roughly three times reduced in percentage in the Notch2IC//LMP1/CD40//CD19-cre mice compared to all other genotypes, while effector T cells are with 39 % markedly increased both compared to mice Notch2IC-and LMP1/CD40-genotypes (27 % and 21 %, respectively, compared to 17 % in CD19-cre animals). Considering that the CD8^{pos} T cells are the largest group as such, the CD8^{pos} effector cells therefore represent the largest T-cell subgroup in the spleen of Notch2IC//LMP1/CD40//CD19-cre mice by far.
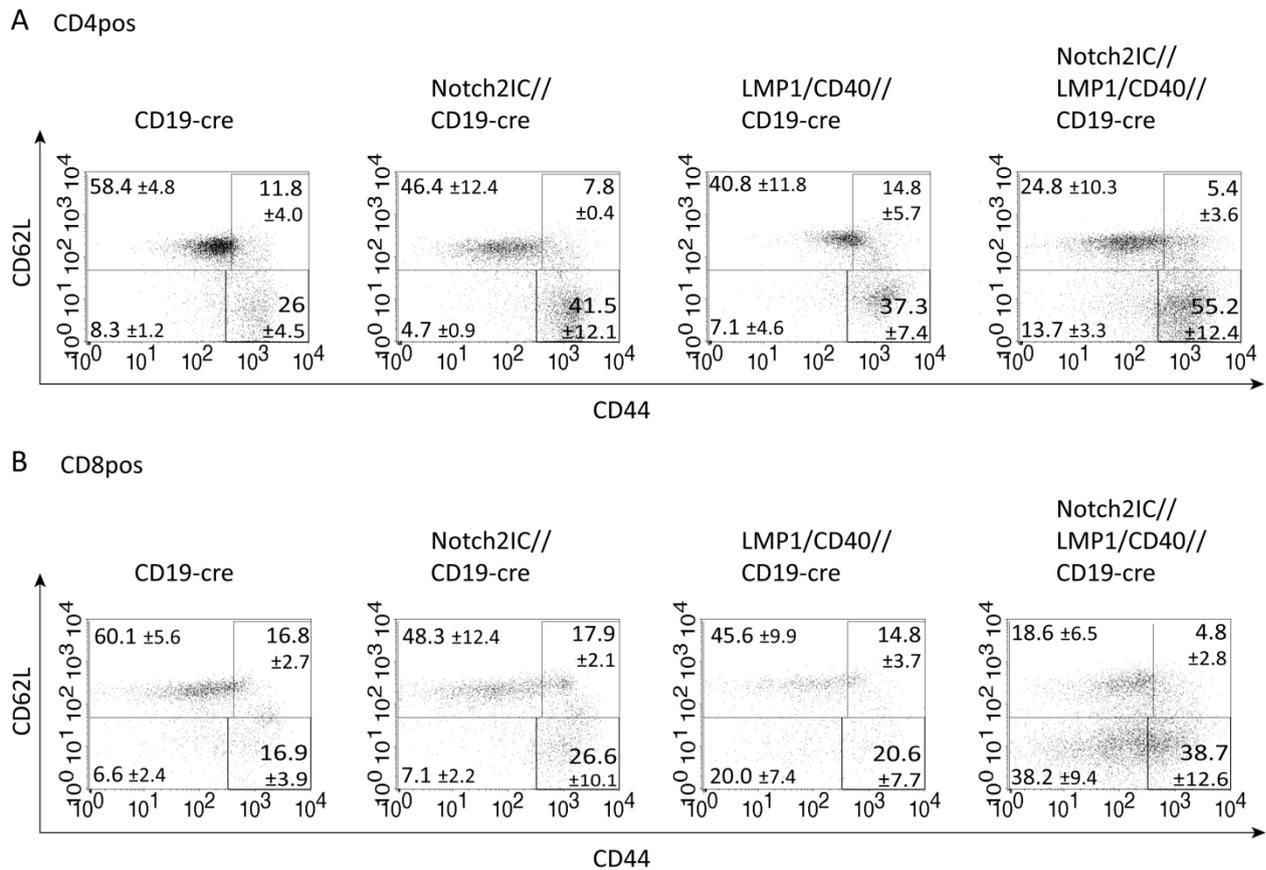
Fig. 3.10 Splenic T cells of Notch2IC//LMP1/CD40//CD19-cre mice show an increase in the percentage of both central memory as well as effector T cells.
Splenic cells were analyzed by flow cytometry for expression of CD62L and CD44 on either CD4^{pos} (A) or CD8^{pos} (B) lymphocyte-gated cells. Averages and standard deviations are calculated from six independent experiments. Naïve T cell compartment (CD62L^{hi} CD44^{low}), central memory T cells (CD62L^{hi} CD44^{hi}), effector T cells (CD62L^{low}, CD44^{hi}), hi, high.

A unique feature in which splenic T cells of LMP1/CD40//CD19-cre and the Notch2IC//LMP1/CD40//CD19-cre strongly resemble each other is the presence of a high percentage of CD8^{pos} T cells that are low for the expression of both CD62L and CD44. This also holds true to a lesser degree in the CD4^{pos} T-cell compartment. This might point towards exhaustion of the splenic T-cell compartment. Exhaustion is a commonly observed phenomenon that has been observed during persistent lymphocytic choriomeningitis virus (LCMV) infection of mice (Zajac et al., 1998) and in other sustained viral infections such as human immunodeficiency virus (HIV) infection and hepatitis B and C virus infection (Yamamoto et al., 2011; Rehermann et al., 2005).

For actual numbers of splenic T-cell populations please refer to Tab. 9.1 (Supplements).

3.5.3 In Notch2IC//LMP1/CD40//CD19-cre mice splenic T cells display a Th1 activation pattern with and without PMA/Ionomycin stimulation

There is not only a surge in myeloid and T cells in the spleens of Notch2IC//LMP1/CD40//CD19-cre mice but splenic T cells of these mice are found to be activated after ex vivo isolation -as shown in the previous section. These findings already point towards the establishment of an inflammatory milieu in the spleens of Notch2IC//LMP1/CD40//CD19-cre mice. Since cyto- and chemokines are important mediators in inflammatory responses this led to the question whether the T cells were also showing an activation pattern with regard to the Th1 and Th2 cytokine production.

CD4^{pos} T cells are regarded as being the most prolific cytokine producers. This subset can be further subdivided into Th1 and Th2, and the cytokines they produce are known as Th1-type cytokines and Th2-type cytokines. Th1-type cytokines tend to produce the pro-inflammatory responses responsible for killing intracellular parasites and for perpetuating autoimmune responses. IFNγ is the main Th1 cytokine, while the Th2-type cytokines include interleukins 4, 5, and 13. Th17 cells produce IL17 and also IL22. This relatively newly discovered T-cell subset is implicated in autoimmunity.

In order to examine cells of all genotypes with regard to their stimulation pattern splenic cell preparations were tested by polyclonal stimulation with phorbol myristate acetate (PMA) and calcium ionophore ionomycin (PMA/Ionomycin). This PMA/Ionomycin-treatment activates all cells in a sample unspecifically and is usually followed by Brefeldin A-treatment. This fungal metabolite interferes with protein transport from the Golgi apparatus to the endoplasmic reticulum and thereby ensures that the respective cytokine under investigation does not diffuse into the medium of the cell suspension. The analysis revealed that the PMA/Ionomycin stimulation of splenic T cells of Notch2IC//CD19-cre mice and of Notch2IC//LMP1/CD40//CD19-cre mice induced a strong increase in the compartment of IFNγ-producing cells (not only in the CD4^{pos} Th1 compartment), which could not be detected in CD19-cre and LMP1/CD40//CD19-cre (Fig. 3.11A, upper panel). Moreover, in splenic cell preparations of both Notch2IC//CD19-cre mice and of Notch2IC//LMP1/CD40//CD19-cre mice there is also an increase in the IFNγ-production in non-CD4^{pos} splenocytes, resulting from the stimulation. IFNγ is known to be produced by a multitude of different cells, e.g. NK and NKT cells. [NK cells were not responsible for the increase in IFNγ in the examined cases. NKT cells were not increased in these mice altogether (data not shown). The level of NKT IFNγ production was not determined].

There were no detectable differences between the four different genotypes tested with regard to the IL4-producing Th2 compartment (Fig. 3.11B, lower panel) or the Th17 subpopulation (data not shown) upon stimulation.
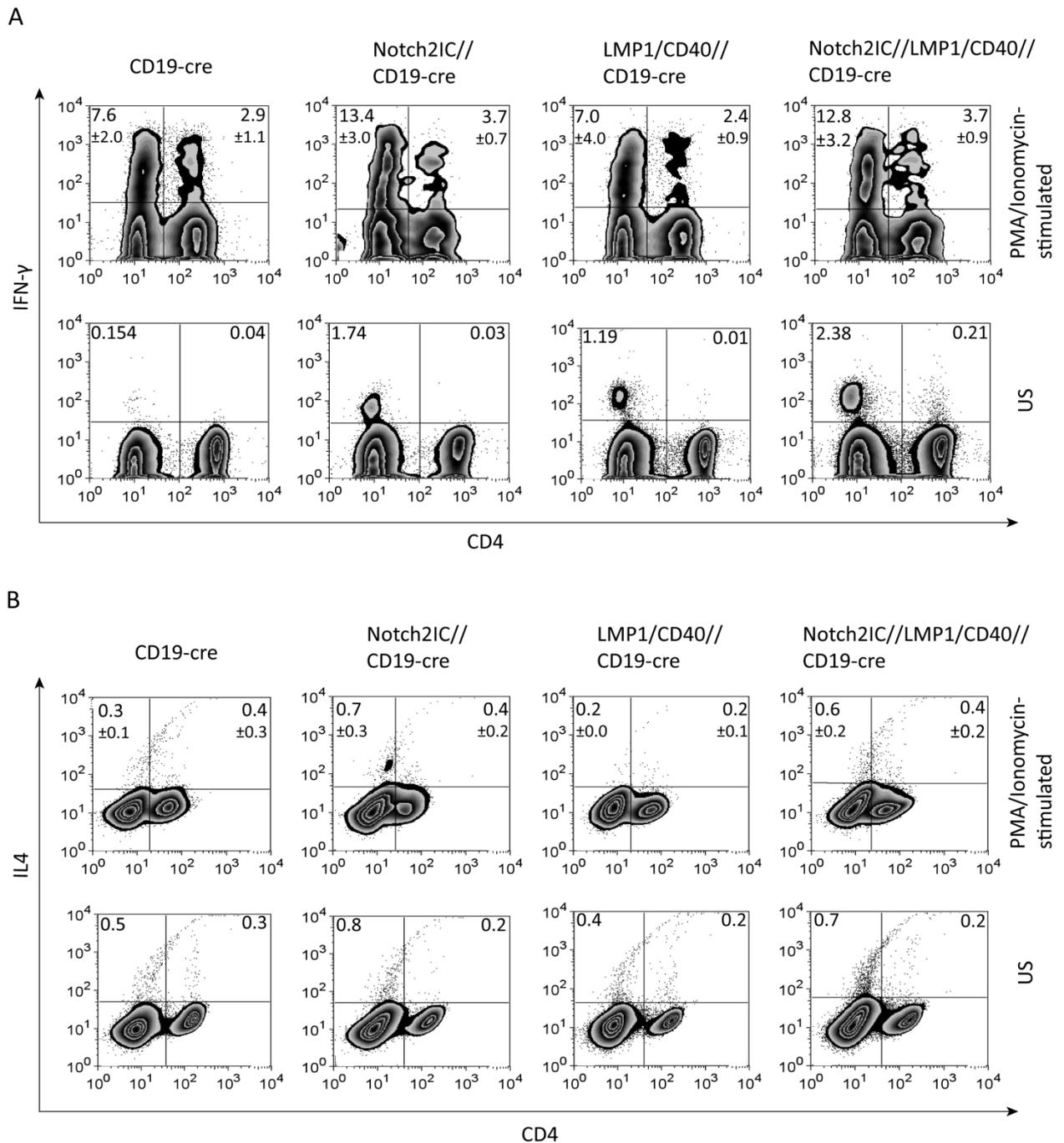
Fig. 3.11 T cells of Notch2IC//LMP1/CD40//CD19-cre and Notch2IC//CD19-cre mice display a Th1 and not a Th2 cytokine profile both with and without stimulation.
(A) Upper panel: IFNγ production of PMA- and Ionomycin-stimulated splenic, lymphocyte-gated cells. Lower panel: IFNγ production of unstimulated splenocytes. (B) Upper panel: IL4 production of PMA- and Ionomycin-stimulated splenic, lymphocyte-gated T cells. Lower panel: IL4 production of unstimulated splenocytes. FACS analysis data was obtained by staining splenocytes with antibodies against the surface marker CD4 and antibodies detecting intracellular level of IL4 or IFNγ. Averages and SDs are calculated from three independent experiments for the stimulated cells and a representative result is shown for two experiments with unstimulated T cells. SD, standard deviation.

It seemed intriguing to evaluate the status of splenic T cells immediately in ex vivo preparations without additional stimulation. Usually the levels of cytokine would be very low and mostly production will be just above or below the detection level. This was indeed the case for the

splenic T cells isolated from spleens of CD19-cre and LMP1/CD40//CD19-cre. In Notch2IC//CD19-cre and the Notch2IC//LMP1/CD40//CD19-cre mice splenic cells showed a Th1 profile and again particularly an increase in non-CD4^{pos} IFNγ secreting cells (Fig. 3.11A and B, lower panel respectively). Furthermore, there is an observable increase in the non-CD4^{pos} fraction of cells that are IL4-producing without stimulation.

Altogether, splenic T cells both in Notch2IC//CD19-cre and in Notch2IC//LMP1/CD40//CD19-cre mice show a tendency towards a Th1 profile both with and without stimulation.

3.5.4 Splenic T$_{reg}$ are increased in splenic preparations of Notch2IC//LMP1/CD40//CD19-cre mice

As shown in section 3.5.2 splenic T cells of Notch2IC//LMP1/CD40//CD19-cre mice exhibit high levels of the surface marker CD25. Cells that are specialized in steering cytokine release are T$_{regs}$, which are characterized by being CD25^{hi}, CD4^{pos} and positive for the transcription factor Foxp3. T$_{regs}$ can regulate immune responses and they are of key importance in maintaining tolerance to self. In fact they can even prohibit the differentiation of naïve into effector T cells. Since the latter cell population is expanded in all transgene-expressing genotypes (except in CD19-cre mice) one could expect a decrease in the population of T$_{regs}$.

When testing via intracellular FACS analysis for the presence of T$_{regs}$ in the spleen of the four genotypes (CD19-cre, Notch2IC//CD19-cre mice, LMP1/CD40//CD19-cre mice, Notch2IC//LMP1/CD40//CD19-cre) there was no significant difference detectable in the percentage of T$_{regs}$ in CD19-cre, Notch2IC//CD19-cre and LMP1/CD40//CD19-cre mice (Fig. 3.12A). But in contrast to all other genotypes analyzed the spleens of Notch2IC//LMP1/CD40//CD19-cre mice display a much larger percentage (marked by a 2-fold increase) of T$_{regs}$ and accordingly –since the spleens also harbor more cells- the actual splenic T$_{reg}$ numbers are increased.

These findings could be confirmed with immunohistochemistry (IHC) on splenic cryosections. Stainings were performed with an antibody against nuclear Foxp3, which serves as a pan-T$_{reg}$ marker and an IgM staining in order to allow for a better localization of the T$_{regs}$ within the follicular structure of the spleen (Fig. 3.12B). In spleens of CD19-cre mice the follicular structures are ordered and smaller and the T$_{regs}$ are confined to the T-cell zone. In Notch2IC//CD19-cre spleens the T$_{regs}$ seem to be somewhat dispersed in the B-cell zone as well. In LMP1/CD40//CD19-cre mice the follicles are much larger as previously observed in the Mac1 stainings (Fig. 3.5D) and the T$_{regs}$ are mainly located in the T-cell zone but also somewhat dispersed within the follicular structures. This observation was also made for the spleens of Notch2IC//LMP1/CD40//CD19-cre

mice. In these spleens however, the increase in T_{regs} becomes evident and the splenic structure almost seems enlarged but also dissolved and the T_{regs} are not so strictly confined to the T cell zone anymore.
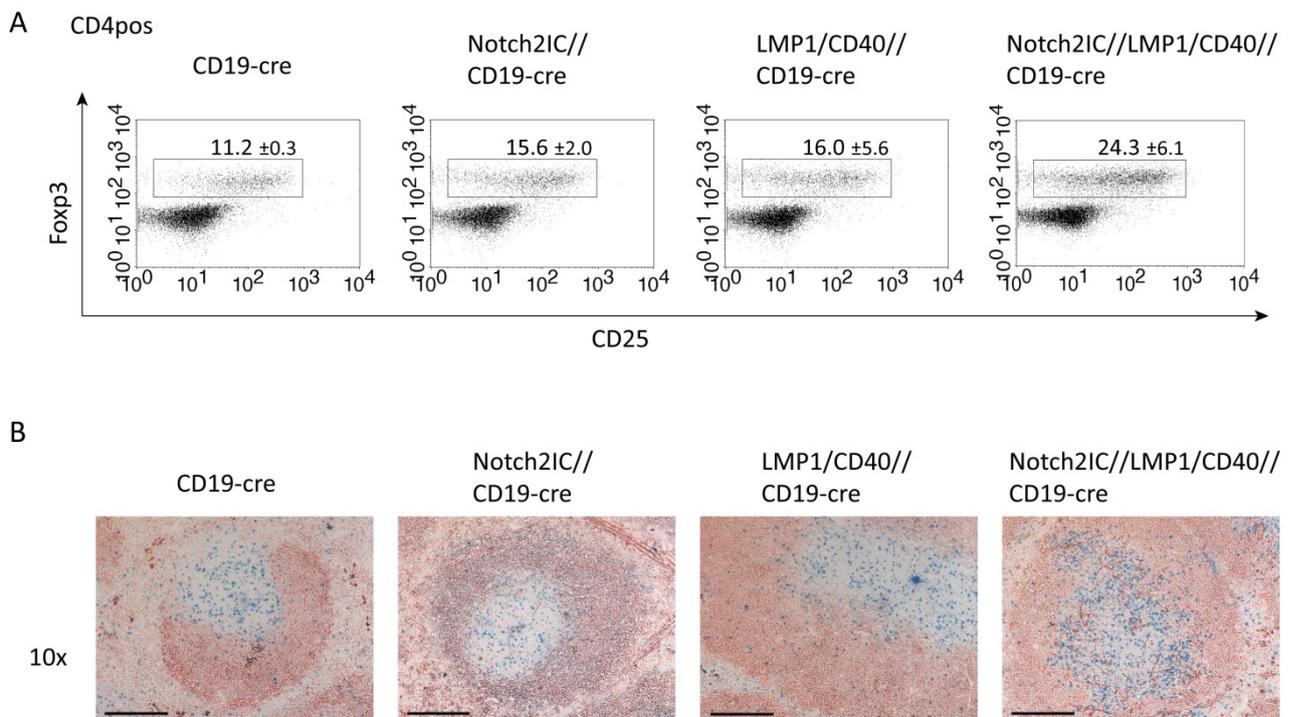
Fig. 3.12 Notch2IC//LMP1/CD40//CD19-cre mice display a substantial increase in T_{regs}.
(A) Splenocytes were stained with antibodies against CD4, CD25 and after cell-permeabilization with α-Foxp3. Dot plots were analyzed after pre-gating on CD4^{pos} cells. Averages and SDs are calculated from three independent experiments. (B) IHC of splenic cryosections with antibodies detecting T_{regs} (Foxp3, blue) and B cells (IgM, red). Bar: 100 µm. IHC, immunohistochemistry. SD, standard deviation.

3.6 Early concomitant expression of constitutive Notch2IC and CD40 partially blocks early B-cell development between pre- and immature B cells in the bone marrow

All these observations described above are however indirect effects of the fact that the Notch2IC//LMP1/CD40//CD19-cre mice express constitutively active Notch2 and constitutively active CD40 in their B cells, which had to be characterized more in detail. As shown in section 3.3 (Fig. 3.3B) splenic B-cell numbers of Notch2IC//LMP1/CD40//CD19-cre mice are overall increased compared to CD19-cre and Notch2IC//CD19-cre mice. However they are significantly reduced compared to LMP1/CD40//CD19-cre. Consequently, it was important to test whether expression of both transgenes has an effect on B-cell development. B-cell precursor subsets and immature B cells in the bone marrow from mice expressing the two transgenes were compared to those in CD19-cre mice alone as well as to that of Notch2IC//CD19-cre and LMP1/CD40//CD19-cre mice. To this end bone marrow samples were prepared from all genotypes for subsequent analysis.

3.6.1 Total and B-cell numbers are normal in bone marrow preparations of Notch2IC//LMP1/CD40//CD19-cre mice, but exhibit significantly increased T-cell numbers

Overall cell numbers in the bone marrow were found to be similar and only slightly elevated in Notch2IC//LMP1/CD40//CD19-cre versus Notch2IC//CD19-cre and LMP1/CD40//CD19-cre mice in comparison to CD19-cre mice (Fig. 3.13A), but this can vary depending on the respective preparation.
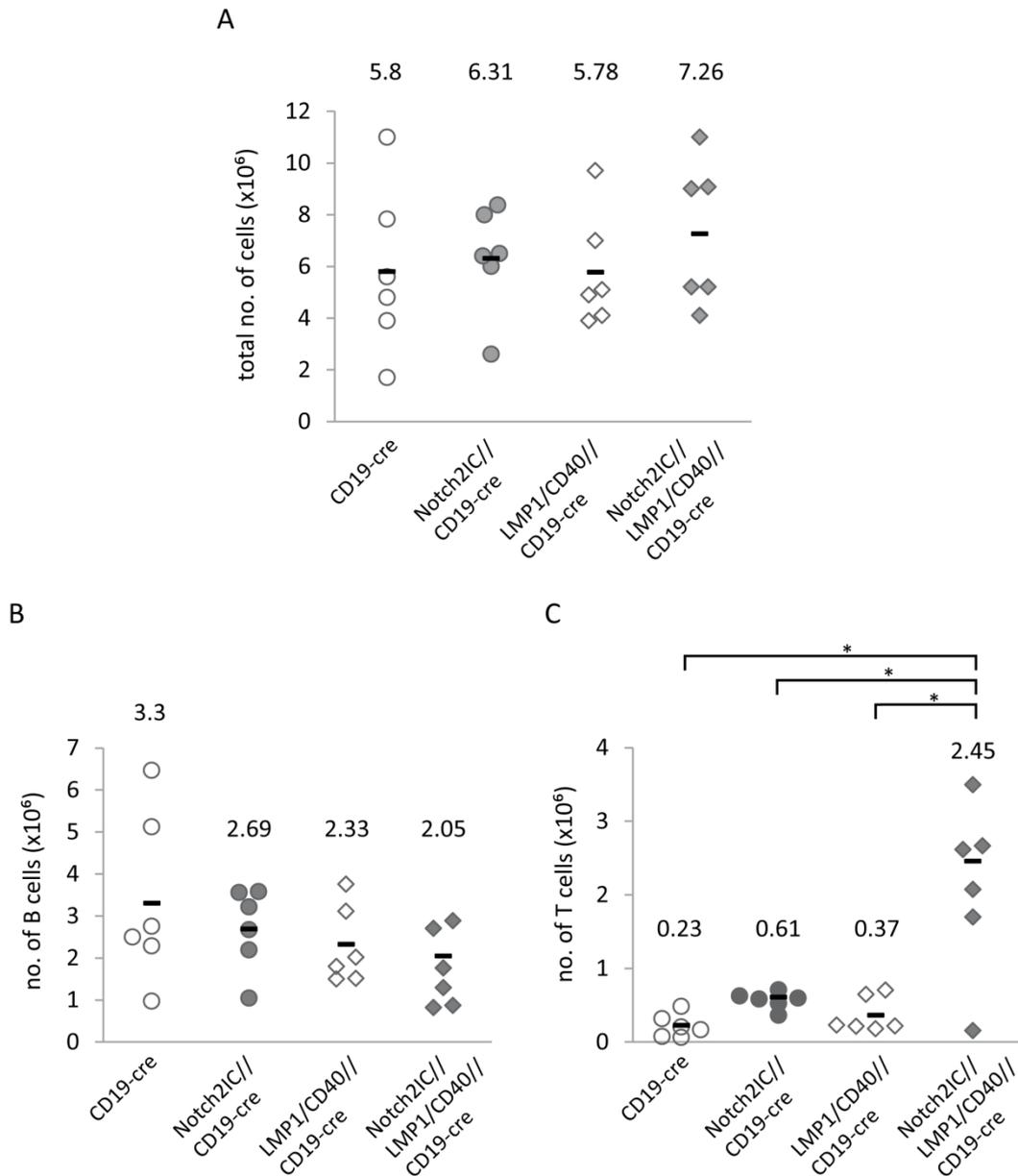
Fig. 3.13 Total and B-cell numbers are normal in bone marrow preparations of Notch2IC//LMP1/CD40//CD19-cre mice, but exhibit significantly increased T-cell numbers.
(A) Total cell, (B) B and (C) T cell numbers of the bone marrow as determined by counting and FACS analysis with α-B220 and α-CD3 antibodies. Topro-3^{pos} (dead) cells were excluded from analysis. Points represent data from individual mouse and horizontal bars mark the mean value indicated in numbers above each data set for the respective genotype. *p < 0.05; SD, standard deviation.

B-cell numbers in bone marrow of Notch2IC//LMP1/CD40//CD19-cre mice are slightly decreased compared to CD19-cre mice, this can also be observed in LMP1/CD40//CD19-cre mice (Fig. 3.13B). By contrast T-cell numbers in bone marrow of Notch2IC//LMP1/CD40//CD19-cre mice are significantly higher than in all other genotypes (Fig. 3.13C). Considering the increase in T cells both in spleen and bone marrow in Notch2IC//LMP1/CD40//CD19-cre mice the T cells were analyzed for the presence of hCD2 on their surface indicating transgene expression which could lead to an increase in this lymphocyte population in the bone marrow. However, as previously shown for the splenic T cells (Fig. 3.3B) the T cells found in the bone marrow were negative for hCD2 (data not shown). It seems likely to assume that these T cells cannot localize all in the spleen and therefore rather home to other secondary lymphoid organs as well as the bone marrow.

3.6.2 Early concomitant expression of constitutive Notch2IC and CD40 leads to a reduction in the pre- and immature B-cell populations in the bone marrow

However, when examining the bone marrow-derived cells there were distinct changes with regard to the different B-cell subpopulations that became evident when staining the cells with antibodies against different surface markers and performing FACS analysis. The percentages of pro- and early pre- B cells (CD43^{pos} B220^{pos}) (Fig. 3.14A, upper panel) are slightly lower in Notch2IC//LMP1/CD40//CD19-cre than in LMP1/CD40//CD19-cre mice which are on level of CD19-cre mice. This was recapitulated in the IgM/B220 staining (Fig. 3.14A, lower panel), where B220^{pos} IgM^{neg} cells represent the pro/pre-B cells. While percentages for the pro/pre-B cells in bone marrow of Notch2IC//CD19-cre are more or less on level of the CD19-cre mice, these are reduced in LMP1/CD40//CD19-cre and are even lower in Notch2IC//LMP1/CD40//CD19-cre mice. Considering the percentages of pre/immature (CD43$^{neg/low}$ B220^{pos}) or only immature B cells (B220^{pos} IgM$^{pos/hi}$), these are always lower in transgene-expressing B-cells and precursors. The levels of these cells in the bone marrow in Notch2IC//CD19-cre animals still resemble CD19-cre mice, percentages are further reduced in LMP1/CD40//CD19-cre and are lowest in Notch2IC//LMP1/CD40//CD19-cre mice (8.4 % CD43 $^{neg/low}$ B220^{pos} cells versus 26.2 % in CD19-cre and 3.8 % B220^{pos} IgM$^{pos/hi}$ cells versus 10.4 % in CD19-cre mice).
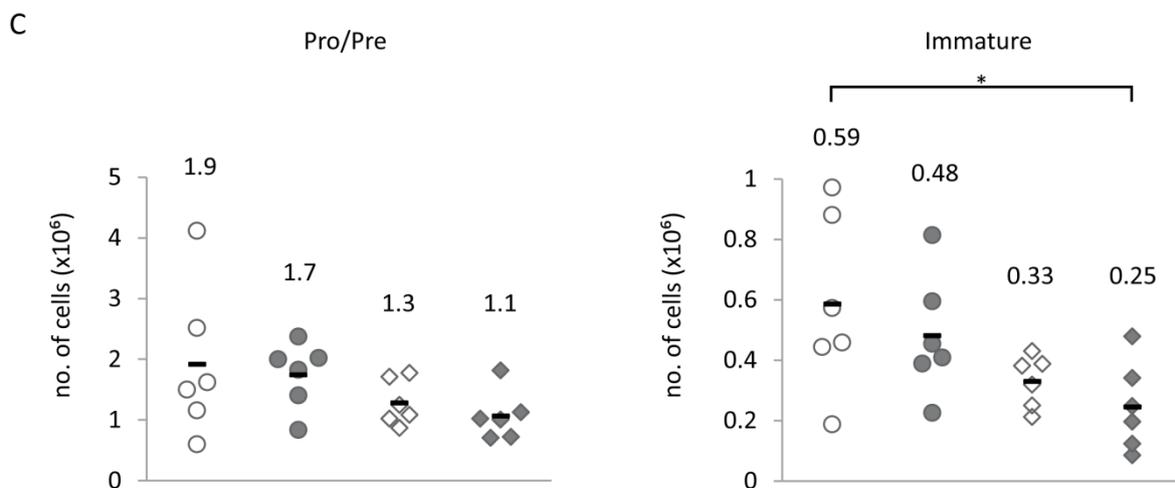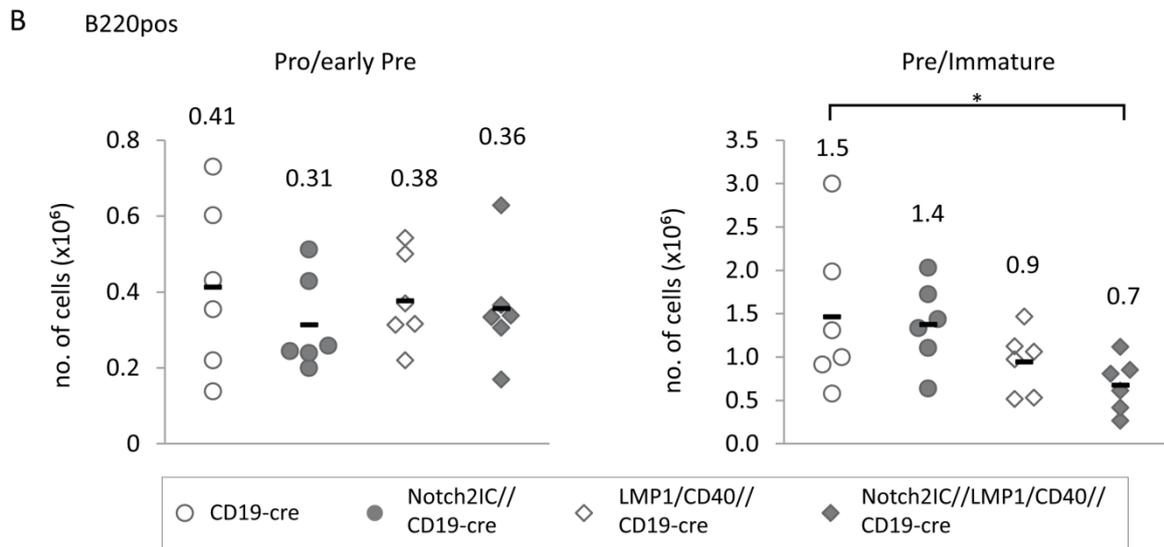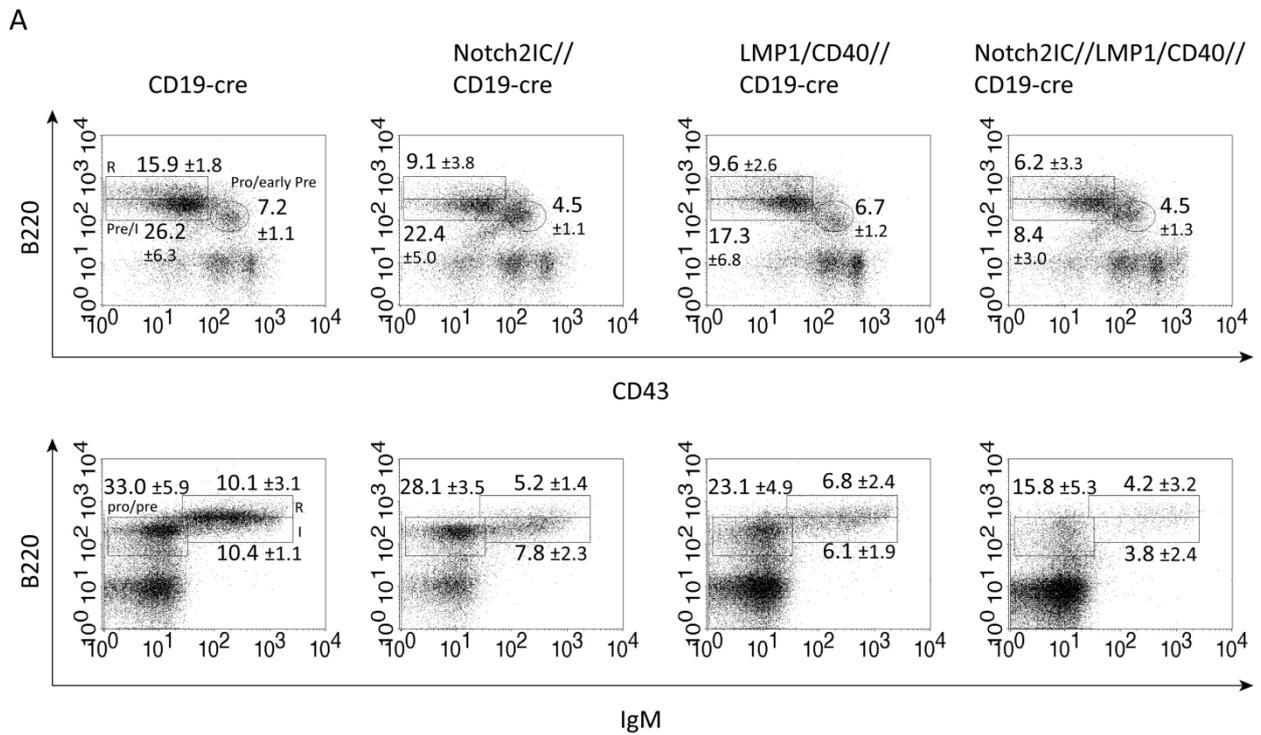
Fig. 3.14 Early concomitant expression of constitutive Notch2IC and LMP1/CD40 affects early B-cell development in the bone marrow leading to a reduction in pre- and immature B cells.

(A) Bone marrow preparations were analyzed by flow cytometry for the expression of B220 and CD43 (upper panel) and B220 and IgM (lower panel), in order to determine the percentages of pro/early pre- (B220^{pos} CD43^{pos}), pre/immature (B220^{pos} CD43$^{neg/low}$), pro/pre (B220^{pos} IgM^{neg}) and immature (B220^{pos} IgM^{hi}) B cells with SD. Cells were pre-gated on lymphocyte gate. (B) Total cell numbers for pro/early pre- and pre/immature B-cell populations as calculated from CD43/B220-stainings (A; upper panel) after B220-pre-gating. (C) Total cell numbers for pro/pre- and immature B cell populations as calculated from IgM/B220-stainings (A; lower panel) FACS plots: Numbers indicate mean percentages and SDs of lymphocyte-gated populations and were calculated from six independent experiments. Cell number calculations: Points represent data from individual mouse and horizontal bars mark the mean value, indicated in numbers above each point column. *p < 0.05; SD, standard deviation; Pro, pro B cells; Pre, pre B cells; R, recirculating B cells; I, immature B cells.

These observations could be reconfirmed when calculating the actual cell numbers from B cell numbers (Fig. 3.14B and C). Considering the pre- to immature B-cell stage one can observe a partial block in the development of immature B cells in bone marrow of the Notch2IC//LMP1/CD40//CD19-cre mice compared to all other genotypes characterized by a significant drop in cell numbers for both of these two developmental stages (1.1×10^6 versus 1.9×10^6 pro/pre B cells in CD19-cre and 0.25×10^6 versus 0.6×10^6 immature B cells in CD19-cre mice).

In the case of Notch2IC//CD19-cre and Notch2IC//LMP1/CD40//CD19-cre mice the surface expression of hCD2 would allow to pinpoint the time point when expression of the transgenes can be observed in the developing B cells. Overall the percentage of hCD2^{pos} B220^{pos} B cells is low (on the average 12.2 % in Notch2IC-expressing B cells and 12.4 % in B cells expressing both transgenes). B cells pro/pre-B-cell and immature B-cell populations as determined by the IgM/B220 staining were gated on hCD2 to see where the reduction in these B-cell stages is stronger.

The results (Tab. 3.1) show that while Notch2IC//CD19-cre mice display on average 38 % immature B cells that are hCD2^{pos} in the bone marrow, Notch2IC//LMP1/CD40//CD19-cre mice only display hCD2^{pos} 31 % immature B cells. With regard to the pro/pre B-cell population in the bone marrow this population is also reduced in Notch2IC//LMP1/CD40//CD19-cre mice with 20 % versus 26 % pro/pre B cells in Notch2IC//CD19-cre mice. These results point towards a partial block in both the pro/pre and the immature B-cell population in Notch2IC//LMP1/CD40//CD19-cre compared to Notch2IC//CD19-cre mice as previously established. However, comparing the ratios derived from the percentages of the respective B-cell compartment (1.2 in the immature and 1.3 in the pre/pro B-cell compartment) it is not possible to determine in which developmental stage the reduction is stronger Notch2IC//LMP1/CD40//CD19-cre mice.

All in all, this strongly suggests that there is either a negative selection of the bone marrow B cells expressing both transgenes in this B-cell stage compared to Notch2IC//CD19-cre mice.

Tab. 3.1 Early concomitant expression of constitutive Notch2IC and LMP1/CD40 affects early B-cell development in the bone marrow leading to an equal reduction in pre - and immature B-cell population. Average percentages with SDs of hCD2pos Pro/Pre and immature B cells as determined from IgM/B220-stainings (Fig. 3.14A; lower panel) after lymphocyte gate-, B220- and hCD2-pre-gating for Notch2IC//CD19-cre and Notch2IC//LMP1/CD40//CD19-cre mice. Calculations based on six independent experiments. SD, standard deviation.

	Immature B cells (hCD2^{pos})	Pro/Pre B cells (hCD2^{pos})
Notch2IC//CD19-cre	37.7 ±8.9	25.8 ±6.8
Notch2IC//LMP1/CD40//CD19-cre	30.5 ±5.2	20.3 ±5.4

3.6.3 Recirculation of mature B cells into the bone marrow is restricted in Notch2IC//LMP1/CD40//CD19-cre mice

The percentages of B220^{hi} cells in the stainings described above (Fig. 3.14A, refer to labeling of gates) hint at a reduction in immature and recirculating B cells in the bone marrow particulariy in the Notch2IC//LMP1CD19-cre compared to CD19-cre mice. A more precise evaluation for recirculating B cells can be achieved via staining of bone marrow cells with IgM/IgD/B220-antibodies and pre-gating on B220^{pos} cells (Fig. 3.15A). The previously observed reduction in mature recirculating B cells could indeed be further confirmed since there is a drop in the percentage of B220^{pos} IgD^{hi} IgM^{pos} cells in all transgene-expressing mice versus the CD19-cre control, but especially in Notch2IC//LMP1/CD40//CD19-cre mice (3 % versus 17 % in CD19-cre mice). This translates to significantly reduced numbers of recirculating B cells in Notch2IC//CD19-cre and LMP1/CD40//CD19-cre versus CD19-cre mice. This is even more pronounced in Notch2IC//LMP1/CD40//CD19-cre mice with 0.06×10^6 recirculating B cells versus 0.57×10^6 in CD19-cre and 0.22×10^6 recirculating B cells in LMP1/CD40//CD19-cre mice (Fig. 3.15B).
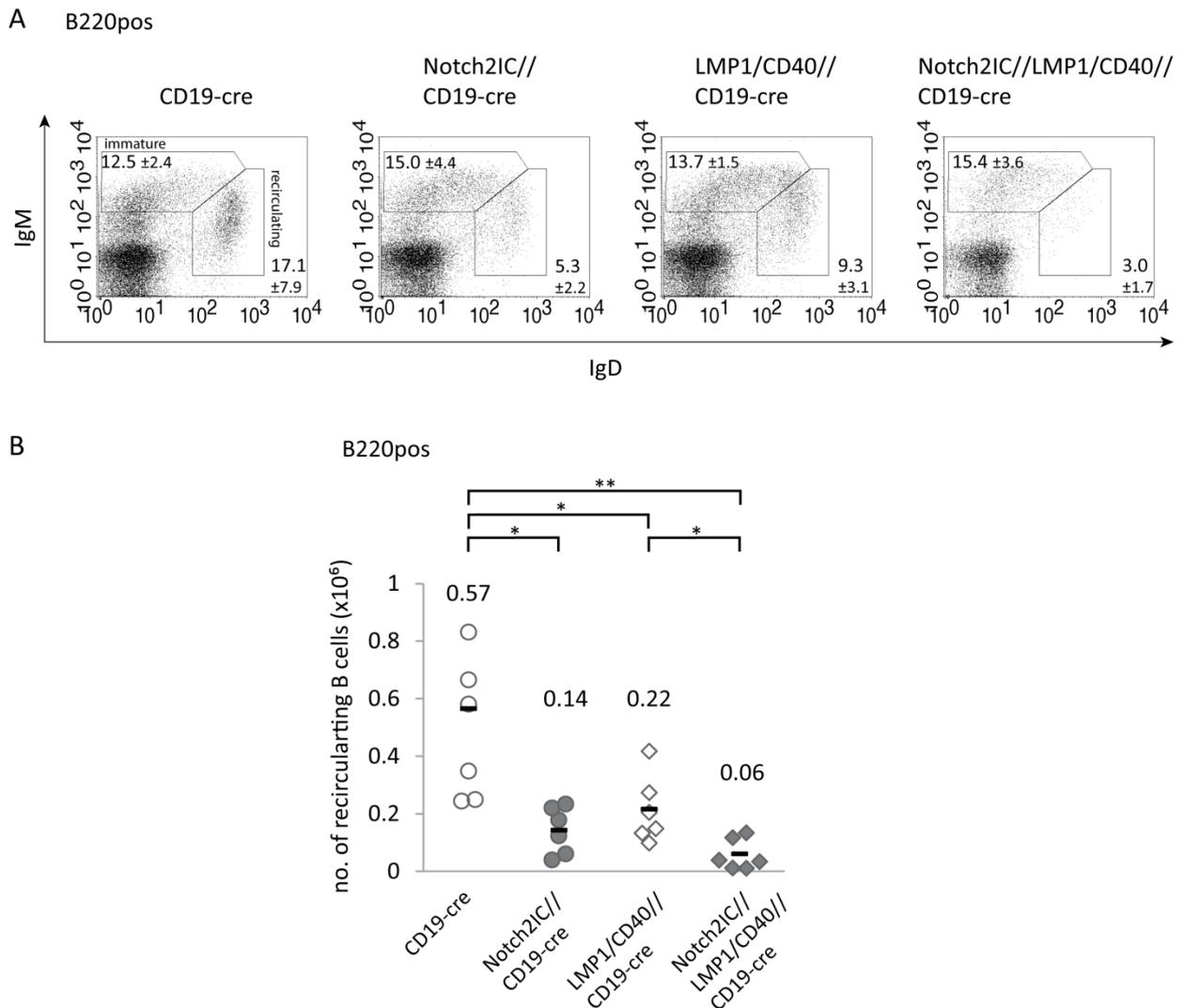
Fig. 3.15 Recirculation of mature B cells into the bone marrow is restricted in Notch2IC//LMP1/CD40//CD19-cre mice.
(A) FACS analysis results for IgM and IgD stainings of B220^{pos} cells to determine percentages of mature recirculating (IgM[pos] IgD[low/pos]) and immature B cells (IgM[pos] IgD[neg]) in the bone marrow with SDs. (B) Total cell numbers for recirculating B220[pos] B-cell populations as calculated from IgM/IgD/B220-stainings (in A) in lymphocyte gate. Numbers indicate mean percentages and SDs of lymphocyte-gated, B220[pos] B-cell populations and were calculated from six independent experiments. Cell number calculations: Points represent data from individual mouse and horizontal bars mark the mean value, indicated in numbers above each point column. SD, standard deviation; R, recirculating B cells; I, immature B cells.

3.7   AA4.1[pos] transitional B cells are not reduced in the spleens of Notch2IC//LMP1/CD40//CD19-cre mice

With the aim to follow up on the reduced numbers of pro-, pre- and immature B cells in Notch2IC//LMP1/CD40//CD19-cre mice, the levels of AA4.1^{pos} cells in the spleens of all four genotypes were examined. The surface marker AA4.1 characterizes transitional B cells that can only be found in the spleen. The flow cytometric analysis revealed that the percentages for transitional B cells of Notch2IC//LMP1/CD40//CD19-cre as well as in LMP1/CD40//CD19-cre mice

are rather reduced than increased compared to CD19-cre and Notch2IC//CD19-cre mice (Fig. 3.16A). This is in line with the finding that Notch2IC//LMP1/CD40//CD19-cre and LMP1/CD40//CD19-cre mice display less immature B cells in the bone marrow. However, since there is an overall increase in B cells both in the spleens of LMP1/CD40//CD19-cre and Notch2IC//LMP1/CD40//CD19-cre mice this percentile decrease does not lead to a reduction but rather a slight yet non-significant increase in overall cell numbers of transitional B cells in these two genotypes (Fig. 3.16B) pointing to an expansion of transitional B cells in the transitional B cell stage in both genotypes.
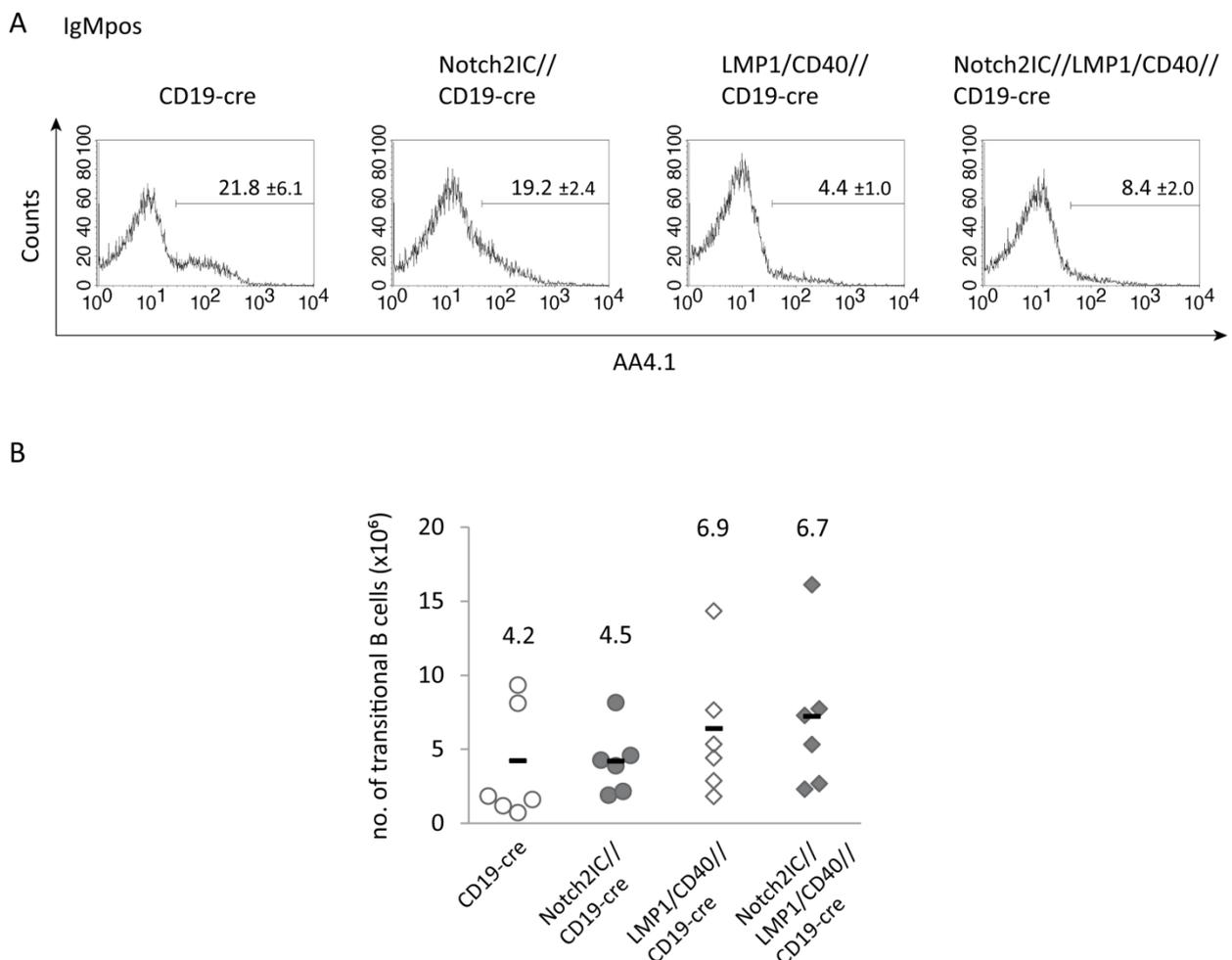
Fig. 3.16 AA4.1^{pos} transitional B-cell numbers are not reduced in spleens of Notch2IC//LMP1/CD40//CD19-cre mice.
Splenocytes were analyzed by flow cytometry for the expression of surface marker AA4.1, which characterize immature (transitional) B cells in the spleen. (A) Numbers indicate mean percentages and SD of lymphocyte-gated, IgM^{pos} AA4.1^{pos} populations. (B) Actual cell numbers were calculated from flow cytometric data in (A). Data was obtained from six independent experiments. Cell number calculations: Points represent data from individual mouse and horizontal bars mark the mean value, indicated in numbers above each point column. SD, standard deviation.

3.8   Marginal zone B cells are expanded in Notch2IC//LMP1//CD40//CD19-cre mice while the follicular B-cell population is decreased

With the aim to better characterize the different B-cell populations splenocytes from all four genotypes (CD19-cre, Notch2IC//CD19-cre, LMP1//CD40//CD19-cre and Notch2IC//LMP1//CD40//CD19-cre) were prepared and stained with antibodies against different surface markers and subjected to flow cytometric analysis. Firstly, surface markers (namely CD21, CD23, IgM and IgD) were employed as to allow making a distinction between MZ B cells and Fo B cells.

The surface CD21/CD23-staining allows for the unambiguous distinction between Fo B cells (CD21^{int} CD23^{pos}) and MZ B cells (CD21^{hi} CD23^{low}). The results of the flow cytometric analysis revealed that spleens of CD19-cre mice harbor few MZ B cells (6 % CD21^{hi} CD23^{low}) as opposed to Fo B cells (75 % CD21^{int} CD23^{pos}). Notch2IC-expressing splenic B cells show a strong shift of B cells adopting a MZ B-cell phenotype (≈63 %) at the expense of the Fo B-cell population (≈17 %). These Notch2IC-expressing B cells exhibit high levels of surface CD21 and have almost completely down-regulated CD23. LMP1/CD40-expressing splenic B cells display an intermediate phenotype (CD21^{hi} CD23^{int}) with B cells strongly trailing off from the Fo B-cell into the MZ B-cell compartment (Fig. 3.17B; upper panel) and display what can be characterized as a MZ B-cell-like phenotype. B cells additionally expressing constitutively active Notch2IC also display a shift of B cells towards adopting a MZ B-cell phenotype (≈48 %, Fig. 3.17A, upper panel), while only few cells exhibit a Fo B-cell type (≈20 %). Interestingly, the Notch2IC//LMP1/CD40-expressing MZ B cells rather resemble the CD19-cre MZ B cells since they do not down-regulate CD23 as strongly as the Notch2IC-expressing B cells do.

The findings concerning the MZ B-cell status of the B cells expressing both constitutively active Notch2IC as well as constitutively active CD40 were confirmed with the help of an IgM/IgD-staining. The gate comprising cells with high IgM and low IgD contains MZ B cells, but also transitional and B1 B cells whereas IgM$^{pos/low}$ IgD^{pos} B cells are Fo B cells. The B cells of CD19-cre mice display a normal distribution pattern with the large majority of cells being IgM$^{pos/low}$ IgD^{pos} and therefore Fo B cells (≈74 %). Only a small percentage of B cells of CD19-cre carries the surface markers characterizing MZ, B1 and transitional B cells (≈17 % IgM^{hi} IgD^{low}).
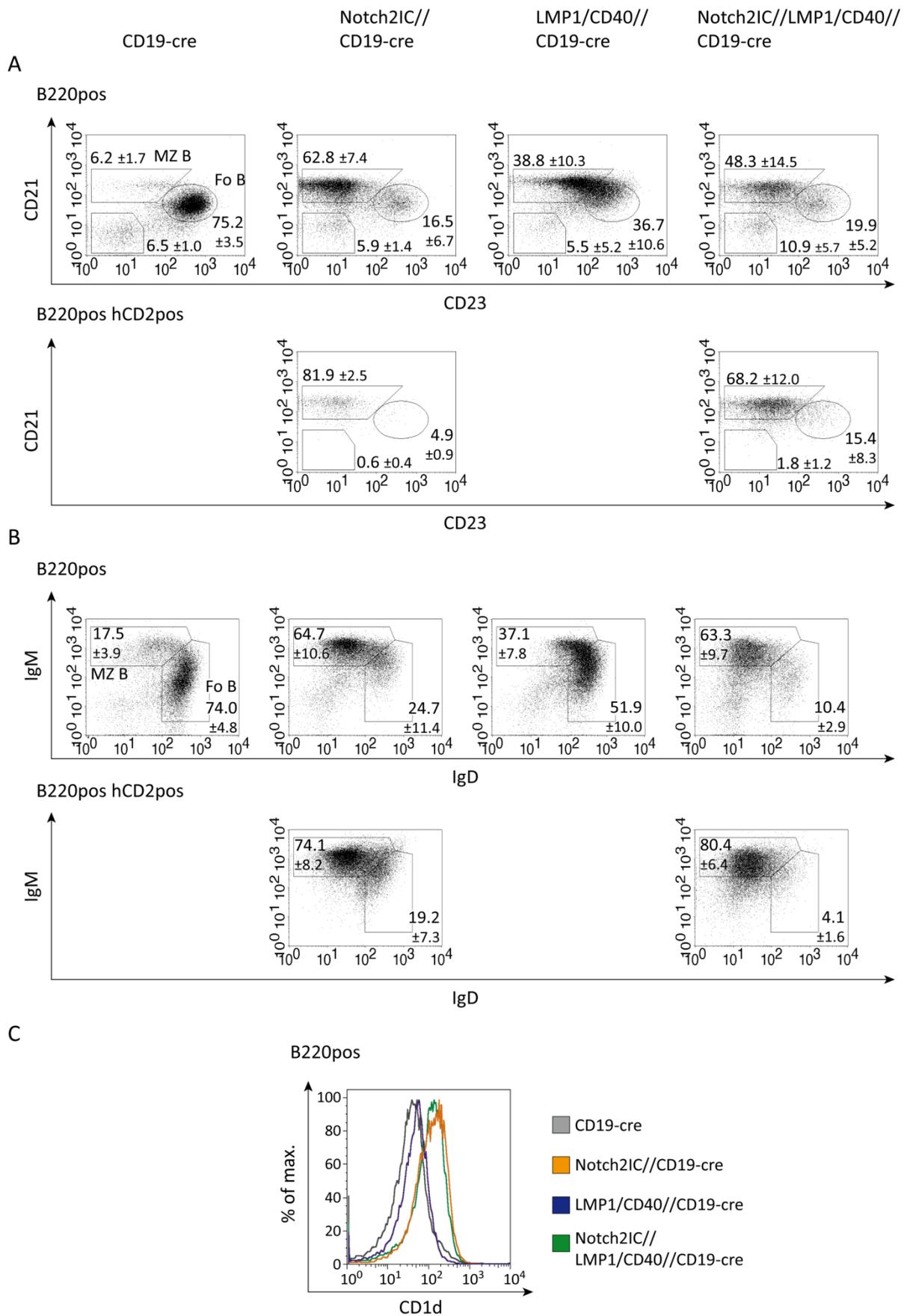
Fig. 3.17 Marginal zone B cells are expanded in Notch2IC//LMP1/CD40//CD19-cre mice while the follicular B-cell population is decreased.

(A) Flow cytometric analysis of Fo (CD21^{int} CD23^{pos}) and MZ B cells (CD21^{hi} CD23^{low}) in the spleen. CD21^{neg} CD23^{neg} cells comprise immature and non-B cells. Numbers indicate mean percentages and SD of lymphocyte-gated, B220^{pos} B cells displaying the respective phenotypes. Re-gating the cells on hCD2 allows for identification of the phenotype of the cells expressing the transgenes (lower panel). Calculations are based on six independent experiments. (B) Splenocytes were analyzed by flow cytometry for the expression of surface IgM and IgD. Numbers indicate mean percentages and SD of lymphocyte-gated populations of B220^{pos} B cells displaying a Fo (IgM^{pos} IgD^{pos}) or MZ and transitional (IgM^{pos} IgD^{low}) B cell phenotype (upper panel). Re-gating the cells on hCD2 allows for identification of the phenotype of the cells expressing the transgenes (lower panel). (C) Histograms show overlays of CD1d-expression of splenic B cells of in CD19-cre (grey line), Notch2IC//CD19-cre mice (orange line), LMP1/CD40//CD19-cre mice (purple line) and Notch2IC//LMP1/CD40//CD19-cre mice (green line). Fo B, follicular B cell; MZ B, marginal zone B cell; SD, standard deviation.

In the flow cytometric analysis of the B cells expressing constitutively active Notch2IC, most B cells exhibit high levels of IgM, while intermediate to low IgD-levels in accordance with their MZ B-cell phenotype. LMP1/CD40-expressing B cells are positive for both IgM and IgD, but the cells strongly trailing off becoming intermediate in their IgD expression, therefore they display an intermediate phenotype similar as observed in the CD21/CD23 staining. However, when B cells express both the Notch2- as well as the CD40-transgene they can be clearly classified as MZ B cells with regard to their high IgM- and low IgD-level (Fig. 3.17B; upper panel), even though the effect is not as pronounced as in Notch2IC-expressing B cells alone (≈48 % MZ B cells versus ≈63 % in Notch2IC//CD19-cre mice).

Overall, constitutive Notch2IC-expression in B cells seems to be the decisive factor whether these cells present with a clear MZ B-cell phenotype.

Re-gating the previous FACS staining results for IgM/IgD and CD21/CD23 on hCD2^{pos} reveals that expression of Notch2IC is indeed correlated with the MZ B-cell phenotype, since the hCD2^{pos} cells of Notch2IC//CD19-cre and Notch2IC//LMP1/CD40//CD19-cre mice can be found within the MZ B cell gates (IgM^{pos} IgD^{low} and CD21^{hi} CD23^{low}, respectively).

Furthermore, splenic B cells of the respective genotype were analyzed for the presence of the MZ B-cell surface marker CD1d. Both Notch2IC-expressing B cells and B cells of Notch2IC//LMP1/CD40//CD19-cre mice are also high in their CD1d expression confirming their MZ B-cell phenotype (Fig. 3.17C)

3.9   Splenic B cells of Notch2IC//LMP1/CD40//CD19-cre mice display an activated phenotype

MZ B cells have a pre-activated phenotype and are larger than their follicular counterparts. Activated lymphocytes generally have a tendency to increase in volume, this was previously observed in LMP1/CD40-expressing splenic B cells which show an increase in cell size and an upregulation of activation markers. This could also be recapitulated in the MZ Notch2IC-expressing B cells. These also express various MZ B-cell-characteristic surface markers such as CD1d, CD36, and CD9 and are increased in size compared to CD19-cre controls (Hampel et al., 2011). This is the reason that could account for the slight, but significant splenomegaly in those Notch2IC//CD19-cre animals versus the CD19-cre mice. Therefore, splenocytes of all genotypes were analyzed with regard to both cell size (through comparison of the FACS FSC, which is indicative of cell size) and with regard to expression of activation surface markers (such as CD80, CD86, CD95, MHCII and ICAM1 (CD54)).

Fig. 3.18A confirms the increase in cell size in both single transgene expressing splenic lymphocytes, which is even furthered in the Notch2IC//LMP1/CD40//CD19-cre animals. Up-regulation of activation marker CD95 is –as shown in section 3.2- a CD40-mediated event and is found to be even slightly increased in the splenic B cells of Notch2IC//LMP1/CD40//CD19-cre mice (Fig. 3.18B). This also seems to be the case for the expression of the B7 protein CD80, which mediates B-T-cell interactions like the B7 protein CD86. CD80 is found to be up-regulated only in B cells of LMP1/CD40//CD19-cre and even slightly stronger in Notch2IC//LMP1/CD40//CD19-cre mice, while levels of CD86 seem widely unchanged in all genotypes with respect to the CD19-cre control.

Concomitant expression of Notch2IC and LMP1/CD40 seems to have an additive effect on the level of ICAM1-expression. The expression levels of this cell surface marker are higher both in Notch2IC-expressing, as well as in LMP1/CD40-expressing B cells compared to CD19-cre mice. ICAM1 levels are even further increased in B cells expressing both transgenes.

MHCII expression however only showed a slight shift towards higher expression in splenic B cells of Notch2IC//CD19-cre, LMP1/CD40//CD19-cre and Notch2IC//LMP1/CD40//CD19-cre mice compared to CD19-cre mice (data not shown).

A

Topro-3neg (living) cells

- CD19-cre
- Notch2IC//CD19-cre
- LMP1/CD40//CD19-cre
- Notch2IC//
  LMP1/CD40//CD19-cre

B

B220pos cells
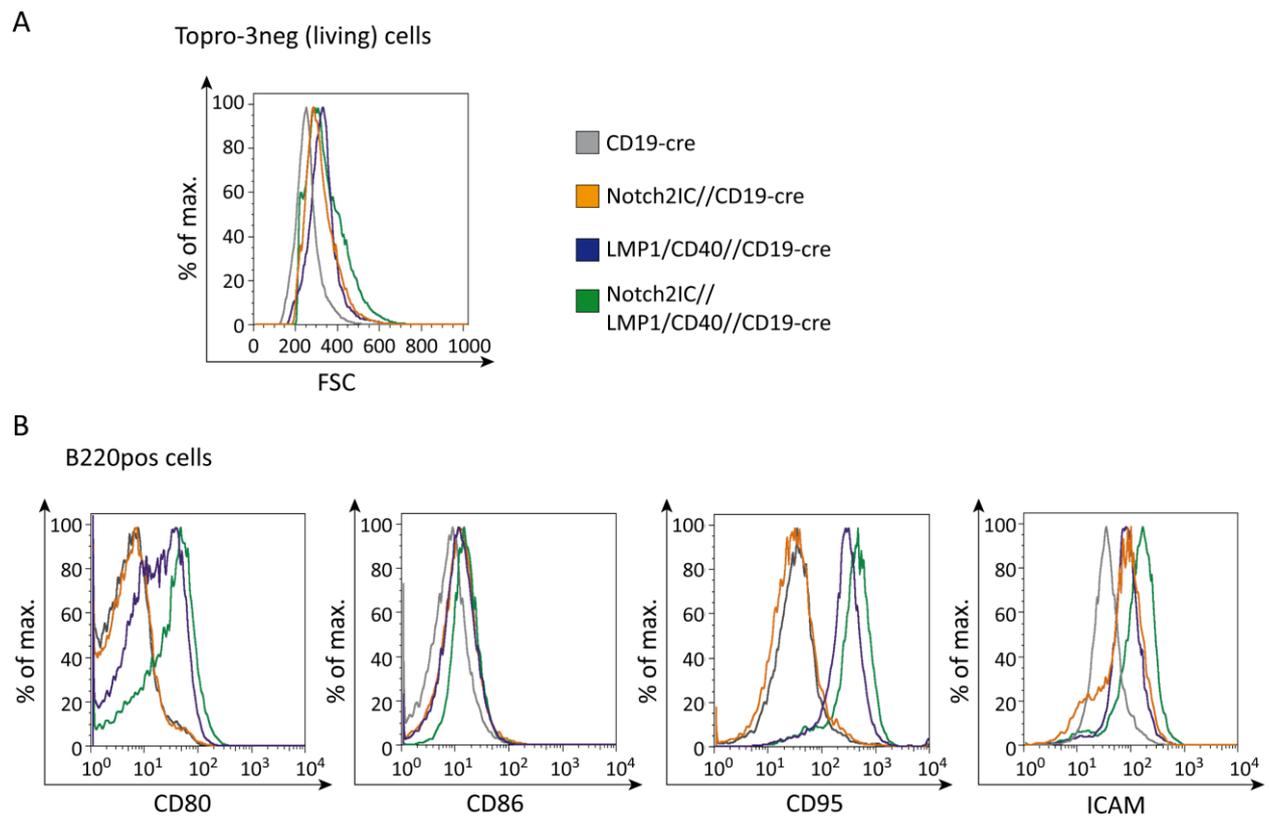
Fig. 3.18 Notch2IC//LMP1/CD40-expressing splenic B cells show an increase in cell size and enhanced expression of cell surface activation markers.
(A) Splenocytes were analyzed for cell size and surface expression of (B) CD80, CD86, CD95 and ICAM1 by flow cytometric analysis. Histograms show overlays of cell size (FSC) or overlays of surface expression of the indicated molecules on lymphocyte-gated, B220^{pos} B cells from CD19-cre (grey line), Notch2IC//CD19-cre mice (orange line), LMP1/CD40//CD19-cre mice (purple line) and Notch2IC//LMP1/CD40//CD19-cre mice (green line). Data are representative for six independent experiments. FSC, forward scatter.

3.10 B-cell numbers are reduced and B-cell subsets are altered in inguinal lymph nodes of Notch2IC//LMP1/CD40//CD19-cre mice

3.10.1 T-cell numbers are normal but B-cell numbers are significantly reduced in inguinal lymph nodes of Notch2IC//LMP1/CD40//CD19-cre mice compared to CD19-cre and LMP1/CD40-cre mice

With the aim to further examining B cells in the periphery inguinal lymph nodes were prepared from mice of all genotypes (CD19-cre, Notch2IC//CD19-cre, LMP1/CD40//CD19-cre and Notch2IC//LMP1/CD40//CD19-cre). Evaluation of the actual B- and T-cell numbers (based on data obtained from flow cytometric analysis) showed that T-cell numbers were overall similar between the different genotypes (Fig. 3.19; right panel). However, B-cell numbers are only increased in lymph nodes of LMP1/CD40//CD19-cre mice, but they are significantly reduced both in Notch2IC//CD19-cre and Notch2IC//LMP1/CD40//CD19-cre compared to CD19-cre mice (Fig. 3.19; left panel).
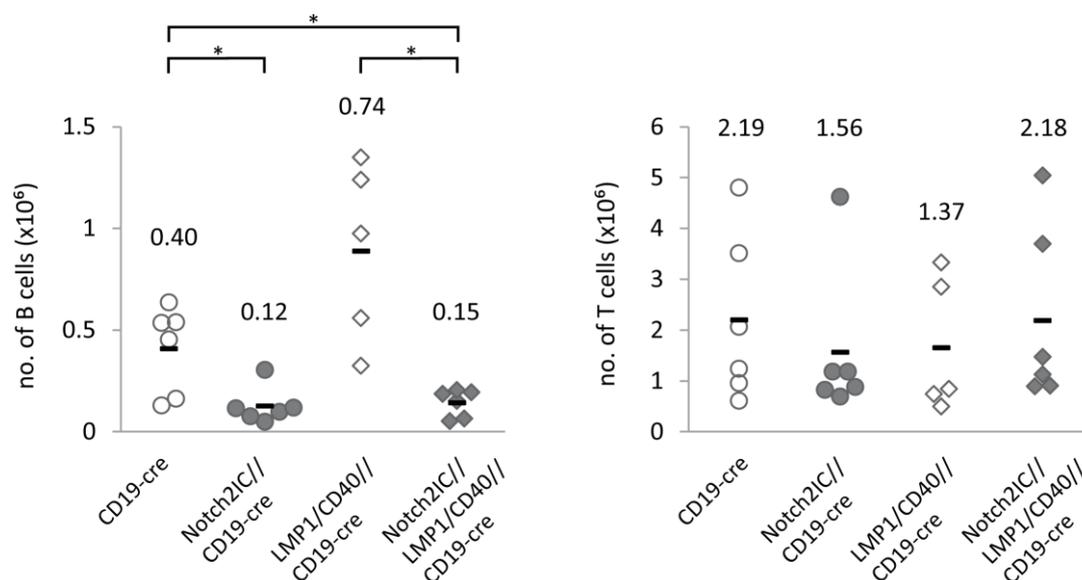
Fig. 3.19 T-cell numbers are normal but B-cell numbers are reduced in inguinal lymph nodes of Notch2IC//LMP1/CD40//CD19-cre mice
Total B-cell (lymphocyte-gated, B220^{pos}) and T-cell (lymphocyte-gated, CD3^{pos}) numbers of iLN. Topro-3^{pos} (dead) cells were excluded from the analysis. Calculations are based on six independent experiments. Points represent data from individual mouse and horizontal bars mark the mean value, indicated in numbers above each point column. iLN, inguinal lymph nodes; SD, standard deviation.

3.10.2 B cells in inguinal lymph nodes of Notch2IC//LMP1/CD40//CD19-cre mice display a shift towards a MZ B-cell phenotype

MZ B cells represent a B-cell population that is rather sessile in the spleen, while Fo B cells can freely circulate in blood and lymph until they encounter antigen. Hence, the presence of MZ B cells in lymph nodes is not expected. Nonetheless, previous analysis of the Notch2IC//CD19-cre (Hampel et al., 2011) also showed that B-cell subsets are altered in the inguinal lymph nodes of Notch2IC//CD19-cre mice in the sense that they display a tendency towards adopting a MZ B-cell phenotype. This prompted further analysis of this secondary lymphoid organ in Notch2IC//LMP1/CD40//CD19-cre mice and controls with respect to their phenotype.

With regard to the results of CD21/CD23 staining the majority of all inguinal lymph node B cells of all genotypes displays a Fo B-cell phenotype (CD21int CD23pos; Fig. 3.21A). These findings could be confirmed with the results of the IgM/IgD staining where B cells were IgMpos/low and IgDpos (Fig. 3.21C).
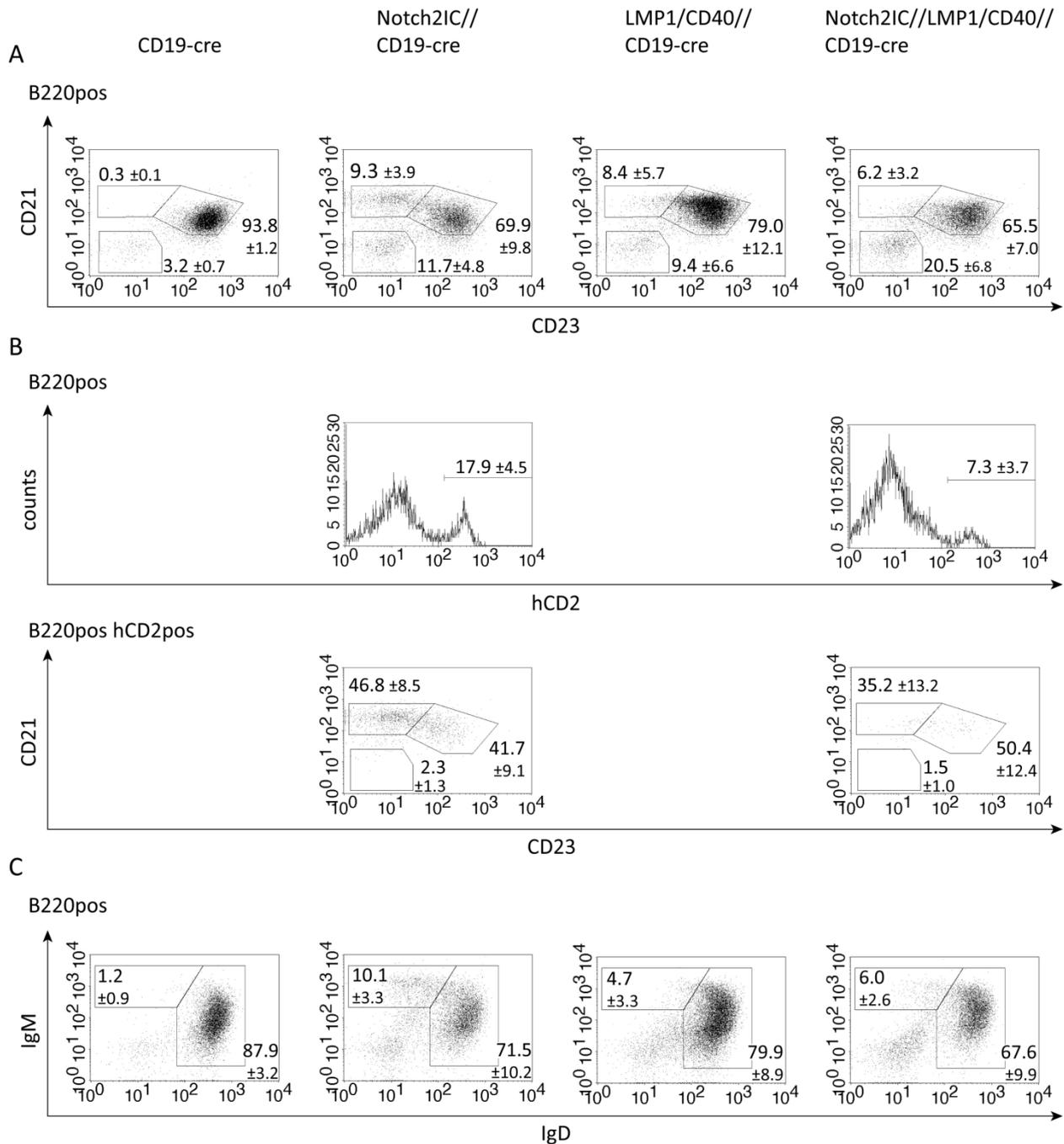
Fig. 3.20 B-cell subsets are altered in the inguinal lymph nodes of Notch2IC//LMP1/CD40//CD19-cre mice.

(A) Lymphocytes of iLN were analyzed by flow cytometry for the expression of IgM and IgD. Numbers indicate mean percentages and SD of lymphocyte-gated populations of B220^{pos} B cells displaying a Fo (IgM[pos] IgD[pos]) or MZ and transitional (IgM[pos] IgD[low]) B-cell phenotype. (B) Average hCD2 percentages with SD in B220^{pos} B cells of iLN as determined by FACS analysis for the respective genotypes. Lower panel: Re-gating the cells in the IgM/IgD staining results on hCD2 allows for identification of the phenotype of the cells expressing the transgenes. (C) Flow cytometric analysis of Fo (CD21^{int} CD23^{pos}) and MZ B cells (CD21^{hi} CD23^{low}) in the iLN. CD21^{neg} CD23^{neg} cells comprise immature and non-B cells. Numbers indicate mean percentages and SD of lymphocyte-gated, B220^{pos} B cells displaying the respective phenotypes (upper panel). Calculations are based on six independent experiments. iLN, inguinal lymph nodes; SD, standard deviation.

Nonetheless, the percentages of B cells that display a MZ B-cell phenotype (CD21^{hi} CD23^{low}) are strongly increased in Notch2IC//CD19-cre, LMP1/CD40//CD19-cre and Notch2IC//LMP1/CD40//CD19-cre mice in the CD21/CD23 staining in comparison to the CD19-cre control mice. This could again be reconfirmed with the results of the IgM/IgD staining where percentages of MZ B-cells (IgM^{pos} IgD^{low}) in inguinal lymph nodes were strongly increased compared to CD19-cre mice. However it has to be kept in mind that the fraction of cells that are IgM^{pos} IgD^{low} comprises besides MZ B cells also B1 B and is a less specific indicator for a MZ B-cell phenotype.

In the inguinal lymph nodes of Notch2IC//CD19-cre and Notch2IC//LMP1/CD40//CD19-cre mice B cells fewer B cells had deleted the stop cassette upstream of the Notch2IC-transgene than in the spleen ($\approx$18 % hCD2^{pos} B cells in inguinal lymph nodes in Notch2IC//CD19-cre and $\approx$7 % in Notch2IC//LMP1/CD40//CD19-cre mice; Fig. 3.20B, upper panel). Pre-gating the inguinal lymph node B cells on hCD2 in the CD21/CD23 staining analysis however shows that roughly half of the B cells that have successfully deleted the stop cassette and express the transgene adopt a MZ B-cell phenotype (47 % in Notch2IC//CD19-cre and 35 % in Notch2IC//LMP1/CD40//CD19-cre mice Fig. 3.21B; lower panel). This is recapitulated in the expression of surface IgM and IgD expression in the hCD2^{pos} lymph node B cells of Notch2IC//CD19-cre and Notch2IC//LMP1/CD40//CD19-cre mice with increased percentages of lymph node B cells that are IgM$^{pos/low}$ IgD^{pos} (data not shown). All in all, considering the low numbers of B cells and particularly hCD2^{pos} B cells in inguinal lymph nodes of Notch2IC//CD19-cre and Notch2IC//LMP1/CD40//CD19-cre mice one could assume that the mature hCD2-expressing B cells are rather retained in the spleen, which would be in line with their physiological sessile character. Nonetheless, the cells in the inguinal lymph nodes that are positive for hCD2 rather display a MZ B-cell phenotype.

3.11 Splenic architecture is grossly disrupted in Notch2IC//LMP1/CD40//CD19-cre mice

In order to better characterize the splenomegaly as well as to define the follicular space and to localize the different B- and T-lymphocyte populations in general immunohistochemistry (IHC) on splenic cryosections was performed (Fig. 3.21). Spleens were stained for IgM^{pos} B cells, for CD3^{pos} T cells and MOMA1, which stains monocytes and metallophilic macrophages. Metallophilic macrophages line the inner border of the MZ and employing the antibody in the staining allows for a visual separation of the MZ B cells from the Fo B cells.
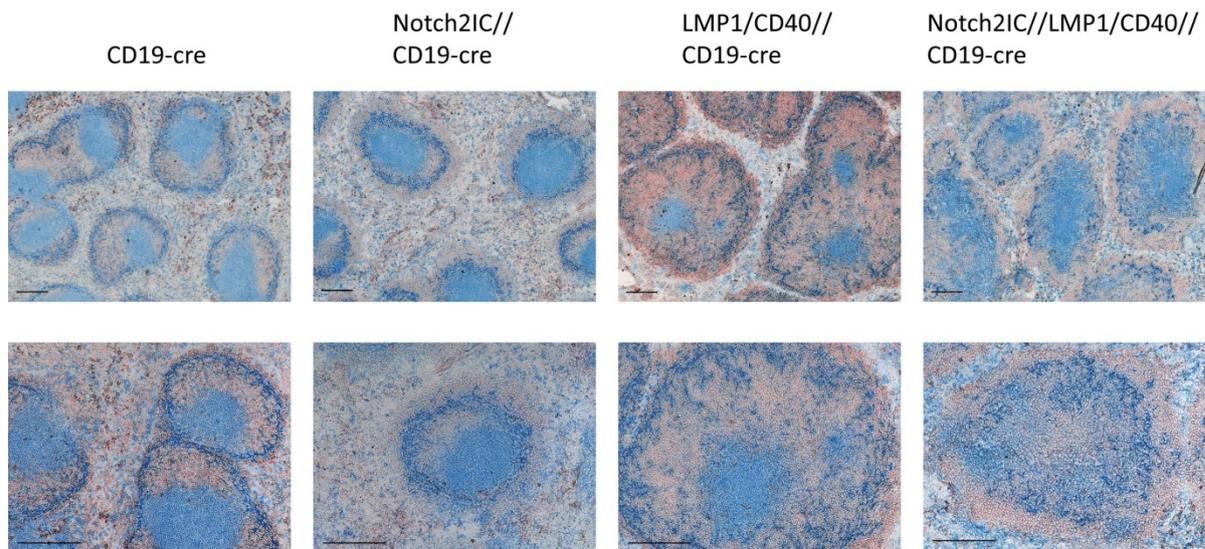
Fig. 3.21 Splenic architecture is grossly disrupted in Notch2IC//LMP1/CD40//CD19-cre mice.
IHC staining of splenic cryosections from Notch2IC//CD19-cre and control mice for monocytes and metallophilic macrophages (α-MOMA-1; dark blue), lining the marginal zone at the sinus, B cells (α-IgM; red) and T cells (α-CD3; light blue). Bar: 100μm. IHC, immunohistochemistry; MZ, marginal zone.

The triple staining showed that the follicles in CD19-cre mice are small with a small ring of MZ B cells surrounding them. The follicle holds the majority of Fo B cells and a well-defined, localized T-cell zone. In Notch2IC//CD19-cre mice as previously documented (Hampel et al., 2011) follicles are still small, which is in accordance with the fact that overall cell numbers are not increased compared to spleens of CD19-cre mice (Fig. 3.1A).

However, the area of MZ B cells is markedly enlarged, and the Fo B cells are rather reduced, but the T-cell zone is equal in size compared to that in CD19-cre mice. Nonetheless, overall follicular structure is retained in Notch2IC//CD19-cre, which is also the case for the spleen of LMP1/CD40//CD19-cre mice. However, the spleens of the latter genotype display an enlargement of follicles as such and of the MZ- and T-cell zone which is in accordance both with the increase in overall spleen size, total cell and lymphocyte numbers. Nonetheless, one can determine that the ring of MOMA1^pos cells is less distinct but rather appears as a rather diffuse pattern that extends well into area of the Fo B cells. The assessment of the IHC of splenic cryosections of Notch2IC//LMP1/CD40//CD19-cre mice delivered completely different results: the follicles are enlarged as was expected according to spleen size, total cell and lymphocyte numbers, but microachitectural order is severely affected. The otherwise defined ring of MOMA1^pos cells is disintegrated and merges with the B and T cells in the follicle. Notch2IC//LMP1/CD40//CD19-cre mice exhibit a strongly enlarged MZ, nonetheless the majority of B cells seems to reside in the Fo area. The T cells are almost dispersed throughout the entire follicle, which allows for constant B- and T-cell interaction.

3.11.1 Splenic B cells of Notch2IC//LMP1/CD40//CD19-cre mice are intermediate in their CXCR4 expression

Chemokine receptors, including CCR7, CXCR4, and CXCR5, are known to be of key importance in the regulation of B-cell trafficking and retention (Cyster, 1999; Okada et al., 2002; Ebisuno et al., 2003). Expression of CXCR5 can be detected on mature B cells and is essentially responsible for guiding B cells into the B-cell zones of secondary lymphoid organs. In CXCR4-deficient mice mature B-cell populations were reduced in the marginal zone and primary follicles and they show defective follicle formation (Nie et al., 2004).

In order to clarify what might be the factors contributing to the observed mispositioning of B cells in the Notch2IC//LMP1/CD40//CD19-cre mice CXCR4 and CXCR5 stainings were performed with splenocytes preparations from all four genotypes and subjected to FACS analysis. Additional staining for the presence of CD21/CD23-surface markers permits to analyze the respective MZ and Fo B-cell populations in greater detail.

The results (Fig. 3.22A) were most distinct with regard to the MZ B cell compartment (CD21^{hi} CD23^{low}). They show that CXCR4–expression is up-regulated in Notch2IC-expressing MZ B cells in comparison to all other genotypes. MZ B cells (CD21^{hi} CD23^{low}) B cells from LMP1/CD40//CD19-cre mice on the other hand displayed the lowest CXCR4 surface marker expression. This might explain that the majority of their B cell residing rather in the follicle, although the population strongly trails off into the MZ B cell compartment. Interestingly, MZ B cells from CD19-cre mice had an intermediate CXCR4 surface marker expression just like the B cells in Notch2IC//LMP1/CD40//CD19-cre mice display a rather intermediate CXCR4-level phenotype. With regard to the Fo B cell compartment (CD21^{int} CD23^{pos}), LMP1/CD40 also exhibited slightly lower levels, Notch2IC-expressing B cells still exhibited higher number for CXCR4^{hi} B cells. This pattern could also be observed to a lesser degree when gating the cells on the B-cell marker CD19 alone without prior pre-gating on MZ and Fo B cells (data not shown) and the levels remained similar with minor shifts in CXCR4 expression strength when Fo B cells were compared to MZ B cells of the same genotype, i.e. CD19-cre (Fig. 3.22B).

CXCR5 levels were equally examined in the four genotypes. However, distinct differences were undetectable among the B cells of the different genotypes (data not shown).

All in all, one could assume that constitutive CD40- and constitutive Notch2-activity oppose each other with regard to positioning of the respective Notch2- or CD40-expressing cell and up- or down-regulation of CXCR4. These might be the forces at work in B cells of Notch2IC//LMP1/CD40//CD19-cre expressing both transgenes. However, CXCR4 levels as such do not provide hints as to where a given B cell will be positioned, since B cells of CD19-cre mice also display rather intermediate level of this chemokine receptor.
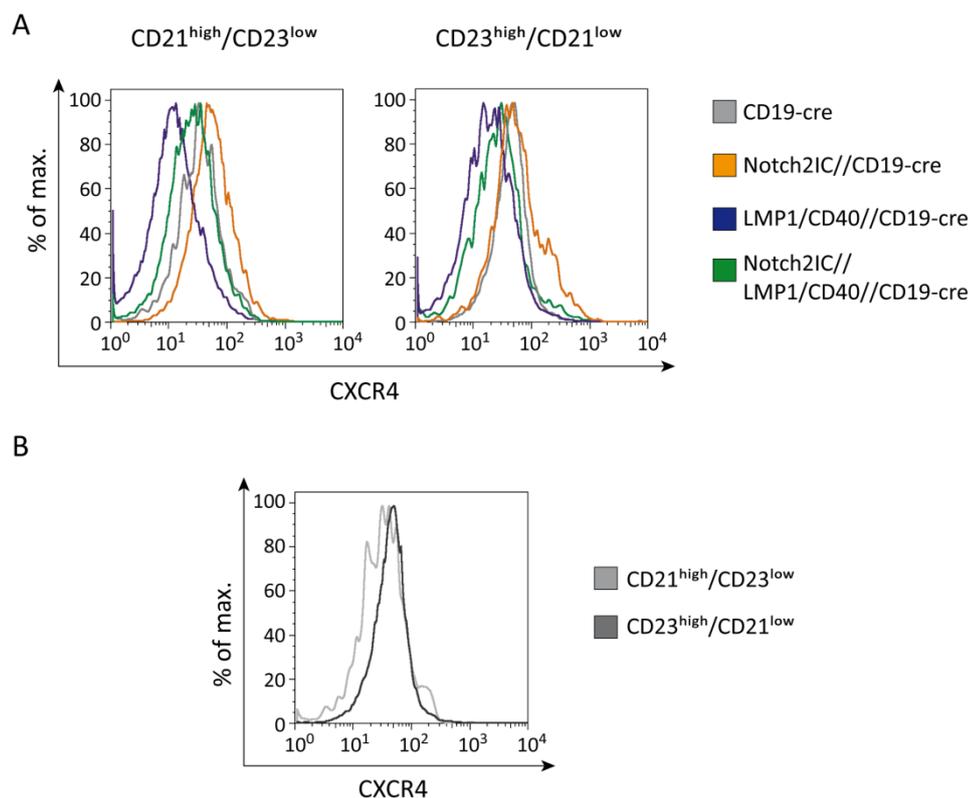
Fig. 3.22 B cells of Notch2IC//LMP1/CD40//CD19-cre mice display intermediate level in their CXCR4 expression.
(A) Flow cytometric analysis results of the CXCR4-levels of pre-gated B cells (CD19^{pos} cells) for the different genotypes. Histogram represents an overlay of all genotypes analyzed. CD19-cre (grey line), Notch2IC//CD19-cre mice (orange line), LMP1/CD40//CD19-cre mice (purple line) and Notch2IC//LMP1/CD40//CD19-cre mice (green line). Data are representative for three independent experiments. (B) Flow cytometric analysis results of the CXCR4-levels of MZ B (light grey) versus Fo B cells (dark grey) of the same genotype (CD19-cre).

3.12 Notch2IC//LMP1/CD40//CD19-cre mice show distinct changes in the expression of cyto- and chemokines

Cyto- and chemokines might be the major factors leading or contributing to the surge in accessory cells and disrupted follicular structures in Notch2IC//LMP1/CD40//CD19-cre mice. These messenger substances can act both over long distances as well as only in situ. Aiming to identify them both on a systemic and local scale, arrays were used to detect changes in serum levels and mRNA-levels specifically in B cells of a broad range of cyto- and chemokines in mice of all four genotypes.

3.12.1 CXCR3 and IL13ra1, IL2Rγ, LTβ and TGFβ mRNA levels in splenic B cells of Notch2IC//LMP1/CD40//CD19-cre mice are differentially up-regulated by Notch2IC and LMP1/CD40

In order to examine the level of cyto- and chemokines that were exclusively produced by the B cells, splenic B cells from all four genotypes were purified using the MACS-separation system to deplete CD43^{pos} (i.e. non-B) cells from the samples. From these splenic B cells mRNA was extracted from which cDNA (complementary DNA) was synthesized. The cDNA was subsequently employed as template in a RT-PCR (real-time polymerase chain reaction) run. The RT-PCR was carried out in a 96-well format obtained from SA Biosciences with pre-spotted primers in each well for each cyto- and chemokine to be analyzed. Results were normalized to values obtained for the control CD19-cre mice (Fig. 3.23).

The mRNA analysis of splenic B cells revealed that only few cyto- and chemokines were up-regulated. Usually the respective cyto- or chemokine was up-regulated in either one of the two transgene-expressing B cells and rather exhibited intermediated mRNA levels in splenic B cells expressing both transgenes simultaneously.

Those cyto- and chemokines that were up-regulated particularly in Notch2IC-expressing B cells were CXCR3 and IL13Rα1.

CXCR3 is highly expressed on activated T cells, but usually not found on resting T lymphocytes, monocytes and granulocytes (Loetscher et al., 1996), but is increased on MZ versus Fo B cells (S. Ehrenberg, personal communication).

IL13ra1 is a subunit of both IL13R and IL4R and together with the common γ chain and other subunits it forms the respective receptor for the Th2 cytokines. Both cytokines are known for their anti-inflammatory character (Watson et al., 1999; Zaccone et al., 1999; Kaminski et al., 2007), however in a B-cell context IL4 together with CD40 can induce a burst in proliferation, division and class switching (Rush et al., 2001).

The cyto- and chemokines that were up-regulated particularly in LMP1/CD40-expressing splenic B cells and to a lesser degree in Notch2IC//LMP1/CD40-expressing splenic B cells were the cytokine receptor IL2Rγ, lymphotoxinβ (LTβ) and TGFβ.
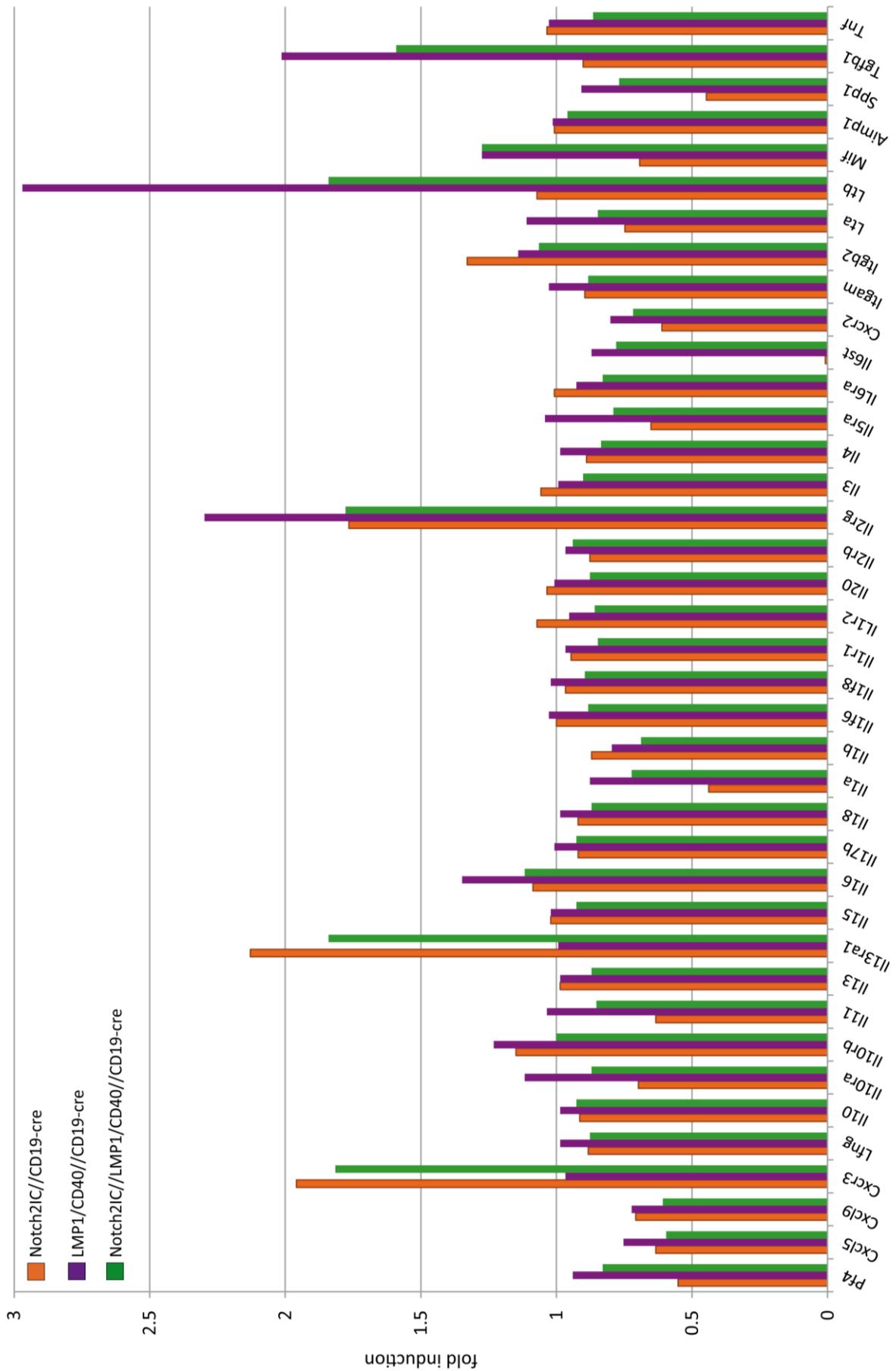
Fig. 3.23 CXCR3 and IL13ra1, IL2Rγ, LTβ and TGFβ mRNA levels in B cells of Notch2IC//LMP1/CD40//CD19-cre mice are differentially up-regulated by Notch2IC and LMP1/CD40.

Splenocytes from all four genotypes were purified by MACS-separation to deplete CD43^{pos} (i.e. non-B) cells from samples. mRNA from B cells was used as template for cDNA synthesis, which was used in a RT-PCR run. The RT-PCR was carried out in a 96-well format obtained from SA Biosciences with pre-spotted primers for each cyto- and chemokine to be analyzed and controls per well. Results were normalized to values obtained for the control CD19-cre mice. LTβ, lymphotoxinβ; MACS, magnetic cell separation, TGFβ, transforming growth factor β.

IL2Rγ also more commonly known as the common γ chain that is a subunit of some different ILRs, not only of IL2R, but also of the IL4-, IL7-, IL9-, IL15- and IL21-receptors (Takeshita et al., 1992; Russell et al., 1993; Asao et al., 1993; Sugamura et al., 1995; Asao et al., 2001) which play a pivotal role in development and function of B-, T- and NK-cells.

TGFβ is known to be influence numberous cellular processes rangeing from cell cycle regulation, differentiation, programmed cell death, adhesion and motility (Padua et al., 2009; Akhurst et al., 2012).

LTβ has been found to be of key importance during the initial organization of the lymphoid tissue during development (Murphy et al., 1998). The stromal cells in the spleen express the receptor while the ligand is majorly found on B cells (McDonald et al., 2005), which is important for positioning processes within the lymphoid follicles and proper development of the T-cell zone (Ngo et al., 2001). Combination of Notch2 and LMP1/CD40 signaling up-regulated genes might lead to the disruption of the splenic architecture.

3.12.2 Notch2IC//LMP1/CD40//CD19-cre mice show an upregulation of CXCL9 and CXCL10 in serum

In order to examine levels of different cytokines on a systemic level, serum samples from mice of all four genotypes were collected and applied to nitrocellulose membranes onto which capture antibodies have been spotted in duplicate. Adding streptavidin-horseradish peroxidase and a common chemiluminescent detection reagents, a signal is produced in proportion to the amount of the respective cytokine bound. Detection is performed as for common Western blots and level of cytokine was quantified from comparative analysis of three cytokine arrays per genotype with the TINA software (Raytest) by Lothar Strobl of our group (Fig. 3.24).

For most cytokines the results were out of range (i.e. either too strong or weak) in the comparative analysis. However, three cytokines were found to be reliably up-regulated in the sera of Notch2IC//LMP1/CD40//CD19-cre mice, namely IL16, chemokine (C-X-C) ligand (CXCL)10 and CXCL9, while IFNγ was slightly and CXCL12 (ligand for CXCR4) was distinctly reduced in these mice.

As suggested by their alternative names monokine-induced by IFN-γ, MIG (CXCL9) and IFNγ inducible protein-10, IP10 (CXCL10) these CXCLs are induced by IFNγ and are therefore also termed Th1-type cytokines.
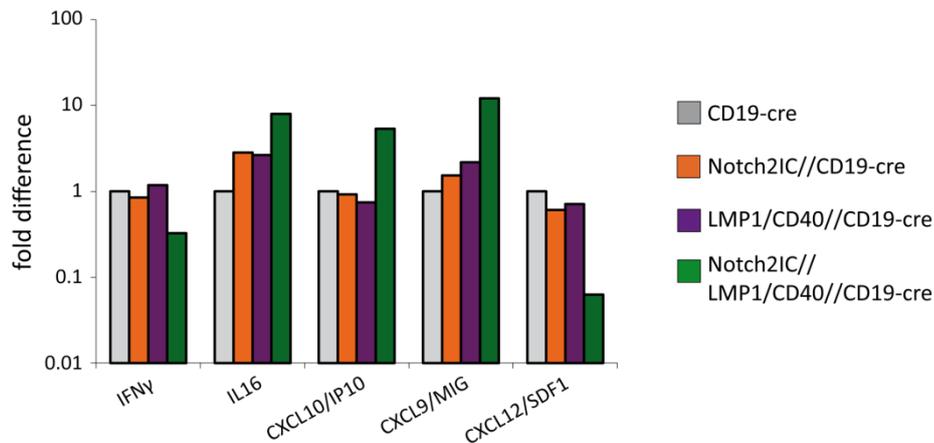
Fig. 3.24 Notch2IC//LMP1/CD40//CD19-cre mice show an up-regulation of CXCL9 and CXCL10 and a down-regulation of CXCL12 in serum.
Serum samples were prepared from heart blood and applied to R&D Proteome Profiler Mouse Cytokine Array Kit membranes. Using SA-HRS peroxidase and detection agents the amount of chemiluminescence is proportional to the amount of cytokine detected. Amount of chemiluminescent signal was quantified using TINA software. The displayed result is derived from comparative analysis of three independent experiments. Values for CD19-cre were set to 1 for normalization. SA-HRS peroxidase, streptavidin-horseradish peroxidase.

3.13 Notch2IC//LMP1/CD40-expressing splenic B cells show an increased proliferation in in vitro culture regardless of the supply of stimuli

Having observed that the splenic B cells are highly activated, it would be interesting to observe their growth behavior under controlled conditions. Primary wild type B cells die within 1 week of in vitro cultures without activating stimuli. The inherently activated phenotype of LMP1/CD40-expressing splenic B cells induces an increase in proliferation as well as enhanced survival in in vitro cultures in comparison to B cells from CD19-cre mice (Homig-Holzel et al., 2008). Also, the pre-activated phenotype of Notch2IC-expressing splenic B cells leads to an increased proliferation rate in comparison to controls (Hampel et al., 2011). Moreover, both CD40 and Notch are found up-regulated in various cancers. Taken together, this led to the assumption that cells expressing both Notch2IC as well as LMP1/CD40 in constitutively active forms would also show enhanced proliferation rates. This hypothesis was tested with the help of Carboxyfluorescein succinimidyl ester (CFSE)-analysis. CFSE is a fluorescent dye that labels intracellular molecules through its succinimidyl group. It is passed on to daughter cells during cell division and thereby provides a

method to measure proliferation of a cell population by the decrease in CFSE-fluorescence of the labeled cells.

Splenocytes from all four genotypes were prepared and depleted of all other cell types by MACS-separation to obtain 95-98 % pure primary B-cell samples. These were thereafter labeled with CFSE and cultivated in 10 % medium with and without stimuli. These stimuli comprised agonistic antibody against CD40 and the cytokine IL4, which are of importance in T-cell-mediated B-cell activation. Stimuli were applied both together and separately. Thereby stimulated or unstimulated splenic B cells were cultivated and analyzed on day 1, 3 and 5 for CFSE-staining intensity after excluding Topro-3^{pos} (dead) cells. Data from day 1 served to set the resting peak of CFSE-labeling intensity.

Evaluating the obtained data with FlowJo software delivers beside the estimates of the percent of culture that divided (percent divided) the division index and the proliferation index. The division index is an overall average of the number of cell divisions that cells in the original population have undergone. It includes the cells that never divided and therefore includes those of the resting or "undivided peak". The proliferation index, however, gives the total number of divisions of a cell that went into division at least once. In contrast to the division index it only takes into account cells that respond in the culture system and therefore considers only the fraction of cells in the "divided peak". One can say that the division index reflects the biology of responding part of the system, while the proliferation index considers also the dynamics of the entire system (www.flowjo.de).

As one can see in Fig. 3.25 there is a clear reduction in the resting peak population on day 3 that transformed into a considerable shift of the "divided peak" in the cultured B cells of Notch2//LMP1/CD40//CD19-cre mice (Fig. 3.25A, upper panel). The same pattern can also be observed for the cultures that received an IL4-stimulus. With roughly 20 % divided B cells expressing both transgenes exhibit the highest proliferation rate of all genotypes tested.

When examining the genotypically different B cells in their entirety (division index) on day 3 the B cells expressing both transgenes display by far the highest division indices both with and without IL4-stimulus (around 0.4 versus 0.1 in CD19-cre and 0.1/0.2 in Notch2//CD19-cre and LMP1/CD40//CD19-cre mice). With regard to the proliferation index one is able to observe that out of the cells that did proliferate, the B cells carrying constitutively active Notch2IC do so most strongly of all genotypes although overall the proliferation index levels of Notch2IC-, LMP1/CD40- and Notch2IC//LMP1/CD40-expressing splenic B cells are similar upon IL4 stimulation and tend to be lower in the CD19-cre splenic B cells. The aforementioned is also recapitulated in the data obtained for day 5 (Fig. S.1; Supplements).
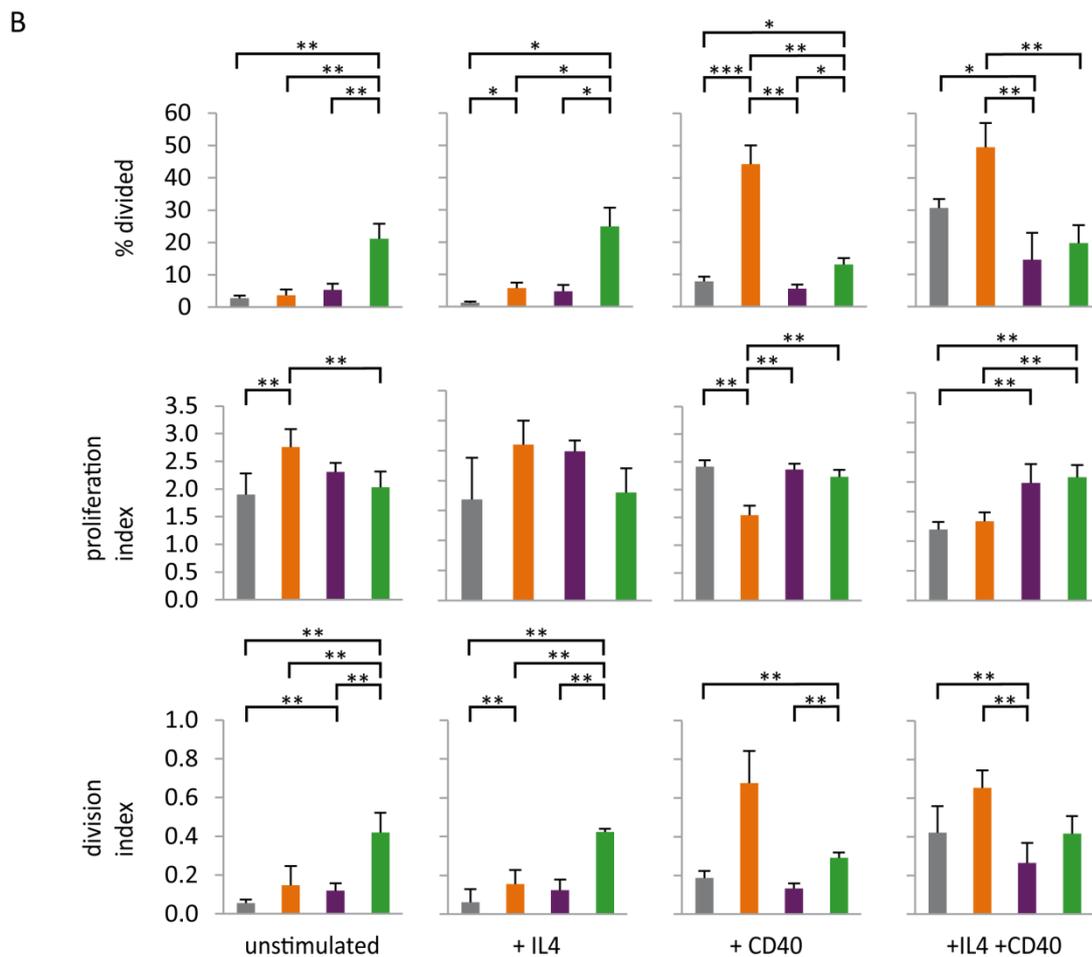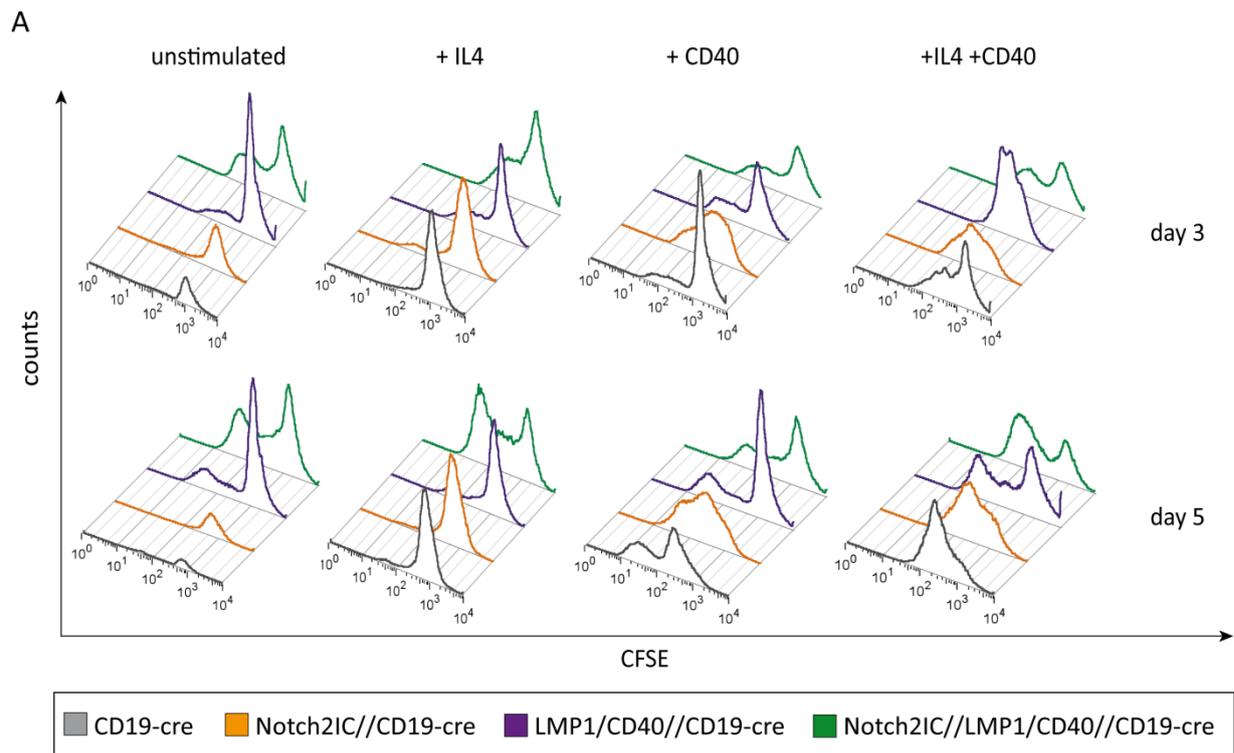
Fig. 3.25 Notch2IC//LMP1/CD40-expressing splenic B cells show an increased proliferation in in vitro culture.
Splenocytes were prepared and splenic cell preparations were depleted of CD43^{pos} (i.e. non-B) cells and labeled with CFSE. The B cells were subsequently cultivated either with or without stimuli. These stimuli

included α-CD40 antibody, IL4 as well as both IL4 and α-CD40 antibody. Cells were analyzed by flow cytometric analysis on day 1, 3 and 5 of culture. Dead cells were excluded from the analysis by excluding Topro-3^{pos} cells. (A) Results for respective genotypes on the indicated days without stimulus, with IL4-stimulus, with CD40-stimulus and with both CD40- and IL4-stimulus. The displayed result is representative for four independent experiments. (B) Statistical evaluation of day 3 of percent divided, proliferation and division index for all genotypes without stimulus, with IL4-stimulus, with CD40-stimulus and both with IL4- and CD40-stimulus. CFSE, Carboxyfluorescein succinimidyl ester. *p < 0.05, ** p < 0.01, *** p < 0.005.

The pattern becomes more divers when adding CD40 or both IL4 and CD40 to the respective cultures. Notch2IC//LMP1/CD40-expressing B cells maintain the previously described high proliferative states for both stimulation scenarios (CD40 or both IL4 and CD40), but the value for percent divided never further increases over 20 %. Furthermore, the division index also remains unchanged. Concerning B cells that already express constitutively active CD40 addition of CD40 antibody alone also has little effect on B-cell proliferation. CD40-stimulation has the strongest effects on cultures of B cells isolated from CD19-cre and Notch2IC//CD19-cre mice. There is a strong increase in the percentage of dividing cells. In the case of B cells expressing constitutively active Notch it even excels those of LMP1/CD40 and Notch2IC//LMP1/CD40-expressing B cells, which is mirrored by the fact that the division index (around 0.7) rises above the levels found in LMP1/CD40 and Notch2IC//LMP1/CD40-expressing B cells (still 0.2 and 0.4. respectively).

As expected this effect is even stronger in B cells that received both IL4 and CD40 in their medium. This leads to a further increase in the percentage of divided cells in the control B-cell population and their division index rises to that of Notch2IC//LMP1/CD40-expressing B cells. However, the Notch2IC-expressing B cells remain those with the highest level percentage of divided cells and division indices of all genotypes in the analysis.

The pattern described above for the proliferative behavior of B cells of the different genotypes on day 3 is recapitulated on day 5. The major difference however is, that by this time simultaneous addition of α-CD40 and IL4 to B-cell cultures leads to a similar division indices in CD19-cre, Notch2IC//CD19-cre and Notch2IC//LMP1/CD40//CD19-cre mice (Fig. S.1; Supplements).

3.13.1 Unstimulated Notch2IC//LMP1/CD40-expressing splenic B cells survive better in culture than Notch2IC-, but not than LMP1/CD40-expressing splenic B cells

The CFSE-labeled and cultured splenic B cells were stained with the fluorescent dye Topro-3, which is only able to penetrate damaged but not intact cellular membranes. It was used in order to ensure the exclusion of dead cells from the analysis. These Topro-3^{pos} cells can also be used as a measure of the amount of dead versus living cells with the respective culture.

The results of the Topro-3^{neg} cells with the respective stimuli at the different time points are summarized in Fig. 3.26.

Fig. 3.26A gives an overview of the B-cell cultures that did not receive any stimulus. Already at day 1 there is a distinct drop in the Notch2IC-expressing cells. By day 3 both B-cell cultures from spleens of CD19-cre and Notch2IC//CD19-cre mice are low in their content of living cells (around 15 %), while LMP1/CD40- and Notch2IC//LMP1/CD40-expressing B cells still harbor 40 % living cells in their cultures. Therefore, the better survival of these cells is an effect mediated by constitutively active CD40, since at day 5, LMP1/CD40-expressing B cells still display 50 % of living cells. However, there is a drop to 25 % living cells in cultures of splenic B cells of Notch2IC//LMP1/CD40//CD19-cre mice. This seems to be a Notch2IC-mediated effect since the Notch2IC-expressing B cells, like the control B cells display on the average a mere 4-6 % of living cells.

Fig. 3.26B gives an overview of the B-cell cultures that did receive an IL4-stimulus with regard to the percentage of living cells in culture. The addition of IL4 enhances the especially survival of B cells of CD19-cre mice. But the overall pattern remains the same as in the cultures that did not receive a stimulus (Fig. 3.26A).

Fig. 3.26C gives an overview of the cell cultures that did receive a CD40-stimulus with regard to the percentage of living cells in culture. As expected the effects of an increased survival are majorly observed for the cells that do not have an intrinsic activated CD40, i.e. B cells of CD19-cre and Notch2IC//CD19-cre mice.

Fig. 3.26D gives an overview of the B-cell cultures that did receive both an IL4- and CD40-stimulus with regard to the percentage of living cells in culture. This combination provides a rather strong stimulus prompting the cells to strongly proliferate, hence there is no loss in viability from day 0 to day 1. At day 3, B cells expressing constitutively active CD40 still display 40 % of viable cells, while all other genotypes including CD19-cre controls display around 28 % viable B cells. At day 5 all genotypes with the exception of LMP1/CD40-expressing B cells (25 % viable cells) drop below values of less than 20 % viable cells. Although those values are still higher than when splenic B cells were left unstimulated at day 5 these values are still lower than when cells were stimulated with α-CD40 only. This is likely due to the fact that splenic B cells receiving a simultaneous CD40- and IL4-stimulation proliferate the strongest and at some point outcompete each other for nutrients. In favor for this hypothesis is the fact that already from day 3 onward the medium starts to turn slightly yellow for all genotypes. Therefore, drop in cell viability also on day 3 can be explained by a number of possible reasons: an overall increase in cell number and at the same time, increasing lack of nutrients and an accumulation of metabolites leading to an increase in

dead cells. Also, cells might die due to a limited number of cell divisions for each cell or cells stop growing and die because of contact inhibition.
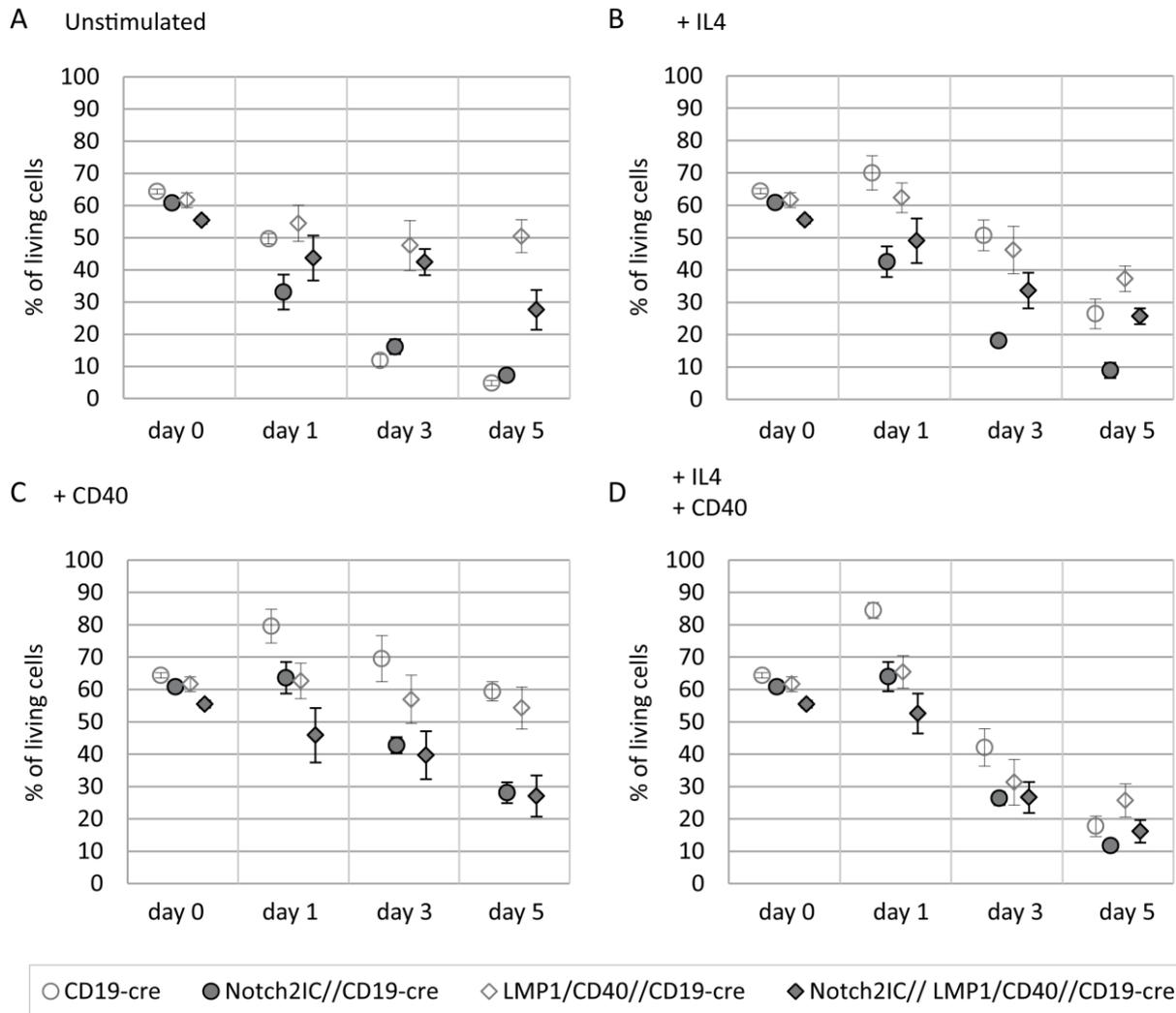
Fig. 3.26 Unstimulated Notch2IC//LMP1/CD40-expressing B cells survive better in culture than Notch2IC-, but not than LMP1/CD40-expressing B cells.
Splenocytes of all genotypes were prepared and B cells were depleted of CD43^{pos} cells. The B cells were subsequently cultivated either with or without stimuli. These stimuli included α-CD40 antibody, IL4 and both (IL4 and α-CD40 antibody). Cells were labeled with Topro-3 prior to flow cytometric analysis on day 0, 1, 3 and 5 of culture. Statistical evaluation of the percentage of living cells is given on the respective days (x-axis) without stimulus (A), with IL4-stimulus (B), with CD40-stimulus (C) and both with IL4- and CD40-stimulus (D). The averages and SDs are calculated from three independent experiments. SD, standard deviation.

3.14 Notch2IC//LMP1/CD40-expressing splenic B cells are highly and actively cycling cells

Previous studies in our lab showed that Notch1IC/2IC were able to drive cells into the S-phase of the cell cycle. However, cell numbers did not increase which was assumed to be due to an increased apoptosis rate in Notch1IC/2IC-expressing cells due to upregulation of pro-apoptotic genes (Kohlhof et al., 2009). All of this is in line with the results obtained in the CFSE-and Topro-3-analysis presented above, considering that compared to CD19-cre B cells Notch2IC-expressing splenic B cells display decreased viability. Constitutive CD40 on the other hand -as was observed with the B cells expressing LMP1/CD40- might deliver the survival signals that enable increased proliferation also in Notch2IC-expressing B cells.

This scenario could be further tested in detail with regard to the cell cycling characteristics in the B cells of Notch2IC//LMP1/CD40//CD19-cre mice supplied with both a constitutively active CD40 as well as a constitutively active Notch2 to see whether these are driven into S-phase of cell cycle –through the activity of Notch-signaling- and allow for continuous proliferation and prevention of apoptosis –through the activity of CD40-signaling.

Therefore, primary splenic B cells depleted of CD43^{pos} cells by MACS-separation were taken into culture for three days and labeled with Bromodesoxyuridine (BrdU) at day 0, day 1 and day 3 for four hours. BrdU is a synthetic nucleoside and thymidine analogue. If given to cells during their proliferative S-phase BrdU-dye will be incorporated into the cell's DNA and can later be visualized by intracellular staining with fluorochrome-coupled α-BrdU antibodies. This allows for inference on the proliferation rate of the cells. Simultaneous staining of the cells with 7-amino-actinomycin D (7AAD; a fluorescent DNA marker) permits to determine the full scope of the cell cycle of any culture of cells under investigation. In order to ensure functionality of the assay LPS was added to B-cell cultures of CD19-cre mice. LPS is a potent, polyclonal stimulus, activating the cells and driving them into proliferation.

On day 0 (Fig. 3.27), reflecting the immediate ex vivo situation splenic B cells from all genotypes still resemble each other with regard to their cells in G0/G1 of the cell cycle (around 80 % of cells) and G2/M (roughly around 5 % of cells). As expected the B cells of CD19-cre mice did hardly proliferate and quickly died in culture without stimulus (as merely roughly 15 % of cells were viable at day 3 as previously shown; Fig. 3.26A). Stimulating control B cells of CD19-cre mice with LPS had little effect after the initial 4 hours of BrdU-labeling and simultaneous LPS-stimulation. But after 1 day of in vitro culture cells with LPS-stimulus displayed a strong increase of cells in S-phase of the cell cycle (6 %), as well as in G2/M-phase (9 %), indicating a strong increase in

proliferation. The effect LPS had on cells was even more pronounced at day 3 of culture with an even expanded percentage of cells in S-phase (35 %), but less cells in G2/M (2 %), hinting at the possibility that cells were so activated that they did not accumulate in the G2 phase but rather re-entered the cell cycle.

Notch2IC- as well as Notch2IC//LMP1/CD40-expressing splenic B cells displayed a much larger percentage of cells in S-phase after ex vivo isolation (about 2 % in both genotypes). This percentage increases over 24 hours: it doubles in Notch2IC-expressing cells and triples in B cells expressing both transgenes. Simultaneously, there is a subtle drop in the percentage of cells in G2/M-phase (from 6 to 4 %) in Notch2IC-expressing B cells, which is also observable in Notch2IC//LMP1/CD40-expressing B cells (from 6 to 5 %). This could either be symptomatic of an increase in B cells re-entering cell cycle or simply of cells dying. The latter seems to be the case for only Notch2IC-expressing B cells since by day 3 of culture these cells display a massive increase of apoptotic/necrotic cells as has been observed in culture of control cells. Moreover, this is accompanied by a considerable drop of viable cells, in all phases of cell cycle but especially in S-phase.

The drop of viable splenic B cells, in all phases of cell cycle but especially in S-phase was not observable for B cells expressing both transgenes, which even displayed a further increase on cells in S-phase (from 6 % on day 1 to 10 % on day 3), with only a small drop of the percentage of cells in G0/G1. This effect was likely to be mediated by CD40. LMP1/CD40-expressing B cells in contrast to CD19-cre control cells already after ex vivo isolation harbor more cells in S-phase, but this portion doubles over 24 hrs (day 1) and triples within 72 hrs (day 3). Furthermore, in line with the anti-apoptotic properties of active CD40-signaling LMP1/CD40-expressing B cells display no drop in cell viability at the analysis endpoint (day 3).

Therefore, the herein presented data strongly support the hypothesis that simultaneous expression of both constitutively active Notch2 and CD40 in B cells leads to an increase in B-cell proliferation by Notch activity driving cells into S-phase but also apoptosis, which can be counteracted by CD40 which can provide strong anti-apoptotic, pro-survival stimuli.

Of note, only medium of wells with Notch2IC//LMP1/CD40-expressing B cells or B cells having received an LPS stimulus (CD19-cre) turned light yellow, indicating a change in pH due to the accumulation of metabolites in the medium (data not shown) and further underlines the highly proliferative state of Notch2IC//LMP1/CD40-expressing B cells.
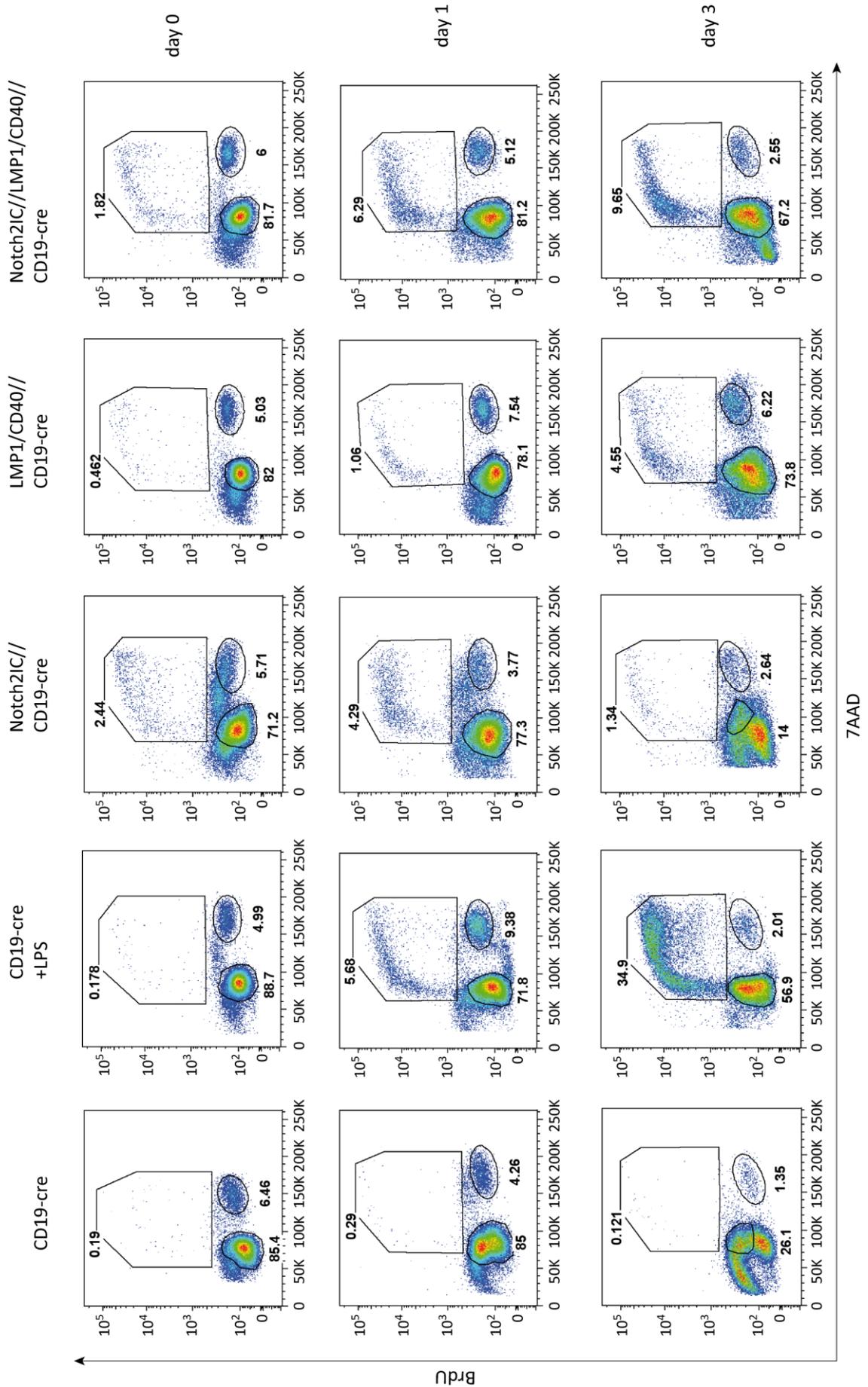
Fig. 3.27 Notch2IC//LMP1/CD40-expressing splenic B cells are highly and actively cycling cells.

Splenocytes were prepared and B cells were depleted of CD43^{pos} (i.e. non-B) cells and labeled with BrdU for 4 hrs. B cells were cultivated either with LPS (in the case of CD19-cre B cells) or without stimuli. Polyclonal stimulus LPS was used on CD19-cre B cells as positive control to test for assay functionality. Cells were analyzed by flow cytometric analysis on day 0 (upper panel), day 1 (middle panel) and day 3 (lower panel) of culture. X-axis shows 7AAD intensity which corresponds to DNA content and y-axis represents APC intensity which corresponds to BrdU-incorporation. In the FSC/SSC cell debris was gated out and by plotting FSC-A versus FSC-W was used to discriminate doublets from single cells. The displayed result is representative for four independent experiments. 7AAD, 7-amino-actinomycin D; APC, allophycocyanin (fluorochrome); BrdU, Bromdesoxyuridine; FSC (-A, -W), foward scatter (-area, -width); hrs, hours; LPS, Lipopolysaccharide; SSC, sideward scatter.

3.15 Aged Notch2IC//LMP1/CD40//CD19-cre mice are prone to develop B-cell lymphomas

As shown before, B cells of Notch2IC//LMP1/CD40//CD19-cre mice have a highly activated phenotype and proliferate strongly in culture. Not surprisingly both Notch and CD40 are found to be up-regulated in a number of cancers (Kuppers et al., 2012). LMP1/CD40//CD19-cre mice develop B- cell lymphomas with a high incidence after 1 year (Hoemig-Hoelzl et al., 2008). Therefore, some mice were saved for over a year (13 to 16 months) to test whether the co-expression of constitutive active Notch2 and CD40 has an impact on lymphomagenesis in Notch2IC//LMP1/CD40//CD19-cre mice.

All five Notch2IC//LMP1/CD40//CD19-cre mice developed hyperplasia, both of the spleens as well as three tissue abnormalities in the lower neck region (Tab. 3.2). There are distinct variations in this small test group, spleens of Notch2IC//LMP1/CD40//CD19-cre mice were up to 13 times heavier than their control counterparts, harboring up to 26-fold more cells in total. The mice can be assigned into two groups: those that do present with overt signs of lymphomas and those that only show mild signs of lymphoma. Both groups can present with or without tumors in the lower neck region.

Three out of five mice (# 3142, # 1779 and # 1778) display a splenic B-cell expansion (3 to 27-fold increase) and a splenic T-cell expansion (8 to 70-fold increase in mouse # 1778 compared to controls). Therefore, the T-cell expansion in the spleen is not lost during ageing of the mice and is still a hallmark of lymphocyte expansion in Notch2IC//LMP1/CD40//CD19-cre mice. Two mice (# 1717 and # 1760) do not present with a splenic B-cell expansion and/or a splenic T-cell expansion but still had an increase in splenic weight and total cell number. Mouse # 1717 had a tumor in the lower neck region which made the sacrifice of the mice necessary. No mice of the Notch2IC//LMP1/CD40//CD19-cre genotype lived longer than 16 months, since all mice developed abnormalities that required putting the animals down. In order to ensure that this is an effect of the constitutive expression of both transgenes in these mice and not of the ageing

process and the accumulation of random mutations over time, one CD19-cre mouse was analyzed along with every Notch2IC//LMP1/CD40//CD19-cre mouse. However, although there are also variations in splenic weight and splenic cell number in CD19-cre control mice none of these mice developed signs of illness.

Tab. 3.2 Overview of 13-16 month-old Notch2IC//LMP1//CD19-cre mice that developed hyperplasia of the spleen or the lower neck region.
The respective aged-matched controls were summarized in the first row, n=5. The data given in the three last columns were obtained through flow cytometric analysis of splenocytes stained for B220^{pos} (B cells), CD3^{pos} (T cells) and hCD2^{pos}/B220^{pos} (B cells expressing transgenes). n.d., not determined; SGT, salivary gland tumor.

	age	splenic weight (g)	total cell no. ($\times 10^7$)	B-cell no. ($\times 10^7$)	T-cell no. ($\times 10^7$)	% of hCD2^{pos} B cells	SGT
CD19-cre	matched	0.22 ±0.1	4.9 ±1.7	2.7 ±1.2	1.2 ±0.3	-	-
Notch2IC//LMP1/CD40// CD19-cre							
# 3142	13 m	2.92	125.0	84.6	19.4	89.4	-
# 1779	14 m	0.72	87.5	37.0	30.4	96.7	1
# 1760	14 m	1.59	64.9	0.8	11.9	5.4	-
# 1778	14 m	n.d.	130.0	30.3	63.4	67.7	1
# 1717	16 m	0.30	9.0	1.3	3.9	23.2	1

3.15.1 Aged Notch2IC//LMP1/CD4//CD19-cre mice display increased numbers of splenic Mac1^{pos} cells

Since some of the old mice examined did not display an increase in the lymphocyte compartment in the spleen the question arose whether these cells could be accessory cells as an expansion of such cells was already observed in the young mice. Preparing splenocytes and analyzing them for Mac1 surface expression, while excluding B220^{pos} B cells, allowed estimating the presence of these cells in the spleens.

While the percentages of Gr1^{hi} cells in aged Notch2IC//LMP1/CD4//CD19-cre were not increased in comparison to CD19-cre mice, only slightly higher in mouse # 1760. But as observed in the younger mice the absolute number of Mac1^{pos} cells were overall elevated in the spleens in aged Notch2IC//LMP1/CD4//CD19-cre mice. Especially in mouse # 1760 (which had almost no B cells in the spleen, while displaying a high splenic weight of 1.59 g), the number of Mac1^{pos} cells is particularly high (16×10^7 versus 0.5×10^7 on the average in CD19-cre mice; Fig. 3.28).
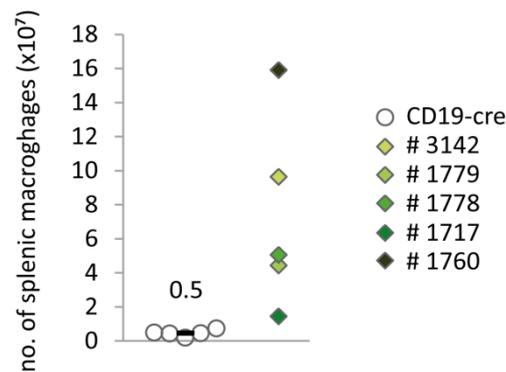
Fig. 3.28 Aged Notch2IC//LMP1/CD4//CD19-cre mice display increased numbers of splenic Mac1^{pos} cells.
Splenocytes were prepared and stained for B220 and Mac1 surface marker expression. Cell numbers of Mac1^{pos} B220^{neg} were determined by flow cytometric analysis and given for each mouse. Data for CD19-cre control mice (n=5) were averaged and SD is given. SD, standard deviation.

3.15.2 Aged Notch2IC//LMP1/CD40-expressing B cells display distinctly altered surface marker expression in the spleen

Young Notch2IC//LMP1/CD40//CD19-cre mice display a MZ B-cell phenotype as previously shown (section 3.8, Fig. 3.17). Therefore, with the aim to test whether this phenotype is maintained in aged mice, splenic B cells of aged mice were analyzed for their MZ B-cell status with the help of IgM/IgD and CD21/CD23 staining and flow cytometric analysis. The FACS analysis revealed that staining overall is very diverse and therefore no averages can be calculated, instead the CD21/CD23- and IgM/IgD-staining pattern of those mice displaying high splenic B-cell numbers (# 3142, # 1779, # 1778 and # 1717) is presented individually (Fig. 3.29).

The CD21/CD23-staining allows for a direct analysis of MZ B- versus Fo B-cell phenotype. Two out of five old Notch2IC//LMP1/CD40//CD19-cre mice (# 1778 and # 1717) still show a tendency to gate into the MZ-B-cell compartment gate as the young mice do. However, they display a tendency towards down-regulation of CD21. In two out of five old mice (# 3142 and # 1779) the majority of B cells showed an clear down-regulation of CD21 (CD21^{low} CD23^{low}). Interestingly, in mouse # 1717 this was particularly the case for the hCD2pos splenic B cells.

With regard to the IgM/IgD-staining of B cells three out of five old Notch2IC//LMP1/CD40//CD19-cre mice (# 3142, # 1778 and # 1717) still gate for majority into the MZ B-cell gate (IgM^{hi} IgD^{low}) however with strongly varying degrees and one out of five mice (# 1779) exhibits a shift towards IgM^{hi} IgD^{low}-MZ B-cell gate with a tendency to acquiring an IgM/IgD double-negative status.

Gating on hCD2 usually allows screening for the status of the actual transgene-expressing cells. The majority of hCD2^{pos} B cells would also gate like the majority of the entire splenic B-cell population in the individual mice, meaning in case there is a down-regulation in one or both markers (either CD21 and CD23 or IgM and IgD) in the entire splenic B-cell population this was found recapitulated in the hCD2 B cells of the mice.
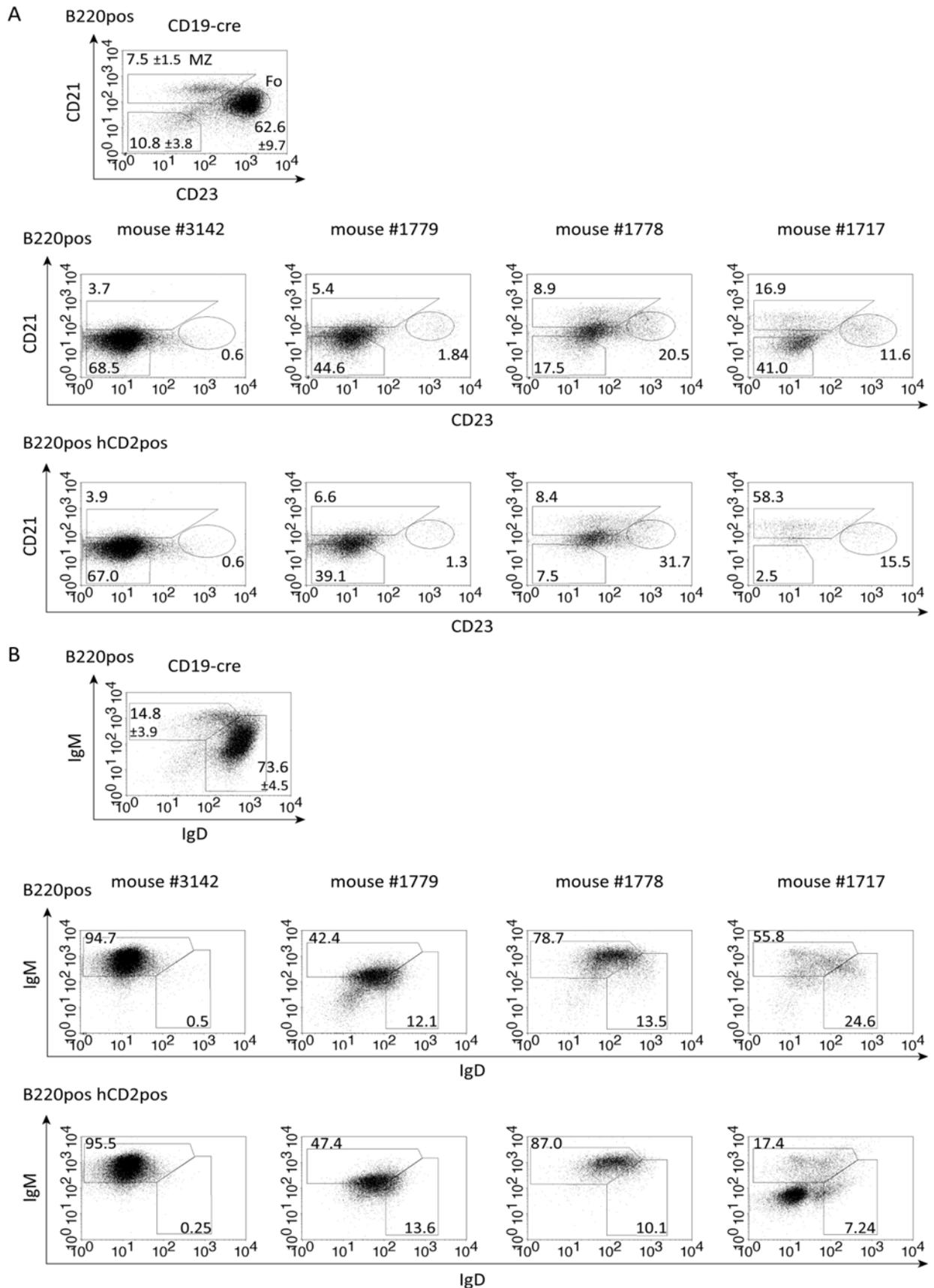
Fig. 3.29 Aged Notch2IC//LMP1/CD40-expressing splenic B cells display distinctly altered surface marker expression in the spleen.
(A) Flow cytometric analysis of Fo (CD21^{hi} CD23^{pos}) and MZ B cells (CD21^{hi} CD23$^{pos/low}$) in the spleen of mice # 3142, # 1779, # 1778, # 1717 and of a representative control CD19-cre mouse (with percentages of

averages and SDs). Numbers indicate percentages of lymphocyte-gated, B220^{pos} B cells displaying the respective phenotypes. Re-gating the cells on hCD2 allows for identification of the phenotype of the cells expressing the transgenes (lower panel). (B) Splenocytes of mice # 3142, # 1779, # 1778, # 1717 and a control CD19-cre mouse were analyzed by flow cytometry for the expression of surface IgM and IgD. Numbers indicate percentages of lymphocyte-gated populations of B220^{pos} B cells displaying a Fo (IgM^{pos} IgD^{pos}) or MZ and transitional (IgM^{pos} IgD^{low}) B cell phenotype (upper panel). Re-gating the cells on hCD2 allows for identification of the phenotype of the cells expressing the transgenes (lower panel). Data for CD19-cre mice (n=5) were averaged and SDs are given. Fo B, follicular B cell; MZ B, marginal zone B cell; SD, standard deviation.

3.15.3 Aged Notch2IC//LMP1/CD40-expressing splenic B cells display differential up-regulation of activation markers

Young Notch2IC//LMP1/CD40//CD19-cre mice display an activated B-cell phenotype as previously shown with the help of various surface markers (section 3.9, Fig. 3.18). However, when analyzing splenic B cells of the aged mice for CD80, CD86 and CD95 the activation marker are still up-regulated, but with varying intensity. Only in mouse # 3142 the same robust, LMP1/CD40-induced upregulation of CD95 can be observed (Fig. 3.30A), leading the entire splenic B-cell population to assume a higher CD95 expression. In all other aged mice (# 1779, # 1778 and # 1717) the up-regulation of CD95-expression is not as strong. Furthermore, the flow cytometric analysis show in all mice analyzed not only the previously observed up-regulation of CD80, but also of CD86 compared to controls (Fig. 3.30B) in their splenic B cells, however with strongly varying levels. Old mice are also diverse with regard to their hCD2-status (Fig. 3.30C), mouse # 1760 for example has almost completely down-regulated hCD2 in its few remaining splenic B cells, when comparing them to a young Notch2IC//LMP1/CD40//CD19-cre mouse.

The different levels of activation marker expression could be explained by activity and up-regulation of different signaling pathways that can differ from mouse to mouse as has previously shown for lymphoma-bearing LMP1/CD40//CD19-cre mice (Homig-Holzel et al., 2008). The variation in expression of transgene reporter (CD95, indirectly or hCD2, directly) might be due to two reasons: A) mainly B cells that do not express the transgenes are expanding or B) there is a transcriptional down-regulation of both transgenes and thereby down-regulation of hCD2- and CD95 expression with age or onset of B- cell lymphomagenesis.
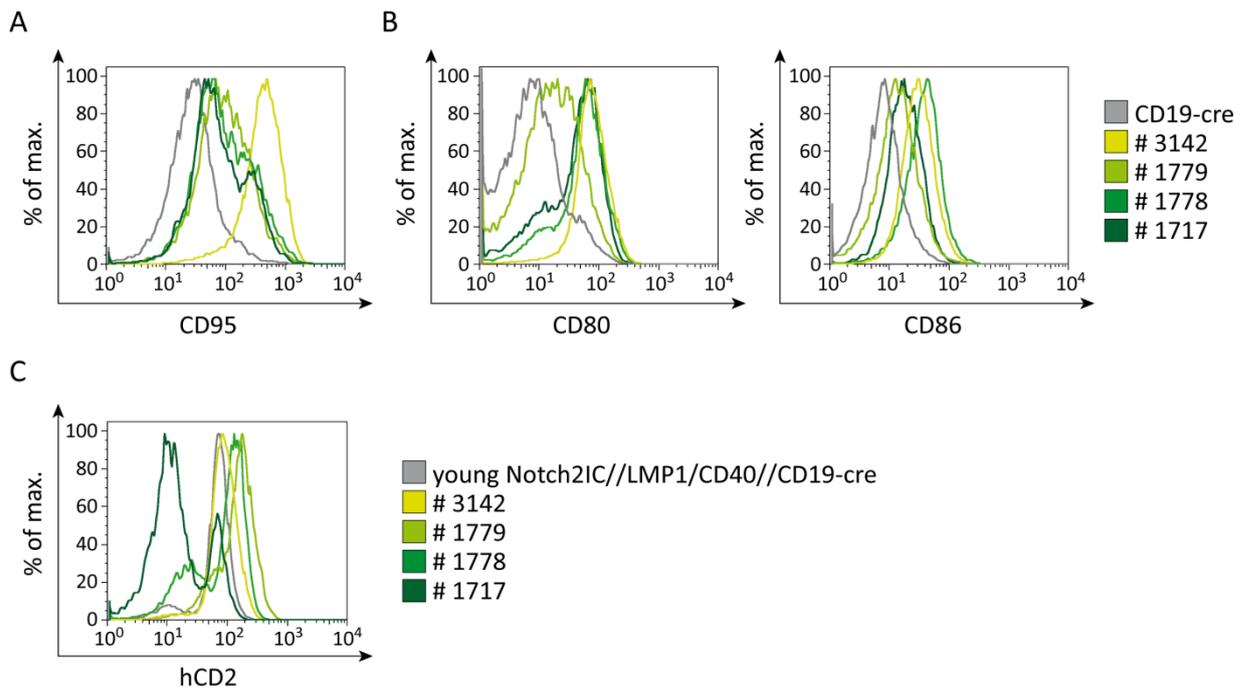
Fig. 3.30 Aged Notch2IC//LMP1/CD40-expressing splenic B cells display up-regulation of activation marker.
Splenocytes were analyzed by FACS for level of surface molecules (A) CD95, (B) CD80 and CD86 (B7-proteins) and C) hCD2. Overlays of surface expression were made of lymphocyte-gated, B220^{pos} B cells from aged Notch2IC//LMP1/CD40//CD19-cre mice (green lines) or controls (CD19-cre or young Notch2IC//LMP1/CD40//CD19-cre mice; grey lines).

CD5 is a surface marker that is usually expressed on T cells as well as B1a cells, but it is also found on activated mature B cells. An up-regulation of activation marker CD5 in splenic B cells could be observed in all aged Notch2IC//LMP1/CD40//CD19-cre mice with the exception of mouse # 1760 (Fig. 3.31 and Tab. 3.3). In this mouse (# 1760) the percentage of CD5^{pos}/B220^{pos} B cells is even diminished compared to the average in CD19-cre (0.3 % versus 4 % in CD19-cre) but overall levels of CD5 are comparable to the CD19-cre control mice. It should be further evaluated whether these splenic B cells adopt a B1 B-cell phenotype.
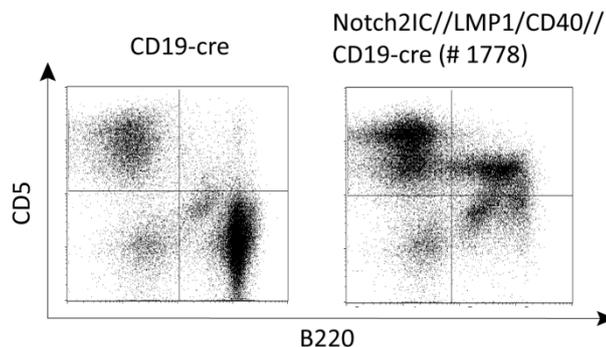
Fig. 3.31 Aged Notch2IC//LMP1/CD40//CD19-cre mice display distinctly altered surface marker expression with regard to CD5 and B220 expression.
Flow cytometric analysis of lymphocyte-gated, CD5^{pos} and B220^{pos} cells in the spleen as analyzed by flow cytometry. Notch2IC//LMP1/CD40//CD19-cre mouse # 1778 is shown along aged-matched CD19-cre control.

Tab. 3.3 Aged Notch2IC//LMP1/CD40//CD19-cre mice display distinctly altered surface marker expression with regard to CD5 and B220 expression.
Flow cytometric analysis of CD5^{pos} and B220^{pos} cells in the spleen as analyzed by flow cytometry. Data for CD19-cre mice (n=5) were averaged and SDs are given. SD, standard deviation.

	CD5 (in %)	CD5^{pos}/B220^{pos} (in %)
CD19-cre	22.5 ±6.5	4.1 ±1.3
Notch2IC//LMP1/CD40//CD19-cre		
# 3142	17.2	54.6
# 1779	36.2	24.2
# 1760	27.1	0.3
# 1778	53.6	27.7
# 1717	55.6	9.5

3.15.4 Aged Notch2IC//LMP1/CD40//CD19-cre mice maintain shift towards effector T-cell compartment

As shown in Tab. 3.2 splenic T-cell expansion (8 to 70-fold increase in mouse # 1778 compared to controls) is preserved in the aged Notch2IC//LMP1/CD40//CD19-cre mice. In order to better characterize the also expanded T-cell population in the old mice the splenic lymphocytes were tested for the expansion of the CD4^{pos} and CD8^{pos} T-cell compartment and furthermore tested for T-cell activation via CD4, CD8, CD44 and CD62L staining and subsequent FACS analysis like the young mice (section 3.5.2).

With respect to the distribution of CD4^{pos} versus CD8^{pos} splenic T cells, one can observe that there is no tendency towards an expansion of a particular T-cell subpopulation (Fig. 3.32).
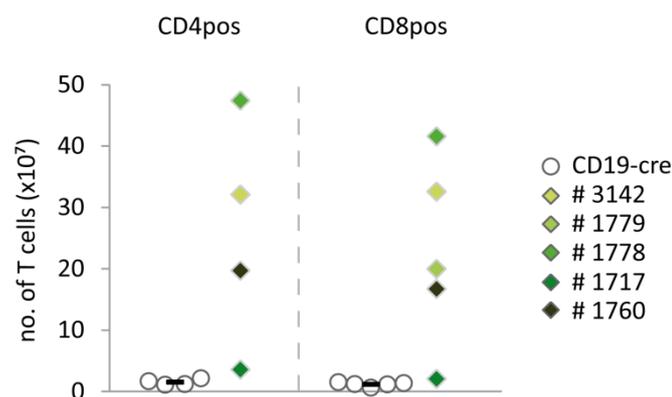
Fig. 3.32 Aged Notch2IC//LMP1/CD4//CD19-cre mice display increased numbers of T cells.
Splenocytes were prepared and analyzed for CD3, CD4 and CD8 surface marker expression. Cell numbers of lymphocyte-gated, CD3^{pos}/CD4^{pos} and CD3^{pos}/CD8^{pos} were determined by flow cytometric analysis. Points represent data from individual mouse and the horizontal bar marks the mean value for CD19-cre control mice (n=5) were averaged and SD is indicated above control mice data set. SD, standard deviation.

With respect to the T-cell activation the aged Notch2IC//LMP1/CD40//CD19-cre mice displayed a similar pattern as in the young mice since they maintain a shift towards T-cell effector

compartment (Fig. 3.33). However, as observed for mainly all other staining results in the old mice they present with variations (Tab. 3.4).
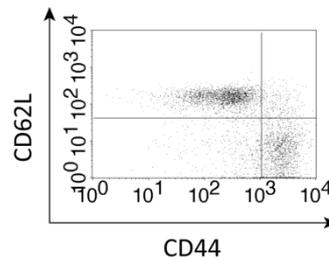
Fig. 3.33 Gating scheme for T-cell activation after CD4^{pos} or CD8^{pos} pre-gating of T cells.
Naïve T-cell compartment (CD62L^{hi} CD44^{low}), central memory T cells (CD62L^{hi} CD44^{hi}), effector T cells (CD62L^{low}, CD44^{hi}). Data for CD19-cre mice (n=5) were averaged and SDs are given. SD, standard deviation.

There is a general reduction in the naïve T-cell compartment and moreover a reduction in central memory (CD62L^{hi} CD44^{hi}) both in CD4^{pos} and CD8^{pos} cells, with the exception of CD4^{pos} T cells of mouse # 1778 in which both effector and memory T-cell compartment are increased at the expense of the naïve T-cell compartment. The marked increase in the effector T-cell compartment (CD62L^{low} CD44^{hi}) in the spleen in the respective CD4^{pos} or CD8^{pos} T-cell population can also still be observed in the old mice, with the exception of CD8^{pos} T cells of mouse # 1779 which resemble CD19-cre mice rather than other aged Notch2IC//LMP1/CD40//CD19-cre mice.

Tab. 3.4 Splenic T cells of aged Notch2IC//LMP1/CD40//CD19-cre mice show an increase in the percentage of both central memory as well as effector memory T cells.
Splenic cells were analyzed by flow cytometry for the CD62L and CD44 expression on either (A) CD4^{pos} or (B) CD8^{pos} T cells.

(A)

CD4^{pos}	naïve T-cells (CD62L^{hi} CD44^{low})	memory T cells (CD62L^{hi} CD44^{hi})	effector T cells (CD62L^{low}, CD44^{hi})	% CD62L^{low}, CD44^{low}
CD19-cre	43.6 ±7.1	6.6 ±1.0	40.7 ±5.6	9.1 ±0.8
Notch2IC//LMP1/CD40// CD19-cre				
# 1760	0.28	2.9	86.3	10.5
# 1778	9.9	23.9	59.4	6.8
# 1717	5.3	4.1	68.4	22.3

(B)

CD8^{pos}	naïve T-cells (CD62L^{hi} CD44^{low})	memory T cells (CD62L^{hi} CD44^{hi})	effector T cells (CD62L^{low}, CD44^{hi})	% CD62L^{low}, CD44^{low}
CD19-cre	22.8 ±12.8	33.7 ±5.7	35.7 ±14.8	8.1 ±3.2
Notch2IC//LMP1/CD40// CD19-cre				
# 1779	34.5	28.7	21.5	15.4
# 1760	2.2	6.1	41.1	50.6
# 1778	10.9	21.4	52.9	14.7
# 1717	5.6	6.2	51.8	36.3

Overall, there is an expansion in the compartment of activated T cells and again not only, but in particular the CD8^{pos} T cells of aged Notch2IC//LMP1/CD40//CD19-cre mice that display the same shift into the CD44^{low} CD62L^{neg} compartment as previously observed in the young mice.

3.15.5 Aged Notch2IC//LMP1/CD40//CD19-cre mice develop monoclonal B-cell lymphoma

In order to determine whether the expansion in splenic size, weight and lymphocyte cell number in aged Notch2IC//LMP1/CD40//CD19-cre mice is due to the expansion of one or several B-cell clones –which would confirm lymphoma development- Southern blots with DNA prepared from total splenocyte samples were prepared. Southern blot analysis also allows to determine whether the lymphoma originates from the expansion of one or more B-cell clones, so whether it is mono- or oligoclonal in nature. Using a radioactively-labeled IgH-probe on membrane-bound DNA that has been digested with the EcoRI-restriction enzyme, one is either able to detect the germline configuration of the IgH-locus or one or more distinct bands signifying the expansion of one or more B-cell clones carrying the same rearrangement of the BCR.

Only four of the five mice could be tested since no DNA was kept from the mouse # 1778. These samples were subjected to analysis along with two control DNA samples from aged-matched CD19-cre mice and one DNA samples from an aged-matched LMP1/CD40//CD19-cre mouse (# 3143). The results of the blot revealed that two of the four samples (# 3142 and # 1779) tested were positive for two further IgH-rearrangements (Fig. 3.34). This could be due to an oligoclonal expansion, however is more likely to be a monoclonal expansion since in most B cells both Ig-alleles tend to be rearranged. This leads to exactly two Ig-gene rearrangements and therefore monoclonal expansions of their splenic B-cell pool that present as oligoclonal. For the LMP1/CD40//CD19-cre DNA sample the band(s) appear very weak, therefore an expansion of one or B-cell clones could not be determined unambiguously.

One of these two mice (# 3142) displayed the highest splenic weight and had the second highest cell numbers of all mice analyzed (2.9 g and 12.5×10^8). The other mouse (# 1779) however, had primarily to be sacrificed since it displayed a tumor in the lower neck region. The mouse had only a slightly elevated splenic weight compared to young Notch2IC//LMP1/CD40//CD19-cre mice (0.72 g versus an average of 0.65 g in young mice). Moreover, the total cell numbers in comparison to young Notch2IC//LMP1/CD40//CD19-cre mice were also only slightly elevated (8.7×10^8 cells versus 5.3×10^8 in young mice).

Despite the comparatively low total cell numbers, the mouse evidently suffered from a B-cell lymphoma. This might be an indication that some B-cell lymphomas in younger mice have gone unnoticed as they do not present themselves as for example those in LMP1/CD40//CD19-cre

mice with an overt splenomegaly and an overt B-cell expansion. On a key note, the two mice that developed monoclonal B-cell lymphomas were also those expressing high hCD2 levels (Tab. 3.2 and Fig. 3.30C) and high levels of CD95 (Fig. 3.30A). This provides further evidence to our hypothesis that if both transgenes are expressed within one B cell this leads to development of lymphoma.
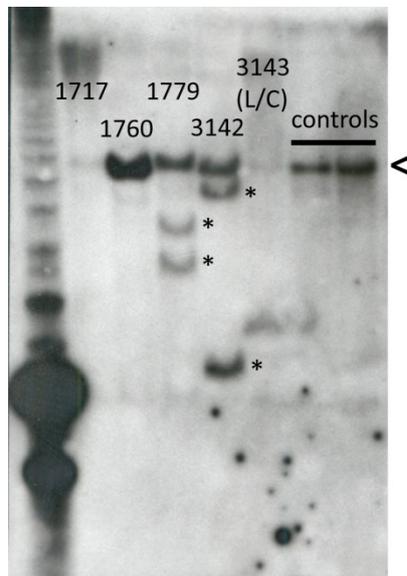
Fig. 3.34 Aged Notch2IC//LMP1/CD40//CD19-cre mice develop monoclonal B-cell lymphoma.
Southern Blot of EcoRI-digested DNA isolated from whole splenocyte preparations. By use of a radioactively-labeled IgH-probe the samples were tested for configurations of their IgH-locus. The arrow points to the band indicating the germline configuration of the respective sample as found in B cells and in any other cell type. The asterisk points to the additional bands indicative of the change in the IgH-locus and monoclonal B-cell expansion in mouse # 3142 and mouse # 1779. The lane carrying the marker is on the left.

Of note, mouse # 1717 and # 1760 that do not display IgH rearrangements are those mice that hardly harbor any B cells in their spleens (Tab. 3.2: # 1717 14 % and # 1760 1,2 % B cells). Since whole splenocyte preparations were used for the Southern blot analysis it is conceivable that the percentage of B cells with a rearranged IgH-locus is simply too small to be noticeable. These mice might carry mono- or oligoclonal expansions in their respective B-cell pools, but they remain undetectable by Southern blot analysis.

3.16 Aged Notch2IC//LMP1/CD40//CD19-cre mice develop salivary gland carcinomas

As shown in Tab. 3.2 (overview of tumor mice) there were mice that had to be sacrificed not only because they developed splenomegalies, but also because three mice developed overt hyperplasias in the lower neck regions (Fig. 3.35A and B). These could be identified by Leticia Quintanilla-Fendt (mouse pathologist, senior physician at the Institute for Pathology, University

of Tübingen) as poorly differentiated carcinomas of the submandibular salivary gland. These carcinomas were henceforth abbreviated to SGTs (salivary gland tumors). She did all the immunohistological characterization of the tissue in the following sections.

The tumor tissue can be visualized by cytokeratin staining on paraffin sections. Fig. 3.35C shows exemplary staining of SGTs of LMP1/CD40//CD19-cre and Notch2IC//LMP1/CD40//CD19-cre mice. In both cases the tumor tissue looks similar and is intergrowing with the rest of the glandular tissue and an ordered gland structure is lost.
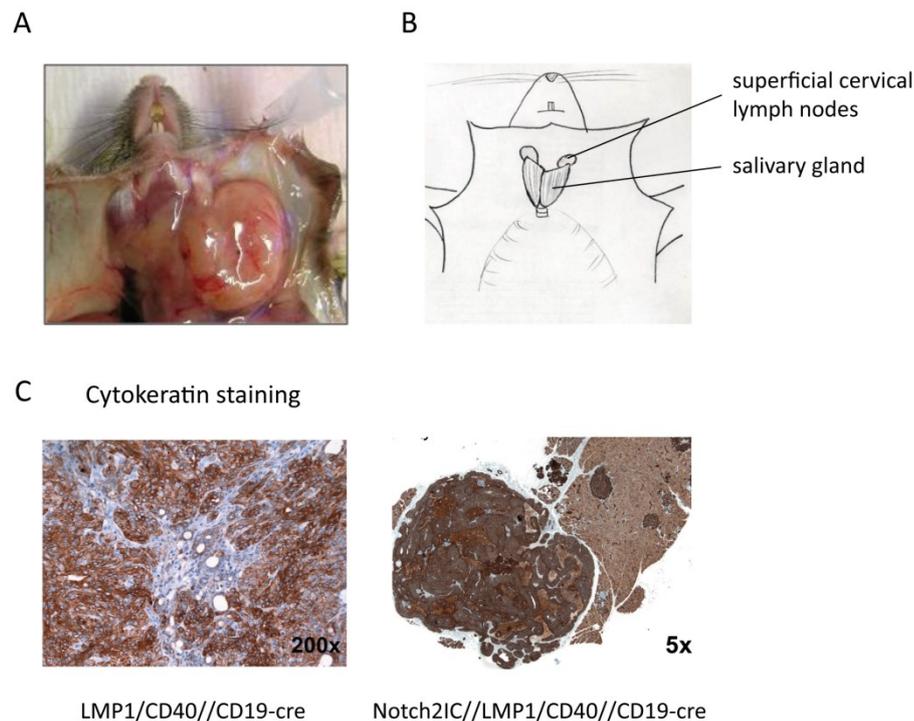
Fig. 3.35 SGT localization in mouse.
(A) SGT on animal (courtesy of C. Hoemig-Hoelzel). (B) Schematic drawing of localization of SG in healthy mice. (C) Tumor tissue as visualized by cytokeratin staining of paraffin sections of SGTs in LMP1/CD40//CD19-cre and Notch2IC//LMP1/CD40//CD19-cre mice. SGT, salivary gland tumor.

These tumor do not only occur in aged Notch2IC//LMP1/CD40//CD19-cre mice, but they have also been observed in LMP1/CD40//CD19-cre mice by former colleagues C. Hoemig-Hoelzel and C. Hojer. An overview of incidence of SGT and/or B-cell lymphoma and age in old LMP1/CD40//CD19-cre mice is given in Tab. 3.5.

Roughly 2/3 of the mice analyzed develop a B-cell lymphoma and half of these have also developed a SGT. However, some few old LMP1/CD40//CD19-cre mice only display SGT development, which means that overall roughly half of the old mice develop a SGT with age.

In aged Notch2IC//LMP1/CD40//CD19-cre mice three out of five mice develop SGTs. From these one mouse (# 1779) has developed an oligoclonal B-cell lymphoma. The two other mice that developed a SGT are # 1778 and # 1717. # 1778 had splenomegaly and a B-cell expansion, presence of a B-cell lymphoma could not be detected by Southern blot analysis due to lack of

DNA material. The other mouse with a SGT (# 1717) had no splenomegaly and rather reduction in B lymphocytes even compared to CD19-cre mice. The other mouse with a B-cell lymphoma (# 3142) had a normal gland. This shows that lymphoma development is not necessarily correlated with development of an SGT.

Tab. 3.5 Overview over LMP1/CD40//CD19-cre mice age in months with SGTs and B-cell lymphoma.
SGT, salivary gland tumor; CH, C. Hojer; CHH, C. Hoemig-Hoelzel

Mouse #	Age (months)	B-cell lymphoma	SGT	Analyzed by
492	10	no	yes	CH
282	12	no	yes	CHH
201	14	no	yes	CHH
740	18	no	yes	CH
947	10	yes	no	CH
849	12	yes	no	CH
445	13	yes	no	CH
787	13	yes	no	CH
197	14	yes	no	CHH
686	14	yes	no	CH
850	14	yes	no	CH
748	18	yes	no	CH
386	18	yes	no	CH
851	19	yes	no	CH
364	12	yes	yes	CHH
685	12	yes	yes	CH
142	14	yes	yes	CHH
247	15	yes	yes	CHH
384	15	yes	yes	CH
34	17	yes	yes	CHH
176	18	yes	yes	CHH

The main question is to uncover the mechanism behind the tumorigenesis. Two scenarios can be envisioned: either the SGTs are elicited by proxy through the activated/lymphatic B- and/or T cells and the SGTs are rather secondary tumors with lymphocytic infiltrates. Or, on the other hand the stop cassette might have been deleted at some time at least in some epithelial cells leading to constitutively active CD40 and constitutively active Notch2IC in the SGs of the respective mice.

With the aim to elucidate this question the paraffin sections of the SGs were stained for the presence of CD3^{pos} and B220^{pos} cells to evaluate them for the presence of lymphocytic infiltrates, for hCD40 (although an antibody detecting the extracellular part of CD40 was used) and hCD2 which is the marker protein that indicates successful deletion of the stop cassette and expression of the targeting construct. hCD2 could deliver clues as to whether carcinogenesis occurs due to a somewhat leaky expression of the transgene(s).

The lymphocyte staining (Fig. 3.36A and B) revealed that both B220^{pos} B cells (B) and also CD3^{pos} T cells (A) are found in higher densities at the capsule lining the SGTs. Interestingly, the B220^{pos} B

cells appear to be rather few compared to the T cells and particularly the CD3^{pos} T cells can also be found in low numbers within the glandular tissue. This staining shows that there are no heavy lymphocyte infiltrates to be found within SGTs, but they rather sit in the surroundings. This is in line with literature findings that strong lymphocyte infiltrates in the salivary glands of wild type mice are only observed upon infection, such as with the Murine cytomegalovirus (MCMV) which displays a strong tropism for the salivary gland (Pilgrim et al., 2007).
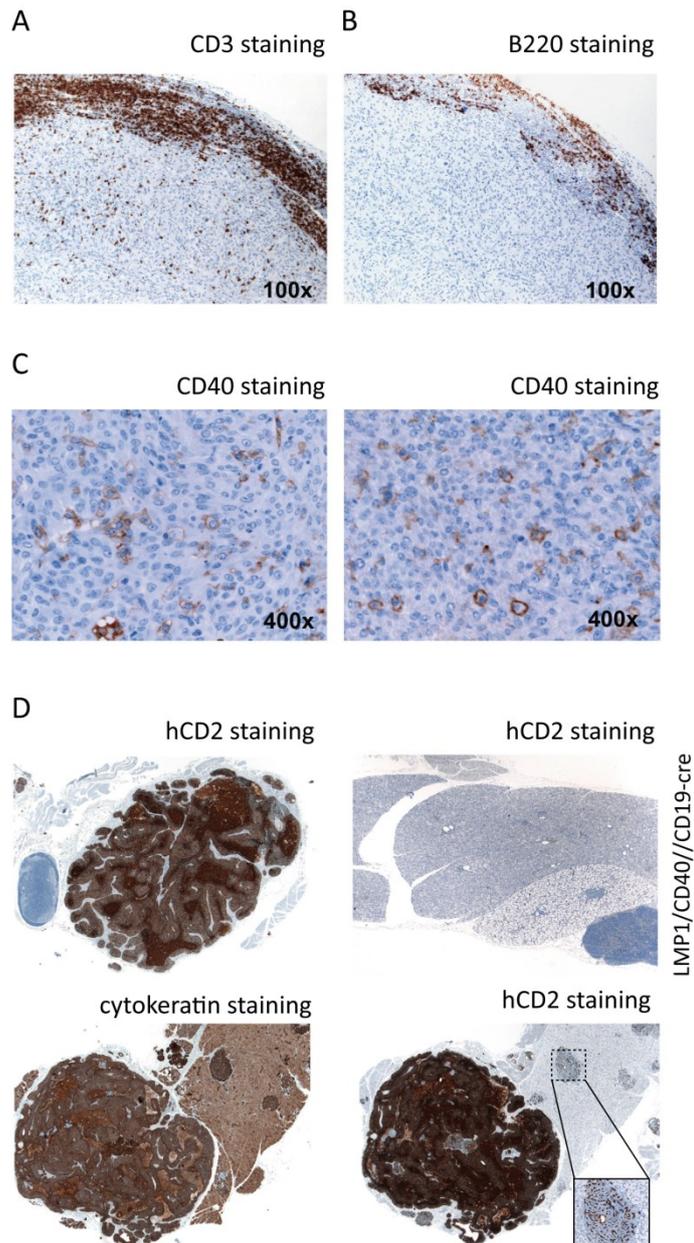
Fig. 3.36 Histological evaluation of lymphocytic infiltrates and surface marker expression in the SGTs of Notch2IC//LMP1/CD40//CD19-cre mice.
IHCs on paraffin sections of SGTs of CD3^{pos} T (A) and B220^{pos} B cells (B), hCD40^{pos} cells (C), hCD2^{pos} cells and cytokeratin (D). IHC, immunohistochemistry; SGT, salivary gland tumor.

The CD40 staining (Fig. 3.36C) shows that only a few cells are positive for CD40. The staining as such appears to be specific since CD40 is a membrane-bound molecule which is where the staining can be observed. These cells could be epithelial cells that up-regulated CD40 independently or infiltrating B cells with CD40.

On the other hand the hCD2 staining (Fig. 3.36D, upper left panel) reveals that the marker surface molecule is prominently distributed throughout the entire tumor tissue in SGTs of Notch2IC//LMP1/CD40//CD19-cre mice, while it is absent in SGTs of LMP1/CD40//CD19-cre mice (Fig. 3.36D, upper right panel) which indicates specificity. Interestingly, the staining patterns appear to be a "photo negative" of the cytokeratin staining, meaning it is especially strong in the areas of the tumor where the cytokeratin staining is weaker and vice versa. (Fig. 3.36D, lower left panel). Furthermore, the hCD2 expression seems to start from the lumen of the vessels that run through the SG tissue (small insert, Fig. 3.36D, lower right panel).

All in all, these histological findings do not deliver final insight what might be the contributing factor for tumor development in the SGs. One would expect the lymphocyte infiltrates to be less discrete at the rim of the tissue, if the infiltrates were the major contributing factor for carcinogenesis. This seems to be supported by the high expression of hCD2 through the entire diseased tissue in the SGTs of Notch2IC//LMP1/CD40//CD19-cre mice, while it is absent in LMP1/CD40//CD19-cre mice.

Southern blot analysis of SGTs shows a partial deletion of stop cassette

The strong hCD2 expression within the tissue (and not just on the connective tissue surrounding the SG where the majority of the hCD2^{pos} B cells are located) rather points toward expression of the transgenes due to excision of the stop cassette in the carcinoma. In order to determine on a molecular level whether the stop cassette has been deleted DNA was extracted from tissue from a normal inconspicuous SG of a LMP1/CD40//CD19-cre mouse and SGT of a LMP1/CD40//CD19-cre mouse and analyzed by Southern blot after EcoRI digest. The probe binds upstream of the first exon of the locus and allows to detect (A) the wild type conformation of the Rosa26 locus, (B) whether the targeting construct has been inserted into the locus and (C) whether there has been a deletion of the stop cassette as part of the targeting locus.

The results of the blot are shown in Fig. 3.37. Only mice having the LMP1/CD40 inserted in only one allele were chosen for analysis. Accordingly one can still see the 15.4 kb band in the blot that indicates the wild type conformation of the targeted locus in one allele. In the SG without tumor there is one additional band at the height 7.2 kb indicative of the successful insertion of the construct into the rosa26-locus, which has been analyzed with the TINA software and was found

to be equimolar to the band at 15.4 kb. In the SGT, there is an additional third band at the height of 5.1 kb that indicates the excision of the stop cassette in the targeting construct that successfully inserted into the Rosa26-locus. This band was again quantitatively analyzed with the TINA software and was found to be equimolar to the band at 7.2 kb in the sample. This is a strong hint that half of the cells in the SGT tissue present with a deleted stop cassette. Considering that the B cells seemed to be rather few that are mainly sitting in the connective tissue capsule it seems unlikely that these account for this amount of deletion of the stop cassette in the tissue. Nonetheless, it cannot be ruled out that these B cells contribute since the material used for the Southern blot analysis was whole tissue preparation because no means of purification of SGT cells were available. DNA material from microdissections of SGT material and controls was prepared, however PCRs detecting the deletion of the stop cassette also remained inconclusive (data not shown).
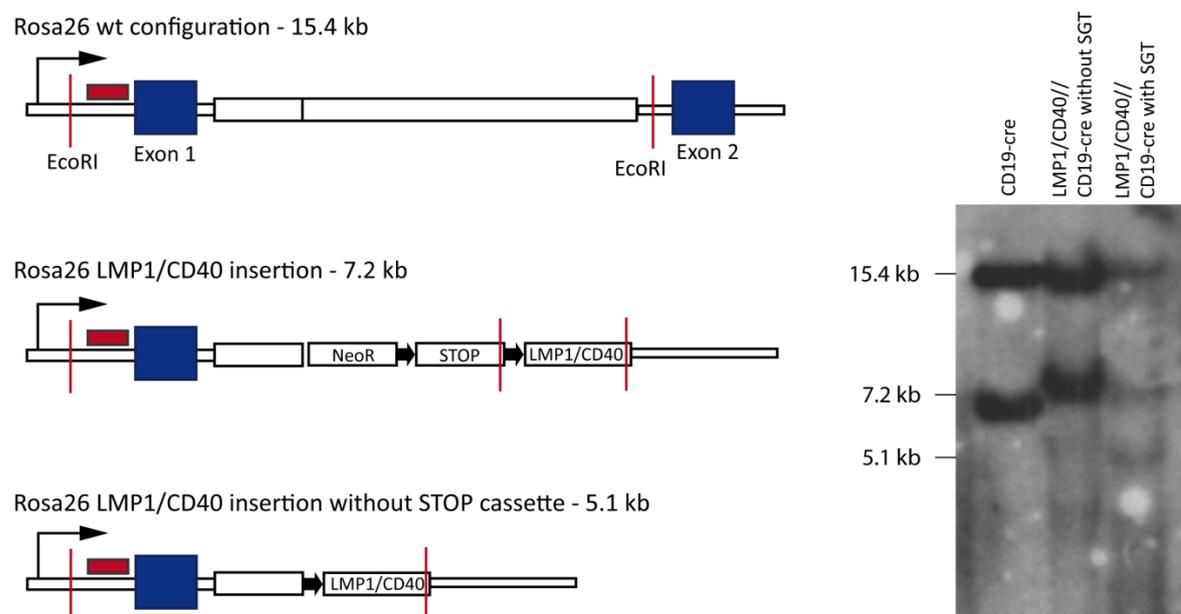
Fig. 3.37 Southern blot analysis of SGTs shows a partial deletion of stop cassette.
(A) Schematic representation of the target locus in wild type configuration (upper panel), with the inserted targeting construct (middle panel) and upon excision of the stop cassette (lower panel). The length (in kb) of the region indicated in the area of the red lines that is detected by the probe (dark red) after EcoRI digest. (B) Southern blot of inconspicuous SG of a LMP1/CD40//CD19-cre mouse and SGT of a LMP1/CD40//CD19-cre mouse showing band sizes upon EcoRI digest and blotting as indicated on the left. kb; kilobase; SG, salivary gland; SGT, salivary gland tumor.

4. DISCUSSION

The rationale behind the cross-breeding mice expressing constitutively active Notch2IC and CD40 in their B cells was to re-create a situation that is found in a number of tumors including B-cell lymphomas such as cHL that display high and constitutive expression of both surface molecules. Indeed with the work at hand it could be shown that such B cells have an activated phenotype, they highly proliferate and cycle actively, that T cell numbers are increased in the spleen and that these T cells are activated and moreover that increased numbers of accessory cells -which also display an activated phenotype- are recruited to the spleen. Moreover, with age these mice seem to be prone to tumorigenesis. These factors shall be examined in more detail in the following sections.

4.1 Notch2IC//LMP1/CD40//CD19-cre mice display an increase in reactive accessory cells in their spleens

The splenomegaly in the Notch2IC//LMP1/CD40//CD19-cre mice is not only due to an increase in the lymphocyte compartment. They also display an increase in accessory cells as for example macrophages. Moreover, macrophages are cells that are –in line with their phagocytic capabilities- inherently larger than most other cell types encountered in the spleen, further adding to the splenomegaly in Notch2IC//LMP1/CD40//CD19-cre mice. The increase in accessory cells in Notch2IC//LMP1/CD40//CD19-cre mice raises of course the question of the mechanism behind the attraction of such cells in the mice. Since the accessory cells as such did not express the transgenes themselves which was demonstrated by the fact that they are hCD2^{neg}, the effect had to be B-cell-mediated. Indeed it has previously been shown that B cells are not necessarily the mere "followers" of inflammatory cues, but in fact can induce inflammation themselves.

This is illustrated by data gathered by Chu and colleagues (Chu et al., 2011). They generated a mouse model with a B-cell-specific knock-out of the ubiquitin-modifying enzyme A20 and demonstrated that this led to a hyperactivation of splenic B cells as well as enhanced proliferation and survival of the B cells. Furthermore, the mice displayed a surge in inflammation-related cells such as myeloid cells (i.e. dendritic cells and macrophages), effector T cells as well as T$_{regs}$ in murine spleens. Ultimately these mice exhibit a severe autoimmune syndrome. The molecule A20 in fact was found to restrict NF-κB signaling downstream of CD40 (Tavares et al., 2010). Therefore it is expectable that B-cell specific loss of a negative regulator of CD40 or constitutive activation of the receptor can lead to the creation of an inflammatory milieu in the spleen of the respective mouse model. This effect seems to be further heightened by

constitutively active Notch2, since the mice expressing both transgenes in their B cells still harbor more granulocytes and significantly more macrophages in their spleens than LMP1/CD40//CD19-cre mice alone.

Interestingly, with regard to LMP1, the viral homologue of CD40 it could also be shown that it can have similar effects even outside of the lymphocyte compartment as was shown by Hannigan and colleagues (Hannigan et al., 2011). They established a transgenic model of multistage carcinogenesis that was induced by epithelial expression of LMP1. Hannigan et al. were able to show an influx of innate immune cells such as macrophages and neutrophils in the skin of mice along with an increase of soluble molecules and inflammatory factors, such as CXCL10, CXCL13, soluble L-selectin and further cytokines. Furthermore, they were able to register that there was a significant increase in activated CD8^{pos} and CD4^{pos} T cells including T$_{regs}$ cells in the dermis of the mice.

Overall the spleens of Notch2IC//LMP1/CD40//CD19-cre mice represent an inflammatory milieu with regard to the influx of reactive innate immune cells. In physiological states upon infection this is desirable and the milieu would subside when infection resolves. However, in states of chronic infection continuous presence of innate immune cells and the sustained release of cyto- and chemokines by these cells themselves as well as the additionally attracted lymphocytes usually have detrimental effect for the individual's health. Recently the term "sterile inflammation" has been coined describing the situation in which the inciting stimulus might not be as harmful to the individual compared to the prolonged "answer" of the immune system towards it (Chen et al., 2010; Rock et al., 2010). Indeed, there is a growing body of evidence illustrating the link between inflammation and tumorigenesis. Prominent examples are gastric cancer which can often be traced back to an initially relatively harmless gastritis induced by *Helicobacter pylori* (Hatakeyama, 2004; Matysiak-Budnik et al., 2006). In the liver chronic hepatitis B virus (HBV) infection can similarly induce hepatocellular carcinoma (Farazi et al., 2006) and 30-50 % of all hepatocellular carcinoma-related deaths can be attributed to HBV-infection (Lavanchy, 2004).

At this point of course it is not clear whether the presence of the accessory cells actually adds to the onset of tumorigenesis or whether they present an innate force that keeps the transgene-expressing B cells in check. Nonetheless, the increase of myeloid cells in general and granulocytes and macrophages in particular rather points towards a tumor-promoting environment.

Macrophages have long been identified as diagnostic markers for in many solid tumors (Qian et al., 2010) and this could also be confirmed with the most recent data from lymphoid tumors with regard to FL and cHL where an increase in macrophages numbers was negatively correlated with disease outcome (Farinha et al., 2005; Kamper et al., 2011). Of note in the latter study, the high

numbers of macrophages were further correlated with presence of EBV in the tumor cell population. Considering the data from LMP1/CD40//CD19-cre and Notch2IC//LMP1/CD40//CD19-cre this effect of macrophage recruitment towards the tumor is likely due to the influence of LMP1 or constitutive CD40 activation.

Nonetheless, tumor-associated macrophages represent a heterogeneous group (Mantovani et al., 2005; Sica, 2010) with diverging roles in tumorigenesis and maintenance: M1 macrophages (classically activated cells) are activated upon LPS and IFNγ-encounter (Th1 phenotype) and rather initiate cytotoxic T cells for an anti-bacterial, anti-viral and anti-tumor response. This could be the case in the spleen of Notch2IC//LMP1/CD40//CD19-cre mice presenting with a tendency for high IFNγ-levels in the tissue. On the other hand, M2 macrophages arise from monocytes upon IL4-and IL13-stimulus. They can promote angiogenesis, tissue-remodeling and dampen the effect of their M1 counterparts (Mantovani et al., 2004a).

Conventional DCs are increased and have an activated phenotype in the spleen of Notch2IC//LMP1/CD40//CD19-cre mice which might hint at a tumor-promoting function by attracting and activating T cells and thereby adding to the inflammatory milieu. In epithelial tumors it was moreover shown that carcinoma cells may condition local DCs to promote proliferation of T$_{regs}$ (Ghiringhelli et al., 2005). On the other hand DCs can act-tumor-suppressing by priming cytotoxic T cells with high efficiency (Steinman et al., 2007). The presence and effect of DCs in solid tumors is quite controversially discussed in the literature (Tsujitani et al., 1990; Troy et al., 1998; Lespagnard et al., 1999). In the field of lymphoma research immature DCs have been proposed to promote survival of malignant T cells (Ni et al., 2011), but mature DCs have also been linked to improved clinical outcomes in cohorts of DLBCL patients (Chang et al., 2007). It has to be kept in mind that they represent a highly heterogeneous group that can be classified by their phenotypes, stages of maturation, degrees of activation and functions and accordingly few generalizations can be made. It was not clarified in the thesis at hand whether the spleens of Notch2IC//LMP1/CD40//CD19-cre mice harbor more DC subtypes than the detected conventional DCs.

Interestingly, in the older Notch2IC//LMP1/CD40//CD19-cre mice the expansion of the macrophages in the spleen is still present, but their presence in numbers can vastly differ between individual mice although of the same genotype, hinting at the fact that the long-term outcome of constitutively active CD40 and Notch2IC can lead to different results or types of tumors and necessitates a "second hit" of signaling deregulation.

Future experiments should also examine the level of lymphocytes and myeloids in the blood in order to clarify whether elevated cell numbers are contained to the spleen or present a systemic response to the transgene expression of the B cells.

4.2 Notch2IC//LMP1/CD40//CD19-cre mice display an increase of activated T cells and increase in the percentage of both central memory as well as effector memory T cells in their spleens

The splenic T-cell population in Notch2IC//LMP1/CD40//CD19-cre mice is significantly larger than the already increased B-cell population in these mice. However, predominance of a T-cell over a B-cell population cannot be regarded as diagnostic marker of malignancy per se. The atypical distribution of CD4^{pos} versus CD8^{pos} T cells however, can count as considerably better criterion whether the situation at hand is abnormal. In Notch2IC//LMP1/CD40//CD19-cre mice both T-cell subsets were increased in the spleen, however with a clear bias towards the CD8^{pos} compartment. In a FACS approach to characterize T-lymphoproliferative disorders Gorczyca and colleagues showed that while in concordance with previous data HL displayed a clear tendency towards CD4^{pos} T-cell expansion (Gorczyca et al., 2002). On the other hand immunocompromised individuals such as HIV^{pos} patients, as well as individuals with certain viral infections such as EBV an expansion of an increased number of CD8^{pos} T cells in relation to CD4^{pos} T cells can be observed (Borowitz et al., 1982; Weisberger et al., 2003).

Notch2IC//LMP1/CD40//CD19-cre mice show a distinct up-regulation of CD25 and CD69 in a subpopulation of their splenic T cells. Moreover a reduction of the naïve T cells can be observed in Notch2IC//LMP1/CD40//CD19-cre mice like in the single transgene-expressing mice. The single transgene-expressing controls resemble the Notch2IC//LMP1/CD40//CD19-cre mice also in the distribution of splenic T cells with regard to CD44 and CD62L marker expression, more precisely in their tendency to adopt an effector phenotype (CD44^{hi} CD62L^{low}). The down-regulation or shedding of CD62L (L-selectin) could be due to a number of reasons. On the one hand, Meijer and colleagues were able to identify tumor-specific type 1 T cells from lymph nodes draining an autologous tumor cell vaccine that are characterized by reduced CD62L expression (Meijer et al., 2004). Furthermore, a group around Morgan was able to show that shedding of CD62L occurs when T cells encountered specific tumor antigen and it regulates lytic activity in human tumor reactive T lymphocytes (Yang et al., 2011). Moreover, myeloid-derived suppressor cells (MDSCs) were found to down-regulate CD62L expression on CD4^{pos} and CD8^{pos} T cells (Hanson et al., 2009). MDSCs represent a population of myeloid cells which -due to interference through tumor-derived factors- are unable to differentiate into granulocytes, macrophages and DCs and accumulate at individual's blood, in lymphoid organs and at tumor sites and might provide an important link between inflammation and cancer (Sinha et al., 2008; Ostrand-Rosenberg et al., 2009). These cells might be of interest in Notch2IC//LMP1/CD40//CD19-cre mice, since they harbor high percentages of myeloid cells in their spleens in general and exhibit a down-regulation not only of CD62L but in fact of both CD62L and CD44 in their splenic T cells. However, this would

have to evaluated carefully since MDSCs exhibit their tumor promoting function by suppressing T-cell activation and proliferation (Bronte et al., 2000; Terabe et al., 2003; Rodriguez et al., 2005; Rodriguez et al., 2008). This seems to argue against presence of such cells in Notch2IC//LMP1/CD40//CD19-cre mice because of the high splenic T-cell number in these mice. However, MDSCs might account for the fact that not all of the T cells in the spleen exhibit high levels of the activation markers (CD65, CD25) throughout and as aforementioned they might be responsible for the overt down-regulation of both CD62L and CD44.

The shift from effector T cells (CD62L^{low} CD44^{hi}) versus CD62L^{low} CD44 $^{low/neg}$ that is discernible in the splenic T cells of Notch2IC//LMP1/CD40//CD19-cre mice could also be observed in LMP1/CD40//CD19-cre mice. This observation might indicate exhaustion of T cells.

Exhaustion is a commonly observed phenomenon for example in sustained viral infections such as HIV infection. This was shown to be reinforced by the presence of the inhibitory receptor PD1 (programmed cell death 1) on T cells (Barber et al., 2006; Blackburn et al., 2009; Mueller et al., 2010). When testing for PD1 expression via flow cytometric analysis in mice of all genotypes tested the obtained results indeed showed a distinct up-regulation of the inhibitory receptor in splenic CD4^{pos} T cells of LMP1/CD40//CD19-cre and Notch2IC//LMP1/CD40//CD19-cre mice compared to CD19-cre controls (data not shown; CD8^{pos} were not tested). However, this up-regulation was unexpectedly also observed for Notch2IC//CD19-cre mice. Hence, PD1 up-regulation might contribute, but does not necessarily lead to the potential T-cell exhaustion in LMP1/CD40//CD19-cre and Notch2IC//LMP1/CD40//CD19-cre mice.

Interestingly, PD1 has been found on T cells only when they are activated (Keir et al., 2008) and it has also been implicated in the development of T$_{regs}$ or inducible iT$_{regs}$ in the periphery. The receptor is highly expressed on this cell type and seems to be involved at various levels in functioning of (i)T$_{regs}$ (Polanczyk et al., 2007; Francisco et al., 2009; Francisco et al., 2010; Gotot et al., 2012). Hence, PD1 expression or up-regulation of the surface molecule could offer an explanation why especially CD8^{pos} T cells display a down-regulation of CD44 and CD62L and also why there is an increase in T$_{regs}$ in the spleen of Notch2IC//LMP1/CD40//CD19-cre mice and should be further evaluated in the future.

4.2.1 T$_{regs}$ are increased in splenic preparations of Notch2IC//LMP1/CD40//CD19-cre mice

As shown, Notch2IC//LMP1/CD40//CD19-cre mice display an increase in T$_{regs}$ in their spleens. T$_{regs}$ are known to play a role in suppressing autoimmunity, but they are also able to dampen anti-tumor response and are suspected to support tumor immune escape (Kryczek et al., 2009; Boursier et al., 2012; Mailloux et al., 2013). All in all, T$_{regs}$ can be "a double-edged sword".

Considering the impact of T_{regs} in patients with B-cell lymphomas, those with a high number of tumor infiltrating Foxp3^{pos} cells (T_{regs}) have a better survival than patients with few Foxp3^{pos} cells as was shown for DLBCL, FL and cHL patients (Alvaro et al., 2005; Carreras et al., 2006; Lee et al., 2008; Tzankov et al., 2008; Wahlin et al., 2010; Koreishi et al., 2010; Kelley et al., 2007). Indeed, in the context of B-cell malignancies T_{regs} seem to have rather tumor-suppressing role owing to their physiological role to keep B cells in check and even kill defective B lymphocytes in order to prevent autoimmunity (Lindqvist et al., 2012).

Thus, the presence of these cells in the spleen of the Notch2IC//LMP1/CD40//CD19-cre mice could be one of the key factors why these mice develop B-cell tumors rather late in their lifetime (from 13 months onward). It will be highly interesting to further evaluate the role of T_{regs} in the Notch2IC//LMP1/CD40//CD19-cre mice: to test for the presence of T_{regs} particularly in older mice and examine whether the expansion of this particular T-cell subgroup is diminished or disappears altogether. The presence of B-cell-derived IL10 is vital for the proper development and maintenance of T_{regs} (Carter et al., 2011), moreover B7 proteins (CD80 and CD86) on B cells have been implicated to play a role in the development and activation of the T-cell subgroup (Tsukahara et al., 2005; Mann et al., 2007). While IL-10 was not found to be up-regulated in serum or in splenic B cells themselves, CD80 was up-regulated in splenic B cells expressing both transgenes whereas CD86-levels were basically unchanged compared to controls in the young mice. Interestingly, these B7 molecules have been suggested to have diverging roles in T_{reg} regulation (Zheng et al., 2004): while blockage of CD86 appears to enhance T_{reg} suppressive function, blockage of CD80 rather seems to lead to T_{reg} division. This might point towards why even high T_{reg} numbers in the mice might not be able to ward off disease in the long run. And finally in the old mice CD80 is also up-regulated, which is likely to be unrelated to presence or absence of T_{regs}, since CD80 is also found to be highly expressed on HRS cells (Vooijs et al., 1997). As aforementioned, it will be interesting to monitor aged mice particularly for the presence of T_{regs} routinely to examine possible correlation of their presence, absence or decline with the onset of tumorigenesis in the Notch2IC//LMP1/CD40//CD19-cre mice. Also, since there is data showing that the effect of T_{regs} in the outcome of disease might be closely linked with the composition of cells in the respective tumor infiltrate (Schreck et al., 2009) this will have to be evaluated in relation to a panel of analysis regarding the presence of different subtypes of accessory cells in the aged Notch2IC//LMP1/CD40//CD19-cre mice .

4.3 Concomitant expression of constitutively active Notch2IC and CD40 has synergistic effects on spleen size and activation status of the splenocytes

Spleens of Notch2IC//LMP1/CD40//CD19-cre animals are significantly larger and heavier than all control counterparts, which is an additive effect of the constitutively active signaling of CD40 and Notch2IC in the B cells of these mice. Any de- or increase in size and weight of the organ is influenced by basically two factors: A) activation status of the splenic cells which influences cell size and which can also be linked to cell type and B) actual cell number.

Notch2IC//LMP1/CD40-expressing splenic B cells are activated with regard to their levels of activation markers -i.e. CD80 and ICAM. This finding can be attributed to expression of both transgenes in the B cells. It is known that activation of cells also leads to an increase in cell size. LMP1/CD40-expressing splenic B cells were previously shown to display a shift in various activation markers (of which CD95 is specific for LMP1/CD40 expression in the cell) and accordingly they display an increase in cell size. Moreover, these mice exhibit an increase both in the splenic B- and T-cell numbers. With regard to Notch2IC//CD19-cre mice, B cells are also activated but in this case this is probably primarily due to the fact that these splenic B cells –as in mice expressing both transgenes- adopt a MZ B-cell phenotype and MZ B cells are inherently pre-activated. This also explains the slight, but significant splenic weight difference between CD19-cre and Notch2IC//CD19-cre mice, even though the splenic B- and T-cell compartments are not expanded in these mice. The overall increase in splenic size in Notch2IC//LMP1/CD40//CD19-cre mice can be attributed to the impact of constitutive CD40 signaling on the lymphocyte compartment leading to an increase of both B- and T-cell compartments and additionally of the macrophage and granulocyte numbers in their spleen, as well as the B-cell size, which is increased due to their activation status. Cell size and increased activation are also due to Notch2IC-induced MZ B-cell phenotype of the Notch2IC//LMP1/CD40-expressing B cells.

4.4 Marginal zone B cells are expanded in Notch2IC//LMP1//CD40//CD19-cre mice at the expense of the follicular B-cell population

It is by now a well-established fact that Notch plays a role in MZ B-cell development (Tanigaki et al., 2002; Saito et al., 2003; Kuroda et al., 2003; Hozumi et al., 2004; Hampel et al., 2011). Therefore it was not unexpected that both in Notch2IC//CD19-cre and Notch2IC//LMP1//CD40//CD19-cre mice this population of mature B cells is expanded at the expense of Fo B cells, with regard to CD21/CD23-, IgM/IgD- and CD1d-status.

Both in vitro and in vivo studies have shown that Notch signaling enhances expression of CD21/35 in B cells (Saito et al., 2003; Strobl et al., 2000). The mechanism behind this being the

fact that the first intron of the murine CD21 gene has three regulatory RBP-J sites and the commitment to high CD21 levels have been suggested to let the B cells develop into MZ B cells (Makar et al., 2001; Zabel et al., 2002).

MZ B cells are suggested be mostly generated from the T1 transitional stage, but are also thought to develop from T2 B cells and pre-MZ B cells (Pillai et al., 2005). T2 and pre-MZ B cells down-regulate surface expression of CD23 as they differentiate into MZ B cells. In the physiological in vivo situation this is likely to be supported by ADAM 10, the metalloproteinase that accounts for the S2 cleavage of the Notch receptor and thereby initiates Notch signaling cascade. Moreover, ADAM10 leads to shedding of CD23 as shown by both in vitro and in vivo studies (Weskamp et al., 2006; Lemieux et al., 2007; Gibb et al., 2010), further defining the MZ B-cell phenotype and amplifying it by inducing Notch signaling.

LMP1/CD40-expressing B cells with regard to CD21/CD23 surface marker rather display an MZ B-cell-like phenotype, whereas Notch2IC-expressing B cells do not only present with a MZ B-cell phenotype but they are almost $CD23^{neg}$. Therefore, additional expression of constitutive CD40 in B cells aside from constitutive expression of Notch2 leads to an attenuation of this almost "overt" MZ B-cell phenotype in Notch2IC//LMP1//CD40//CD19-cre mice. Splenic B cells expressing both transgenes indeed rather resemble MZ B cells of CD19-cre controls. Also, LMP1/CD40 signaling leads to different localization cues in splenic B cells compared to constitutive Notch2 signaling alone. This shall be further discussed in the next chapter.

4.5 Splenic architecture is grossly disrupted in Notch2IC//LMP1/CD40//CD19-cre mice

In the FACS analysis the B cells of LMP1/CD40//CD19-cre mice appear to have an MZ B-cell-like phenotype. Nonetheless, for the majority the B cells in these mice were still able to reside within the follicle. The border separating follicle from MZ can -in IHC analysis- be optically determined by the localization of $MOMA1^{pos}$ macrophages. These are already quite dispersed in spleens of LMP1/CD40//CD19-cre in contrast to CD19-cre and Notch2IC//CD19-cre mice, which might hint at a very mild disruption of structure and a very low difficulty of the B cells to localize properly. Notch2IC-expressing B cells display a clear MZ B-cell phenotype at the expense of Fo B cells, both in the FACS analysis results as well as with regarding to the localization of the B cells in the actual MZ. Surface marker expression in Notch2IC//LMP1/CD40//CD19-cre mice as shown in the FACS analysis- suggests that B cells expressing both transgenes exhibit a clear MZ B-cell phenotype and did not insinuate a diffuse splenic structure as observed in the IHC staining. However, the splenic architecture of Notch2IC//LMP1/CD40//CD19-cre mice is very unique with still high number of B

cells residing in the Fo zone despite the MZ marker expression profile on the one hand and loss of defined T- and B-cell zones on the other.

CXCR4 is known to be responsible for homing of B cells to the bone marrow (Petit et al., 2002). CXCR4-deficient mice are impaired in B-lymphopoeisis, myelopoeisis and unable to produce normal numbers of viable mature B cells (Ma et al., 1998; Nie et al., 2004). CXCR4 was previously not reported to influence the MZ versus Fo B-cell lineage decision (Nie et al., 2004). This was underlined by the data presented in this thesis finding no noticeable difference in expression level between Fo and MZ B cells in control mice. However, the difference in expression levels between LMP1/CD40-expressing splenic B cells and Notch2IC-expressing splenic B cells were quite large and considering the localization of the majority of B cells in the respective mouse (LMP1/CD40-expressing rather in the Fo; Notch2IC-expressing rather in the MZ), there could be a however complex connection between these observations (CXCR4 level and localization of B cells in the spleen). However, this positional information conveyed by CXCR4 is lost in splenic B cells expressing both transgenes, since they express intermediate level between Notch2IC- and LMP1/CD40-expressing B cells. This could add to the effect that these B cells despite their MZ B-cell phenotype rather reside in the Fo area. It would be interesting to determine the level of the CXCR4 ligand SDF1 (stromal-derived factor1) in the cells of the red pulp where SDF1 level are usually high (Cyster, 2005). This could deliver clues as the actual positional clues that Notch2IC//LMP1/CD40-expressing splenic B cells are actually exposed to with regard to CXCR4 signaling.

The evaluation of normal CXCR4 levels in correlation with low serum levels of the ligand SDF1 (i.e. lower than in the CD19-cre controls and single transgene expressing mice) might also account in part to the low B-cell numbers in inguinal lymph nodes and low numbers of recirculating B cells in the bone marrow. Yet, this still leaves low numbers of Notch2IC-expressing B cells in the aforementioned compartments unexplained.

Another factor that could have implications for the localization of splenic B cells is LTβ, which was found up-regulated with regard to its mRNA levels both in LMP1/CD40-expressing and in Notch2IC//LMP1/CD40-expressing B cells. In physiological conditions signaling disruption via the LTα/β complex leads to severe impairment in development even complete loss of secondary lymphoid organs (Rennert et al., 1996; De Togni et al., 1994). The signaling axis is also important during the remodeling of lymphoid tissue during viral infections and the process is mediated by B lymphocytes (Kumar et al., 2010). More precisely loss of LTβ signaling leads to loss of splenic MZs marginal zones and T/B-cell segregation (Futterer et al., 1998). Inversely, adverse effects could also be anticipated if LTβ expression is unusually high as found in splenic B cells of LMP1/CD40//CD19-cre and Notch2IC//LMP1/CD40//CD19-cre mice.

This leads to the other aspect of abnormal splenic architecture in these mice. As aforementioned it is not only an open question why the B cells expressing both transgenes do not localize strictly in the MZ according to their surface marker expression, but also what is the reason for the loss of a defined T/B-cell zone. Also under this aspect it would be valuable to examine the increased LTβ level since the engagement of LTβR on splenic stroma cells prompts them to release further cytokines such as CCl21. CCL21, like CCL19, is a ligand for CCR7. CCR7 level and those of its ligands play an important role both for B- as well as T cells in order to localize properly in the spleen (Forster et al., 1999; Luther et al., 2000; Okada et al., 2007). In fact this receptor although it is only subtly expressed on B cells enables them -along with CXCR4 and CXCR5- to leave the blood stream and to enter secondary lymphoid tissues such as lymph nodes and intestinal Peyer's patches (Okada et al., 2002; Ebisuno et al., 2003). Moreover, it can be hypothesized that the loss of structure contributes to the activation of the B- and especially the T cells, since the region of interaction between the lymphocytes is not limited to the T/B-cell border.

4.6   Notch2IC//LMP1/CD40//CD19-cre mice show distinct changes in the expression level of cyto- and chemokines in serum and splenic B cells

CXCR3 and IL13rα1, IL2Rγ, LTβ and TGFβ mRNA levels in splenic B cells of Notch2IC//LMP1/CD40//CD19-cre mice were found to be differentially up-regulated by Notch2IC and LMP1/CD40. Cyto- and chemokines that were up-regulated on mRNA level particularly in Notch2IC-expressing B cells were CXCR3 and IL13Rα1. The cyto- and chemokines that were up-regulated particularly in LMP1/CD40-expressing B cells and to a lesser degree in Notch2IC//LMP1/CD40-expressing B cells were IL2Rγ, LTβ and TGFβ. Notch2IC//LMP1/CD40//CD19-cre mice furthermore show an up-regulation of CXCL9 and CXCL10 and IL16 in serum compared to all other genotypes.

It effect that the up-regulation of the mRNA levels of interleukin receptor subunits IL13Rα1 and IL2Rγ has in splenic B cells of Notch2IC//LMP1CD40//CD19-cre mice is probably complex, since both are subunits function as part of a number of different ILRs. IL13R mediates both IL13 as well as IL4 signaling. Both IL4 and IL13 were shown to have anti-inflammatory capabilities, e.g. they have been related to the protection of pancreatic β-cells (Zaccone et al., 1999; Kaminski et al., 2007) and the prevention of destructive insulitis (Rabinovitch et al., 1998). However IL4 is also a potent B-cell stimulus necessary for class switching and B-cell proliferation (Mandler et al., 1993; Rush et al., 2002; Kim et al., 2007). IL2Rγ on the other hand is also known as the common γ-chain and is part of the respective ILR mediating IL2-, IL4-, IL7-, IL9-, IL15- and IL21-responses (Takeshita et al., 1992; Russell et al., 1993; Asao et al., 1993; Sugamura et al., 1995; Asao et al., 2001), which

are involved in a number of developmental processes not only in B cells, but also T- and NK cells. Taken together these findings of higher subunit level suggest an increased responsiveness of Notch2IC//LMP1/CD40-expressing B cells towards further cytokine stimulation.

TGFβ has been implicated to play a role in numerous biological processes, i.e. cell growth, inflammation, matrix synthesis and apoptosis (Taipale et al., 1998). With regard to tumorigenesis in solid tissues TGFβ has been implicated in metastasis and angiogeneisis (Yu et al., 2000; Padua et al., 2009). On the other hand, in the context of B-cell lymphoma it has been shown to induce growth arrest (Bakkebo et al., 2010), moreover TGFβ has also been implicated in recently discovered regulatory function of B cells in the tumor environment (Yang et al., 2010). The latter rather points towards a counter reaction to overt B-cell activation and proliferation in the LMP1/CD40//CD19-cre and Notch2IC//LMP1/CD40//CD19-cre animals.

LTβ is likely to have implications in the localization of Notch2IC//LMP1/CD40-expressing B cells as laid out in the previous section. Furthermore, signaling via the LTβ receptor in classical DCs has been shown to be of importance in their development (Kabashima et al., 2005). Blocking the pathway also leads to an decrease in T_{regs} but also inflammation in mice treated with a receptor antagonist (Nakayama et al., 2012). Considering this, overt LTβ signaling -besides its implications in T/B-cell positioning- might be a contributing factor leading to the surge in T_{regs} and DCs in the spleen of Notch2IC//LMP1/CD40//CD19-cre mice. Moreover a role for this signaling pathway has been proposed in establishing a lymphoma-supporting niche in the spleen fostering a microenvironment with the involvement of various cell types as observed in cHL (Kuppers, 2011; Rehm et al., 2011).

Along the lines of accessory cell recruitment one can interpret the data for increased IL16 serum levels. IL16 is a chemoattractant for all CD4-expressing cells. It is a cytokine that can as well attract myeloid cells, DCs, macrophages and other cell types as was observed in the spleens of Notch2IC//LMP1/CD40/CD19-cre animals. Furthermore, IL16 is able to induce up-regulation of IL2R (CD25) on T cells (Parada et al., 1998). Therefore it can influence T-cell dynamics 3-fold: it can lead to a better reactivity towards T-cell-activating IL2, and lead to both the increase in $CD25^{pos}$ T cells as well as the overall increase of T_{regs} (which are $CD25^{pos}$).

Most interestingly is probably the finding of increased CXCR3 mRNA level in splenic B cells as well as increased serum level of CXCL9 and CXCL10 (its ligands) in the Notch2IC//LMP1/CD40//CD19-cre mice liking data from the mRNA and serum analysis

Although hardly detectable on Fo B cells, CXCR3 is known to be higher expressed on MZ B cells, which is in line with the higher level of the receptor in Notch2IC- and Notch2IC//LMP1/CD40//CD19-cre mice that display a MZ B-cell phenotype. This was further

underlined by results of an mRNA array by Stefanie Ehrenberg from our lab (personal communication). Therefore, it is not so surprising that the level of the receptor are also high in B-cell lymphomas associated with this particular entity of mature B cells i.e. the MZ B cells. For example, strong expression of CXCR3 was observed patients with B-CLL, FL, in SMZL and in the monocytoid and plasmacytic cells in extranodal marginal zone lymphoma (Jones et al., 2000; Ohshima et al., 2003).

The level of ligands for CXCR3, i.e. CXCL11, CXCL10 and CXCL9 are increased in serum of Notch2IC//LMP1/CD40//CD19-cre mice. Together they form a group of homologous proteins that elicit their chemotactic function via binding to the G-protein-coupled receptor CXCR3 (Loetscher et al., 1996; Luster et al., 1995; Lasagni et al., 2003). CXCR3 is also rapidly induced on naïve T cells following activation (Groom et al., 2011). In fact, engagement of CXCR3 facilitates the shift of CD8^{pos} cells towards differentiation into effector cells (Kurachi et al., 2011). Receptor blockage via an agonist leads to strong inhibition of the migration of T cells and the role of CXCL10 and CXCL9 in the recruitment of effector T lymphocytes to sites of inflammation has been documented (O'Boyle et al., 2012). Moreover, these cytokines are secreted not just by T cells through a positive feedback loop but CXCL9 and CXCL10 are also produced by DCs, B cells, and macrophages (Park et al., 2002) and the receptor was also found on endothelial cells and in infiltrating lymphocytes with an activated phenotype in inflammatory diseases. The fact that the ligands can be produced by B cells as well combined with the fact of higher level of their receptor strongly supports the hypothesis of a positive feedback loop in Notch2IC- and Notch2IC//LMP1/CD40//CD19-cre mice. Interestingly, CXCR3 is expressed by certain DC subsets, specifically myeloid-derived CD11c^{pos} cells in normal and inflammatory conditions (Garcia-Lopez et al., 2001). This supports the findings that there is a distinct increase in accessory cells such as macrophages and CD11c^{pos} DCs of an activated phenotype in the Notch2IC//LMP1/CD40//CD19-cre mice due to systemic presence of these ligands. Up-regulation of CXCR3 in splenic B cells compliments the high serum level of its ligands in these mice and might help to establish and maintain the inflammatory milieu in these mice and maybe even the MZ B-cell phenotype.

A factor that was synergistically down-regulated in serum of Notch2IC//LMP1/CD40/CD19-cre mice was CXCL12, also termed SDF1 which is a homeostatic chemokine. The major function of this chemokine is to regulate hematopoietic cell trafficking, since it induces intracellular actin polymerization needed for cell motility (Bleul et al., 1996) and also secondary lymphoid tissue architecture (Teicher et al., 2010). The chemokine has two receptors, i.e. CXCR4 and CXCR7, the former of which was not found to be down- or up-regulated in splenic B cells of Notch2IC//LMP1/CD40//CD19-cre compared to CD19-cre animals, but found to be up-regulated

in Notch2IC//CD19-cre and down-regulated in LMP1/CD40//CD19-cre mice. In the spleen CXCL12 is mainly found in the red pulp (Cyster, 2005), and its down-regulation with constant CXCR4-levels might contribute to the positioning defects observed in the spleen of Notch2IC//LMP1/CD40//CD19-cre mice.

It would be highly interesting to evaluate the cyto- and chemokine profile of the splenic cells in situ in order to decipher the respective contribution of the different cellular compartment that were found to be expanded in mice expressing both transgenes in their B cells.

4.7 Notch2IC//LMP1/CD40-expressing splenic B cells show an increased proliferation in in vitro culture regardless of the supply of stimuli

Many of the parameters that were examined in the Notch2IC//LMP1/CD40//CD19-cre mice were clearly due to the expression of one or the other transgene, for example the MZ B-cell phenotype is an effect that can be clearly be attributed to constitutively active Notch2IC in the B cells of these animals. By contrast, the effect concomitant expression of both transgenes in the splenic B cells has on their proliferative behavior is derived from both LMP1/CD40 and Notch2IC signaling.

As has been shown before Notch can convey proliferative signals to the cell in which it is expressed, however activity of the pathway also leads to apoptotic signals (Kohlhof et al., 2009). This outcome can differ depending on cell type and potential disease state. On the one hand pharmacological inhibition of the Notch pathway can lead to apoptosis in immortalized Kaposi's sarcoma and B-CLL cells (Curry et al., 2005; Rosati et al., 2013) and Notch inhibition has been discussed as a possible approach in treatment of cancer especially with regard to subduing cancer stem cells (Purow, 2012). On the other hand Notch2 signaling was found to sensitize endothelial cells to apoptosis through negative regulation of apoptosis regulator Survivin (Quillard et al., 2009), to induce apoptosis in neural progenitor cells through a p53-dependent pathway (Sakurada et al., 1992). Generally, Notch signaling has been recognized as a powerful initiator of growth arrest and apoptosis in a number of B-cell malignancies (Zweidler-McKay et al., 2005). In the data presented here it could also be observed that Notch2IC-expressing splenic B cells survived less well in in vitro culture without stimulus than LMP1/CD40-expressing splenic B cells or B cells expressing both transgenes. However, the results of the BrdU analysis also showed a high percentage of Notch2IC-expressing B cells in S-phase of the cell cycle which underlines that Notch signaling strongly supports the proliferation of the splenic B cells. The proliferative state of Notch2IC-expressing cells is in line with data showing that Notch can in fact induce a number of cell cycling genes such as CyclinE1, CyclinE2, CyclinA2 and CDK6 (cyclin-dependent kinase6) and CDK4 (Kohlhof et al., 2009). Moreover, Notch is known to induce the transcription factor c-myc,

which plays a key role in inducing cell cycle regulation, proliferation and growth (Palomero et al., 2006). C-myc is deregulated in a number of cancers, in the field of hematopoietic malignancies it is probably best characterized for its Notch-induced role in T-ALL (Weng et al., 2006; Riz et al., 2010) and Burkitt lymphoma (Li et al., 2003; Mirandola et al., 2009).

CD40 is vital for the growth, survival and differentiation processes of the B cell (Gordon, 1995; Kehry, 1996) and has moreover shown to also enhance survival in DCs and other cells (van Kooten et al., 1997), it can also induce apoptosis in hepatocytes through up-regulation of CD95 (Afford et al., 1999; Afford et al., 2001). These effects can be overpowered by TRAF-signaling-induced up-regulation of the anti-apoptotic proteins Bcl-x_L and Bfl-1/A1 that is NF-κB-mediated (Lee et al., 1999).

In the in vitro culture one could clearly see the survival advantage LMP1/CD40-expressing B cells had over Notch2IC-expressing B cells, due to the effects of constitutively active CD40 relaying strong survival signals to the B cell. However, with regard to their proliferation state or more precisely the percentage of strongly proliferating B cells in S-phase they actually lagged behind Notch2IC-expressing B cells. Examining the dynamics of cell cycle and survival of B cells of Notch2IC//LMP1/CD40//CD19-cre mice one can observe the synergies that arise from the combination of both constitutively active CD40 and Notch2IC: While these B cells display better overall survival (CFSE- and Topro-3-staining data) without any stimulus, they display higher percentages of B cells that are actively cycling in S-phase of the cell cycle (BrdU data), leading in the sum to proliferation rates surpassing those of all genotypes tested in parallel.

At this point one can only hypothesize as to what the exact mechanisms behind these proliferative capacities are. As aforementioned c-myc is a potential candidate, but this should be evaluated carefully. A further candidate for evaluation would be the cell cycle regulator p53 for which Notch1 has been described to be a target and various crosstalk levels between the two signaling pathways have been suggested (Dotto, 2009; Wickremasinghe et al., 2011; Roemer, 2012). p53 could also be regulated by active CD40 signaling as has been shown for multiple myeloma cell lines (Teoh et al., 2000; Tai et al., 2002).

4.8 Aged Notch2IC//LMP1/CD40//CD19-cre mice are prone to develop B-cell lymphomas

With regard to B-cell lymphoma development one year-old LMP1/CD40//CD19-cre mice started to develop lymphomas with a high incidence, whereas with one year none of the Notch2IC//CD19-cre mice developed obvious signs of lymphoma (Homig-Holzel et al., 2008; Hampel et al., 2011), which implies that in contrast to constitutively active CD40, constitutively

active Notch2 signaling alone is not sufficient to drive B-cell lymphomagenesis. However, as seen in the in vitro data the combination of both transgenes greatly enhances proliferation and survival of the cells. And in fact, although the test population that was kept for long-term observation was rather small, it seems that these mice also develop lymphomas with a high incidence: since three out of five mice showed a vast increase in the lymphocyte compartment and two out of five mice could be diagnosed with a monoclonal expansion of their splenic B-cell population. However, although the Southern blot did not deliver definite confirmation for the expansion of several B-cell clones in the other mice, does not confirm their absence. Especially in the aged mice with low B cell numbers the method of Southern blot analysis might not be sensitive enough to detect several, maybe more subtle expansion of B cells with different clonalities. This is indeed the case in cHL, where only a fraction of the tumor mass consists of the actual lymphoma cells which are surrounded by large numbers of various accessory cells.

Furthermore, it is conceivable that some of the mice developed T-cell lymphoma. Already in young mice the splenic T-cell population is expanded and activated and is still present in the aged Notch2IC//LMP1/CD40//CD19-cre mice. Therefore, these aged mice should be examined for the presence of T-cell tumors. This could be accomplished via special probes for the TCR similar as done for the IgH-locus in the B cell of the whole cell preparations in Southern blot analysis. In a faster approach the clonality of T cells of aged mice could be characterized by FACS analysis with regard to their TCR-Vβ chain repertoire (Pechloff et al., 2010). Similar to the young mice the old mice shall be routinely examined for presence and status of accessory cells.

Interestingly, a staining for the reporter cell surface marker hCD2 revealed that only in two out of the five mice tested, the splenic B-cell population displayed a large percentage of hCD2^{pos} B cells. This might be an indication that although Notch2IC//LMP1/CD40//CD19-cre mice in contrast to the control mice did develop overt hyperplasia, that the expression of the transgenes (which can be monitored by staining for surface hCD2) might provide the tipping point towards lymphoma development but might not be necessary to be maintained afterwards.

Furthermore, the fact that all splenic B cells of aged Notch2IC//LMP1/CD40//CD19-cre mice -with exception of CD80 and CD86- showed a great diversification of surface markers, might be suggestive of a higher than detected tumor incidence. In the tumors observed in LMP1/CD40//CD19-cre mice (Homig-Holzel et al., 2008) all mice exhibited differential activation of examined signaling pathways.

Another crucial point to consider when evaluating the observed tumor incidence in mice is the weight of the spleen, since one of the aged mice with a tumor detectable by Southern blot did not exhibit increased splenic weight nor overtly increased B-cell numbers (# 1779). This might hint at the fact that a number of tumors might have gone unnoticed in the young mice simply

because they did not manifest themselves with an overt splenomegaly. Therefore, mice that are considerably younger than 12 months of age should be routinely checked for tumor development.

With regard to the increase of accessory cells and especially the T$_{regs}$ in the younger mice and the potential impact they are having, i.e. whether they act rather tumor-promoting or tumor-suppressing, it will be of utmost importance to examine the outgrowth behavior of B cells transplanted into NSG mice (i.e. NOD/LtS z-scid IL2Rγnull or NOD/SCID/γ mice). These have no T-, B- and NK cells and moreover many defects in the innate immune compartment (Shultz et al., 2005). Consequently, they rank amongst the most immunodeficient strains of mice. If the onset of tumorigenesis is accelerated, these transplantation experiments could provide valuable hints as to whether the onset of B-cell lymphoma is kept in check by innate immune cells and T cells. Together with further analysis of the chemo- and cytokine panel of these accessory cells this could provide a rather comprehensive picture of the mechanisms at work concerning tumorigenesis due to deregulated CD40- and Notch2IC-signaling in vivo.

4.9   Aged Notch2IC//LMP1/CD40//CD19-cre mice develop salivary gland carcinomas

Apart from the observed B-cell lymphomas the old Notch2IC//LMP1/CD40//CD19-cre mice also develop salivary gland carcinomas, this phenomenon had also been observed for aged LMP1/CD40//CD19-cre mice by former colleagues C. Hoemig-Hoelzel and C. Hojer (unpublished data). Like in LMP1/CD40//CD19-cre mice carcinoma development in Notch2IC//LMP1/CD40//CD19-cre mice seemed rather independent of whether these mice also developed an overt B-cell lymphoma or not. Some old Notch2IC//CD19-cre mice also showed hyperplasia in their SGs, however with a much lower incidence and the animals were older (> 18 months; S. Ehrenberg, personal communication); therefore, it was assumed that the SGT development was majorly a CD40-mediated event.

The question is however, whether tumorigenesis in the SGs is a B-cell-mediated effect or whether there was an aberrant expression of LMP1/CD40 or rather Notch2IC//LMP1/CD40. Both scenarios seem equally likely since CD40 rather conveys survival promoting qualities to the expressing epithelial cell and on the other hand overt activation of the lymphocyte compartment -as seen in chronic inflammation- can in fact lead to cancer (Coussens et al., 2002). Unfortunately, with the data at hand the question what the causative behind carcinogenesis could not be resolved unambiguously.

CD40 was originally identified as a B-cell costimulatory receptor and a tumor-antigen expressed in bladder carcinoma (Paulie et al., 1985) and the transforming capacity of LMP1 –the viral homologue of CD40- was first shown in rodent fibroblasts (Wang et al., 1985; Baichwal et al., 1988; Moorthy et al., 1993). Moreover, initial studies on the functions of CD40 have been primarily performed in transiently transformed epithelial cells since B lymphocytes used to be more challenging to manipulate experimentally, thereby it became obvious that the functions of CD40 can vary depending on the cell type in which it is expressed. The function of active CD40-signaling in an epithelial cell context has been well-characterized, but even within the same compartment the outcome of CD40 expression can vary. On the one hand activity of the CD40 pathway can contribute to the proinflammatory function of intestinal epithelial cells in pathological states like inflammatory bowel disease and expression of its viral homologue LMP1 is closely associated with nasopharyngeal cancer, it can promote cell survival through activation of the phosphatidylinositol 3-(PI3) kinase/Akt pathway and inhibit epithelial cell differentiation (Dawson et al., 1990; Raab-Traub, 2002; Dawson et al., 2003; Lo et al., 2004; Borcherding et al., 2010). Moreover, the SGTs under investigation were all carcinomas with a low differentiation degree resembling a human neoplasm called "lymphoepithelioma-like carcinoma of the submandibular salivary gland associated with Epstein-Barr virus" (L. Quintanilla-Fendt, personal communication). Furthermore, the high tumor incidence in the mice, the fact that a considerable portion of the tumor tissue displayed the deletion of the stop cassette (Southern blot data), the high presence of hCD2 while B cells were virtually absent from the tumor sites, all argue in favor of a temporarily ectopic expression of the Cre-recombinase (Schmidt-Supprian et al., 2007), leading to deletion of the stop-cassette and ultimately to tumorigenesis due to the growth promoting effects of CD40.

When evaluating the hypothesis that SG tumorigenesis could be due to a B cell intrinsic effect we could actually identify a possible human correlate called Sjogren's syndrome. Sjogren's syndrome is an autoimmune disease which is characterized by obstruction of the lacrimal and salivary glands. This is accompanied among other symptoms by parotitis (i.e. an inflammation of the major SG) and its most serious complication of Sjogren's is the development of non-HL (Johnsen et al., 2012). B cells have been shown to play a pivotal role in this disease (Mackay et al., 2007; Coca et al., 2009). A number of models have been developed which try to facilitate studying the diverse aspects of the disease in mice (Delaleu et al., 2011). The model proposed by Qian and colleagues displays similarities with Notch2IC//LMP1/CD40//CD19-cre mice (Qian et al., 2008). Qian et al. showed that genetic deficiency of a negative regulator (Act1) of CD40 and B-lymphocyte-activating factor (BAFF) leads to development of Sjogren's syndrome in those mice. This is manifested by an overall increase in B-cell number in those mice, hyperactivation and

enhanced survival of B cells, enlarged lymph nodes and SGs. All these features are also found in Notch2IC//LMP1/CD40//CD19-cre mice. Howver, Qian et al., also found α-La-, as well as α-Ro autoantibodies in the sera of the knock-out mice. The presence of these could not expected in LMP1/CD40//CD19-cre or Notch2IC//LMP1/CD40//CD19-cre mice, since these transgenic mice are impaired in their Ig isotype switching.

Nonetheless, the involvement of B cells as mediators cannot be ruled out categorically, if only as mediators of inflammation. Another point to consider is that even though no B cells were found in the SG of Notch2IC//LMP1/CD40//CD19-cre mice, B cells have been demonstrated to exert procarcinogenic capabilities even distal from the site of tumor origin as demonstrated by de Visser and colleagues (de Visser et al., 2005).

Considering the strong hCD2 staining in the SGTs one has to keep that expression of CD2 can be up-regulated in basal cell carcinoma, human urogenital system and in adult kidney tumours (Taylor et al., 1990; Tienari et al., 2005) and has been implicated in mutagenesis in human embryonic carcinoma cells (Do et al., 2009). Therefore strong expression of hCD2 could rather be a consequence of carcinomagenesis in the SGT cells and not marker of transgene expression.

The SGs seem a peculiar organ to develop tumors, however it is conceivable that this organ even when mice kept in ultra-clean conditions is still exposed to certain amounts of antigen, similar as Peyer's patches in the intestines of the animals. Again, antigenic insult would rather hint towards involvement of B cells in development of SGT.

5. SUMMARY

CD40- and Notch-receptor signaling were found to be deregulated in a number of tumors such as Hodgkin lymphoma. Mice expressing either one of the receptors in a constitutively active form and B-cell-specific fashion have previously been established and characterized in our lab (LMP1/CD40//CD19-cre and Notch2IC//CD19-cre; Homig-Holzel et al., 2008; Hampel et al., 2011). In order to study the effects of the constitutive activation of both receptors in B cells in an in vivo setting, mice expressing constitutively active Notch2 and mice expressing constitutively active CD40 were cross-bred so that offspring concomitantly express both receptors in a CD19-dependent and hence B-cell-specific manner. This resulted in the Notch2IC//LMP1/CD40//CD19-cre. All mouse analyses were carried out with aged-matched CD19-cre, Notch2IC//CD19-cre and LMP1/CD40//CD19-cre as controls.

Notch2IC//LMP1/CD40//CD19-cre mice display a significant increase in splenic size and weight. There was a significant increase in total splenic cell numbers and splenic B-cell numbers in Notch2IC//LMP1/CD40//CD19-cre compared to CD19-cre and Notch2IC//CD19-cre mice, however splenic B-cell numbers were significantly lower than in LMP1/CD40//CD19-cre mice. Therefore, it was evaluated what other cell types contribute to the enlarged spleen and increased total cell numbers.

Increased numbers of accessory cells, namely myeloid cells, macrophages, granulocytes and dendritic cells could be identified in spleens of Notch2IC//LMP1/CD40//CD19-cre mice. Moreover, these mice display significantly increased numbers of splenic T cells compared to controls. The T cells in the Notch2IC//LMP1/CD40//CD19-cre mice display an enhanced expression of the T-cell activation markers and an increase in the percentage of both central memory, as well as effector memory T cells. Furthermore, regulatory T cells (T_{regs}) that represent important regulators of cellular immune responses are increased in spleens of Notch2IC//LMP1/CD40//CD19-cre mice.

Mice of the Notch2IC//LMP1/CD40//CD19-cre genotype exhibit a partial block in early B-cell development between pre- and immature B cell stage in the bone marrow, probably due to deleterious effects that early expression of both transgenes has on the developing B cell. Considering the pool of mature B cells in Notch2IC//LMP1/CD40//CD19-cre animals they display - like Notch2IC//CD19-cre mice - an expansion of the marginal zone (MZ) B cells and decrease of the follicular (Fo) B cells as determined by flow cytometric analysis. Although they unambiguously display MZ B-cell surface marker expression, the splenic architecture was observed to be disrupted in Notch2IC//LMP1/CD40//CD19-cre mice with very diffuse B- and T-cell zones. Distinct

changes in the expression of cyto- and chemokines in Notch2IC//LMP1/CD40//CD19-cre mice (both with regard to mRNA levels of the respective splenic B cells as well as serum levels) could be contributing to this. There was an up-regulation of CXCL9 and CXCL10 in serum and an increase of CXCR3 and IL13 receptor α1, IL2 receptor γ, Lymphotoxin β and Transforming Growth Factor β mRNA levels in splenic B cells of Notch2IC//LMP1/CD40//CD19-cre mice in comparison to all other genotypes.

Generally the splenic B cells of Notch2IC//LMP1/CD40//CD19-cre mice display an activated phenotype and better survival in culture than Notch2IC-, but not than LMP1/CD40-expressing B cells. B cells of Notch2IC//LMP1/CD40//CD19-cre mice display enhanced proliferation in in vitro culture surpassing that of splenic B cells expressing either Nocth2IC or LMP1/CD40.

A small group of mice was left to age in order to observe potential B-cell lymphoma development. Indeed it was found that from an age of 13 months onward Notch2IC//LMP1/CD40//CD19-cre mice are prone to develop monoclonal B-cell lymphoma and strongly suggest further studies with larger cohorts. Aged mice still display an increased number of macrophages in their spleens and they maintain the shift towards effector T-cell compartment as observed in the young mice. However, they vastly differ from young mice regarding their MZ B-cell phenotype since aged Notch2IC//LMP1/CD40-expressing splenic B cells display distinctly altered surface marker expression profile. Moreover, old Notch2IC//LMP1/CD40-expressing B cells display up-regulation of activation-induced of both B7-proteins and CD5. Furthermore, aged Notch2IC//LMP1/CD40//CD19-cre mice develop salivary gland carcinomas, as has also been observed for LMP1/CD40//CD19-cre mice. The origin of these carcinomas however could not be unambiguously identified within the scope of this work.

All in all, the data presented fit with the hypothesis that constitutive CD40 signaling can deliver survival signal to the B cells that can counteract constitutive Notch-signaling-induced apoptosis signals which ultimately results in a profound increase in proliferation rates in the splenic B cells of mice that expressing constitutively active Notch2 and constitutively active CD40.

6. ZUSAMMENFASSUNG

Der CD40- und der Notch-Rezeptor-Signalweg sind in verschiedenen Tumoren dereguliert, u.a. im Hodgkin-Lymphom. In unserem Labor sind Mäuse mit B-zellspezifischer Expression jeweils einer der beiden Rezeptoren, die zudem konstitutiv aktiv sind, generiert und charakterisiert worden; LMP1/CD40//CD19-cre und Notch2IC//LMP1/CD40//CD19-cre-Mäuse (Homig-Holzel et al., 2008; Hampel et al., 2011). Um die Effekte deregulierter Signale dieser beider Rezeptoren in B-Zellen in vivo zu studieren, wurden Mäuse, die konstitutiv aktives Notch2 exprimieren, mit Mäusen, die konstitutiv aktives CD40 exprimieren, miteinander verpaart. Hierdurch exprimiert die Nachkommengeneration (Notch2IC//LMP1/CD40//CD19-cre-Mäuse) gleichzeitig beide Rezeptoren in CD19-abhängiger und damit B-zellspezifischer Form. Alle Mausanalysen sind mit CD19-cre, Notch2IC//CD19-cre und LMP1/CD40//CD19-cre Kontrollmäusen gleichen Alters durchgeführt worden.

Die Notch2IC//LMP1/CD40//CD19-cre-Mäuse haben synergistische Effekte sowohl auf die Milzgröße, als auch auf das Milzgewicht. Die absoluten Zell- und der B-Zellzahlen in der Milz der Notch2IC//LMP1/CD40//CD19-cre-Mäuse waren gegenüber denen der CD19-cre und Notch2IC//CD19-cre-Mäusen signifikant erhöht. Jedoch waren die Anzahl der B-Zellen in der Milz der Notch2IC//LMP1/CD40//CD19-cre-Mäuse im Vergleich zu den LMP1/CD40//CD19-cre-Mäusen signifikant geringer. Es wurde daraufhin untersucht, welche anderen Zelltypen für die erhöhten absoluten Milzzellzahlen verantwortlich sind.

Es konnte eine erhöhte Anzahl an akzessorischen Zellen, und zwar myeloider Zellen, Makrophagen, Granulozyten und Dendritischer Zellen in Milzen der Notch2IC//LMP1/CD40//CD19-cre Mäusen identifiziert werden. Darüber hinaus zeichnen sich diese Mäuse durch eine signifikant erhöhte Anzahl an T-Zellen in ihren Milzen verglichen mit den Kontrollen aus. Die T-Zellen in den Notch2IC//LMP1/CD40//CD19-cre-Mäusen zeigen eine erhöhte Expression T-zellspezifischer Aktivierungsmarker und einen prozentualen Anstieg von zentralen Gedächtniszellen sowie Effektor-T-Zellen. Zudem sind regulatorische T-Zellen (T$_{regs}$), die wichtige Regulatoren in der zellulären Immunantwort repräsentieren, in den Milzen von Notch2IC//LMP1/CD40//CD19-cre-Mäusen erhöht.

Mäuse des Notch2IC//LMP1/CD40//CD19-cre Genotyps weisen einen partiellen Block in der frühen B-Zellentwicklung im Knochenmark zwischen dem pre- und unreifen B-Zellstadium auf, wahrscheinlich aufgrund abträglicher Auswirkungen, die die frühe Expression beider Transgene auf die sich entwickelnde B-Zelle hat. Reife B-Zellen in Notch2IC//LMP1/CD40//CD19-cre Tieren zeigen – wie auch Notch2IC//CD19-cre-Mäuse – in der durchflusszytometrischen Analyse eine

Expansion der Marginalzonen (MZ) B-Zellen und eine Verminderung der Follikulären (Fo) B-Zellen. Obwohl sie eindeutig MZ B-Zelloberflächenmarker in der FACS-Analyse aufweisen und B-Zellen auch in der MZ lokalisierbar sind, saß doch ein unerwartet großer Anteil der B-Zellen in Notch2IC//LMP1/CD40//CD19-cre-Mäusen auch im Follikel und die Milzarchitektur wies in der Immunhistochemischen-Analyse sehr diffuse B- und T-Zellzonen auf. Distinkte Abweichungen hinsichtlich der Expression von Zyto- und Chemokinen in Notch2IC//LMP1/CD40//CD19-cre-Mäusen (sowohl im Niveau an mRNA in den B-Zellen als solche, als auch im Serum) könnten an diesem Effekt beteiligt sein. Im Vergleich zu allen anderen analysierten Mäusen ergab sich in Notch2IC//LMP1/CD40//CD19-cre-Mäusen eine Hochregulierung von CXCL9 und CXCL10 im Serum und eine Zunahme an CXCR3 und IL13-IL13-Rezeptor α1, IL2-Rezeptor γ, Lymphotoxin β und Transforming-Growth-Factor β mRNA der Milz-B-Zellen.

Allgemein zeigen die Milz-B-Zellen in Notch2IC//LMP1/CD40//CD19-cre-Mäusen einen aktivierten Phänotyp und verbessertes Überleben in in-vitro-Kultur verglichen zu Notch2IC-, aber nicht zu LMP1/CD40-exprimierenden Milz-B-Zellen. Zudem zeigen die Milz-B-Zellen von Notch2IC//LMP1/CD40//CD19-cre-Mäusen eine gesteigerte Proliferation in In-vitro-Kultur, die die von B-Zellen übertreffen, die entweder Notch2IC oder LMP1/CD40 exprimieren.

Eine kleine Gruppe Mäuse wurde zur Analyse in erhöhtem Alter verwahrt, um die potenzielle Entstehung von B-Zelllymphomen beobachten zu können. Tatsächlich konnte beobachtet werden, dass sie ab einem Alter von 13 Monaten fortschreitend anfällig für die Entstehung von monoklonalen B-Zelllymphomen sind, was weitere Studien mit größeren Kohorten empfiehlt. Alte Mäuse zeigen immer noch eine erhöhte Anzahl an Makrophagen und eine Verschiebung der T-Zell-Population zu den Effektor-T-Zell-Phänotyp in der Milz wie bei jungen Mäusen. Sie unterscheiden sich jedoch stark von jungen Mäusen hinsichtlich ihres MZ-B-Zellphänotyps, da alte Notch2IC//LMP1/CD40//CD19-cre-Mäuse ein verändertes Oberflächenmarkerprofil aufweisen. Darüber hinaus zeigen alte Notch2IC//LMP1/CD40//CD19-cre-Mäuse eine Hochregulierung beider aktivierungsinduzierter B7-Proteine und CD5 auf ihren Milz-B-Zellen auf. Außerdem entwickeln Notch2IC//LMP1/CD40//CD19-cre-Mäuse Tumore der Speicheldrüse, wie es auch bei LMP1/CD40//CD19-cre-Mäusen beobachtet wurde. Der Ursprung dieser Tumore konnte im Rahmen dieser Arbeit nicht eindeutig identifiziert werden.

Insgesamt untermauern die gezeigten Daten die Hypothese, dass ein konstitutives CD40-Signal B-Zellen ein Überlebenssignal zuführen kann, das dem Notch-Signalweg-induzierten Apoptose-Signal entgegenwirken kann. Dies resultiert schließlich in einer profunden Zunahme der Proliferationsraten in Milz-B-Zellen von Mäusen, die sowohl konstitutiv aktives Notch2 und konstitutiv aktives CD40 exprimieren.

7. MATERIAL

Bacteria

DH5α (Escherchia coli): Genotype: F- endA1 glnV44 thi-1 recA1 relA1 gyrA96 deoR nupG Φ80d lacZ ΔM15 Δ(lacZYAargF)U169 hsdR17 (rK- mK+), λ- .

DNA probes for Southern blotting

Rosa26-probe: The probe is 550 bp large and was prepared from the pRosa26-5-pBS KS plasmid by restriction digest with the enzymes EcoRI und Pac1.

IgH-probe: The IgH-probe is the sequence between the J4 and Emicro segments of the IgH locus and was excised with the enzymes EcoRI and NaeI. It was subsequently cloned into a Bluescript Vector from which it can be prepared by digest with the enzymes EcoRI und HindIII (Gao et al., 2000).

Enzymes

Restriction endonucleases were purchased from New England BioLabs and MBI Fermentas. Taq DNA polymerase was purchased from Invitrogen Life Technologies.

B-cell medium

1 x RPMI 1640
5 % (v/v) fetal calf serum (FCS; PAA/ 10% (v/v) if used for culture
1 % (v/v) Penicillin-Streptomycin
1 % (v/v) non-essential aminoacids
1 % (v/v) sodiumpyruvate
1 % (v/v) L-Glutamin
50 µM β-Mercaptoethanol
All reagents by Gibco.

Mouse strains

All mice were kept on a mixed background (BALB/c x C57BL/6).

LMP1/CD40flSTOPP (Homig-Holzel et al., 2008)

The LMP1/CD40fl STOPP It is conditional transgenic for the chimeric LMP1/CD40 gene that has been inserted into the murine Rosa26 locus. A STOP cassette flanked by loxP sites is located upstream of the *LMP1/CD40* gene and prevents its expression. In the presence of Cre, the STOP cassette can be excised and LMP1/CD40 is expressed under control of the endogenous Rosa26 promoter.

Notch2IC (Hampel et al., 2011)

The Notch2ICflSTOPP strain is conditional transgenic for the conditional notch2IC allele. The notch2ICflSTOP construct was inserted together with an IRES-hCD2 coding sequence into the murine Rosa26 locus. A STOP cassette flanked by loxP sites is located upstream of the *notch2IC* gene and prevents its expression. In the presence of Cre, the STOP cassette can be excised and Notch2IC is expressed under control of the constitutively active CAGGS promoter. This leads to the expression of the Notch2IC transgene under the transcriptional control of promoter, while hCD2 is concomitantly expressed on the surface to the respective Notch2IC-expressing cell.

CD19-cre (Rickert et al., 1997)

CD19-cre are a C57BL/6 mouse strain that has the *Cre* recombinase gene inserted into the CD19 locus, thereby disrupting the CD19 gene. The expression of the *cre* gene is regulated by the endogenous CD19 promoter.

Primers for PCR and sequencing reactions

Primer name	Primer sequence (5´ to 3´)	Annealing Temp (°C)
CD19c	AACCAGTCAACACCCTTCC	57
CD19d	CCAGACTAGATACAGACCAG	57
Cre 7	TCAGCTACACCAGAGACGG	57
CD40 PCR3	CTG AGA TGC GAC TCT CTT TGC CAT	55
Ex1Fw1 LMP1	AGG AGC CCT CCT TGT CCT CTA	55
Notch2IC 25 rev (T)	ATCCCGGTCTCCGTATAGTG	59
Notch2IC 33 fw (T)	CCCTTGCCCTCTATGTACCA	59
Rosa fw1 (60)	CTCTCCCAAAGTCGCTCTG	59
Rosa rev2 (62)	TACTCCGAGGCGGATCACAAGC	59

Antibodies for immunohistochemistry

Antigen	Source	Coupled to	Dilution	Manufacturer
Murine CD3	Dog		1:2	By courtesy of E. Kremmer
Murine IgM	Goat	Peroxidase	1:100	Sigma
Murine MOMA1	Rat		1:100	Biomedicals
Rat IgG2	Mouse	Biotin	1:250	Jackson Laboratories
Mac1	Rat	Biotin	1:100	BD
Foxp3	Rat	Biotin	1:100	eBioscience
Streptavidin-conjugated		Alkaline Phosphatase	1:400	Sigma

8. METHODS

Mouse breeding

Mice carrying the notch2ICflSTOP and the LMP1/CD40 allele were crossed to the CD19-cre mouse strain to generate mice expressing one or the other or both transgenes. Transgenes were expressed upon in Cre-mediated excision of the stop cassette upstream the respective or both targeting constructs in the Rosa26 locus. Transgenes are expressed from the pro-B cell stage onward with a gradual increase during proceeding B cell differentiation (Rickert et al., 1997). Analyses were performed on a mixed background and mice were analyzed at eight to 16 weeks of age, unless stated otherwise. Mice that were monitored for the development of lymphomas or leukemic disease (>13months) were kept under special observation by designated personnel.

All mice were bred and maintained in specific pathogen-free conditions. All experiments were performed in compliance with the German animal welfare law and have been approved by the Institutional Committee on Animal Experimentation and the government of Upper Bavaria.

Isolation of primary lymphocytes

Mice were euthanized by CO_2 gassing and subsequently dissected. Spleen, thymus, and lymph nodes were taken out as whole organs and were maintained in medium until further procedures. Cells from the bone marrow were prepared by dissecting tibia bones, cut at neck of the tibia and the cavity was flushed with medium. Splenic weight was obtained by placing spleens in sterile petri dishes on a microscale. In case small pieces were cut off for histologic preparations (see section "Histology", pp.110-111), the larger piece of spleen was weighed again to be able to equate weight with total cell number and finally FACS percentages of particular cell populations (see section "Cell number calculations", p. 108).

Single cell suspensions from lymph nodes and spleens were obtained by passing the organs through a 70 µm cell strainer (Becton Dickinson). Erythrocytes were depleted from single cell suspensions from spleen and bone marrow by lysis with a hypotonic buffer (1x RBC lysis buffer; eBiosciences) for three minutes or longer for LMP1/CD40//CD19-cre and Notch2IC//LMP1/CD40//CD19-cre at RT. All cell suspensions were kept on ice the entire time and washing steps with medium or PBS/1% (w/v) BSA were carried out by centrifuging cell suspensions for 10 minutes at 300 x g at 4 °C. Cell numbers were determined by Neubauer chamber countings.

Magnetic Cell Separation (MACS)

Splenic B cells were isolated from single cells suspensions by depletion of CD43^{pos} non-B cells by MACS, using α-CD43 beads and LS columns according to the manufacturer's specifications (Miltenyi Biotec). Thereby, B-cell populations of 85 to 98% purity were obtained as confirmed via FACS-analysis.

Cell number calculations

Total cell number of any given cell suspension was determined by use of a Neubauer counting chamber and a light microscope counting only the light cells (darker cells are probably dead having disrupted cell membranes that allows for diffusion of the counting medium into the cell). Cell numbers of a cell population can be calculated from the total cell number as determined by Neubauer chamber counting and the percentage of the respective population in the organ under investigation as determined by FACS.

In case no small piece was cut off for histologic preparations:

Total cell no. (as counted)/100 × percentage of respective cell population (as determined by FACS) = total no. of respective cell population.

In case a small piece was cut off for histologic preparations:

Spleen = x gram,

i.e. larger piece (as weighed) = $x-y_1 = y_2 = z_2 \times 10^7$ cells

i.e. smaller piece = $x-y_2 = y_1 = z_1 \times 10^7$ cells

Hence, Total cell no. $(z_1 + z_2)$/100 × percentage of respective cell population (as determined by FACS) = total no. of respective cell population.

Surface marker Flow Cytometry (FACS)

Single cell suspension prepared from BM, LN and SP were surface-stained with a combination of FITC-, PE-, PerCP- and APC-conjugated monoclonal antibodies, diluted in MACS buffer (Miltenyi Biotec). Antibodies specific for the respective surface antibody employed were purchased from BD Biosciences or eBiosciences. Usually 3×10^4 cells were used for stainings and stained in 25 microL staining mix for at least 20 min on ice. If indicated cells were additionally labeled with TOPRO-3 or propidium iodide (PI) staining (both from Molecular Probes) in order to exclude dead cells from analysis. These intercalating fluorescent dyes are able to bind to DNA and thus only stain dead cells with damaged cell membranes which allow the dye to diffuse into the nucleus. The staining of cells was determined with a four-color FACSCaliburTM flow cytometer (BD Biosciences) and results were analyzed using CELLQuest and FlowJo software.

Intracellular FACS-analysis

$4×10^6$ cells previously washed in PBS/1 % (w/v) BSA were resuspended in 25 microL surface marker staining mix and incubated for at least 20 min on ice. After another washing step, cells are resuspended in PBS/4 % paraformaldehyde or Histofix (Carl Roth) and left for 10 min at RT. Cells are washed with PBS (then they can be left o/n at 4 °C in PBS), afterwards they are washed with intracellular FACS buffer (PBS/1 % (w/v) BSA/1 % (w/v) saponin) and afterwards incubated in intracellular FACS buffer for 10 min at RT. Respective staining mixes were prepared in 20 microL buffer and incubated for 30 min at RT. Cells were washed twice in 1 mL intracellular FACS buffer and cell pellets were resuspended in PBS for FACS measurement.

Foxp3 staining was performed according to manufactures specifications of the Foxp3 staining kit from eBiosciences.

In vitro culture of primary lymphocytes

Short term cultivation for stimulation of T-cell responses (Th1/Th2)

$4×10^7$ whole splenic cells/mL were kept in B-cell medium with 10 % (v/v) FCS, supplemented with phorbol myristate acetate (PMA; 1:50.000 dilution from 1 mM stock) and calcium ionophore ionomycin (Ionomycin; 1:10.000 dilution from 10 mM stock).

PMA/Ionomycin-treatment provides a polyclonal stimulus activating all cells in a sample unspecifically. The cells were incubated at 37 °C for 2 to 2 ½ hrs. Subsequently cells were treated with by Brefeldin A (1:500 dilution from 5 mg/ml stock) for no longer than 2 ½ hrs at 37 °C. Brefeldin A-treatment is done to ensure that the cytokine under investigation does not diffuse from the cell into the medium of the cell suspension.

Afterwards cells were washed with PBS and in order to stain intracellular cytokines the protocol for Intracellular FACS-analysis was followed.

Proliferation assay (CSFE assay)

Splenic, MACS-purified B cells were labeled with carboxyfluorescein diacetate succinimidyl ester (CFSE, Molecular Probes, final concentration 5 µM) in serum-free B cell medium for 5 min at 37 °C for 10 min. CFSE is a fluorescent dye that labels intracellular molecules by its succinimidyl group. It is passed on to daughter cells during cell division and thereby provides a method to measure proliferation of a cell population by the decrease in CFSE-fluorescence of the labeled cells.

B cells were cultured ($5×10^6$ cells/ml) in B-cell medium with 10 % (v/v) FCS with or without stimuli up to five days in 96-well plates ($5×10^5$ cells/well). Stimuli were either IL4 (10 ng/ml; mouse recombinant; Sigma) or α-CD40 antibody (2.5 µg/ml; eBioscience) or both. At different time

points (day 1, day 3 and day 5), cells were analyzed with a FACSCalibur. The percentage of living cells was determined by staining and excluding dead cells by Topro-3.

Cell cycle analysis (BrdU assay)

To perform cell cycle analysis B cells were isolated and cultured as described above, at least 5 wells with 5×10^5 cells of a 96-well plate were cultivated. Splenic B cells were analyzed on day 0 as to determine the immediate ex vivo situation and subsequently on day 1 and day 3 after bromdesoxyuridine (BrdU) labeling for four hours. BrdU is a synthetic nucleoside and thymidine analogue. If given to cells during their proliferative S-phase BrdU-dye will be incorporated into the cell's DNA and can later be visualized by α-BrdU antibodies. This allows for inference on the proliferation rate of the cells. Simultaneous staining of the cells with 7-amino-actinomycin D (7AAD; a fluorescent DNA marker) shortly before analysis, permits to determine the full scope of the cell cycle of any culture of cells under investigation. In order to ensure functionality of the assay LPS (25 µg/ml; E. coli 055:B5; Sigma) was added to B-cell cultures of CD19-cre mice. LPS is a potent, polyclonal stimulus, activating the cells and driving them into proliferation.

BrdU incorporation into the DNA of B cells was analyzed by using the APC BrdU Flow Kit (Becton Dickinson) according to manufacturer's instructions on a LSRII Fortessa (Becton Dickinson).

Preparation of serum from murine blood

Blood was collected directly from the heart with a Pasteur pipette. Afterwards, the blood was stored on ice for at least four hours and was subsequently centrifuged at 9.000 xg and 4 C for 10 min. The supernatant was transferred to a new tube and the procedure was repeated once to yield pure serum.

Equal amounts of serum were analyzed for the presence of cyto- and chemokines with the Proteome ProfilerTM Array according to manufacturer's specifications (Mouse Cytokine Array Panel A; R&D Sytems) and the obtained data subsequently analyzed with Tina 2.0 software.

Histology
Immunohistochemistry

Spleens were embedded in O.C.T. Tissue Tek (Sakura) in medium-sized cryomolds (Sakura) and placed them on dry ice until completely frozen. Embedded spleens were stored at -20 °C, wrapped in aluminum foil and ziplock bags to avoid air contact. 5-8 µm thick sections were cut with a cryostat (Leica Microsystems), collected on gelatin-coated microscope slides (Thermo Scientific) and air-dried overnight. Sections were subsequently fixed for ten minutes in 100 % (v/v) acetone.

Slides with sections were then rehydrated with PBS, and incubated for 20 minutes in quenching buffer (PBS containing 10 % (v/v) goat serum, 1 % (w/v) BSA) to block endogenous peroxidase. Afterwards, sections were incubated for each 15 min in two different blocking buffers, first an Avidin, then a Biotin blocking buffer (Avidin-Biotin Blocking Kit; Vector Laboratories) to prevent unspecific binding of Avidin- and Biotin-coupled antibodies. Between incubation steps, sections were washed for 5 min in PBS. Subsequently, staining was performed by incubating sections with different antibodies diluted in PBS/1 % (w/v) BSA for one hour each. Before and after antibody stainings, sections were washed with PBS each three times for 5 minutes. Phosphatase-conjugated antibodies were detected in blue using Blue Alkaline Phosphatase Substrate Kit III (Vector laboratories). Peroxidase-conjugated antibodies were detected in red due to a reaction with aminoethylcarbazole (AEC) after treatment with Peroxidase Substrate Kit AEC (Vector laboratories). Staining reactions were stopped at the latest after 10 min by washing with PBS. All incubation steps were performed at 22 °C in a wet chamber. Sections were air-dried and subsequently embedded in Kaiser gelatin (Merck) and sealed off with a coverslip.

For Foxp3 stainings, sections were rehydrated in PBS/1 % (w/v) BSA/1 % (w/v) saponin. Also all antibodies were diluted in PBS/1 % (w/v) BSA/1 % (w/v) saponin.

Stainings were analyzed using a fluorescent microscope (Zeiss). Pictures were obtained with a digital camera (AxioCam MRm) and the AxioVision programme.

Fluorescent microscopy

Sections of specimen were prepared, blocked and stained as described for immunohistochemistry ultimately using antibodies coupled to flourochromes. Analysis was carried out on a confocal microscope (Axiovert 200M, Zeiss) and Pictures were obtained with a digital camera (AxioCam MRm) and OpenLab programme and edited using Adobe Photoshop.

DNA isolation
Plasmid isolation from bacteria

Plasmids were produced and isolated from competent bacteria with the EndoFree Plasmid Maxi Kit (Qiagen) according to manufacturer's instructions. The air-dried pellet was resolved in TE buffer and DNA concentration was determined with a photometer (Eppendorf).

Isolation of genomic DNA from murine tails and whole splenocyte pellets

Murine tail clippings, splenic cell pellets or SGTs were incubated shaking at 56 °C o/n in at least 500 µl lysis buffer (100 mM Tris/HCl pH 8,5 mM EDTA, 0.2 % (w/v) SDS, 200 mM NaCl,) supplemented with 100 µg/ml proteinase K (Invitrogen). 1/3 volume of a saturated NaCl (at least 5 M) were added to precipitate proteins and samples were centrifuged 10 min at 10.000 xg. The

supernatant was transferred into a new tube and DNA was precipitated by adding 2x volume 100 % (v/v) isopropyl alcohol and inverting the sample-containing tube. After another round of centrufgation samples were centrifuged and the DNA was washed with 70 % (v/v) ethanol. Samples were air-dried, and ultimately dissolved in appropriate volume of TE buffer by shaking at 37 °C for one hr for genotypings or at least 4 hrs for Southern blots.

DNA analysis

Polymerase Chain Reaction (PCR) for genotyping

The method of PCR was used to analyze DNA of transgenic mice for the configuration of the Rosa26 locus (insertion of transgenes) and presence of Cre-recombinase in the CD19-locus in the genome. All materials were obtained from Invitrogen. A basic reaction mixture with different primers was used:

Master Mix	Per reaction (µl)
H20	19,65
Taq Puffer (10x)	2,5
MgCl2 (25 mM)	1
dNTP (10mM)	0,5
Primer 1	0,1
Primer 2	0,1
Taq Polymerase (5U/µl)	0,15
DNA	1
total	25

Agarose gel electrophoresis of DNA

Agarose gel electrophoresis was performed to determine PCR reaction results and size-fractionate restriction-digested DNA molecules, which were either eluted from the gel (Southern blot probe) or blotted on a nitrocellulose membrane (Southern blot). Gels were prepared with 1x TAE (40 mM Tris/HCl, 20 mM acetic acid, 1 mM EDTA pH 8.5), 5 µg/ml ethidium bromide and 0.8 % (Southern blot) or 2 % (w/v; genotyping) agarose.

Electrophoresis was performed in a gel electrophoresis chamber (Peqlab) with 1x TAE buffer at 90 V for PCR samples or run at 25 V o/n. Results were visualized and documented with a geldocumentation system (Vilbert Lourmat).

DNA fragment for Southern blot probe was excised from agarose gel containing correctly-sized fragment with a clean scalpel and the DNA probe was isolated with QIAquick Gel Extraction Kit (Qiagen) according to manufacturer's instructions.

Restriction digest of DNA for Southern blot

Restriction digest of plasmid DNA was performed using specific restriction enzymes according to manufacturer's instructions for appropriate conditions and buffers.

Genomic DNA from splenic cells and SGTs was digested with EcoRI for both Southern blots. Restriction buffer mix (1 mM Spermidin, 1 mM DTT, 100 µg/ml BSA, 50 µg/ml RNase, 1x EcoRI buffer, 100 to 150 U of EcoRI enzyme) was added to respective DNA in TE buffer. DNA was digested for at least 16 hrs at 37 °C.

Southern blot (Southern, 1975)

This method was used for the identification of mono- or oligoclonal B cell lymphomas (whole splenic cell preparations) and the deletion of the transgene up-stream the inserted transgene (SGTs). After the restriction digest treatment, DNA is electrophoretically separated and transferred from the agarose gel to a nitrocellulose membrane. A radioactively-labeled DNA probe (Rosa- or IgH-probe) is allowed to hybridize to the denatured DNA on the membrane o/n. This allows for the detection of distinct DNA fragments as definite bands on the membrane.

After digestion as described in the previous section, the respective samples were size-fractionated on a 0.8 % (w/v) agarose gel along with a standard 1 kb DNA ladder (Invitrogen) at 25 V o/n. The restriction-digested DNA in the gel was visualized and documented on a UV luminescent screen together with a ruler to determine the height of the desired fragment in the gel so that the gel could be cut down to a smaller size and only the part containing the fragement of interest would be kept. Subsequently, the gel was incubated in 0.25 N HCl for 25 min in order to denature the DNA. Afterwards the gel has to be equilibrated for transfer onto the membrane: the gel was shortly rinsed in water and incubated in alkaline transfer buffer (0.4 M NaOH, 0.6 M NaCl) for 40 min. DNA blotting onto the membrane (ImmobilonTM Ny+ membrane, Millipore) was achieved via capillary pressure from transfer buffer flow top to bottom of the set-up. The next morning the position of slots of the gel were marked on the membrane. The membrane was rinsed shortly in 2x SSC buffer (0.3 M NaCl, 0.03 M NaCitrate, pH 6.5) for neutralization. DNA was cross-linked to the membrane by baking it for one hr at 80 °C. In order to limit unspecific binding of the respective probe, the membrane was pre-hybridized in pre-heated (65 °C) hybridization solution (1 M NaCl, 50 mM Tris, pH 7.5, 10 % (w/v) dextran sulfate, 1 % (w/v) SDS, 250 µg salmon sperm DNA/ml) for at least 6 hrs at 65 °C, before incubation with the respective radioactively labeled probe.

The probe was prepared by excision through restrictions digest and 100 ng were labeled by Random Prime Labeling Kit (GE Healthcare) according to manufacturer's instructions with 50 µCi ^{32}P-dCTP (Hartmann Analytic). The labeled probe was purified using a G50 sephadex column (GE Healthcare) according to manufacturer's instructions. In order to denaturate the probe to enable binding to membrane-bound DNA, it was incubated for five minutes at 100 °C and placed for two

minutes on ice. The membrane was incubated for at least 16 hrs at 65 °C in the hybridization solution, containing pre-hybridization buffer with the respective DNA probe.

Afterwards, the membrane was rinsed three times or more each for 10 min in pre-heated washing buffer (0.2x SSC, 0.5 % (w/v) SDS) at 58 °C to wash off unbound or unspecifically-bound probe until radioactivity dropped to 60 to 70 counts. The membrane was placed in transparent foil and radioactively-labeled probe was visualized on the membrane by autoradiography with radiosensitive films (Biomax MS PE Applied Biosystems 35x43 cm, KODAK), exposed for one day or longer at -80 °C in a Biomax cassette.

RNA analysis
RNA preparation

Total RNA that was isolated by using RNaeasy Mini Kit (Quiagen). In order to use defined and equal amounts of total RNA for cDNA synthesis, undiluted 2 µl RNA were applied to a spectrophotometer (NanoDrop) and its absorbance at 260 nm was determined to calculate RNA concentration. RNA integrity was tested on a Nothern Blot gel (kindly provided by M. Kellner).

cDNA synthesis

RNA can be reversely transcribed into a single-stranded DNA intermediate, i.e. complementary DNA (cDNA). Using oligo-dT primers, reverse transcriptase synthesizes a cDNA strand starting at the 3´-end of the poly(A)-mRNA. 1 µg total RNA of all samples was simultaneously in the same PCR run reversely transcribed with > 10 U of viral AMV Reverse Transcriptase, using 1st Strand cDNA Synthesis Kit for RT-PCR [AMV] (Roche Diagnostics) with 0.02 A260 units (0.8 µg) Oligo-p(dT)15 primers, amount of 10x reaction buffer, 10 mM dNTPs, 25 mM MgCl2 and 50 U RNase Inhibitor according to manufacturer's instructions, adding to a final reaction volume of 25 µl. Each RNA preparation was transcribed in quadruplicate. RNA was restored at -80 °C. The resulting first strand cDNA was stored at -20 °C and was used as a template for qPCR.

Mouse Inflammatory Cytokines & Receptors qRT PCR Array

The Array used was obtained from SA Biosciences and is based on the principles of quantitative real-time PCR (q RT PCR). This method allows studying mRNA expression in a comparative manner between different samples (as in this case) genotypes and was carried out using the LightCycler system (Roche Diagnostics).

SYBR green fluorescent dye is included in the reaction and this dye intercalates into the growing DNA strands during PCR reaction (unbound dye exhibits very little fluorescence and therefore does not have to be taken into account). The process of increase in fluorescence is measured by

the LightCycler during each completion of reaction cycle in realtime and the amount of RNA can be reversely determined by the amount of bound SYBR green in the sample.

100 µl of a genotype cDNA was mixed with the reaction mix supplied with array according to manufactures instructions. 100 µl of the resulting mix were immidiately added to each of the well of the 96-well array with pre-spotted primers for each cytokine and cytokine receptor to be analyzed and was centrifuged before placing into the LightCycler instrument. The array was always kept on ice during the preparation.

For each sample the crossing point (CP) was determined. The crossing point describes the cycle in which the fluorescence exceeds background signal and the lower the CT, the higher the content of the respective amplicon in the respective sample.

In order to determine the specificity of each DNA product by examining the melting temperature of the resulting qRTPCR products, melting curve analysis was performed according to manufacturer's instructions.

Data analyses were carried out using Excel software (Microsoft).

REFERENCES

AFFORD, S. C., AHMED-CHOUDHURY, J., RANDHAWA, S., RUSSELL, C., YOUSTER, J., CROSBY, H. A., ELIOPOULOS, A., HUBSCHER, S. G., YOUNG, L. S. & ADAMS, D. H. 2001. CD40 activation-induced, Fas-dependent apoptosis and NF-kappaB/AP-1 signaling in human intrahepatic biliary epithelial cells. *FASEB J,* 15**,** 2345-54.

AFFORD, S. C., RANDHAWA, S., ELIOPOULOS, A. G., HUBSCHER, S. G., YOUNG, L. S. & ADAMS, D. H. 1999. CD40 activation induces apoptosis in cultured human hepatocytes via induction of cell surface fas ligand expression and amplifies fas-mediated hepatocyte death during allograft rejection. *J Exp Med,* 189**,** 441-6.

AKHURST, R. J. & HATA, A. 2012. Targeting the TGFbeta signalling pathway in disease. *Nat Rev Drug Discov,* 11**,** 790-811.

ALDINUCCI, D., GLOGHINI, A., PINTO, A., DE FILIPPI, R. & CARBONE, A. 2010. The classical Hodgkin's lymphoma microenvironment and its role in promoting tumour growth and immune escape. *J Pathol,* 221**,** 248-63.

ALLMAN, D. M., FERGUSON, S. E., LENTZ, V. M. & CANCRO, M. P. 1993. Peripheral B cell maturation. II. Heat-stable antigen(hi) splenic B cells are an immature developmental intermediate in the production of long-lived marrow-derived B cells. *J Immunol,* 151**,** 4431-44.

ALVARO, T., LEJEUNE, M., SALVADO, M. T., BOSCH, R., GARCIA, J. F., JAEN, J., BANHAM, A. H., RONCADOR, G., MONTALBAN, C. & PIRIS, M. A. 2005. Outcome in Hodgkin's lymphoma can be predicted from the presence of accompanying cytotoxic and regulatory T cells. *Clin Cancer Res,* 11**,** 1467-73.

AMSEN, D., SPILIANAKIS, C. G. & FLAVELL, R. A. 2009. How are T(H)1 and T(H)2 effector cells made? *Curr Opin Immunol,* 21**,** 153-60.

ANASTASI, E., CAMPESE, A. F., BELLAVIA, D., BULOTTA, A., BALESTRI, A., PASCUCCI, M., CHECQUOLO, S., GRADINI, R., LENDAHL, U., FRATI, L., GULINO, A., DI MARIO, U. & SCREPANTI, I. 2003. Expression of activated Notch3 in transgenic mice enhances generation of T regulatory cells and protects against experimental autoimmune diabetes. *J Immunol,* 171**,** 4504-11.

APOSTOLOU, I. & VON BOEHMER, H. 2004. In vivo instruction of suppressor commitment in naive T cells. *J Exp Med,* 199**,** 1401-8.

ARTAVANIS-TSAKONAS, S., RAND, M. D. & LAKE, R. J. 1999. Notch signaling: cell fate control and signal integration in development. *Science,* 284**,** 770-6.

ASAO, H., OKUYAMA, C., KUMAKI, S., ISHII, N., TSUCHIYA, S., FOSTER, D. & SUGAMURA, K. 2001. Cutting edge: the common gamma-chain is an indispensable subunit of the IL-21 receptor complex. *J Immunol,* 167**,** 1-5.

ASAO, H., TAKESHITA, T., ISHII, N., KUMAKI, S., NAKAMURA, M. & SUGAMURA, K. 1993. Reconstitution of functional interleukin 2 receptor complexes on fibroblastoid cells: involvement of the cytoplasmic domain of the gamma chain in two distinct signaling pathways. *Proc Natl Acad Sci U S A,* 90**,** 4127-31.

ATTANAVANICH, K. & KEARNEY, J. F. 2004. Marginal zone, but not follicular B cells, are potent activators of naive CD4 T cells. *J Immunol,* 172**,** 803-11.

BAICHWAL, V. R. & SUGDEN, B. 1988. Transformation of Balb 3T3 cells by the BNLF-1 gene of Epstein-Barr virus. *Oncogene,* 2**,** 461-7.

BAKKEBO, M., HUSE, K., HILDEN, V. I., SMELAND, E. B. & OKSVOLD, M. P. 2010. TGF-beta-induced growth inhibition in B-cell lymphoma correlates with Smad1/5 signalling and constitutively active p38 MAPK. *BMC Immunol,* 11**,** 57.

BANCHEREAU, J., BAZAN, F., BLANCHARD, D., BRIERE, F., GALIZZI, J. P., VAN KOOTEN, C., LIU, Y. J., ROUSSET, F. & SAELAND, S. 1994. The CD40 antigen and its ligand. *Annu Rev Immunol,* 12**,** 881-922.

BARBER, D. L., WHERRY, E. J., MASOPUST, D., ZHU, B., ALLISON, J. P., SHARPE, A. H., FREEMAN, G. J. & AHMED, R. 2006. Restoring function in exhausted CD8 T cells during chronic viral infection. *Nature,* 439**,** 682-7.

BATRLA, R., LINNEBACHER, M., RUDY, W., STUMM, S., WALLWIENER, D. & GUCKEL, B. 2002. CD40-expressing carcinoma cells induce down-regulation of CD40 ligand (CD154) and impair T-cell functions. *Cancer Res,* 62**,** 2052-7.

BENSON, M. J., PINO-LAGOS, K., ROSEMBLATT, M. & NOELLE, R. J. 2007. All-trans retinoic acid mediates enhanced T reg cell growth, differentiation, and gut homing in the face of high levels of co-stimulation. *J Exp Med,* 204**,** 1765-74.

BENSON, R. J., HOSTAGER, B. S. & BISHOP, G. A. 2006. Rapid CD40-mediated rescue from CD95-induced apoptosis requires TNFR-associated factor-6 and PI3K. *Eur J Immunol,* 36**,** 2535-43.

BLACKBURN, S. D., SHIN, H., HAINING, W. N., ZOU, T., WORKMAN, C. J., POLLEY, A., BETTS, M. R., FREEMAN, G. J., VIGNALI, D. A. & WHERRY, E. J. 2009. Coregulation of CD8+ T cell exhaustion by multiple inhibitory receptors during chronic viral infection. *Nat Immunol,* 10**,** 29-37.

BLASIUS, A. L., BARCHET, W., CELLA, M. & COLONNA, M. 2007. Development and function of murine B220+CD11c+NK1.1+ cells identify them as a subset of NK cells. *J Exp Med,* 204**,** 2561-8.

BLEUL, C. C., FUHLBRIGGE, R. C., CASASNOVAS, J. M., AIUTI, A. & SPRINGER, T. A. 1996. A highly efficacious lymphocyte chemoattractant, stromal cell-derived factor 1 (SDF-1). *J Exp Med,* 184**,** 1101-9.

BORCHERDING, F., NITSCHKE, M., HUNDORFEAN, G., RUPP, J., VON SMOLINSKI, D., BIEBER, K., VAN KOOTEN, C., LEHNERT, H., FELLERMANN, K. & BUNING, J. 2010. The CD40-CD40L pathway contributes to the proinflammatory function of intestinal epithelial cells in inflammatory bowel disease. *Am J Pathol,* 176**,** 1816-27.

BOROWITZ, M. J., CROKER, B. P. & METZGAR, R. S. 1982. Immunohistochemical analysis of the distribution of lymphocyte subpopulations in Hodgkin's disease. *Cancer Treat Rep,* 66**,** 667-74.

BOURSIER, G., SIRI, A. & DE BOYSSON, H. 2012. [Use of regulatory T cells in cellular therapies in autoimmune diseases]. *Med Sci (Paris),* 28**,** 757-63.

BROCKER, T., RIEDINGER, M. & KARJALAINEN, K. 1997. Driving gene expression specifically in dendritic cells. *Adv Exp Med Biol,* 417**,** 55-7.

BRONTE, V., APOLLONI, E., CABRELLE, A., RONCA, R., SERAFINI, P., ZAMBONI, P., RESTIFO, N. P. & ZANOVELLO, P. 2000. Identification of a CD11b(+)/Gr-1(+)/CD31(+) myeloid progenitor capable of activating or suppressing CD8(+) T cells. *Blood,* 96**,** 3838-46.

CAILHIER, J. F., SAWATZKY, D. A., KIPARI, T., HOULBERG, K., WALBAUM, D., WATSON, S., LANG, R. A., CLAY, S., KLUTH, D., SAVILL, J. & HUGHES, J. 2006. Resident pleural macrophages are key orchestrators of neutrophil recruitment in pleural inflammation. *Am J Respir Crit Care Med,* 173**,** 540-7.

CARBONE, A., GLOGHINI, A., GRUSS, H. J. & PINTO, A. 1995. CD40 ligand is constitutively expressed in a subset of T cell lymphomas and on the microenvironmental reactive T cells of follicular lymphomas and Hodgkin's disease. *Am J Pathol,* 147**,** 912-22.

CARIAPPA, A., TANG, M., PARNG, C., NEBELITSKIY, E., CARROLL, M., GEORGOPOULOS, K. & PILLAI, S. 2001. The follicular versus marginal zone B lymphocyte cell fate decision is regulated by Aiolos, Btk, and CD21. *Immunity,* 14**,** 603-15.

CARRERAS, J., LOPEZ-GUILLERMO, A., FOX, B. C., COLOMO, L., MARTINEZ, A., RONCADOR, G., MONTSERRAT, E., CAMPO, E. & BANHAM, A. H. 2006. High numbers of tumor-infiltrating FOXP3-positive regulatory T cells are associated with improved overall survival in follicular lymphoma. *Blood,* 108**,** 2957-64.

CARTER, N. A., VASCONCELLOS, R., ROSSER, E. C., TULONE, C., MUNOZ-SUANO, A., KAMANAKA, M., EHRENSTEIN, M. R., FLAVELL, R. A. & MAURI, C. 2011. Mice lacking endogenous IL-10-producing regulatory B cells develop exacerbated disease and present with an increased frequency of Th1/Th17 but a decrease in regulatory T cells. *J Immunol,* 186**,** 5569-79.

CASOLA, S. 2010. Mouse models for miRNA expression: the ROSA26 locus. *Methods Mol Biol,* 667**,** 145-63.

CASSATELLA, M. A. 1999. Neutrophil-derived proteins: selling cytokines by the pound. *Adv Immunol,* 73**,** 369-509.

CHANG, K. C., HUANG, G. C., JONES, D. & LIN, Y. H. 2007. Distribution patterns of dendritic cells and T cells in diffuse large B-cell lymphomas correlate with prognoses. *Clin Cancer Res,* 13**,** 6666-72.

CHEN, G. Y. & NUNEZ, G. 2010. Sterile inflammation: sensing and reacting to damage. *Nat Rev Immunol,* 10**,** 826-37.

CHEN, W., JIN, W., HARDEGEN, N., LEI, K. J., LI, L., MARINOS, N., MCGRADY, G. & WAHL, S. M. 2003. Conversion of peripheral CD4+CD25- naive T cells to CD4+CD25+ regulatory T cells by TGF-beta induction of transcription factor Foxp3. *J Exp Med,* 198**,** 1875-86.

CHIODONI, C., IEZZI, M., GUIDUCCI, C., SANGALETTI, S., ALESSANDRINI, I., RATTI, C., TIBONI, F., MUSIANI, P., GRANGER, D. N. & COLOMBO, M. P. 2006. Triggering CD40 on endothelial cells contributes to tumor growth. *J Exp Med,* 203**,** 2441-50.

CHU, Y., VAHL, J. C., KUMAR, D., HEGER, K., BERTOSSI, A., WOJTOWICZ, E., SOBERON, V., SCHENTEN, D., MACK, B., REUTELSHOFER, M., BEYAERT, R., AMANN, K., VAN LOO, G. & SCHMIDT-SUPPRIAN, M. 2011. B cells lacking the tumor suppressor TNFAIP3/A20 display impaired differentiation and hyperactivation and cause inflammation and autoimmunity in aged mice. *Blood,* 117**,** 2227-36.

CHUNG, J. B., SILVERMAN, M. & MONROE, J. G. 2003. Transitional B cells: step by step towards immune competence. *Trends Immunol,* 24**,** 343-9.

CINAMON, G., MATLOUBIAN, M., LESNESKI, M. J., XU, Y., LOW, C., LU, T., PROIA, R. L. & CYSTER, J. G. 2004. Sphingosine 1-phosphate receptor 1 promotes B cell localization in the splenic marginal zone. *Nat Immunol,* 5**,** 713-20.

CLARK, G. J., ANGEL, N., KATO, M., LOPEZ, J. A., MACDONALD, K., VUCKOVIC, S. & HART, D. N. 2000. The role of dendritic cells in the innate immune system. *Microbes Infect,* 2**,** 257-72.

COCA, A. & SANZ, I. 2009. B cell depletion in lupus and Sjogren's syndrome: an update. *Curr Opin Rheumatol,* 21**,** 483-8.

COOMBES, J. L., SIDDIQUI, K. R., ARANCIBIA-CARCAMO, C. V., HALL, J., SUN, C. M., BELKAID, Y. & POWRIE, F. 2007. A functionally specialized population of mucosal CD103+ DCs induces Foxp3+ regulatory T cells via a TGF-beta and retinoic acid-dependent mechanism. *J Exp Med,* 204**,** 1757-64.

CORNELL, M., EVANS, D. A., MANN, R., FOSTIER, M., FLASZA, M., MONTHATONG, M., ARTAVANIS-TSAKONAS, S. & BARON, M. 1999. The Drosophila melanogaster Suppressor of deltex gene, a regulator of the Notch receptor signaling pathway, is an E3 class ubiquitin ligase. *Genetics,* 152**,** 567-76.

COUSSENS, L. M. & WERB, Z. 2002. Inflammation and cancer. *Nature,* 420**,** 860-7.

CURRY, C. L., REED, L. L., GOLDE, T. E., MIELE, L., NICKOLOFF, B. J. & FOREMAN, K. E. 2005. Gamma secretase inhibitor blocks Notch activation and induces apoptosis in Kaposi's sarcoma tumor cells. *Oncogene,* 24**,** 6333-44.

CYSTER, J. G. 1999. Chemokines and cell migration in secondary lymphoid organs. *Science,* 286**,** 2098-102.

CYSTER, J. G. 2005. Chemokines, sphingosine-1-phosphate, and cell migration in secondary lymphoid organs. *Annu Rev Immunol,* 23**,** 127-59.

D'ACQUISTO, F. & CROMPTON, T. 2011. CD3+CD4-CD8- (double negative) T cells: saviours or villains of the immune response? *Biochem Pharmacol,* 82**,** 333-40.

DALY, T. M., OKUYAMA, T., VOGLER, C., HASKINS, M. E., MUZYCZKA, N. & SANDS, M. S. 1999a. Neonatal intramuscular injection with recombinant adeno-associated virus results in prolonged beta-glucuronidase expression in situ and correction of liver pathology in mucopolysaccharidosis type VII mice. *Hum Gene Ther,* 10**,** 85-94.

DALY, T. M., VOGLER, C., LEVY, B., HASKINS, M. E. & SANDS, M. S. 1999b. Neonatal gene transfer leads to widespread correction of pathology in a murine model of lysosomal storage disease. *Proc Natl Acad Sci U S A,* 96**,** 2296-300.

DAWSON, C. W., RICKINSON, A. B. & YOUNG, L. S. 1990. Epstein-Barr virus latent membrane protein inhibits human epithelial cell differentiation. *Nature,* 344**,** 777-80.

DAWSON, C. W., TRAMOUNTANIS, G., ELIOPOULOS, A. G. & YOUNG, L. S. 2003. Epstein-Barr virus latent membrane protein 1 (LMP1) activates the phosphatidylinositol 3-kinase/Akt pathway to promote cell survival and induce actin filament remodeling. *J Biol Chem,* 278**,** 3694-704.

DE STROOPER, B., ANNAERT, W., CUPERS, P., SAFTIG, P., CRAESSAERTS, K., MUMM, J. S., SCHROETER, E. H., SCHRIJVERS, V., WOLFE, M. S., RAY, W. J., GOATE, A. & KOPAN, R. 1999. A presenilin-1-dependent gamma-secretase-like protease mediates release of Notch intracellular domain. *Nature,* 398**,** 518-22.

DE TOGNI, P., GOELLNER, J., RUDDLE, N. H., STREETER, P. R., FICK, A., MARIATHASAN, S., SMITH, S. C., CARLSON, R., SHORNICK, L. P., STRAUSS-SCHOENBERGER, J. & ET AL. 1994. Abnormal development of peripheral lymphoid organs in mice deficient in lymphotoxin. *Science,* 264**,** 703-7.

DE VISSER, K. E., KORETS, L. V. & COUSSENS, L. M. 2005. De novo carcinogenesis promoted by chronic inflammation is B lymphocyte dependent. *Cancer Cell,* 7**,** 411-23.

DEJACO, C., DUFTNER, C., GRUBECK-LOEBENSTEIN, B. & SCHIRMER, M. 2006. Imbalance of regulatory T cells in human autoimmune diseases. *Immunology,* 117**,** 289-300.

DELALEU, N., NGUYEN, C. Q., PECK, A. B. & JONSSON, R. 2011. Sjogren's syndrome: studying the disease in mice. *Arthritis Res Ther,* 13**,** 217.

DELEEUW, R. J., KOST, S. E., KAKAL, J. A. & NELSON, B. H. 2012. The prognostic value of FoxP3+ tumor-infiltrating lymphocytes in cancer: a critical review of the literature. *Clin Cancer Res,* 18**,** 3022-9.

DENKERS, E. Y., DEL RIO, L. & BENNOUNA, S. 2003. Neutrophil production of IL-12 and other cytokines during microbial infection. *Chem Immunol Allergy,* 83**,** 95-114.

DING, A. H., NATHAN, C. F. & STUEHR, D. J. 1988. Release of reactive nitrogen intermediates and reactive oxygen intermediates from mouse peritoneal macrophages. Comparison of activating cytokines and evidence for independent production. *J Immunol,* 141**,** 2407-12.

DO, H. J., LEE, W. Y., LIM, H. Y., OH, J. H., KIM, D. K., KIM, J. H., KIM, T. & KIM, J. H. 2009. Two potent transactivation domains in the C-terminal region of human NANOG mediate transcriptional activation in human embryonic carcinoma cells. *J Cell Biochem,* 106**,** 1079-89.

DOTTO, G. P. 2009. Crosstalk of Notch with p53 and p63 in cancer growth control. *Nat Rev Cancer,* 9**,** 587-95.

DRUTMAN, S. B., KENDALL, J. C. & TROMBETTA, E. S. 2012. Inflammatory spleen monocytes can upregulate CD11c expression without converting into dendritic cells. *J Immunol,* 188**,** 3603-10.

EBISUNO, Y., TANAKA, T., KANEMITSU, N., KANDA, H., YAMAGUCHI, K., KAISHO, T., AKIRA, S. & MIYASAKA, M. 2003. Cutting edge: the B cell chemokine CXC chemokine ligand 13/B lymphocyte chemoattractant is expressed in the high endothelial venules of lymph nodes and Peyer's patches and affects B cell trafficking across high endothelial venules. *J Immunol,* 171**,** 1642-6.

ELLISEN, L. W., BIRD, J., WEST, D. C., SORENG, A. L., REYNOLDS, T. C., SMITH, S. D. & SKLAR, J. 1991. TAN-1, the human homolog of the Drosophila notch gene, is broken by chromosomal translocations in T lymphoblastic neoplasms. *Cell,* 66**,** 649-61.

FARAZI, P. A. & DEPINHO, R. A. 2006. Hepatocellular carcinoma pathogenesis: from genes to environment. *Nat Rev Cancer,* 6**,** 674-87.

FARINHA, P., MASOUDI, H., SKINNIDER, B. F., SHUMANSKY, K., SPINELLI, J. J., GILL, K., KLASA, R., VOSS, N., CONNORS, J. M. & GASCOYNE, R. D. 2005. Analysis of multiple biomarkers shows that lymphoma-associated macrophage (LAM) content is an independent predictor of survival in follicular lymphoma (FL). *Blood,* 106**,** 2169-74.

FITZGERALD, K. & GREENWALD, I. 1995. Interchangeability of Caenorhabditis elegans DSL proteins and intrinsic signalling activity of their extracellular domains in vivo. *Development,* 121**,** 4275-82.

FLOESS, S., FREYER, J., SIEWERT, C., BARON, U., OLEK, S., POLANSKY, J., SCHLAWE, K., CHANG, H. D., BOPP, T., SCHMITT, E., KLEIN-HESSLING, S., SERFLING, E., HAMANN, A. & HUEHN, J. 2007. Epigenetic control of the foxp3 locus in regulatory T cells. *PLoS Biol,* 5**,** e38.

FONTENOT, J. D., RASMUSSEN, J. P., GAVIN, M. A. & RUDENSKY, A. Y. 2005. A function for interleukin 2 in Foxp3-expressing regulatory T cells. *Nat Immunol,* 6**,** 1142-51.

FORSTER, R., MATTIS, A. E., KREMMER, E., WOLF, E., BREM, G. & LIPP, M. 1996. A putative chemokine receptor, BLR1, directs B cell migration to defined lymphoid organs and specific anatomic compartments of the spleen. *Cell,* 87**,** 1037-47.

FORSTER, R., SCHUBEL, A., BREITFELD, D., KREMMER, E., RENNER-MULLER, I., WOLF, E. & LIPP, M. 1999. CCR7 coordinates the primary immune response by establishing functional microenvironments in secondary lymphoid organs. *Cell,* 99**,** 23-33.

FOSTIER, M., EVANS, D. A., ARTAVANIS-TSAKONAS, S. & BARON, M. 1998. Genetic characterization of the Drosophila melanogaster Suppressor of deltex gene: A regulator of notch signaling. *Genetics,* 150**,** 1477-85.

FRANCISCO, L. M., SAGE, P. T. & SHARPE, A. H. 2010. The PD-1 pathway in tolerance and autoimmunity. *Immunol Rev,* 236**,** 219-42.

FRANCISCO, L. M., SALINAS, V. H., BROWN, K. E., VANGURI, V. K., FREEMAN, G. J., KUCHROO, V. K. & SHARPE, A. H. 2009. PD-L1 regulates the development, maintenance, and function of induced regulatory T cells. *J Exp Med,* 206**,** 3015-29.

FUNAKOSHI, S., LONGO, D. L., BECKWITH, M., CONLEY, D. K., TSARFATY, G., TSARFATY, I., ARMITAGE, R. J., FANSLOW, W. C., SPRIGGS, M. K. & MURPHY, W. J. 1994. Inhibition of human B-cell lymphoma growth by CD40 stimulation. *Blood,* 83**,** 2787-94.

FUTTERER, A., MINK, K., LUZ, A., KOSCO-VILBOIS, M. H. & PFEFFER, K. 1998. The lymphotoxin beta receptor controls organogenesis and affinity maturation in peripheral lymphoid tissues. *Immunity,* 9**,** 59-70.

GAPIN, L., MATSUDA, J. L., SURH, C. D. & KRONENBERG, M. 2001. NKT cells derive from double-positive thymocytes that are positively selected by CD1d. *Nat Immunol,* 2**,** 971-8.

GARCIA-LOPEZ, M. A., SANCHEZ-MADRID, F., RODRIGUEZ-FRADE, J. M., MELLADO, M., ACEVEDO, A., GARCIA, M. I., ALBAR, J. P., MARTINEZ, C. & MARAZUELA, M. 2001. CXCR3 chemokine receptor distribution in normal and inflamed tissues: expression on activated lymphocytes, endothelial cells, and dendritic cells. *Lab Invest,* 81**,** 409-18.

GAY, D., SAUNDERS, T., CAMPER, S. & WEIGERT, M. 1993. Receptor editing: an approach by autoreactive B cells to escape tolerance. *J Exp Med,* 177**,** 999-1008.

GENESTIER, L., TAILLARDET, M., MONDIERE, P., GHEIT, H., BELLA, C. & DEFRANCE, T. 2007. TLR agonists selectively promote terminal plasma cell differentiation of B cell subsets specialized in thymus-independent responses. *J Immunol,* 178, **7779-86.**

GIVAN, A., Flow Cytometry - First Principles. 2nd ed. Wiley-Liss, 2001.

GHIRINGHELLI, F., PUIG, P. E., ROUX, S., PARCELLIER, A., SCHMITT, E., SOLARY, E., KROEMER, G., MARTIN, F., CHAUFFERT, B. & ZITVOGEL, L. 2005. Tumor cells convert immature myeloid dendritic cells into TGF-beta-secreting cells inducing CD4+CD25+ regulatory T cell proliferation. *J Exp Med,* 202, **919-29.**

GIBB, D. R., EL SHIKH, M., KANG, D. J., ROWE, W. J., EL SAYED, R., CICHY, J., YAGITA, H., TEW, J. G., DEMPSEY, P. J., CRAWFORD, H. C. & CONRAD, D. H. 2010. ADAM10 is essential for Notch2-dependent marginal zone B cell development and CD23 cleavage in vivo. *J Exp Med,* 207, **623-35.**

GIRKONTAITE, I., MISSY, K., SAKK, V., HARENBERG, A., TEDFORD, K., POTZEL, T., PFEFFER, K. & FISCHER, K. D. 2001. Lsc is required for marginal zone B cells, regulation of lymphocyte motility and immune responses. *Nat Immunol,* 2, **855-62.**

GIRKONTAITE, I., SAKK, V., WAGNER, M., BORGGREFE, T., TEDFORD, K., CHUN, J. & FISCHER, K. D. 2004. The sphingosine-1-phosphate (S1P) lysophospholipid receptor S1P3 regulates MAdCAM-1+ endothelial cells in splenic marginal sinus organization. *J Exp Med,* 200, **1491-501.**

GORCZYCA, W., WEISBERGER, J., LIU, Z., TSANG, P., HOSSEIN, M., WU, C. D., DONG, H., WONG, J. Y., TUGULEA, S., DEE, S., MELAMED, M. R. & DARZYNKIEWICZ, Z. 2002. An approach to diagnosis of T-cell lymphoproliferative disorders by flow cytometry. *Cytometry,* 50, **177-90.**

GORDON, J. 1995. CD40 and its ligand: central players in B lymphocyte survival, growth, and differentiation. *Blood Rev,* 9, **53-6.**

GOTOT, J., GOTTSCHALK, C., LEOPOLD, S., KNOLLE, P. A., YAGITA, H., KURTS, C. & LUDWIG-PORTUGALL, I. 2012. Regulatory T cells use programmed death 1 ligands to directly suppress autoreactive B cells in vivo. *Proc Natl Acad Sci U S A,* 109, **10468-73.**

GROOM, J. R. & LUSTER, A. D. 2011. CXCR3 in T cell function. *Exp Cell Res,* 317, **620-31.**

HAAS, W., PEREIRA, P. & TONEGAWA, S. 1993. Gamma/delta cells. *Annu Rev Immunol,* 11, **637-85.**

HAMANN, J., FIEBIG, H. & STRAUSS, M. 1993. Expression cloning of the early activation antigen CD69, a type II integral membrane protein with a C-type lectin domain. *J Immunol,* 150, **4920-7.**

HAMPEL, F., EHRENBERG, S., HOJER, C., DRAESEKE, A., MARSCHALL-SCHROTER, G., KUHN, R., MACK, B., GIRES, O., VAHL, C. J., SCHMIDT-SUPPRIAN, M., STROBL, L. J. & ZIMBER-STROBL, U. 2011. CD19-independent instruction of murine marginal zone B-cell development by constitutive Notch2 signaling. *Blood,* 118, **6321-31.**

HANISSIAN, S. H. & GEHA, R. S. 1997. Jak3 is associated with CD40 and is critical for CD40 induction of gene expression in B cells. *Immunity,* 6, **379-87.**

HANSON, E. M., CLEMENTS, V. K., SINHA, P., ILKOVITCH, D. & OSTRAND-ROSENBERG, S. 2009. Myeloid-derived suppressor cells down-regulate L-selectin expression on CD4+ and CD8+ T cells. *J Immunol,* 183, **937-44.**

HARDY, R. R., HAYAKAWA, K., PARKS, D. R. & HERZENBERG, L. A. 1983. Demonstration of B-cell maturation in X-linked immunodeficient mice by simultaneous three-colour immunofluorescence. *Nature,* 306, **270-2.**

HARTLEY, S. B., COOKE, M. P., FULCHER, D. A., HARRIS, A. W., CORY, S., BASTEN, A. & GOODNOW, C. C. 1993. Elimination of self-reactive B lymphocytes proceeds in two stages: arrested development and cell death. *Cell,* 72, **325-35.**

HATAKEYAMA, M. 2004. Oncogenic mechanisms of the Helicobacter pylori CagA protein. *Nat Rev Cancer,* 4, **688-94.**

HE, F., WANG, L., HU, X. B., YIN, D. D., ZHANG, P., LI, G. H., WANG, Y. C., HUANG, S. Y., LIANG, Y. M. & HAN, H. 2009. Notch and BCR signaling synergistically promote the proliferation of Raji B-lymphoma cells. *Leuk Res,* 33, **798-802.**

HO, F., LORTAN, J. E., MACLENNAN, I. C. & KHAN, M. 1986. Distinct short-lived and long-lived antibody-producing cell populations. *Eur J Immunol,* 16, **1297-301.**

HOGG, N., TAKACS, L., PALMER, D. G., SELVENDRAN, Y. & ALLEN, C. 1986. The p150,95 molecule is a marker of human mononuclear phagocytes: comparison with expression of class II molecules. *Eur J Immunol,* 16, **240-8.**

HOMIG-HOLZEL, C., HOJER, C., RASTELLI, J., CASOLA, S., STROBL, L. J., MULLER, W., QUINTANILLA-MARTINEZ, L., GEWIES, A., RULAND, J., RAJEWSKY, K. & ZIMBER-STROBL, U. 2008. Constitutive CD40 signaling in B cells selectively activates the noncanonical NF-kappaB pathway and promotes lymphomagenesis. *J Exp Med,* 205, **1317-29.**

HOZUMI, K., NEGISHI, N., SUZUKI, D., ABE, N., SOTOMARU, Y., TAMAOKI, N., MAILHOS, C., ISH-HOROWICZ, D., HABU, S. & OWEN, M. J. 2004. Delta-like 1 is necessary for the generation of marginal zone B cells but not T cells in vivo. *Nat Immunol*, 5**,** 638-44.

HSIEH, J. J., NOFZIGER, D. E., WEINMASTER, G. & HAYWARD, S. D. 1997. Epstein-Barr virus immortalization: Notch2 interacts with CBF1 and blocks differentiation. *J Virol*, 71**,** 1938-45.

HUBBARD, E. J., WU, G., KITAJEWSKI, J. & GREENWALD, I. 1997. sel-10, a negative regulator of lin-12 activity in Caenorhabditis elegans, encodes a member of the CDC4 family of proteins. *Genes Dev*, 11**,** 3182-93.

HUBMANN, R., SCHWARZMEIER, J. D., SHEHATA, M., HILGARTH, M., DUECHLER, M., DETTKE, M. & BERGER, R. 2002. Notch2 is involved in the overexpression of CD23 in B-cell chronic lymphocytic leukemia. *Blood*, 99**,** 3742-7.

JOHNSEN, S. J., BRUN, J. G., GORANSSON, L. G., SMASTUEN, M. C., JOHANNESEN, T. B., HALDORSEN, K., HARBOE, E., JONSSON, R., MEYER, P. A. & OMDAL, R. 2012. The risk of non-hodgkin lymphoma in primary sjogren's syndrome, a population-based study. *Arthritis Care Res (Hoboken)*.

JONES, D., BENJAMIN, R. J., SHAHSAFAEI, A. & DORFMAN, D. M. 2000. The chemokine receptor CXCR3 is expressed in a subset of B-cell lymphomas and is a marker of B-cell chronic lymphocytic leukemia. *Blood*, 95**,** 627-32.

JUNDT, F., ACIKGOZ, O., KWON, S. H., SCHWARZER, R., ANAGNOSTOPOULOS, I., WIESNER, B., MATHAS, S., HUMMEL, M., STEIN, H., REICHARDT, H. M. & DORKEN, B. 2008. Aberrant expression of Notch1 interferes with the B-lymphoid phenotype of neoplastic B cells in classical Hodgkin lymphoma. *Leukemia*, 22**,** 1587-94.

JUNO, J. A., KEYNAN, Y. & FOWKE, K. R. 2012. Invariant NKT cells: regulation and function during viral infection. *PLoS Pathog*, 8**,** e1002838.

KABASHIMA, K., BANKS, T. A., ANSEL, K. M., LU, T. T., WARE, C. F. & CYSTER, J. G. 2005. Intrinsic lymphotoxin-beta receptor requirement for homeostasis of lymphoid tissue dendritic cells. *Immunity*, 22**,** 439-50.

KAMINSKI, A., KAMINSKI, E. R. & MORGAN, N. G. 2007. Pre-incubation with interleukin-4 mediates a direct protective effect against the loss of pancreatic beta-cell viability induced by proinflammatory cytokines. *Clin Exp Immunol*, 148**,** 583-8.

KAMPER, P., BENDIX, K., HAMILTON-DUTOIT, S., HONORE, B., NYENGAARD, J. R. & D'AMORE, F. 2011. Tumor-infiltrating macrophages correlate with adverse prognosis and Epstein-Barr virus status in classical Hodgkin's lymphoma. *Haematologica*, 96**,** 269-76.

KANZLER, H., KUPPERS, R., HANSMANN, M. L. & RAJEWSKY, K. 1996. Hodgkin and Reed-Sternberg cells in Hodgkin's disease represent the outgrowth of a dominant tumor clone derived from (crippled) germinal center B cells. *J Exp Med*, 184**,** 1495-505.

KAWABE, T., NAKA, T., YOSHIDA, K., TANAKA, T., FUJIWARA, H., SUEMATSU, S., YOSHIDA, N., KISHIMOTO, T. & KIKUTANI, H. 1994. The immune responses in CD40-deficient mice: impaired immunoglobulin class switching and germinal center formation. *Immunity*, 1**,** 167-78.

KEHRY, M. R. 1996. CD40-mediated signaling in B cells. Balancing cell survival, growth, and death. *J Immunol*, 156**,** 2345-8.

KEIR, M. E., BUTTE, M. J., FREEMAN, G. J. & SHARPE, A. H. 2008. PD-1 and its ligands in tolerance and immunity. *Annu Rev Immunol*, 26**,** 677-704.

KELLEY, T. W., POHLMAN, B., ELSON, P. & HSI, E. D. 2007. The ratio of FOXP3+ regulatory T cells to granzyme B+ cytotoxic T/NK cells predicts prognosis in classical Hodgkin lymphoma and is independent of bcl-2 and MAL expression. *Am J Clin Pathol*, 128**,** 958-65.

KIEL, M. J., VELUSAMY, T., BETZ, B. L., ZHAO, L., WEIGELIN, H. G., CHIANG, M. Y., HUEBNER-CHAN, D. R., BAILEY, N. G., YANG, D. T., BHAGAT, G., MIRANDA, R. N., BAHLER, D. W., MEDEIROS, L. J., LIM, M. S. & ELENITOBA-JOHNSON, K. S. 2012. Whole-genome sequencing identifies recurrent somatic NOTCH2 mutations in splenic marginal zone lymphoma. *J Exp Med*, 209**,** 1553-65.

KIM, R. J., KIM, H. A., PARK, J. B., PARK, S. R., JEON, S. H., SEO, G. Y., SEO, D. W., SEO, S. R., CHUN, G. T., KIM, N. S., YIE, S. W., BYEON, W. H. & KIM, P. H. 2007. IL-4-induced AID expression and its relevance to IgA class switch recombination. *Biochem Biophys Res Commun*, 361**,** 398-403.

KOCH, U., FIORINI, E., BENEDITO, R., BESSEYRIAS, V., SCHUSTER-GOSSLER, K., PIERRES, M., MANLEY, N. R., DUARTE, A., MACDONALD, H. R. & RADTKE, F. 2008. Delta-like 4 is the essential, nonredundant ligand for Notch1 during thymic T cell lineage commitment. *J Exp Med*, 205**,** 2515-23.

KOCHERT, K., ULLRICH, K., KREHER, S., ASTER, J. C., KITAGAWA, M., JOHRENS, K., ANAGNOSTOPOULOS, I., JUNDT, F., LAMPRECHT, B., ZIMBER-STROBL, U., STEIN, H., JANZ, M., DORKEN, B. & MATHAS, S. 2011.

High-level expression of Mastermind-like 2 contributes to aberrant activation of the NOTCH signaling pathway in human lymphomas. *Oncogene,* 30**,** 1831-40.

KOHLHOF, H., HAMPEL, F., HOFFMANN, R., BURTSCHER, H., WEIDLE, U. H., HOLZEL, M., EICK, D., ZIMBER-STROBL, U. & STROBL, L. J. 2009. Notch1, Notch2, and Epstein-Barr virus-encoded nuclear antigen 2 signaling differentially affects proliferation and survival of Epstein-Barr virus-infected B cells. *Blood,* 113**,** 5506-15.

KOREISHI, A. F., SAENZ, A. J., PERSKY, D. O., CUI, H., MOSKOWITZ, A., MOSKOWITZ, C. H. & TERUYA-FELDSTEIN, J. 2010. The role of cytotoxic and regulatory T cells in relapsed/refractory Hodgkin lymphoma. *Appl Immunohistochem Mol Morphol,* 18**,** 206-11.

KRYCZEK, I., LIU, R., WANG, G., WU, K., SHU, X., SZELIGA, W., VATAN, L., FINLAYSON, E., HUANG, E., SIMEONE, D., REDMAN, B., WELLING, T. H., CHANG, A. & ZOU, W. 2009. FOXP3 defines regulatory T cells in human tumor and autoimmune disease. *Cancer Res,* 69**,** 3995-4000.

KUMAR, V., SCANDELLA, E., DANUSER, R., ONDER, L., NITSCHKE, M., FUKUI, Y., HALIN, C., LUDEWIG, B. & STEIN, J. V. 2010. Global lymphoid tissue remodeling during a viral infection is orchestrated by a B cell-lymphotoxin-dependent pathway. *Blood,* 115**,** 4725-33.

KUPPERS, R. 2009. Molecular biology of Hodgkin lymphoma. *Hematology Am Soc Hematol Educ Program***,** 491-6.

KUPPERS, R. 2011. CCR7 & lymphotoxin in lymphoma niche. *Blood,* 118**,** 831-2.

KUPPERS, R., ENGERT, A. & HANSMANN, M. L. 2012. Hodgkin lymphoma. *J Clin Invest,* 122**,** 3439-47.

KURACHI, M., KURACHI, J., SUENAGA, F., TSUKUI, T., ABE, J., UEHA, S., TOMURA, M., SUGIHARA, K., TAKAMURA, S., KAKIMI, K. & MATSUSHIMA, K. 2011. Chemokine receptor CXCR3 facilitates CD8(+) T cell differentiation into short-lived effector cells leading to memory degeneration. *J Exp Med,* 208**,** 1605-20.

KURODA, K., HAN, H., TANI, S., TANIGAKI, K., TUN, T., FURUKAWA, T., TANIGUCHI, Y., KUROOKA, H., HAMADA, Y., TOYOKUNI, S. & HONJO, T. 2003. Regulation of marginal zone B cell development by MINT, a suppressor of Notch/RBP-J signaling pathway. *Immunity,* 18**,** 301-12.

KUROOKA, H., KURODA, K. & HONJO, T. 1998. Roles of the ankyrin repeats and C-terminal region of the mouse notch1 intracellular region. *Nucleic Acids Res,* 26**,** 5448-55.

LAKE, R. J., GRIMM, L. M., VERAKSA, A., BANOS, A. & ARTAVANIS-TSAKONAS, S. 2009. In vivo analysis of the Notch receptor S1 cleavage. *PLoS One,* 4**,** e6728.

LAM, N. & SUGDEN, B. 2003. CD40 and its viral mimic, LMP1: similar means to different ends. *Cell Signal,* 15**,** 9-16.

LAN, K., MURAKAMI, M., BAJAJ, B., KAUL, R., HE, Z., GAN, R., FELDMAN, M. & ROBERTSON, E. S. 2009. Inhibition of KSHV-infected primary effusion lymphomas in NOD/SCID mice by gamma-secretase inhibitor. *Cancer Biol Ther,* 8**,** 2136-43.

LAN, K., VERMA, S. C., MURAKAMI, M., BAJAJ, B., KAUL, R. & ROBERTSON, E. S. 2007. Kaposi's sarcoma herpesvirus-encoded latency-associated nuclear antigen stabilizes intracellular activated Notch by targeting the Sel10 protein. *Proc Natl Acad Sci U S A,* 104**,** 16287-92.

LASAGNI, L., FRANCALANCI, M., ANNUNZIATO, F., LAZZERI, E., GIANNINI, S., COSMI, L., SAGRINATI, C., MAZZINGHI, B., ORLANDO, C., MAGGI, E., MARRA, F., ROMAGNANI, S., SERIO, M. & ROMAGNANI, P. 2003. An alternatively spliced variant of CXCR3 mediates the inhibition of endothelial cell growth induced by IP-10, Mig, and I-TAC, and acts as functional receptor for platelet factor 4. *J Exp Med,* 197**,** 1537-49.

LAURENCE, A., TATO, C. M., DAVIDSON, T. S., KANNO, Y., CHEN, Z., YAO, Z., BLANK, R. B., MEYLAN, F., SIEGEL, R., HENNIGHAUSEN, L., SHEVACH, E. M. & O'SHEA J, J. 2007. Interleukin-2 signaling via STAT5 constrains T helper 17 cell generation. *Immunity,* 26**,** 371-81.

LAVANCHY, D. 2004. Hepatitis B virus epidemiology, disease burden, treatment, and current and emerging prevention and control measures. *J Viral Hepat,* 11**,** 97-107.

LEE, H. H., DADGOSTAR, H., CHENG, Q., SHU, J. & CHENG, G. 1999. NF-kappaB-mediated up-regulation of Bcl-x and Bfl-1/A1 is required for CD40 survival signaling in B lymphocytes. *Proc Natl Acad Sci U S A,* 96**,** 9136-41.

LEE, N. R., SONG, E. K., JANG, K. Y., CHOI, H. N., MOON, W. S., KWON, K., LEE, J. H., YIM, C. Y. & KWAK, J. Y. 2008. Prognostic impact of tumor infiltrating FOXP3 positive regulatory T cells in diffuse large B-cell lymphoma at diagnosis. *Leuk Lymphoma,* 49**,** 247-56.

LEE, S. Y., KUMANO, K., NAKAZAKI, K., SANADA, M., MATSUMOTO, A., YAMAMOTO, G., NANNYA, Y., SUZUKI, R., OTA, S., OTA, Y., IZUTSU, K., SAKATA-YANAGIMOTO, M., HANGAISHI, A., YAGITA, H., FUKAYAMA, M., SETO,

M., KUROKAWA, M., OGAWA, S. & CHIBA, S. 2009. Gain-of-function mutations and copy number increases of Notch2 in diffuse large B-cell lymphoma. *Cancer Sci,* 100**,** 920-6.

LEMIEUX, G. A., BLUMENKRON, F., YEUNG, N., ZHOU, P., WILLIAMS, J., GRAMMER, A. C., PETROVICH, R., LIPSKY, P. E., MOSS, M. L. & WERB, Z. 2007. The low affinity IgE receptor (CD23) is cleaved by the metalloproteinase ADAM10. *J Biol Chem,* 282**,** 14836-44.

LESPAGNARD, L., GANCBERG, D., ROUAS, G., LECLERCQ, G., DE SAINT-AUBAIN SOMERHAUSEN, N., DI LEO, A., PICCART, M., VERHEST, A. & LARSIMONT, D. 1999. Tumor-infiltrating dendritic cells in adenocarcinomas of the breast: a study of 143 neoplasms with a correlation to usual prognostic factors and to clinical outcome. *Int J Cancer,* 84**,** 309-14.

LI, Z., VAN CALCAR, S., QU, C., CAVENEE, W. K., ZHANG, M. Q. & REN, B. 2003. A global transcriptional regulatory role for c-Myc in Burkitt's lymphoma cells. *Proc Natl Acad Sci U S A,* 100**,** 8164-9.

LINDQVIST, C. A. & LOSKOG, A. S. 2012. T regulatory cells in B-cell malignancy - tumour support or kiss of death? *Immunology,* 135**,** 255-60.

LO, K. W., TO, K. F. & HUANG, D. P. 2004. Focus on nasopharyngeal carcinoma. *Cancer Cell,* 5**,** 423-8.

LODER, F., MUTSCHLER, B., RAY, R. J., PAIGE, C. J., SIDERAS, P., TORRES, R., LAMERS, M. C. & CARSETTI, R. 1999. B cell development in the spleen takes place in discrete steps and is determined by the quality of B cell receptor-derived signals. *J Exp Med,* 190**,** 75-89.

LOETSCHER, M., GERBER, B., LOETSCHER, P., JONES, S. A., PIALI, L., CLARK-LEWIS, I., BAGGIOLINI, M. & MOSER, B. 1996. Chemokine receptor specific for IP10 and mig: structure, function, and expression in activated T-lymphocytes. *J Exp Med,* 184**,** 963-9.

LOGEAT, F., BESSIA, C., BROU, C., LEBAIL, O., JARRIAULT, S., SEIDAH, N. G. & ISRAEL, A. 1998. The Notch1 receptor is cleaved constitutively by a furin-like convertase. *Proc Natl Acad Sci U S A,* 95**,** 8108-12.

LOSSOS, I. S. & LEVY, R. 2003. Higher grade transformation of follicular lymphoma: phenotypic tumor progression associated with diverse genetic lesions. *Semin Cancer Biol,* 13**,** 191-202.

LUSTER, A. D., GREENBERG, S. M. & LEDER, P. 1995. The IP-10 chemokine binds to a specific cell surface heparan sulfate site shared with platelet factor 4 and inhibits endothelial cell proliferation. *J Exp Med,* 182**,** 219-31.

LUTHER, S. A., TANG, H. L., HYMAN, P. L., FARR, A. G. & CYSTER, J. G. 2000. Coexpression of the chemokines ELC and SLC by T zone stromal cells and deletion of the ELC gene in the plt/plt mouse. *Proc Natl Acad Sci U S A,* 97**,** 12694-9.

MA, Q., JONES, D., BORGHESANI, P. R., SEGAL, R. A., NAGASAWA, T., KISHIMOTO, T., BRONSON, R. T. & SPRINGER, T. A. 1998. Impaired B-lymphopoiesis, myelopoiesis, and derailed cerebellar neuron migration in CXCR4- and SDF-1-deficient mice. *Proc Natl Acad Sci U S A,* 95**,** 9448-53.

MACKAY, F., GROOM, J. R. & TANGYE, S. G. 2007. An important role for B-cell activation factor and B cells in the pathogenesis of Sjogren's syndrome. *Curr Opin Rheumatol,* 19**,** 406-13.

MAILLARD, I., WENG, A. P., CARPENTER, A. C., RODRIGUEZ, C. G., SAI, H., XU, L., ALLMAN, D., ASTER, J. C. & PEAR, W. S. 2004. Mastermind critically regulates Notch-mediated lymphoid cell fate decisions. *Blood,* 104**,** 1696-702.

MAILLOUX, A. W. & EPLING-BURNETTE, P. K. 2013. Effector memory regulatory T-cell expansion marks a pivotal point of immune escape in myelodysplastic syndromes. *Oncoimmunology,* 2**,** e22654.

MAKAR, K. W., ULGIATI, D., HAGMAN, J. & HOLERS, V. M. 2001. A site in the complement receptor 2 (CR2/CD21) silencer is necessary for lineage specific transcriptional regulation. *Int Immunol,* 13**,** 657-64.

MANDLER, R., FINKELMAN, F. D., LEVINE, A. D. & SNAPPER, C. M. 1993. IL-4 induction of IgE class switching by lipopolysaccharide-activated murine B cells occurs predominantly through sequential switching. *J Immunol,* 150**,** 407-18.

MANN, M. K., MARESZ, K., SHRIVER, L. P., TAN, Y. & DITTEL, B. N. 2007. B cell regulation of CD4+CD25+ T regulatory cells and IL-10 via B7 is essential for recovery from experimental autoimmune encephalomyelitis. *J Immunol,* 178**,** 3447-56.

MANTOVANI, A., SICA, A. & LOCATI, M. 2005. Macrophage polarization comes of age. *Immunity,* 23**,** 344-6.

MANTOVANI, A., SICA, A., SOZZANI, S., ALLAVENA, P., VECCHI, A. & LOCATI, M. 2004. The chemokine system in diverse forms of macrophage activation and polarization. *Trends Immunol,* 25**,** 677-86.

MARTIN, F. & KEARNEY, J. F. 2000. Positive selection from newly formed to marginal zone B cells depends on the rate of clonal production, CD19, and btk. *Immunity,* 12**,** 39-49.

MATSUNAMI, N., HAMAGUCHI, Y., YAMAMOTO, Y., KUZE, K., KANGAWA, K., MATSUO, H., KAWAICHI, M. & HONJO, T. 1989. A protein binding to the J kappa recombination sequence of immunoglobulin genes contains a sequence related to the integrase motif. *Nature,* 342**,** 934-7.

MATSUNO, Y., COELHO, A. L., JARAI, G., WESTWICK, J. & HOGABOAM, C. M. 2012. Notch signaling mediates TGF-beta1-induced epithelial-mesenchymal transition through the induction of Snai1. *Int J Biochem Cell Biol,* 44**,** 776-89.

MATYSIAK-BUDNIK, T. & MEGRAUD, F. 2006. Helicobacter pylori infection and gastric cancer. *Eur J Cancer,* 42**,** 708-16.

MCDONALD, K. G., MCDONOUGH, J. S. & NEWBERRY, R. D. 2005. Adaptive immune responses are dispensable for isolated lymphoid follicle formation: antigen-naive, lymphotoxin-sufficient B lymphocytes drive the formation of mature isolated lymphoid follicles. *J Immunol,* 174**,** 5720-8.

MCHEYZER-WILLIAMS, M. G. & AHMED, R. 1999. B cell memory and the long-lived plasma cell. *Curr Opin Immunol,* 11**,** 172-9.

MCNALLY, A., HILL, G. R., SPARWASSER, T., THOMAS, R. & STEPTOE, R. J. 2011. CD4+CD25+ regulatory T cells control CD8+ T-cell effector differentiation by modulating IL-2 homeostasis. *Proc Natl Acad Sci U S A,* 108**,** 7529-34.

MEIJER, S. L., DOLS, A., HU, H. M., CHU, Y., ROMERO, P., URBA, W. J. & FOX, B. A. 2004. Reduced L-selectin (CD62LLow) expression identifies tumor-specific type 1 T cells from lymph nodes draining an autologous tumor cell vaccine. *Cell Immunol,* 227**,** 93-102.

MELTER, M., REINDERS, M. E., SHO, M., PAL, S., GEEHAN, C., DENTON, M. D., MUKHOPADHYAY, D. & BRISCOE, D. M. 2000. Ligation of CD40 induces the expression of vascular endothelial growth factor by endothelial cells and monocytes and promotes angiogenesis in vivo. *Blood,* 96**,** 3801-8.

METLAY, J. P., WITMER-PACK, M. D., AGGER, R., CROWLEY, M. T., LAWLESS, D. & STEINMAN, R. M. 1990. The distinct leukocyte integrins of mouse spleen dendritic cells as identified with new hamster monoclonal antibodies. *J Exp Med,* 171**,** 1753-71.

MILLER, J. A. & MILLER, E. C. 1975. Metabolic activation and reactivity of chemical carcinogens. *Mutat Res,* 33**,** 25-6.

MINTER, L. M., TURLEY, D. M., DAS, P., SHIN, H. M., JOSHI, I., LAWLOR, R. G., CHO, O. H., PALAGA, T., GOTTIPATI, S., TELFER, J. C., KOSTURA, L., FAUQ, A. H., SIMPSON, K., SUCH, K. A., MIELE, L., GOLDE, T. E., MILLER, S. D. & OSBORNE, B. A. 2005. Inhibitors of gamma-secretase block in vivo and in vitro T helper type 1 polarization by preventing Notch upregulation of Tbx21. *Nat Immunol,* 6**,** 680-8.

MIRANDOLA, L., BASILE, A., COMI, P. & CHIARAMONTE, R. 2009. Burkitt lymphoma translocation turns Notch over to the dark side. *Leuk Res,* 33**,** 750-1.

MOORTHY, R. K. & THORLEY-LAWSON, D. A. 1993. All three domains of the Epstein-Barr virus-encoded latent membrane protein LMP-1 are required for transformation of rat-1 fibroblasts. *J Virol,* 67**,** 1638-46.

MORIMURA, T., GOITSUKA, R., ZHANG, Y., SAITO, I., RETH, M. & KITAMURA, D. 2000. Cell cycle arrest and apoptosis induced by Notch1 in B cells. *J Biol Chem,* 275**,** 36523-31.

MOSSER, D. M. 2003. The many faces of macrophage activation. *J Leukoc Biol,* 73**,** 209-12.

MOSSER, D. M. & EDWARDS, J. P. 2008. Exploring the full spectrum of macrophage activation. *Nat Rev Immunol,* 8**,** 958-69.

MUCIDA, D., PARK, Y., KIM, G., TUROVSKAYA, O., SCOTT, I., KRONENBERG, M. & CHEROUTRE, H. 2007. Reciprocal TH17 and regulatory T cell differentiation mediated by retinoic acid. *Science,* 317**,** 256-60.

MUELLER, S. N., VANGURI, V. K., HA, S. J., WEST, E. E., KEIR, M. E., GLICKMAN, J. N., SHARPE, A. H. & AHMED, R. 2010. PD-L1 has distinct functions in hematopoietic and nonhematopoietic cells in regulating T cell responses during chronic infection in mice. *J Clin Invest,* 120**,** 2508-15.

MURPHY, M., WALTER, B. N., PIKE-NOBILE, L., FANGER, N. A., GUYRE, P. M., BROWNING, J. L., WARE, C. F. & EPSTEIN, L. B. 1998. Expression of the lymphotoxin beta receptor on follicular stromal cells in human lymphoid tissues. *Cell Death Differ,* 5**,** 497-505.

MURTHY, A., SHAO, Y. W., NARALA, S. R., MOLYNEUX, S. D., ZUNIGA-PFLUCKER, J. C. & KHOKHA, R. 2012. Notch activation by the metalloproteinase ADAM17 regulates myeloproliferation and atopic barrier immunity by suppressing epithelial cytokine synthesis. *Immunity,* 36**,** 105-19.

NAGASAWA, T. 2006. Microenvironmental niches in the bone marrow required for B-cell development. *Nat Rev Immunol,* 6**,** 107-16.

NAKAYAMA, Y. & BROMBERG, J. S. 2012. Lymphotoxin-beta receptor blockade induces inflammation and fibrosis in tolerized cardiac allografts. *Am J Transplant,* 12**,** 2322-34.

NAM, Y., ASTER, J. C. & BLACKLOW, S. C. 2002. Notch signaling as a therapeutic target. *Curr Opin Chem Biol,* 6**,** 501-9.

NEMAZEE, D. & BUERKI, K. 1989. Clonal deletion of autoreactive B lymphocytes in bone marrow chimeras. *Proc Natl Acad Sci U S A,* 86**,** 8039-43.

NGO, V. N., CORNALL, R. J. & CYSTER, J. G. 2001. Splenic T zone development is B cell dependent. *J Exp Med,* 194**,** 1649-60.

NI, X. & DUVIC, M. 2011. Dendritic cells and cutaneous T-cell lymphomas. *G Ital Dermatol Venereol,* 146**,** 103-13.

NICOLAS, M., WOLFER, A., RAJ, K., KUMMER, J. A., MILL, P., VAN NOORT, M., HUI, C. C., CLEVERS, H., DOTTO, G. P. & RADTKE, F. 2003. Notch1 functions as a tumor suppressor in mouse skin. *Nat Genet,* 33**,** 416-21.

NIE, Y., WAITE, J., BREWER, F., SUNSHINE, M. J., LITTMAN, D. R. & ZOU, Y. R. 2004. The role of CXCR4 in maintaining peripheral B cell compartments and humoral immunity. *J Exp Med,* 200**,** 1145-56.

NIWA, H., YAMAMURA, K. & MIYAZAKI, J. 1991. Efficient selection for high-expression transfectants with a novel eukaryotic vector. *Gene,* 108**,** 193-9.

NUNEZ, C., NISHIMOTO, N., GARTLAND, G. L., BILLIPS, L. G., BURROWS, P. D., KUBAGAWA, H. & COOPER, M. D. 1996. B cells are generated throughout life in humans. *J Immunol,* 156**,** 866-72.

NUTT, S. L., HEAVEY, B., ROLINK, A. G. & BUSSLINGER, M. 1999. Commitment to the B-lymphoid lineage depends on the transcription factor Pax5. *Nature,* 401**,** 556-62.

O'BOYLE, G., FOX, C. R., WALDEN, H. R., WILLET, J. D., MAVIN, E. R., HINE, D. W., PALMER, J. M., BARKER, C. E., LAMB, C. A., ALI, S. & KIRBY, J. A. 2012. Chemokine receptor CXCR3 agonist prevents human T-cell migration in a humanized model of arthritic inflammation. *Proc Natl Acad Sci U S A,* 109, 4598-603.

OBERG, C., LI, J., PAULEY, A., WOLF, E., GURNEY, M. & LENDAHL, U. 2001. The Notch intracellular domain is ubiquitinated and negatively regulated by the mammalian Sel-10 homolog. *J Biol Chem,* 276**,** 35847-53.

OETTINGER, M. A. 1996. Cutting apart V(D)J recombination. *Curr Opin Genet Dev,* 6**,** 141-5.

OHASHI, S., NATSUIZAKA, M., NAGANUMA, S., KAGAWA, S., KIMURA, S., ITOH, H., KALMAN, R. A., NAKAGAWA, M., DARLING, D. S., BASU, D., GIMOTTY, P. A., KLEIN-SZANTO, A. J., DIEHL, J. A., HERLYN, M. & NAKAGAWA, H. 2011. A NOTCH3-mediated squamous cell differentiation program limits expansion of EMT-competent cells that express the ZEB transcription factors. *Cancer Res,* 71**,** 6836-47.

OHSHIMA, K., SUEFUJI, H., KARUBE, K., HAMASAKI, M., HATANO, B., TUTIYA, T., YAMAGUCHI, T., SUZUKI, K., SUZUMIYA, J. & KIKUCHI, M. 2003. Expression of chemokine receptor CXCR3 and its ligand, mig, in gastric and thyroid marginal zone lymphomas. Possible migration and autocrine mechanism. *Leuk Lymphoma,* 44**,** 329-36.

OKADA, T. & CYSTER, J. G. 2007. CC chemokine receptor 7 contributes to Gi-dependent T cell motility in the lymph node. *J Immunol,* 178**,** 2973-8.

OKADA, T., NGO, V. N., EKLAND, E. H., FORSTER, R., LIPP, M., LITTMAN, D. R. & CYSTER, J. G. 2002. Chemokine requirements for B cell entry to lymph nodes and Peyer's patches. *J Exp Med,* 196**,** 65-75.

OKI, S., CHIBA, A., YAMAMURA, T. & MIYAKE, S. 2004. The clinical implication and molecular mechanism of preferential IL-4 production by modified glycolipid-stimulated NKT cells. *J Clin Invest,* 113**,** 1631-40.

OKUYAMA, R., NGUYEN, B. C., TALORA, C., OGAWA, E., TOMMASI DI VIGNANO, A., LIOUMI, M., CHIORINO, G., TAGAMI, H., WOO, M. & DOTTO, G. P. 2004. High commitment of embryonic keratinocytes to terminal differentiation through a Notch1-caspase 3 regulatory mechanism. *Dev Cell,* 6**,** 551-62.

OLIVER, A. M., MARTIN, F. & KEARNEY, J. F. 1999. IgMhighCD21high lymphocytes enriched in the splenic marginal zone generate effector cells more rapidly than the bulk of follicular B cells. *J Immunol,* 162**,** 7198-207.

ONG, C. T., SEDY, J. R., MURPHY, K. M. & KOPAN, R. 2008. Notch and presenilin regulate cellular expansion and cytokine secretion but cannot instruct Th1/Th2 fate acquisition. *PLoS One,* 3**,** e2823.

OSMOND, D. G. 1986. Population dynamics of bone marrow B lymphocytes. *Immunol Rev,* 93**,** 103-24.

OSMOND, D. G. 1991. Proliferation kinetics and the lifespan of B cells in central and peripheral lymphoid organs. *Curr Opin Immunol,* 3**,** 179-85.

OSTRAND-ROSENBERG, S. & SINHA, P. 2009. Myeloid-derived suppressor cells: linking inflammation and cancer. *J Immunol,* 182**,** 4499-506.

OYAMA, T., HARIGAYA, K., MURADIL, A., HOZUMI, K., HABU, S., OGURO, H., IWAMA, A., MATSUNO, K., SAKAMOTO, R., SATO, M., YOSHIDA, N. & KITAGAWA, M. 2007. Mastermind-1 is required for Notch signal-dependent steps in lymphocyte development in vivo. *Proc Natl Acad Sci U S A,* 104**,** 9764-9.

PADUA, D. & MASSAGUE, J. 2009. Roles of TGFbeta in metastasis. *Cell Res,* 19**,** 89-102.

PARADA, N. A., CENTER, D. M., KORNFELD, H., RODRIGUEZ, W. L., COOK, J., VALLEN, M. & CRUIKSHANK, W. W. 1998. Synergistic activation of CD4+ T cells by IL-16 and IL-2. *J Immunol,* 160**,** 2115-20.

PARK, M. K., AMICHAY, D., LOVE, P., WICK, E., LIAO, F., GRINBERG, A., RABIN, R. L., ZHANG, H. H., GEBEYEHU, S., WRIGHT, T. M., IWASAKI, A., WENG, Y., DEMARTINO, J. A., ELKINS, K. L. & FARBER, J. M. 2002. The CXC chemokine murine monokine induced by IFN-gamma (CXC chemokine ligand 9) is made by APCs, targets lymphocytes including activated B cells, and supports antibody responses to a bacterial pathogen in vivo. *J Immunol,* 169**,** 1433-43.

PAULIE, S., EHLIN-HENRIKSSON, B., MELLSTEDT, H., KOHO, H., BEN-AISSA, H. & PERLMANN, P. 1985. A p50 surface antigen restricted to human urinary bladder carcinomas and B lymphocytes. *Cancer Immunol Immunother,* 20**,** 23-8.

PECHLOFF, K., HOLCH, J., FERCH, U., SCHWENEKER, M., BRUNNER, K., KREMER, M., SPARWASSER, T., QUINTANILLA-MARTINEZ, L., ZIMBER-STROBL, U., STREUBEL, B., GEWIES, A., PESCHEL, C. & RULAND, J. 2010. The fusion kinase ITK-SYK mimics a T cell receptor signal and drives oncogenesis in conditional mouse models of peripheral T cell lymphoma. *J Exp Med,* 207**,** 1031-44.

PESCHON, J. J., MORRISSEY, P. J., GRABSTEIN, K. H., RAMSDELL, F. J., MARASKOVSKY, E., GLINIAK, B. C., PARK, L. S., ZIEGLER, S. F., WILLIAMS, D. E., WARE, C. B., MEYER, J. D. & DAVISON, B. L. 1994. Early lymphocyte expansion is severely impaired in interleukin 7 receptor-deficient mice. *J Exp Med,* 180**,** 1955-60.

PETIT, I., SZYPER-KRAVITZ, M., NAGLER, A., LAHAV, M., PELED, A., HABLER, L., PONOMARYOV, T., TAICHMAN, R. S., ARENZANA-SEISDEDOS, F., FUJII, N., SANDBANK, J., ZIPORI, D. & LAPIDOT, T. 2002. G-CSF induces stem cell mobilization by decreasing bone marrow SDF-1 and up-regulating CXCR4. *Nat Immunol,* 3**,** 687-94.

PILGRIM, M. J., KASMAN, L., GREWAL, J., BRUORTON, M. E., WERNER, P., LONDON, L. & LONDON, S. D. 2007. A focused salivary gland infection with attenuated MCMV: an animal model with prevention of pathology associated with systemic MCMV infection. *Exp Mol Pathol,* 82**,** 269-79.

PILLAI, S. & CARIAPPA, A. 2009. The follicular versus marginal zone B lymphocyte cell fate decision. *Nat Rev Immunol,* 9**,** 767-77.

PILLAI, S., CARIAPPA, A. & MORAN, S. T. 2005. Marginal zone B cells. *Annu Rev Immunol,* 23**,** 161-96.

POLANCZYK, M. J., HOPKE, C., VANDENBARK, A. A. & OFFNER, H. 2007. Treg suppressive activity involves estrogen-dependent expression of programmed death-1 (PD-1). *Int Immunol,* 19**,** 337-43.

PUI, J. C., ALLMAN, D., XU, L., DEROCCO, S., KARNELL, F. G., BAKKOUR, S., LEE, J. Y., KADESCH, T., HARDY, R. R., ASTER, J. C. & PEAR, W. S. 1999. Notch1 expression in early lymphopoiesis influences B versus T lineage determination. *Immunity,* 11**,** 299-308.

PUROW, B. 2012. Notch inhibition as a promising new approach to cancer therapy. *Adv Exp Med Biol,* 727**,** 305-19.

QIAN, B. Z. & POLLARD, J. W. 2010. Macrophage diversity enhances tumor progression and metastasis. *Cell,* 141**,** 39-51.

QIAN, Y., GILTIAY, N., XIAO, J., WANG, Y., TIAN, J., HAN, S., SCOTT, M., CARTER, R., JORGENSEN, T. N. & LI, X. 2008. Deficiency of Act1, a critical modulator of B cell function, leads to development of Sjogren's syndrome. *Eur J Immunol,* 38**,** 2219-28.

QUILLARD, T., DEVALLIERE, J., CHATELAIS, M., COULON, F., SEVENO, C., ROMAGNOLI, M., BARILLE NION, S. & CHARREAU, B. 2009. Notch2 signaling sensitizes endothelial cells to apoptosis by negatively regulating the key protective molecule survivin. *PLoS One,* 4**,** e8244.

RAAB-TRAUB, N. 2002. Epstein-Barr virus in the pathogenesis of NPC. *Semin Cancer Biol,* 12**,** 431-41.

RABINOVITCH, A. & SUAREZ-PINZON, W. L. 1998. Cytokines and their roles in pancreatic islet beta-cell destruction and insulin-dependent diabetes mellitus. *Biochem Pharmacol,* 55**,** 1139-49.

RADTKE, F., FASNACHT, N. & MACDONALD, H. R. 2010. Notch signaling in the immune system. *Immunity,* 32**,** 14-27.

RADTKE, F., WILSON, A., STARK, G., BAUER, M., VAN MEERWIJK, J., MACDONALD, H. R. & AGUET, M. 1999. Deficient T cell fate specification in mice with an induced inactivation of Notch1. *Immunity,* 10**,** 547-58.

RANGARAJAN, A., TALORA, C., OKUYAMA, R., NICOLAS, M., MAMMUCARI, C., OH, H., ASTER, J. C., KRISHNA, S., METZGER, D., CHAMBON, P., MIELE, L., AGUET, M., RADTKE, F. & DOTTO, G. P. 2001. Notch signaling is a direct determinant of keratinocyte growth arrest and entry into differentiation. *EMBO J,* 20**,** 3427-36.

REBAY, I., FLEMING, R. J., FEHON, R. G., CHERBAS, L., CHERBAS, P. & ARTAVANIS-TSAKONAS, S. 1991. Specific EGF repeats of Notch mediate interactions with Delta and Serrate: implications for Notch as a multifunctional receptor. *Cell,* 67**,** 687-99.

REEDIJK, M., ODORCIC, S., CHANG, L., ZHANG, H., MILLER, N., MCCREADY, D. R., LOCKWOOD, G. & EGAN, S. E. 2005. High-level coexpression of JAG1 and NOTCH1 is observed in human breast cancer and is associated with poor overall survival. *Cancer Res,* 65**,** 8530-7.

REEDIJK, M., PINNADUWAGE, D., DICKSON, B. C., MULLIGAN, A. M., ZHANG, H., BULL, S. B., O'MALLEY, F. P., EGAN, S. E. & ANDRULIS, I. L. 2008. JAG1 expression is associated with a basal phenotype and recurrence in lymph node-negative breast cancer. *Breast Cancer Res Treat,* 111**,** 439-48.

REHERMANN, B. & NASCIMBENI, M. 2005. Immunology of hepatitis B virus and hepatitis C virus infection. *Nat Rev Immunol,* 5**,** 215-29.

REHM, A., MENSEN, A., SCHRADI, K., GERLACH, K., WITTSTOCK, S., WINTER, S., BUCHNER, G., DORKEN, B., LIPP, M. & HOPKEN, U. E. 2011. Cooperative function of CCR7 and lymphotoxin in the formation of a lymphoma-permissive niche within murine secondary lymphoid organs. *Blood,* 118**,** 1020-33.

RENNERT, P. D., BROWNING, J. L., MEBIUS, R., MACKAY, F. & HOCHMAN, P. S. 1996. Surface lymphotoxin alpha/beta complex is required for the development of peripheral lymphoid organs. *J Exp Med,* 184**,** 1999-2006.

RENSHAW, B. R., FANSLOW, W. C., 3RD, ARMITAGE, R. J., CAMPBELL, K. A., LIGGITT, D., WRIGHT, B., DAVISON, B. L. & MALISZEWSKI, C. R. 1994. Humoral immune responses in CD40 ligand-deficient mice. *J Exp Med,* 180**,** 1889-900.

RICH, B. E. 1997. Autocrine expression of interleukin-7 rescues lymphoid expansion in interleukin-7-deficient mice. *Immunology,* 92**,** 374-80.

RICKERT, R. C., ROES, J. & RAJEWSKY, K. 1997. B lymphocyte-specific, Cre-mediated mutagenesis in mice. *Nucleic Acids Res,* 25**,** 1317-8.

RIZ, I., HAWLEY, T. S., LUU, T. V., LEE, N. H. & HAWLEY, R. G. 2010. TLX1 and NOTCH coregulate transcription in T cell acute lymphoblastic leukemia cells. *Mol Cancer,* 9**,** 181.

ROCK, K. L., LATZ, E., ONTIVEROS, F. & KONO, H. 2010. The sterile inflammatory response. *Annu Rev Immunol,* 28**,** 321-42.

RODRIGUEZ, P. C., HERNANDEZ, C. P., QUICENO, D., DUBINETT, S. M., ZABALETA, J., OCHOA, J. B., GILBERT, J. & OCHOA, A. C. 2005. Arginase I in myeloid suppressor cells is induced by COX-2 in lung carcinoma. *J Exp Med,* 202**,** 931-9.

RODRIGUEZ, P. C. & OCHOA, A. C. 2008. Arginine regulation by myeloid derived suppressor cells and tolerance in cancer: mechanisms and therapeutic perspectives. *Immunol Rev,* 222**,** 180-91.

ROEMER, K. 2012. Notch and the p53 clan of transcription factors. *Adv Exp Med Biol,* 727**,** 223-40.

ROLINK, A. G., ANDERSSON, J. & MELCHERS, F. 1998. Characterization of immature B cells by a novel monoclonal antibody, by turnover and by mitogen reactivity. *Eur J Immunol,* 28**,** 3738-48.

ROLINK, A. G., NUTT, S. L., MELCHERS, F. & BUSSLINGER, M. 1999. Long-term in vivo reconstitution of T-cell development by Pax5-deficient B-cell progenitors. *Nature,* 401**,** 603-6.

ROMER, S., SAUNDERS, U., JACK, H. M. & JEHN, B. M. 2003. Notch1 enhances B-cell receptor-induced apoptosis in mature activated B cells without affecting cell cycle progression and surface IgM expression. *Cell Death Differ,* 10**,** 833-44.

ROSATI, E., SABATINI, R., DE FALCO, F., DEL PAPA, B., FALZETTI, F., DI IANNI, M., CAVALLI, L., FETTUCCIARI, K., BARTOLI, A., SCREPANTI, I. & MARCONI, P. 2013. gamma-Secretase inhibitor I induces apoptosis in chronic lymphocytic leukemia cells by proteasome inhibition, endoplasmic reticulum stress increase and notch down-regulation. *Int J Cancer,* 132**,** 1940-53.

ROSSI, D., TRIFONOV, V., FANGAZIO, M., BRUSCAGGIN, A., RASI, S., SPINA, V., MONTI, S., VAISITTI, T., ARRUGA, F., FAMA, R., CIARDULLO, C., GRECO, M., CRESTA, S., PIRANDA, D., HOLMES, A., FABBRI, G., MESSINA, M., RINALDI, A., WANG, J., AGOSTINELLI, C., PICCALUGA, P. P., LUCIONI, M., TABBO, F., SERRA, R., FRANCESCHETTI, S., DEAMBROGI, C., DANIELE, G., GATTEI, V., MARASCA, R., FACCHETTI, F., ARCAINI, L., INGHIRAMI, G., BERTONI, F., PILERI, S. A., DEAGLIO, S., FOA, R., DALLA-FAVERA, R., PASQUALUCCI, L., RABADAN, R. & GAIDANO, G. 2012. The coding genome of splenic marginal zone lymphoma: activation of NOTCH2 and other pathways regulating marginal zone development. *J Exp Med,* 209**,** 1537-51.

RUSH, J. S., HASBOLD, J. & HODGKIN, P. D. 2002. Cross-linking surface Ig delays CD40 ligand- and IL-4-induced B cell Ig class switching and reveals evidence for independent regulation of B cell proliferation and differentiation. *J Immunol,* 168**,** 2676-82.

RUSH, J. S. & HODGKIN, P. D. 2001. B cells activated via CD40 and IL-4 undergo a division burst but require continued stimulation to maintain division, survival and differentiation. *Eur J Immunol,* 31**,** 1150-9.

RUSSELL, S. M., KEEGAN, A. D., HARADA, N., NAKAMURA, Y., NOGUCHI, M., LELAND, P., FRIEDMANN, M. C., MIYAJIMA, A., PURI, R. K., PAUL, W. E. & ET AL. 1993. Interleukin-2 receptor gamma chain: a functional component of the interleukin-4 receptor. *Science,* 262**,** 1880-3.

SAITO, T., CHIBA, S., ICHIKAWA, M., KUNISATO, A., ASAI, T., SHIMIZU, K., YAMAGUCHI, T., YAMAMOTO, G., SEO, S., KUMANO, K., NAKAGAMI-YAMAGUCHI, E., HAMADA, Y., AIZAWA, S. & HIRAI, H. 2003. Notch2 is preferentially expressed in mature B cells and indispensable for marginal zone B lineage development. *Immunity,* 18**,** 675-85.

SAKURADA, M., OKOCHI, N., KATO, H., SATOMI, S., SASAKI, T., TAGUCHI, Y. & MORI, S. 1992. [Mitochondrial energy synthesis during cold preservation and after reperfusion in liver transplantation]. *Nihon Geka Gakkai Zasshi,* 93**,** 709-15.

SANTAGATA, S., DEMICHELIS, F., RIVA, A., VARAMBALLY, S., HOFER, M. D., KUTOK, J. L., KIM, R., TANG, J., MONTIE, J. E., CHINNAIYAN, A. M., RUBIN, M. A. & ASTER, J. C. 2004. JAGGED1 expression is associated with prostate cancer metastasis and recurrence. *Cancer Res,* 64**,** 6854-7.

SAVAGE, P. A., MALCHOW, S. & LEVENTHAL, D. S. 2012. Basic principles of tumor-associated regulatory T cell biology. *Trends Immunol.*

SCHMIDT-SUPPRIAN, M. & RAJEWSKY, K. 2007. Vagaries of conditional gene targeting. *Nat Immunol,* 8**,** 665-8.

SCHRECK, S., FRIEBEL, D., BUETTNER, M., DISTEL, L., GRABENBAUER, G., YOUNG, L. S. & NIEDOBITEK, G. 2009. Prognostic impact of tumour-infiltrating Th2 and regulatory T cells in classical Hodgkin lymphoma. *Hematol Oncol,* 27**,** 31-9.

SHI, T. P., XU, H., WEI, J. F., AI, X., MA, X., WANG, B. J., JU, Z. H., ZHANG, G. X., WANG, C., WU, Z. Q. & ZHANG, X. 2008. Association of low expression of notch-1 and jagged-1 in human papillary bladder cancer and shorter survival. *J Urol,* 180**,** 361-6.

SHIBATA, K., YAMADA, H., SATO, T., DEJIMA, T., NAKAMURA, M., IKAWA, T., HARA, H., YAMASAKI, S., KAGEYAMA, R., IWAKURA, Y., KAWAMOTO, H., TOH, H. & YOSHIKAI, Y. 2011. Notch-Hes1 pathway is required for the development of IL-17-producing gammadelta T cells. *Blood,* 118**,** 586-93.

SHULTZ, L. D., LYONS, B. L., BURZENSKI, L. M., GOTT, B., CHEN, X., CHALEFF, S., KOTB, M., GILLIES, S. D., KING, M., MANGADA, J., GREINER, D. L. & HANDGRETINGER, R. 2005. Human lymphoid and myeloid cell development in NOD/LtSz-scid IL2R gamma null mice engrafted with mobilized human hemopoietic stem cells. *J Immunol,* 174**,** 6477-89.

SICA, A. 2010. Role of tumour-associated macrophages in cancer-related inflammation. *Exp Oncol,* 32**,** 153-8.

SINHA, P., OKORO, C., FOELL, D., FREEZE, H. H., OSTRAND-ROSENBERG, S. & SRIKRISHNA, G. 2008. Proinflammatory S100 proteins regulate the accumulation of myeloid-derived suppressor cells. *J Immunol,* 181**,** 4666-75.

SMITH, K. G., HEWITSON, T. D., NOSSAL, G. J. & TARLINTON, D. M. 1996. The phenotype and fate of the antibody-forming cells of the splenic foci. *Eur J Immunol,* 26**,** 444-8.

SOUTHERN, E. M. 1975. Detection of specific sequences among DNA fragments separated by gel electrophoresis. *J Mol Biol,* 98**,** 503-17.

STEIN, M., KESHAV, S., HARRIS, N. & GORDON, S. 1992. Interleukin 4 potently enhances murine macrophage mannose receptor activity: a marker of alternative immunologic macrophage activation. *J Exp Med,* 176**,** 287-92.

STEINMAN, R. M. & BANCHEREAU, J. 2007. Taking dendritic cells into medicine. *Nature,* 449**,** 419-26.

STROBL, L. J., HOFELMAYR, H., MARSCHALL, G., BRIELMEIER, M., BORNKAMM, G. W. & ZIMBER-STROBL, U. 2000. Activated Notch1 modulates gene expression in B cells similarly to Epstein-Barr viral nuclear antigen 2. *J Virol,* 74**,** 1727-35.

SU, T. T. & RAWLINGS, D. J. 2002. Transitional B lymphocyte subsets operate as distinct checkpoints in murine splenic B cell development. *J Immunol,* 168**,** 2101-10.

SUGAMURA, K., ASAO, H., KONDO, M., TANAKA, N., ISHII, N., NAKAMURA, M. & TAKESHITA, T. 1995. The common gamma-chain for multiple cytokine receptors. *Adv Immunol,* 59**,** 225-77.

SUN, C. M., HALL, J. A., BLANK, R. B., BOULADOUX, N., OUKKA, M., MORA, J. R. & BELKAID, Y. 2007. Small intestine lamina propria dendritic cells promote de novo generation of Foxp3 T reg cells via retinoic acid. *J Exp Med,* 204**,** 1775-85.

SUN, J., KRAWCZYK, C. J. & PEARCE, E. J. 2008. Suppression of Th2 cell development by Notch ligands Delta1 and Delta4. *J Immunol,* 180**,** 1655-61.

TAI, Y. T., PODAR, K., GUPTA, D., LIN, B., YOUNG, G., AKIYAMA, M. & ANDERSON, K. C. 2002. CD40 activation induces p53-dependent vascular endothelial growth factor secretion in human multiple myeloma cells. *Blood,* 99**,** 1419-27.

TAIPALE, J., SAHARINEN, J. & KESKI-OJA, J. 1998. Extracellular matrix-associated transforming growth factor-beta: role in cancer cell growth and invasion. *Adv Cancer Res,* 75**,** 87-134.

TAKESHITA, T., ASAO, H., OHTANI, K., ISHII, N., KUMAKI, S., TANAKA, N., MUNAKATA, H., NAKAMURA, M. & SUGAMURA, K. 1992. Cloning of the gamma chain of the human IL-2 receptor. *Science,* 257**,** 379-82.

TANIGAKI, K., HAN, H., YAMAMOTO, N., TASHIRO, K., IKEGAWA, M., KURODA, K., SUZUKI, A., NAKANO, T. & HONJO, T. 2002. Notch-RBP-J signaling is involved in cell fate determination of marginal zone B cells. *Nat Immunol,* 3**,** 443-50.

TAVARES, R. M., TURER, E. E., LIU, C. L., ADVINCULA, R., SCAPINI, P., RHEE, L., BARRERA, J., LOWELL, C. A., UTZ, P. J., MALYNN, B. A. & MA, A. 2010. The ubiquitin modifying enzyme A20 restricts B cell survival and prevents autoimmunity. *Immunity,* 33**,** 181-91.

TAYLOR, R. S., GRIFFITHS, C. E., BROWN, M. D., SWANSON, N. A. & NICKOLOFF, B. J. 1990. Constitutive absence and interferon-gamma-induced expression of adhesion molecules in basal cell carcinoma. *J Am Acad Dermatol,* 22**,** 721-6.

TEICHER, B. A. & FRICKER, S. P. 2010. CXCL12 (SDF-1)/CXCR4 pathway in cancer. *Clin Cancer Res,* 16**,** 2927-31.

TEOH, G., TAI, Y. T., URASHIMA, M., SHIRAHAMA, S., MATSUZAKI, M., CHAUHAN, D., TREON, S. P., RAJE, N., HIDESHIMA, T., SHIMA, Y. & ANDERSON, K. C. 2000. CD40 activation mediates p53-dependent cell cycle regulation in human multiple myeloma cell lines. *Blood,* 95**,** 1039-46.

TERABE, M., MATSUI, S., PARK, J. M., MAMURA, M., NOBEN-TRAUTH, N., DONALDSON, D. D., CHEN, W., WAHL, S. M., LEDBETTER, S., PRATT, B., LETTERIO, J. J., PAUL, W. E. & BERZOFSKY, J. A. 2003. Transforming growth factor-beta production and myeloid cells are an effector mechanism through which CD1d-restricted T cells block cytotoxic T lymphocyte-mediated tumor immunosurveillance: abrogation prevents tumor recurrence. *J Exp Med,* 198**,** 1741-52.

THOMAS, M., CALAMITO, M., SRIVASTAVA, B., MAILLARD, I., PEAR, W. S. & ALLMAN, D. 2007. Notch activity synergizes with B-cell-receptor and CD40 signaling to enhance B-cell activation. *Blood,* 109**,** 3342-50.

TIEGS, S. L., RUSSELL, D. M. & NEMAZEE, D. 1993. Receptor editing in self-reactive bone marrow B cells. *J Exp Med,* 177**,** 1009-20.

TIENARI, J., LEHTONEN, S. & LEHTONEN, E. 2005. CD2-associated protein in human urogenital system and in adult kidney tumours. *Virchows Arch,* 446**,** 394-401.

TRAVERT, M., AME-THOMAS, P., PANGAULT, C., MORIZOT, A., MICHEAU, O., SEMANA, G., LAMY, T., FEST, T., TARTE, K. & GUILLAUDEUX, T. 2008. CD40 ligand protects from TRAIL-induced apoptosis in follicular lymphomas through NF-kappaB activation and up-regulation of c-FLIP and Bcl-xL. *J Immunol,* 181**,** 1001-11.

TROY, A., DAVIDSON, P., ATKINSON, C. & HART, D. 1998. Phenotypic characterisation of the dendritic cell infiltrate in prostate cancer. *J Urol,* 160**,** 214-9.

TSUJITANI, S., KAKEJI, Y., WATANABE, A., KOHNOE, S., MAEHARA, Y. & SUGIMACHI, K. 1990. Infiltration of dendritic cells in relation to tumor invasion and lymph node metastasis in human gastric cancer. *Cancer,* 66**,** 2012-6.

TSUKAHARA, R., TAKEUCHI, M., AKIBA, H., KEZUKA, T., TAKEDA, K., USUI, Y., USUI, M., YAGITA, H. & OKUMURA, K. 2005. Critical contribution of CD80 and CD86 to induction of anterior chamber-associated immune deviation. *Int Immunol,* 17**,** 523-30.

TU, L., FANG, T. C., ARTIS, D., SHESTOVA, O., PROSS, S. E., MAILLARD, I. & PEAR, W. S. 2005. Notch signaling is an important regulator of type 2 immunity. *J Exp Med,* 202**,** 1037-42.

TZANKOV, A., MEIER, C., HIRSCHMANN, P., WENT, P., PILERI, S. A. & DIRNHOFER, S. 2008. Correlation of high numbers of intratumoral FOXP3+ regulatory T cells with improved survival in germinal center-like diffuse large B-cell lymphoma, follicular lymphoma and classical Hodgkin's lymphoma. *Haematologica,* 93**,** 193-200.

UCHIDA, J., YASUI, T., TAKAOKA-SHICHIJO, Y., MURAOKA, M., KULWICHIT, W., RAAB-TRAUB, N. & KIKUTANI, H. 1999. Mimicry of CD40 signals by Epstein-Barr virus LMP1 in B lymphocyte responses. *Science,* 286**,** 300-3.

URASHIMA, M., CHAUHAN, D., UCHIYAMA, H., FREEMAN, G. J. & ANDERSON, K. C. 1995. CD40 ligand triggered interleukin-6 secretion in multiple myeloma. *Blood,* 85**,** 1903-12.

VAN DEN OORD, J. J., MAES, A., STAS, M., NUYTS, J., BATTOCCHIO, S., KASRAN, A., GARMYN, M., DE WEVER, I. & DE WOLF-PEETERS, C. 1996. CD40 is a prognostic marker in primary cutaneous malignant melanoma. *Am J Pathol,* 149**,** 1953-61.

VAN KOOTEN, C. & BANCHEREAU, J. 1997. Functions of CD40 on B cells, dendritic cells and other cells. *Curr Opin Immunol,* 9**,** 330-7.

VIGOUROUX, S., YVON, E., WAGNER, H. J., BIAGI, E., DOTTI, G., SILI, U., LIRA, C., ROONEY, C. M. & BRENNER, M. K. 2003. Induction of antigen-specific regulatory T cells following overexpression of a Notch ligand by human B lymphocytes. *J Virol,* 77**,** 10872-80.

VON BOEHMER, H. 2005. Notch in lymphopoiesis and T cell polarization. *Nat Immunol,* 6**,** 641-2.

VON FREEDEN-JEFFRY, U., VIEIRA, P., LUCIAN, L. A., MCNEIL, T., BURDACH, S. E. & MURRAY, R. 1995. Lymphopenia in interleukin (IL)-7 gene-deleted mice identifies IL-7 as a nonredundant cytokine. *J Exp Med,* 181**,** 1519-26.

VOOIJS, W. C., OTTEN, H. G., VAN VLIET, M., VAN DIJK, A. J., DE WEGER, R. A., DE BOER, M., BOHLEN, H., BOLOGNESI, A., POLITO, L. & DE GAST, G. C. 1997. B7-1 (CD80) as target for immunotoxin therapy for Hodgkin's disease. *Br J Cancer,* 76**,** 1163-9.

WAHLIN, B. E., AGGARWAL, M., MONTES-MORENO, S., GONZALEZ, L. F., RONCADOR, G., SANCHEZ-VERDE, L., CHRISTENSSON, B., SANDER, B. & KIMBY, E. 2010. A unifying microenvironment model in follicular lymphoma: outcome is predicted by programmed death-1--positive, regulatory, cytotoxic, and helper T cells and macrophages. *Clin Cancer Res,* 16**,** 637-50.

WALDSCHMIDT, T. J., CONRAD, D. H. & LYNCH, R. G. 1988. The expression of B cell surface receptors. I. The ontogeny and distribution of the murine B cell IgE Fc receptor. *J Immunol,* 140**,** 2148-54.

WANG, D., LIEBOWITZ, D. & KIEFF, E. 1985. An EBV membrane protein expressed in immortalized lymphocytes transforms established rodent cells. *Cell,* 43**,** 831-40.

WANG, J. & KE, X. Y. 2011. The four types of T_{regs} in malignant lymphomas. *J Hematol Oncol,* 4**,** 50.

WANG, Z., LI, Y., KONG, D. & SARKAR, F. H. 2010. The role of Notch signaling pathway in epithelial-mesenchymal transition (EMT) during development and tumor aggressiveness. *Curr Drug Targets,* 11**,** 745-51.

WATSON, M. L., WHITE, A. M., CAMPBELL, E. M., SMITH, A. W., UDDIN, J., YOSHIMURA, T. & WESTWICK, J. 1999. Anti-inflammatory actions of interleukin-13: suppression of tumor necrosis factor-alpha and antigen-induced leukocyte accumulation in the guinea pig lung. *Am J Respir Cell Mol Biol,* 20**,** 1007-12.

WEISBERGER, J., CORNFIELD, D., GORCZYCA, W. & LIU, Z. 2003. Down-regulation of pan-T-cell antigens, particularly CD7, in acute infectious mononucleosis. *Am J Clin Pathol,* 120**,** 49-55.

WENG, A. P., MILLHOLLAND, J. M., YASHIRO-OHTANI, Y., ARCANGELI, M. L., LAU, A., WAI, C., DEL BIANCO, C., RODRIGUEZ, C. G., SAI, H., TOBIAS, J., LI, Y., WOLFE, M. S., SHACHAF, C., FELSHER, D., BLACKLOW, S. C., PEAR, W. S. & ASTER, J. C. 2006. c-Myc is an important direct target of Notch1 in T-cell acute lymphoblastic leukemia/lymphoma. *Genes Dev,* 20**,** 2096-109.

WESKAMP, G., FORD, J. W., STURGILL, J., MARTIN, S., DOCHERTY, A. J., SWENDEMAN, S., BROADWAY, N., HARTMANN, D., SAFTIG, P., UMLAND, S., SEHARA-FUJISAWA, A., BLACK, R. A., LUDWIG, A., BECHERER, J. D., CONRAD, D. H. & BLOBEL, C. P. 2006. ADAM10 is a principal 'sheddase' of the low-affinity immunoglobulin E receptor CD23. *Nat Immunol,* 7**,** 1293-8.

WICKREMASINGHE, R. G., PRENTICE, A. G. & STEELE, A. J. 2011. p53 and Notch signaling in chronic lymphocytic leukemia: clues to identifying novel therapeutic strategies. *Leukemia,* 25**,** 1400-7.

WILSON, A., MACDONALD, H. R. & RADTKE, F. 2001. Notch 1-deficient common lymphoid precursors adopt a B cell fate in the thymus. *J Exp Med,* 194**,** 1003-12.

WOLFER, A., WILSON, A., NEMIR, M., MACDONALD, H. R. & RADTKE, F. 2002. Inactivation of Notch1 impairs VDJbeta rearrangement and allows pre-TCR-independent survival of early alpha beta Lineage Thymocytes. *Immunity,* 16**,** 869-79.

WON, W. J. & KEARNEY, J. F. 2002. CD9 is a unique marker for marginal zone B cells, B1 cells, and plasma cells in mice. *J Immunol,* 168**,** 5605-11.

WU, G., LYAPINA, S., DAS, I., LI, J., GURNEY, M., PAULEY, A., CHUI, I., DESHAIES, R. J. & KITAJEWSKI, J. 2001. SEL-10 is an inhibitor of notch signaling that targets notch for ubiquitin-mediated protein degradation. *Mol Cell Biol,* 21**,** 7403-15.

WU, L., MAILLARD, I., NAKAMURA, M., PEAR, W. S. & GRIFFIN, J. D. 2007. The transcriptional coactivator Maml1 is required for Notch2-mediated marginal zone B-cell development. *Blood,* 110**,** 3618-23.

YAMAMOTO, T., PRICE, D. A., CASAZZA, J. P., FERRARI, G., NASON, M., CHATTOPADHYAY, P. K., ROEDERER, M., GOSTICK, E., KATSIKIS, P. D., DOUEK, D. C., HAUBRICH, R., PETROVAS, C. & KOUP, R. A. 2011. Surface expression patterns of negative regulatory molecules identify determinants of virus-specific CD8+ T-cell exhaustion in HIV infection. *Blood,* 117**,** 4805-15.

YANG, L., PANG, Y. & MOSES, H. L. 2010. TGF-beta and immune cells: an important regulatory axis in the tumor microenvironment and progression. *Trends Immunol,* 31**,** 220-7.

YANG, S., LIU, F., WANG, Q. J., ROSENBERG, S. A. & MORGAN, R. A. 2011. The shedding of CD62L (L-selectin) regulates the acquisition of lytic activity in human tumor reactive T lymphocytes. *PLoS One,* 6**,** e22560.

YOKOYAMA, W. M., MAXFIELD, S. R. & SHEVACH, E. M. 1989. Very early (VEA) and very late (VLA) activation antigens have distinct functions in T lymphocyte activation. *Immunol Rev,* 109**,** 153-76.

YU, Q. & STAMENKOVIC, I. 2000. Cell surface-localized matrix metalloproteinase-9 proteolytically activates TGF-beta and promotes tumor invasion and angiogenesis. *Genes Dev,* 14**,** 163-76.

ZABEL, M. D., WHEELER, W., WEIS, J. J. & WEIS, J. H. 2002. Yin Yang 1, Oct1, and NFAT-4 form repeating, cyclosporin-sensitive regulatory modules within the murine CD21 intronic control region. *J Immunol,* 168**,** 3341-50.

ZACCONE, P., PHILLIPS, J., CONGET, I., GOMIS, R., HASKINS, K., MINTY, A., BENDTZEN, K., COOKE, A. & NICOLETTI, F. 1999. Interleukin-13 prevents autoimmune diabetes in NOD mice. *Diabetes,* 48**,** 1522-8.

ZAJAC, A. J., BLATTMAN, J. N., MURALI-KRISHNA, K., SOURDIVE, D. J., SURESH, M., ALTMAN, J. D. & AHMED, R. 1998. Viral immune evasion due to persistence of activated T cells without effector function. *J Exp Med,* 188**,** 2205-13.

ZAMBROWICZ, B. P., IMAMOTO, A., FIERING, S., HERZENBERG, L. A., KERR, W. G. & SORIANO, P. 1997. Disruption of overlapping transcripts in the ROSA beta geo 26 gene trap strain leads to widespread expression of beta-galactosidase in mouse embryos and hematopoietic cells. *Proc Natl Acad Sci U S A,* 94**,** 3789-94.

ZAVADIL, J., CERMAK, L., SOTO-NIEVES, N. & BOTTINGER, E. P. 2004. Integration of TGF-beta/Smad and Jagged1/Notch signalling in epithelial-to-mesenchymal transition. *EMBO J,* 23**,** 1155-65.

ZHENG, Y., MANZOTTI, C. N., LIU, M., BURKE, F., MEAD, K. I. & SANSOM, D. M. 2004. CD86 and CD80 differentially modulate the suppressive function of human regulatory T cells. *J Immunol,* 172**,** 2778-84.

ZOHREN, F., SOUROULLAS, G. P., LOU, M., GERDEMANN, U., IMPERATO, M.R., WILSON, N. K., GOETTGENS, B., LUKOV, G. L., GOODELL, M. A. 2012. The transcription factor Lyl-1 regulates lymphoid specification and the maintenance of early T lineage progenitors. *Nature Immunol,* 13, 761–769.

ZWEIDLER-MCKAY, P. A., HE, Y., XU, L., RODRIGUEZ, C. G., KARNELL, F. G., CARPENTER, A. C., ASTER, J. C., ALLMAN, D. & PEAR, W. S. 2005. Notch signaling is a potent inducer of growth arrest and apoptosis in a wide range of B-cell malignancies. *Blood,* 106**,** 3898-906.

SUPPLEMENTARY DATA

Tab. S.1 Overview over cell numbers of splenic T cell populations of CD19-cre, Notch2IC//CD19-cre, LMP1/CD40//CD19-cre and Notch2IC//LMP1/CD40//CD19-cre mice.
Splenic cells were analyzed by flow cytometry CD62L and CD44 expression on either (A) CD4^{pos} or (B) CD8^{pos} lymphocyte-gated T cells. Calculations are based on five independent experiments.

(A)

CD4^{pos}	Total cell numbers ($\times 10^7$)	naïve T-cells (CD62L^{hi} CD44^{low}) ($\times 10^7$)	memory T cells (CD62L^{hi} CD44^{hi}) ($\times 10^7$)	effector T cells (CD62L^{low} CD44^{hi}) ($\times 10^7$)	CD62L^{low}, CD44^{low} ($\times 10^7$)
CD19-cre	1.2 ±0.2	0.6 ±0.1	0.1 ±0.0	0.3 ±0.1	0.0 ±0.0
Notch2IC// CD19-cre	1.3 ±0.5	0.6 ±0.2	0.1 ±0.0	0.5 ±0.2	0.1 ±0.0
LMP1/CD40// CD19-cre	7.7 ±1.9	2.4 ±1.4	0.8 ±0.3	2.1 ±0.7	0.4 ±0.2
Notch2IC//LMP1/CD40// CD19-cre	8.7± 5.4	1.9 ±1.6	0.4 ±0.4	3.3 ±1.0	1.0 ±0.7

(B)

| CD8^{pos}	Total cell numbers ($\times 10^7$)	naïve T-cells (CD62L^{hi} CD44^{low}) ($\times 10^7$)	memory T cells (CD62L^{hi} CD44^{hi}) ($\times 10^7$)	effector T cells (CD62L^{low}, CD44^{hi}) ($\times 10^7$)	CD62L^{low}, CD44^{low} ($\times 10^7$)
CD19-cre	0.5 ±0.2	0.3 ±0.1	0.1 ±0.0	0.1 ±0.0	0.0 ±0.0
Notch2IC// CD19-cre	0.8 ±0.2	0.4 ±0.4	0.2 ±0.2	0.2 ±0.2	0.1 ±0.0
LMP1/CD40// CD19-cre	1.9 ±0.8	0.7 ±0.3	0.2 ±0.1	0.3 ±0.1	0.3 ±0.2
Notch2IC//LMP1/CD40// CD19-cre	5.7 ±2.5	1.0 ±0.8	0.2 ±0.2	2.0 ±0.9	2.3 ±1.8
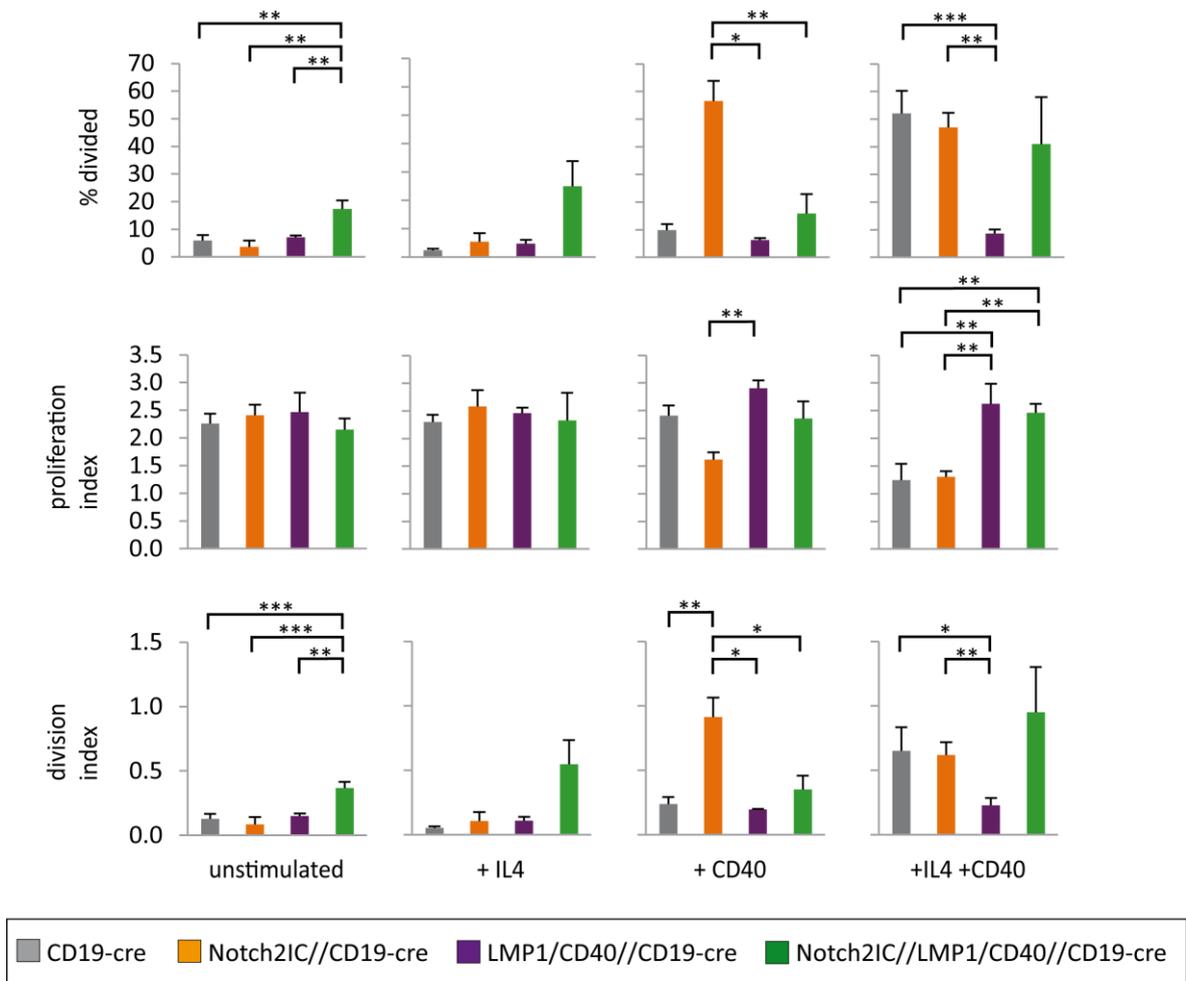
Fig. S.1 Notch2IC//LMP1/CD40-expressing B cells show an increased proliferation in in vitro culture.
Splenocytes were prepared and splenic cell preparations were depleted of CD43^{pos} (i.e. non-B) cells and labeled with CFSE. The B cells were subsequently cultivated either with or without stimuli. These stimuli included α-CD40 antibody, IL4 as well as both IL4 and α-CD40 antibody. Cells were analyzed by flow cytometric analysis on day 1, 3 and 5 of culture. Dead cells were excluded from the analysis by excluding Topro-3^{pos} cells. Statistical evaluation of day 5 of percent divided, proliferation and division index for all genotypes without stimulus, with IL4-stimulus, with CD40-stimulus and both with IL4- and CD40-stimulus. CFSE, Carboxyfluorescein succinimidyl ester. *p < 0.05, ** p < 0.01, *** p < 0.005.